

Magnetic Resonance Guided Radiotherapy for the Treatment of Bladder and Pancreatic Cancer

A thesis submitted for the degree of

MD(Res)

Arabella Katrina Hunt

Joint Department of Radiotherapy and Imaging

The Institute of Cancer Research and the Royal Marsden

NHS Foundation Trust

University of London

Abstract

Magnetic resonance guided radiotherapy (MRgRT) has many postulated benefits over conventional radiotherapy treatment techniques. Its superior soft tissue definition, lack of imaging related ionising radiation and the integration of daily adaptive re-planning offers the potential for improved radiotherapy related outcomes for patients with pancreatic and muscle invasive bladder cancers. However, as with any new technology, robust pre-clinical and early stage workflow studies must be undertaken in order for this potential to be reached.

This thesis focuses on pre-clinical research into the use of magnetic resonance imaging (MRI) within the radiotherapy pathway and the development of clinically deliverable MRgRT workflows for use by my institution for the treatment of pancreatic and muscle invasive bladder cancers.

The thesis investigates inter-observer MRI based contouring variability within the bladder cancer radiotherapy community and shows how this can be improved through education/guideline creation. Intra-fraction target motion is modelled and suitable treatment margins for use in an online adaptive hypofractionated bladder cancer radiotherapy workflow are recommended. A pilot study shows that MRgRT to the bladder is feasible and well tolerated.

The thesis describes the development and evaluation of MRI sequences for use within a pancreatic cancer MRgRT pathway. The feasibility of abdominal compression to reduce intra-fraction pancreatic target motion during an MRgRT fraction is evaluated and found to be both effective and tolerated by volunteers. A hypofractionated, 15 fraction MRgRT protocol for locally advanced pancreatic cancer is proposed utilising mid-ventilation planning techniques to enable personalisation of treatment margins.

This work serves as a foundation for MRgRT for bladder and pancreatic cancer patients at The Royal Marsden. It also provides the basis for further work on the development of dose escalated treatments for these two cancer types which will hopefully lead to improved patient outcomes in the future.

Acknowledgements

This thesis would not have been possible without the help, knowledge and guidance of many supportive people.

First and foremost, my thanks to my supervisors Robert Huddart, Shaista Hafeez and Katharine Aitken. Your wise words, enthusiasm and gentle guidance have helped make me a better clinician and scientist and I will be forever grateful for the opportunity you gave me to experience the world of research.

To the many physicists who I worked with along the way, thank you. To Ian Hanson, Alex Dunlop, Adam Mitchell, Simeon Nill, Dualta McQuaid, Jon Mohajer and Joan Chick, thank you for being so generous with your time and helping me (amongst other things) get to grips with Monaco planning, MR Linac workflow development and margin recipes. Without your support much of this thesis would not have been possible. To Oliver Gurney-Champion and Andreas Wetscherek thank you for your knowledgeable guidance and help with MR sequence development in both the online and offline settings.

To the MR Linac radiographers, Helen McNair, Trina Herbert, Sophie Alexander, Rebekah Lawes, Gill Smith, Helen Barnes and Cynthia Eccles it has been a pleasure collaborating with you. Thank you for your enthusiasm, insight and ideas. My thanks especially to Sophie and Rebekah who helped drive forward the pancreas work when I returned to training.

To Lorna Bower and Toby Morgan MR Linac trial co coordinators thank you for your support with trial recruitment and vital admin.

To my fellow research buddies- Hannah, Ingrid, Priya, Angela, Doug, Kobika, Anna, Sarah, Teresa, Adham and Brian, thanks for sharing your know-how and being there to listen to my moans when things got tough!

To my collaborators in both the bladder and pancreatic radiotherapy communities, thank you for being so welcoming and keen to help and for giving your time despite packed clinical schedules.

Closer to home, thank you to my family. To my parents, for their loyal support in all my endeavours and my husband Dan who bore the brunt of my grumpiness when things didn't go to plan but who was always there to pick me up and drive me forward. And to Sophia, my daughter, whose early arrival, slightly delayed this write up but who I love beyond measure.

Thank you to my funders. This research was supported by the National Institute for Health Research (NIHR) Biomedical Research Centre at The Royal Marsden NHS Foundation Trust and the Institute of Cancer Research and by Cancer Research UK programme grants (C33589/A19727).

And finally, thank you to the patients and volunteers who altruistically gave up their precious time in the hope of improving treatment for others, I will be forever grateful.

Contents

Declaration

Abstract

Acknowledgements

Contents

List of Figures

List of Tables

List of Acronyms

Chapter 1 Introduction	21
1.1 Disease Background	21
1.2 Role of radiotherapy in muscle invasive bladder cancer (MIBC) ..	22
1.2.1 The role of radical radiotherapy in the management of MIBC	22
1.2.2 The role of radiotherapy in the high dose palliative setting.....	25
1.2.3 Challenges of radiotherapy for MIBC	26
1.3 Role of radiotherapy in locally advanced pancreatic cancer (LAPC)	29
1.3.1 The role of conventionally fractionated chemoradiotherapy in the management of LAPC	30
1.3.2 Challenges of pancreatic radiotherapy	34
1.3.3 Role of hypofractionated (including stereotactic) radiotherapy in locally advanced pancreatic cancer	36
1.3.4 Role of Dose Escalation in Locally Advanced Pancreatic Cancer .	40
1.4 Magnetic resonance guided online adaptive radiotherapy	45
1.4.1 MR guided online adaptation for LAPC and MIBC	46
1.5 The Elekta Unity MR Linac	48

1.6 Key issues to be addressed in this thesis- with reference to relevant chapters	49
1.6.1 MR based contouring assessment and MR sequence development.	49
1.6.2 Management of intra-fraction motion.....	50
1.6.3 Development of hypofractionated workflows and protocols.....	51
1.7 References	51
Chapter 2 MRI based inter-observer contouring variability in bladder cancer radiotherapy and consensus guidance generation.....	61
2.1 Introduction.....	61
2.2 Part 1: Interobserver contouring variation and the impact of consensus guidance generation- Methods.....	62
2.2.1 Participant selection	63
2.2.2 Contouring case selection	63
2.2.3 Contouring method.....	63
2.2.4 Additional tasks completed by participants.....	65
2.2.5 Determining inter-observer contouring variability	65
2.2.6 Analysis of inter-observer variation	66
2.2.7 Assessment of the impact of consensus guidance on inter-observer variability.....	67
2.2.8 Exploratory assessment of effect of consensus generation on simulated target coverage.....	67
2.2.9 Statistical analysis	69
2.3 Part 1: Results.....	70
2.3.1 Participant Characteristics.....	70
2.3.2 Case Characteristics	71
2.3.3 Contours completed	73
2.3.4 Analysis of inter-observer variation	73

2.3.5	Impact of consensus guidance generation on interobserver variation	98
2.3.6	Effect of consensus guidance generation on simulated target coverage.....	100
2.4	Part 1: Discussion	102
2.4.1	Choice of IOV metrics used.....	103
2.4.2	Use of gold standard structures	104
2.4.3	Impact of case selection.....	105
2.4.4	Examples of others using consensus guidance to improve contouring variability.	107
2.4.5	Statistical testing	108
2.4.6	Impact of guidance on simulated dosimetry	109
2.5	Part 1: Conclusion	110
2.6	Part 1 References	110
2.7	Part 2: Consensus guidance generation- Method.....	114
2.8	Part 2: Results.....	115
2.8.1	Agreed consensus statements	115
2.9	Part 2: Discussion	120
2.9.1	GTV delineation.....	120
2.9.2	CTV delineation.....	121
2.9.3	Delineation of Organs at risk	122
2.10	Part 2 Conclusion	123
2.11	Part 2 References	123
Chapter 3 Workflow development for the treatment of bladder cancer on the Elekta Unity.....		128
3.1	Introduction.....	128
3.2	Methods	132
3.2.1	Development of intra-fraction treatment margins	132

3.2.2	Impact of other bowel re-contouring	139
3.3	Results.....	141
3.3.1	Development of intra-fraction treatment margins	141
3.3.2	Impact of other bowel re-contouring	146
3.4	Discussion.....	151
3.4.1	Development of intra-fraction treatment margins	151
3.4.2	Impact of other bowel re-contouring	154
3.5	Conclusion	155
3.6	References	156
Chapter 4	Feasibility of Magnetic Resonance Guided Radiotherapy for the Treatment of Muscle-Invasive Bladder Cancer.	159
4.1	Introduction.....	159
4.2	Methods	160
4.2.1	Patient eligibility.....	160
4.2.2	Reference plan generation	161
4.2.3	Online adaptive workflow	164
4.2.4	Workflow feasibility	165
4.2.5	Offline assessment.....	166
4.2.6	Patient experience.....	168
4.3	Results.....	168
4.3.1	Online adaptive workflow	169
4.3.2	Inter- and intra-fraction CTV variation	170
4.3.3	Target coverage and Conformity Index	173
4.3.4	Patient tolerability	176
4.4	Discussion.....	176
4.5	Conclusions and future directions.....	180
4.6	References	181

Chapter 5 MRI sequence optimisation for pancreatic MR guided radiotherapy.	184
5.1 Introduction	184
5.1.1 Use of MRI in radiotherapy workflows	184
5.1.2 Challenges of developing offline and online radiotherapy planning MRI sequences for pancreatic cancer	185
5.1.3 Sequence optimisation	188
5.2 Methods	189
5.2.1 Development of radiotherapy simulation MRIs	189
5.2.2 Optimising sequences for online use on the Elekta Unity	191
5.2.3 Evaluation of sequences optimised for the Elekta Unity	191
5.3 Results	192
5.3.1 Development of radiotherapy simulation MRIs	192
5.3.2 Evaluation of sequences for use in an online radiotherapy workflow on the MR Linac	197
5.4 Discussion	208
5.5 Conclusion	211
5.6 References	211
Chapter 6 Investigation into the use of abdominal compression in pancreatic MR guided radiotherapy	214
6.1 Introduction	214
6.2 Methods	215
6.2.1 Volunteer selection	215
6.2.2 Identification of suitable abdominal compression devices	216
6.2.3 Assessment of the impact of abdominal compression on respiratory motion	217
6.2.4 Assessment of the impact of compression devices on image clarity.	219
6.2.5 Assessment of volunteer tolerability	219

6.2.6	Assessment of compatibility with 4DCT	219
6.3	Results.....	220
6.3.1	Assessment of the impact of abdominal compression on diaphragmatic motion	220
6.3.2	Assessment of the impact on image clarity of the presence of compression devices	221
6.3.3	Assessment of volunteer tolerability	223
6.3.4	Assessment of compatibility with 4DCT	225
6.4	Discussion.....	225
6.5	Conclusion	227
6.6	References	228
Chapter 7	Pancreatic cancer MRgRT treatment protocol.....	230
7.1	Introduction.....	230
7.2	Methods.....	230
7.2.1	Rationale for use of a non-dose escalated 15 fraction protocol...230	
7.2.2	Integration of the optimised MRI sequences into the pancreatic workflow and PTV margin calculations	233
7.3	Results- The protocol.....	239
7.3.1	Objectives and Scope	239
7.3.2	Indications	240
7.3.3	Pre-radiotherapy investigations.....	240
7.3.4	Therapeutic schemata.....	240
7.3.5	Pre-treatment	240
7.3.6	Volume definition.....	241
7.3.7	Treatment planning	243
7.3.8	Treatment delivery.....	244
7.3.9	Follow up after treatment.....	245
7.4	Discussion.....	245

7.5	Conclusion	248
7.6	References	248
Chapter 8	Summary, conclusions and future directions.....	252
8.1	MRI based inter-observer contouring variability in bladder cancer radiotherapy and consensus guidance generation.....	252
8.2	Workflow development for the treatment of bladder cancer on the Elekta Unity.....	254
8.3	Feasibility of Magnetic Resonance Guided Radiotherapy for the Treatment of Muscle-Invasive Bladder Cancer.....	255
8.4	MRI sequence optimisation for pancreatic MR guided radiotherapy.	258
8.5	Investigation into the use of abdominal compression in pancreatic MR guided radiotherapy	260
8.6	Pancreatic cancer MRgRT treatment protocol	260
8.7	The future of MRgRT	263
8.8	Conclusion	265
8.9	References	265
Appendix 2.1	268
Appendix 2.2	274
Appendix 2.3	276
Appendix 4.1	277
Appendix 5.1	279
Appendix 5.2	280
Appendix 6.1	281
Appendix 7.1	283
Appendix 7.2	290

List of Tables

Table 1.1 Table of studies comparing surgery to TMT	23
Table 1.2 Randomised phase II/III chemoradiotherapy trials for locally advanced pancreatic cancer (published post year 2000).	32
Table 1.3 Prospective SBRT trials of LAPC	37
Table 2.1 Stage 1 contouring guidance	64
Table 2.2 Margin sizes	68
Table 2.3 Participant Characteristics	71
Table 2.4 Case Characteristics	72
Table 2.5 Stage 1 GTV variation.....	73
Table 2.6 Stage 1 CTV variation.....	78
Table 2.7 Stage 1 Outer bladder wall variation.	82
Table 2.8 Table of median DICE scores depending on years of bladder radiotherapy experience.	86
Table 2.9 Stage 3 GTV variation.....	86
Table 2.10 Stage 3 CTV variation	91
Table 2.11 Stage 3 Outer bladder wall variation	95
Table 2.12 Effect of consensus guidance generation on interobserver variability.	99
Table 2.13 Effect of consensus guidance generation on interobserver variability, case 3 alone.....	99
Table 2.14 Results of simulated target coverage	101
Table 2.15 Comparison between STAPLE contour and Gold standard STAPLE contour.....	105
Table 2.16 Results of Delphi consensus.....	118
Table 3.1 PTV expansions	134
Table 3.2 Planning dose constraints used	136
Table 3.3 Patients where OAR dose constraints were missed when using medium margin.....	138
Table 3.4 Characteristics of APPLY patients n=44	142
Table 3.5 Characteristics of IDEAL n=20	142

Table 3.6 APPLY patients coverage of CTV ₃₀ by differing PTV margins around CTV ₀	143
Table 3.7 Coverage of CTV ₆₀ by differing PTV margins around CTV ₃₀	144
Table 3.8 Coverage of CTV ₃₀ by 95% isodose, n=34	145
Table 4.1 Dose constraints	162
Table 4.2 Template Settings	163
Table 4.3 Patient Characteristics	169
Table 4.4 Intra-fraction CTV change	173
Table 5.1 Typical imaging protocol for pancreatic cancer.	186
Table 5.2 Differences between diagnostic and radiotherapy planning MRIs for pancreatic cancer.....	187
Table 5.3 Summary of observations from imaging session of patients 1-4 and their potential roles within an offline workflow.	193
Table 5.4 Results of formal image clarity assessment.	207
Table 5.5 Wilcoxon Signed Ranks Test	208
Table 6.1 Median Likert score for the different sequences with the differing compression devices.	222
Table 6.2 Post hoc analysis of T1W and mDixon (water) comparisons.	223
Table 7.1 Table of dose equivalence	232
Table 7.2 Initial margin calculations	238
Table 7.3 Proposed PTV margins.....	239
Table 7.4 PTV motion adapted margin.	242
Table 7.5 PTV constraints for 45Gy/15# simultaneous integrated boost	243
Table 7.6 OAR constraints.....	244
Table 7.7 Follow up schedule for locally advanced pancreatic cancer.....	245

List of figures

Figure 1.1 Pancreatic cancer disease status	30
Figure 1.2 Close proximity of GI OARs to target volume.	35
Figure 1.3 Kaplan Meier plot from Krishnan et al (73).....	42
Figure 1.4 Kaplan Meier plot from Chung et al (75)	43
Figure 1.5 Online adaptive workflow	46
Figure 1.6 The Elekta Unity	48
Figure 2.1 Flow chart of study stages and their relevant chapter parts.....	62
Figure 2.2 Geometric inter-observer comparison metrics	67
Figure 2.3 Assessment of gold standard PTV coverage.....	69
Figure 2.4 Representative axial slices of the 6 cases.	72
Figure 2.5 Inter-observer contouring variability for case 3.	75
Figure 2.6 Inter-observer GTV contouring variability for case 1	76
Figure 2.7 Inter-observer GTV contouring variability for case 2.....	77
Figure 2.8 Inter-observer CTV contouring variability for case 1.	79
Figure 2.9 Inter-observer CTV contouring variability for case 2.	80
Figure 2.10 Inter-observer CTV contouring variability for case 3.	81
Figure 2.11 Inter-observer outer bladder wall contouring variability for case 1.	83
Figure 2.12 Inter-observer outer bladder wall contouring variability for case 2.	84
Figure 2.13 Inter-observer outer bladder wall contouring variability for case 3.	85
Figure 2.14 Inter-observer contouring variability for case 3 post consensus. ...	88
Figure 2.15 Inter-observer contouring variability for case 4.	89
Figure 2.16 Inter-observer contouring variability for case 5.	90
Figure 2.17 Inter-observer contouring variability for case 3.	92
Figure 2.18 Inter-observer contouring variability for case 4.	93
Figure 2.19 Inter-observer contouring variability for case 5.	94
Figure 2.20 Inter-observer contouring variability for case 3.	96
Figure 2.21 Inter-observer contouring variability for case 4.	97
Figure 2.22 Inter-observer contouring variability for case 5.	98
Figure 3.1 Adapt to shape workflow	129
Figure 3.2 Demonstration of deformable image registration (DIR) performance for bowel.	130

Figure 3.3 Standard DVH based planning approach.....	131
Figure 3.4 Gradient based planning approach.	132
Figure 3.5 Steps involved in margin analysis, using an APPLY patient scan..	135
Figure 3.6 Planning study for APPLY dataset.	137
Figure 3.7 Bowel re-contouring study pathway.	141
Figure 3.8 Predominant direction of target miss for APPLY cohort	143
Figure 3.9 Predominant direction of target miss for IDEAL cohort	144
Figure 3.10 ROC curve results using small margins.	146
Figure 3.11 Variability of other bowel volume across 5 patients	147
Figure 3.12 CTV ₃₀ V95% coverage	148
Figure 3.13 Volume of other bowel receiving ≥ 36 Gy.	148
Figure 3.14 Volume of other bowel receiving ≥ 33 Gy.	149
Figure 3.15 Volume of other bowel receiving ≥ 31 Gy.	149
Figure 3.16 Volume of other bowel receiving ≥ 28 Gy.	150
Figure 3.17 Volume of other bowel receiving ≥ 25 Gy.	150
Figure 4.1 Flow chart of adaptive workflow	165
Figure 4.2 example of offline CTV re-contouring.....	166
Figure 4.3 Time taken for online adaptive workflow stages.	170
Figure 4.4 Variation in CTV at MRI _{session} (top graph), Variation in intra-fraction volume change, (bottom graph).	172
Figure 4.5 Intra-fraction fill rates	173
Figure 4.6 Box and Whisker plot (as per figure 4.3) depicting CTV coverage by 95% isodose on verification and post treatment MRIs.	174
Figure 4.7 Intra-fraction changes to rectal shape.....	175
Figure 4.8 Conformity index based on session anatomy versus post treatment anatomy.	175
Figure 5.1 Examples of sequences acquired on the 1.5T diagnostic scanner.	195
Figure 5.2 Axial slices of CE marked Elekta provided sequences.	198
Figure 5.3 Impact of the addition of a water bolus given 15 minutes prior to imaging.	199
Figure 5.4 T1 mDixon (water component) developed by UMC Utrecht.....	200
Figure 5.5 Imaging development of Wisconsin mDixon.	202
Figure 5.6 Comparison of in-house developed breath-hold Dixon.	203

Figure 5.7 Comparison between finalised Wisconsin sequence (A) and In house version (B).....	204
Figure 5.8 Comparison of 3DVANE vs T1W free breathing	205
Figure 5.9 In house Dixon (high resolution) in arms down position with varying encoding directions.	206
Figure 6.1 Abdominal compression devices tested.....	217
Figure 6.2 Measurement of diaphragmatic motion.....	218
Figure 6.3 Graph showing the reduction in mean motion across the 5 volunteers in Cohort 2 with use of ZiFix compression device.	220
Figure 6.4 Results of volunteer questionnaires following Dynabelt sessions. .	224
Figure 6.5 Results of volunteer questionnaires for ZiFix sessions.	225

List of Acronyms

3D	Three Dimensional
4D	Four Dimensional
5- FU	Fluorouracil
ABC	Active breath control
AC	Abdominal compression
ART	Adaptive radiotherapy
ATP	Adapt to position
ATS	Adapt to shape
BED	Biologically equivalent dose
BPT	Bladder preservation therapy
BRPC	Borderline resectable pancreatic cancer
C κ	Cohen Kappa
CBCT	Cone beam computer tomography
CC	Cubic centimetre
CECT	Contrast enhanced computer tomography
CI	Confidence interval
cm	Centimetres
CT	Computer tomography
CTCAE	Common terminology criteria for adverse events
CTV	Clinical target volume

CRT	Chemoradiotherapy
DCE	DICE similarity coefficient
DIR	Deformable image registration
Dmax	Maximum dose
DSS	Disease specific survival
DVH	Dose volume histogram
DWI	Diffusion weighted image
FOV	Field of view
FOLFIRINOX	Fluorouracil, irinotecan, oxaliplatin
GI	Gastrointestinal
GTV	Gross tumour volume
HD	Hausdorff distance
HR	Hazard ratio
IMRT	Intensity modulated radiotherapy
ICR	Institute of Cancer Research
IOV	Interobserver variability
ITV	Internal target volume
KPS	Kamofsky performance score
LAPC	Locally advanced pancreatic cancer
MDA	Mean distance to agreement
MDT	Multidisciplinary team
MIBC	Muscle invasive bladder cancer

MidV	Mid ventilation
mm	Millimetre
MR	Magnetic resonance
MRgRT	Magnetic resonance guided radiotherapy
MRI	Magnetic resonance imaging
MVR	Maximum variability ratio
N	Number
OAR	Organ at risk
OS	Overall survival
PRV	Planning organ at risk volume
PTV	Planning treatment volume
RC	Radical cystectomy
RCR	Royal College of Radiologists
RMH	The Royal Marsden Hospital
ROI	Region of interest
RPM	Real time position management
RT	Radiotherapy
SBRT	Stereotactic body radiotherapy
SFOV	Small field of view
SIB	Simultaneous integrated boost
SNR	Signal to noise ratio
SSO	Segment shape optimisation

STAPLE	Simultaneous truth and performance level estimate
T	Tesla
T1W	T1 weighted
T2W	T2 weighted
TCC	Transitional cell carcinoma
TMT	Tri-modality treatment
TPS	Treatment planning system
TSE	Turbo spin ECHO
TURBT	Transurethral resection of bladder tumour
VGA	Visual graded analysis
VIBE	Volumetric interpolated breath-hold sequence
VMAT	Volumetric modulated arc therapy

Chapter 1 Introduction

Sections of this introduction have been published:

Original articles:

Hunt A, Hansen VN, Oelfke U, Nill S, Hafeez S. Adaptive Radiotherapy Enabled by MRI Guidance. *Clinical oncology (Royal College of Radiologists (Great Britain))*. 2018;30(11):711-9.

Bertholet J, Hunt A, Dunlop A, Bird T, Mitchell RA, Oelfke U, et al. Comparison of the dose escalation potential for two hypofractionated radiotherapy regimens for locally advanced pancreatic cancer. *Clinical and translational radiation oncology*. 2019;16:21-7.

Chapter 1 **Introduction**

1.1 Disease Background

Bladder cancer is the 10th most common malignancy in the UK with approximately 10,000 new cases diagnosed each year (1). Incidence rates are higher in men than in women and increase with age. In Europe/North America, transitional cell carcinoma (TCC) accounts for 90% of cases (2), with non-urothelial histologies, for example squamous, adenocarcinoma and small cell histologies, making up the remainder. The majority of diagnoses are of non-muscle invasive disease but 25% present with muscle invasive bladder cancer (MIBC) which carries a 5 year overall survival of ~50% (3). For the MIBC cohort who present with localised disease, radical cystectomy is regarded by many as the standard of care. However, in recent years, radical radiotherapy, as part of a tri-modality treatment (TMT) approach (transurethral resection in conjunction with chemoradiotherapy), is increasingly being recognised as an alternative to cystectomy for selected patients (4-8).

Pancreatic adenocarcinoma represents the 11th most common UK cancer but it is the 6th most common cause of UK cancer death (9). Five year overall survival is poor at <5% and despite some recent advances in systemic therapy has changed little in the last 40 years. As such, pancreatic cancer has been designated a cancer of unmet need by Cancer Research UK (9). Unlike bladder cancer, the majority of patients present with either locally advanced (30%) or metastatic disease (50%) (10). For patients with locally advanced pancreatic cancer (LAPC), standard of care involves either systemic treatment alone or in combination with radiotherapy (11). Historical median survival for this group is between 6-15 months (12), however, for those fit enough to receive newer chemotherapy combinations such as FOLFIRINOX (Fluorouracil [5-FU], Leucovorin, Irinotecan, Oxaliplatin) median survival can now reach up to 24 months (13).

1.2 Role of radiotherapy in muscle invasive bladder cancer (MIBC)

1.2.1 The role of radical radiotherapy in the management of MIBC

Approximately 25% of bladder cancer patients present with localised MIBC (14), with a further subset of patients progressing from non-muscle invasive disease. MIBC requires more aggressive treatment than non-muscle invasive disease and historically radical cystectomy with lymphadenectomy has been the standard of care for this patient cohort. However, with a median age at diagnosis of ≥ 75 years (1) and its close association with smoking, many patients make poor surgical candidates especially as radical cystectomy is associated with significant treatment related morbidity and mortality (15). In those not fit for surgery, or who decline it, radiotherapy with its potential for organ preservation offers an alternative to cystectomy and has been shown in two UK run trials (16, 17) to provide acceptable rates of local control, be well tolerated and give 5 year overall survival rates of ~50% when combined with radiosensitization, either in the form of chemotherapy or hypoxia modification with carbogen and nicotinamide.

In recent years, the use of radiotherapy for those who *are* cystectomy candidates has also begun to gain popularity with guidelines now recognising the tri-modality treatment (TMT) approach of transurethral resection in conjunction with radiotherapy and concurrent radiosensitization as an alternative radical treatment option for a select group of patients with MIBC (5, 7). The exact criteria for suitability for 'selective bladder preservation' varies but tends to include (amongst others) patients with unifocal disease, good bladder function and limited/no carcinoma in situ. In addition, patients must be willing and able to undergo post treatment cystoscopic surveillance as disease recurrence and subsequent salvage cystectomy may be necessary in ~7-11% of patients (16, 17).

There is no prospective randomised evidence directly comparing surgery to radiotherapy for MIBC. The UK Selective bladder Preservation Against Radical Excision (SPARE) trial (18) attempted to answer this question but closed early due to poor accrual citing clinician and patient treatment preferences impacting on the ability to accept the offered randomised treatment. As a result, data on the

comparative efficacy of TMT versus surgery comes in the form of (often contradictory) retrospective series.

In the absence of randomised data, the US National Cancer Database has been used by multiple studies in an attempt to answer whether surgery and radiotherapy are comparable. Ritch et al(19), Cahn et al(20) and Seisen et al (21) all used types of propensity matched analysis to understand whether radiotherapy (usually in the form of TMT) gave comparable survival outcomes, (Table 1.1). In all three cases, radiotherapy/TMT appeared to give worse outcomes than radical cystectomy (RC). However, although propensity matching of some kind was used in all three studies, these types of observational cohorts remain at significant risk of bias particularly from unknown confounders. This is particularly significant in bladder cancer patients where differences in the typical populations undergoing cystectomy versus radiotherapy are significant. In addition, for this database, details around the quality of TMT performed are difficult to tease out, for example, the degree of TURBT is not recorded nor the exact timing of chemotherapy with respect to radiotherapy (neo-adjuvant versus concomitant versus adjuvant). Both these factors are known to impact on the success of TMT, with those undergoing a complete TURBT with concomitant radiosensitization doing better than those having an incomplete resection and radiotherapy alone (16, 22).

Table 1.1 Table of studies comparing surgery to TMT

Author	Evidence type	Number of patients and sample period	Treatment definitions	Outcomes
Ritch et al 2018	Retrospective propensity score-matched review of National Cancer Data Base (USA)	Total N= 8379 RC = 6606 CRT = 1773 1683 matched 2004-2013	RC = radical cystectomy or pelvic exenteration CRT= chemotherapy within 90 days of radiation, RT dose $\geq 40\text{Gy}$	Median 5 year survival worse for CRT compared to RC 30% vs 38% $p < 0.004$ Initial improved mortality for CRT, HR 0.84 (0.74-0.96) which then

				worsened over time, suggesting higher initial mortality following RC
Cahn et al 2017	Retrospective, propensity score-matched review of National Cancer Data Base (USA)	Total N = 32300 RC = 22680 BPT = 9620 2004-2013	RC = radical cystectomy +/- lymphadenectomy BPT = stratified into 1) received any RT = 9620 2) definitive RT (50-80Gy) = 2540 3) definitive RT with chemotherapy (within 3 months of RT) = 1489	BPT associated with decreased 5 year OS compared to RC, 20.6% vs 48.3% But when considering CRT group alone difference reduced, 29.9% vs 48.3% Note: high rates of suboptimal RT- only 4.6% of total population received CRT
Seisen et al 2017	Retrospective, propensity score-matched review of National Cancer Data Base (USA) using inverse probability of treatment weighting adjusted analysis	Total N = 12843 RC = 11586 TMT = 1257 2004-2011	RC = radical cystectomy plus lymphadenectomy TMT = >39Gy of RT plus chemotherapy (exact relation to RT unknown)	Similar median OS When time-varying co-variant added TMT was associated with worsening HR after 25 months HR 1.37 (1.16-1.59) p<0.001
Fahmy et al 2018	Systematic review of 57 studies reporting outcomes after TMT or RC	Total N = 30293 RC = 26891 TMT = 3402 1990-2017	RC = radical cystectomy +/- lymphadenectomy TMT = TURBT + RT with radiosensitization (various RT regimens and radiosensitization techniques used)	Mean 10 year OS 30.9% TMT vs 35.1% RC (p=0.32) Mean 10 year DSS 50.9% TMT vs 57.8% RC (p=0.26) The addition of NAC

				significantly improved survival in RC cohort (p= 0.025) but not TMT cohort (p= 0.078)
Giacalone et al 2017	Single centre (USA), retrospective case series	Total N = 475 (TMT only) 1986-2013	TMT = TURBT followed by RT with concurrent chemotherapy Split course RT used as per RTOG studies	5 year and 10 year OS: 57% and 39% 5 year and 10 year DSS: 66% and 59% Salvage cystectomy rate at 5 years: 29% Noted improvement in outcomes in later cohort (2005-2013) vs older cohorts (1986-1995)

In comparison, a systematic review and meta-analysis of 57 studies reporting outcomes for patients undergoing RC or TMT by Fahmy et al (23) suggested that there is no difference in overall or disease specific survival when RC is compared to TMT. This is backed up by single centre experiences from Massachusetts General Hospital (24) and The University of Toronto (8) which also suggest similar survival outcomes from the two treatment modalities. However, the inherent weakness in both single centre, and non-randomised inter- trial outcome comparisons must be acknowledged.

Unfortunately, given the challenges of performing a randomised study in this treatment space it is unlikely that level one evidence comparing surgery versus TMT in those fit for cystectomy will be forthcoming.

1.2.2 The role of radiotherapy in the high dose palliative setting

Although radiotherapy with radiosensitization is generally well tolerated (16, 25, 26), there is still a cohort of patients for whom a daily fractionation of 4-6 weeks with concurrent chemotherapy will be too challenging to deliver. While the use of

carbogen and nicotinamide as a radiosensitizer can be considered, as used in the BCON trial (17), another option to consider is that of hypofractionated weekly treatments. The APPLY trial (27), a single centre UK trial, recruited 55 MIBC patients deemed unfit for radical therapy to receive 36Gy in 6 fractions over 6 weeks with treatment delivered using an adaptive planning technique. In this elderly, co-morbid cohort, this dose fractionation and planning technique resulted in local control rates at 3 months of at least 51% and an estimated 1 year survival of 62% (95% CI 48%-74%). This work was then extended in the multicentre HYBRID trial (NCT01810757) which randomised a similar patient cohort to 36Gy in 6 fractions delivered using either a standard or adaptive planning technique. The study found that hypofractionated radiotherapy was well tolerated and provided good local control rates (81.3% at 3 months) (28).

In our centre, this option is also considered (using a dose fractionation of 30Gy/5#) in those with low volume metastatic disease where control of the primary is required.

1.2.3 Challenges of radiotherapy for MIBC

Delivering radiotherapy to the bladder is not without its challenges.

Firstly, the bladder is a moving target with large inter-fraction variation in position, shape and size due to variable urinary filling and nearby organ motion (29-31). Historically this has necessitated the use of large population based treatment margins in order to achieve reliable target coverage. However, this approach is often over-generous resulting in excessive normal tissue irradiation (32) and is still prone to target miss (33).

In order to overcome this, some centres (such as my own) have adopted a “plan of the day” or library of plans approach. Here, a selection of plans are created for each patient with varying CTV to PTV margin sizes. Prior to each fraction a cone-beam CT is then used to select the most appropriate plan based on the size, shape and position of the bladder on that day. Use of this technique has been shown to both improve target coverage while simultaneously reducing dose to normal tissues compared to conventional techniques (34-36). However, the library of plans approach is unable to account completely for the variation seen

on a day-to-day basis and so conformality of treatment plans remains modest. In order to personalise our radiotherapy margins further we should therefore investigate other potential solutions such as online adaptive replanning which will be discussed in more detail later.

Secondly, within the radiation oncology community there is variation in target volume definition and dose/fractionation schedules used to treat patients with MIBC (23). This lack of consensus makes cross trial/country data comparison difficult. In the UK, 'radical' patients are commonly treated with either 60- 64Gy in 1.8-2Gy per fractions or 55Gy in 20 fractions with the whole bladder included in the target volume with no additional lymph node irradiation (37). In comparison, in the US and Canada, a split course approach is often utilised (8, 24) whereby radiotherapy is delivered to the bladder and pelvic nodes up to around 40-45Gy with an additional tumour boost of ~20Gy. Whilst it might not be possible to converge these different treatment styles, attempts should be made to standardise treatments as much as possible, in particular with respect to target and OAR definition in order to allow cross institution/trial comparisons.

Finally, although current radiotherapy protocols give reasonable rates of local control, most episodes of localised disease recurrence happen at the site of original disease (38) suggesting that for some patients current doses are insufficient. Dose-response studies for MIBC suggest that rates of local control can be improved with dose escalation (39). The potential benefit of dose escalation is currently under investigation in the Phase II RAIDER trial (NCT02447549) having shown promise in a pilot study (40). In this study the tumour is boosted to 70Gy/32# or 60Gy/20# with the remaining bladder receiving 52Gy or 46Gy respectively. The boost level to 70Gy was selected based on bladder brachytherapy studies which have reached doses of ~70Gy (2Gy equivalent) with acceptable toxicity (41). The magnitude of effect expected with dose escalation is influenced by the α/β ratio of bladder cancer. Bladder cancers are generally regarded as rapidly proliferating, with a high α/β ratio of around 10-15Gy (42). This means that escalation from 64Gy to 70Gy gives a biologically effective dose increase of 8.46Gy (BED_{10}) or 7.64Gy (BED_{15}) when using the following formula:

$$BED = nd \left[1 + \frac{d}{\alpha/\beta} \right]$$

Where n is the number of fractions, d is the dose per fraction.

However, the data from clinical studies which supports an α/β ratio of 10-15 is limited and the confidence intervals wide (42, 43). In a recently published meta-analysis of the BCON and BC2001 studies (44) results would suggest the α/β ratio may be less than 10. If this is the case, then biologically effective dose increase would be greater than expected.

It is likely that any effect of dose escalation will not be seen uniformly across the MIBC cohort. However, the patient group most likely to benefit from dose escalation is currently unknown. Logically, dose escalation may be particularly important for those patients with residual disease post TURBT as higher doses of radiation are typically needed for the treatment of macroscopic versus microscopic disease¹. In a pooled analysis of Radiation Therapy Oncology Group Protocols (22), patients with a visibly complete TURBT had higher complete response rates following bladder preservation therapy (using concurrent CRT and doses up to 64Gy in 2 Gy per fraction) compared to those patients with incomplete TURBT. However, in the combined analysis of the BCON and BC2001 trials, complete resection was not found to be a significant variable in locoregional disease control (44). Other aspects of a patient's tumour, such as the tumour microenvironment and molecular and genomic differences are therefore likely to be important in predicting a patient's response to radiotherapy. Research into potential genomic biomarkers for treatment response is ongoing (45) but imaging biomarkers may also have utility in this area. MRI is increasingly recognised as a valuable way of providing non-invasive measurement of the tumour microenvironment. Established techniques such as diffusion weighted imaging have been shown in single centre studies to have utility in predicting

¹ In RAIDER, patients with and without visible disease post TURBT were eligible for enrolment. In cases where there is no visible disease, the tumour bed (i.e., the location of the tumour pre resection, defined using pre-TURBT imaging and surgical bladder maps) is boosted to 70Gy. In this protocol no distinction is made between patients with and without visible disease in terms of dose given to boosted region. The tumour bed is labelled as a GTV although strictly speaking the tumour bed is a CTV as there is no visible tumour remaining.

response to bladder radiotherapy in both the pre (46) and post treatment setting (47). Multicentre validation is awaited. Other techniques quantifying tumour hypoxia such as T2*-weighted blood-oxygenation-level-dependent MRI (BOLD) and tumour oxygenation level dependent MRI (TOLD) can map areas of hypoxia within a tumour and although not yet shown to predict treatment response in human studies have shown promise in predicting radiotherapy response in rodent studies (48). Although further studies are needed, functional imaging may well provide a valuable tool in selecting patients most likely to benefit from escalated doses.

In order to safely dose escalate without excess toxicity it is important to identify and boost the tumour rather than the whole bladder. For MIBC, while the whole bladder is relatively easy to identify on a radiotherapy planning CT and standard cone beam CT, the tumour is less so increasing the risk of target miss and necessitating the use of larger treatment margins. As a result, alternative imaging modalities should be explored as a way to improve target accuracy. MRI has been shown to improve staging accuracy compared to CT (49-51). Incorporation of MRI into the radiotherapy contouring process may therefore enable greater confidence in tumour delineation. This could in turn lead to smaller treatment margins, greater dose escalation and potentially improved patient outcomes.

1.3 Role of radiotherapy in locally advanced pancreatic cancer (LAPC)

Patients with pancreatic adenocarcinoma can be broadly divided into those with and without metastatic disease. In the cohort with localised disease further subdivisions can be made into those with resectable, borderline resectable and locally advanced disease states. See Figure 1.1

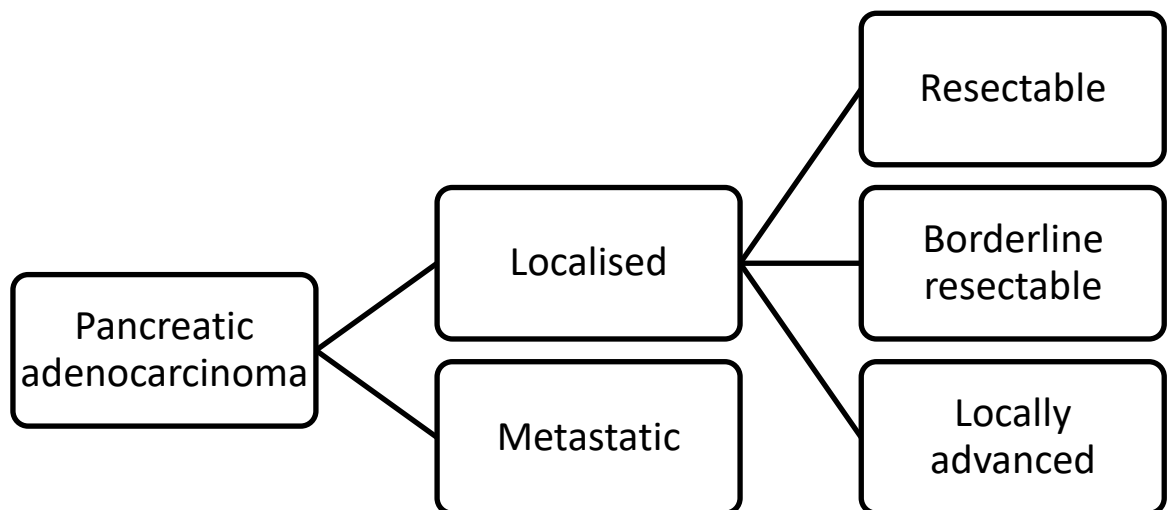


Figure 1.1 Pancreatic cancer disease status

Although exact definitions vary, locally advanced pancreatic cancer is typically defined as disease without distant metastasis (including non-regional lymph node metastasis) where the primary is surgically inoperable due to the extent of involvement of local vasculature or critical nearby organs. Exact definitions for surgical resectability vary between guidelines and clinical trials (52-54) however, common to all these definitions is the degree of involvement of the superior mesenteric artery, the common hepatic artery, the coeliac axis and the superior mesenteric vein/portal veins.

1.3.1 The role of conventionally fractionated chemoradiotherapy in the management of LAPC

Similar to MIBC, treatment of LAPC and in particular the use of radiotherapy is controversial. Some regard LAPC as a systemic disease with an inevitable progression to metastasize which is therefore best suited to treatment with systemic regimens. Others would argue that although the majority of LAPC patients will at some stage progress to metastatic disease, a minority (around 30% (55)) will die with localised disease for which a localised treatment as part of a multi-modality approach is more appropriate. In addition, as local disease progression can cause significant and difficult to control symptoms, treatments which can improve local control are of value.

The controversy over the role of conventional chemoradiotherapy stems largely from conflicting results from historical randomised trials, Table 1.2.

Table 1.2 Randomised phase II/III chemoradiotherapy trials for locally advanced pancreatic cancer (published post year 2000).

Author and Title	Phase	Number of patients	Intervention and Comparator	Outcomes	CRT OS benefit
Hammel et al 2016 LAP07	III	449 (442 eligible) in whole study 269 in radiotherapy randomisation	2 phases Phase 1: Induction chemo of Gemcitabine + Erlotinib vs Gemcitabine alone Phase 2: For non progressors only, CRT vs continuing with chemo 3D conformal RT, 54Gy/30# concurrent Capecitabine	Median OS: 15.2 months with addition of CRT vs 16.5 months with chemo alone (p=0.83) CRT group had decreased local progression 32% vs 46% Toxicity: CRT resulted in more G3/4 nausea than chemo alone (all other toxicity difference NS)	No
Mukherjee et al 2013 SCALOP	II	114 (74 eligible)	Induction Gemcitabine and Capecitabine followed by either Capecitabine+RT or Gemcitabine+RT 3D conformal or IMRT, 50.4Gy/28# concurrent Capecitabine or Gemcitabine	Median OS (primary analysis): 15.2 months Capecitabine vs 13.4 months Gemcitabine (p=0.01)	N/A
Loehrer et al 2011 An Eastern Cooperative Oncology Group Trial	III	74 (71 evaluable)	Gemcitabine alone vs Gemcitabine plus CRT 3D conformal encouraged, no IMRT 50.4Gy/28# with concurrent Gem	Median OS: 11.1 months Gemcitabine Plus CRT vs 9.2 months Gemcitabine alone (P=0.017)	Yes
Chauffert et al 2008 FFCD/SFRO study	III	119	Induction CRT (with 5FU and cisplatin) followed by maintenance Gemcitabine Vs Gemcitabine alone	Median OS: 8.6 months for CRT vs 13 months Gem alone (p=0.03)	No

			3D conformal RT, 60Gy/30# concurrent 5FU/cisplatin)	Toxicity: Higher G3/4 in CRT arm during induction (36% vs 22%) and maintenance (32% vs 18%)	
--	--	--	---	---	--

Studies identified via Pubmed search performed in October 2019. Search limited to published, randomised phase II/III trials comparing chemotherapy to chemoradiotherapy for LAPC. Only studies published post the year 2000 included. Search terms- pancreatic cancer [MESH], chemoradiotherapies [MESH] with additional manual searches following review of reference lists. Search cross referenced against Palto et al (46) ASTRO Pancreatic Guideline Full Evidence Table which performed a systematic review of trials between May 2007-June 2017. Mukherjee et al included in table as this UK trial provided the basis for the current standard of care in the UK.

Proponents of systemic therapy alone would point to the LAP 07 (12) and FFCD/SFRO (56) studies which failed to show an overall survival (OS) advantage for the addition of chemoradiotherapy (CRT) to chemotherapy alone. In LAP 07, 449 patients with LAPC (442 eligible for analysis) were randomised to induction Gemcitabine versus Gemcitabine and Erlotinib followed by, in non-progressors only, continuation of chemotherapy versus CRT (54Gy/30# with concurrent Capecitabine). The addition of CRT did not lead to an improvement in the primary endpoint of median OS (16.5 months in the chemotherapy group versus 15.2 months in the CRT group (p=0.83)). However, an improvement in local control was observed and participants in the CRT arm experienced a longer time off treatment. In the FFCD/SFRO study, induction CRT (60Gy/30# with concurrent 5FU and cisplatin) followed by maintenance Gemcitabine gave a worse OS compared to Gemcitabine alone (median OS 8.6 months for CRT versus 13 months for Gemcitabine alone, p=0.03) with higher rates of toxicity in the CRT arm (36% vs 22% Grade 3/4). However, both LAP 07 and FFCD/SFRO can be criticised for their radiotherapy delivery, with only 30% of patients receiving per protocol treatment in the former and a non-standard, untested, toxic radiotherapy dose/ fraction schedule used in the latter.

Proponents for the addition of CRT to induction chemotherapy would point to the OS benefit seen in another (albeit smaller) phase 3 trial by Loehrer et al (57) where chemotherapy in the form of Gemcitabine was compared to Gemcitabine

plus CRT. A statically significant improvement in OS was seen in favour of chemotherapy plus CRT (9.2 months chemotherapy alone vs 11.1 months chemotherapy plus CRT ($p=0.017$)) with similar rates of toxicity.

As a result of the controversies in the data, both treatment strategies (chemotherapy alone versus chemotherapy followed by CRT) are considered as acceptable treatment options in the management of LAPC (54, 58).

Survival for patients with LAPC is poor whichever treatment strategy is deployed and work is needed to improve patient outcomes. Recent advances in chemotherapy regimens, in particular the use of FOLFIRINOX chemotherapy, have demonstrated an improvement in OS in the metastatic setting and have also been shown to be beneficial to the LAPC cohort. A meta-analysis of outcomes in LAPC patients suggests a median OS of 24.2 months (95% CI 21.7-26.8) can now be achieved, although it should be noted that no phase 3 or randomised trials were available for this analysis (13). This raises the question as to whether the adoption of newer radiotherapy techniques such as stereotactic, dose escalated and adaptive radiotherapy can have a similar positive impact on patient outcomes particularly as with longer metastatic survival times, local control becomes more important.

1.3.2 Challenges of pancreatic radiotherapy

Similar to bladder cancer radiotherapy, the actual delivery of pancreatic radiotherapy has many challenges.

Firstly, one of the main difficulties in delivering radiotherapy to the pancreas is its close proximity to dose sensitive organs at risk (OARs), particularly the duodenum and stomach (see figure 1.2). Conventionally planned, single dose level radiotherapy, results in significant dose to OARs in order to maintain planning target volume (PTV) coverage. To avoid excessive toxicity, the dose which can be delivered to the PTV must therefore be limited with implications for the rates of local control. In the two most recent randomised controlled trials LAP 07(12) and SCALOP (59) which both utilised 3D conformal radiotherapy with planning margins in the region of 2cm superiorly/inferiorly and 1.5cm in other directions, gastrointestinal (GI) grade 3/4 toxicity rates were not insignificant at

23% and 12% respectively and while the use of intensity modulated radiotherapy (IMRT) and volumetric arc therapy (VMAT) may help reduce this to a degree, concern remains around attempting to increase dose using conventional margins and single dose level techniques.



Figure 1.2 Close proximity of GI OARs to target volume.

Left to right, radiotherapy planning scan with gross tumour volume outlined in red, duodenum in aqua, bowel in green, stomach in orange, liver in yellow and kidneys in blue. Middle image: addition of CTV (in yellow) and PTV (in pink) margins resulting in target extending into duodenum. Right image: isodose lines from VMAT plan (54Gy/30#) highlighting the inevitable high dose given to the duodenum in order to maintain PTV coverage.

Another important consideration is the impact of inter- and intra-fraction motion. Like other organs of the upper abdomen, the pancreas is subject to motion as a result of respiration and to a lesser extent the peristalsis of nearby organs. Although motion varies on an individual basis, typical average motion over a respiratory cycle is in the order of 17mm in the superior/inferior direction (60). This means that in order to avoid target miss, strategies to mitigate/accommodate this motion must be employed in radiotherapy planning and treatment. At a basic level, this can be achieved by using large population based CTV to PTV planning margins but this increases normal tissue irradiation and the potential for toxicity. Individualised margins which are typically smaller, can be achieved using the internal target volume (ITV) approach by mapping motion over a respiratory cycle using a 4DCT, but this still results in larger than desired treatment margins. Other strategies include physical reductions in respiratory motion such as breath-hold delivery techniques or abdominal compression devices. More recently, gated treatments have become available on some treatment platforms.

Finally, challenges in defining the pancreatic GTV should not be overlooked both at the contouring and treatment setup stage. A recent study comparing contours drawn on CT versus those drawn on MRI found comparable Dice coefficient scores of 0.73 and 0.72 respectively, suggesting that inter-observer variation is not insignificant (61). Exploring the use of MRI as an adjunct to contouring is therefore important. In addition, replacements for the cone beam CT which is often of poor quality in the abdomen should be sought to help improve set up accuracy.

1.3.3 Role of hypofractionated (including stereotactic) radiotherapy in locally advanced pancreatic cancer

A potential solution for the problem of close OAR proximity and overlapping treatment margins is the use of stereotactic body radiotherapy (SBRT). This involves the delivery of high dose, highly conformal radiotherapy to a well-defined tumour target. By deploying a rapid dose fall off at the target edge (by allowing higher doses to the centre of the target compared to conventional CRT), exposure to adjacent tissue and organs can be minimized with the potential for increased local control whilst maintaining acceptable toxicity (62). Strictly defined, SBRT refers to ablative fractionation regimens of 5 fractions or less although the same principles can be deployed with longer hypofractionation schedules (such as 6-15 fraction regimens) as long as high rates of conformality are still achieved (referred to in this thesis in the context of LAPC as hypofractionated treatments). Within the context of locally advanced pancreatic cancer, interest in SBRT is increasing. This is largely due to the fact that, conventional CRT appears to offer at best only a modest survival benefit with not insignificant toxicity. SBRT offers shorter treatment times which minimises the time off systemic treatment and improves patient convenience. The smaller treatment margins also have the potential for improved toxicity profiles if successfully combined with advanced radiotherapy techniques such as image guided radiotherapy and strict motion control.

A review of the literature shows a wide spectrum of stereotactic dose/fractionations in previous/current clinical use, the majority only assessed in the retrospective setting (58). With respect to *prospective* trials, summarised in

Table 1.3, modern SBRT techniques and fractionations (post 2010) show promise in providing well tolerated treatments with good rates of local control. However, while rates of toxicity might be improved compared to CRT, improvements in OS have been limited, with median OS in the region of 10.6-19 months (63-69). If the data from retrospective studies is also included, as done by Petrelli et al in their systematic review of 19 trials (including retrospective datasets), OS ranged from 5.7 to 47 months with a median of 17 months (70).

Table 1.3 Prospective SBRT trials of LAPC

Clinical Trial	Phase	Country	Patient cohort	Intervention	Outcomes
Quan et al 2018(63)	II	USA, single centre	N= 35, 16 LAPC/ 19 BRPC	Induction chemotherapy (Gem/Cap) if no progression then 36Gy/3# Surgical resection post SABR if feasible Chemotherapy post SABR allowed Radiotherapy BED ₁₀ = 79.2Gy	Combined 2-year LPFS: 44.9% (1 year result not reported) Median BRPC OS (estimated) : 28.3 months Median LAPC OS: 14.3 months Toxicity: no ≥G3 acute toxicity related to SBRT, no late toxicity Median follow up 15.4 months
Comito et al 2017(69)	II	Italy, single centre	N= 45 all LAPC	Pre and post SBRT chemotherapy allowed but not mandated 45Gy/6# Surgical resection post SBRT allowed (patients excluded from final	Median FFLP: 26 months 1 year FFLP: 87% Median OS from SBRT 13 months, from diagnosis 19 months Toxicity: no ≥G3 acute

				analysis N=3) Radiotherapy BED ₁₀ = 78.5Gy	or late toxicity Median follow up 13.5 months
Herman et al 2015(64)	II	USA, multiple centres	N= 49 all LAPC	3 doses of gemcitabine followed by 33Gy/5# then gemcitabine until progression (surgery allowed) Radiotherapy BED ₁₀ = 54.78Gy	FFLP at 1 year: 78% Median OS: 13.9 months Toxicity: acute and late GI ≥G2 toxicity: 2% and 11% respectively Median follow up 13.9 months
Gurka et al 2013(65)	I	USA, single centre	N= 11 (10 evaluable) all LAPC	6 cycles of full dose Gemcitabine in total, during week 4 received 25Gy/5# (elective nodal volume included) OGD to assess impact on duodenum at baseline, 2 and 6 months Radiotherapy BED ₁₀ = 37.5Gy	Overall local control: 60% FFLP at 1 year: 70% Median OS: 12.2 months Toxicity: no ≥G3 acute radiation related toxicity, no late GI toxicity
Tozzi et al 2013(66)	I	Italy, single centre	N= 30, 21 LAPC, 9 local recurrence post-surgery	Induction gemcitabine based chemotherapy 45Gy/6# (reduced to 36Gy/6# if dose constraints not met, N=5) Radiotherapy BED ₁₀ = 78.5Gy	Local Control: 86%11 months, 75% at 2 years Median OS from SBRT: 11 months Median OS from start of treatment: 14 months Toxicity: no ≥G3 acute or late radiation

					related toxicity
Schellenberg et al 2011(67)	II	USA, single centre	N=20 all LAPC	3 doses Gemcitabine followed by single 25Gy fraction, weekly Gemcitabine restarted after 2 weeks for 3-5 additional cycles Radiotherapy BED ₁₀ = 87.5Gy	FFLP: 94% at 1 year Median OS: 11.8 months Toxicity: no acute ≥G3 toxicity, 5% ≥G3 late toxicity
Polistina et al 2010(68)	I	Italy, single centre	N= 23 all LAPC	6 weeks Gemcitabine followed by 30Gy/3# then continuation of Gemcitabine Radiotherapy BED ₁₀ = 60Gy	Local control 82.6% at 3 months, 50% at 12 months Median OS: 10.6 months Toxicity: No acute or late ≥G3 GI toxicity Median follow up 9 months
Hoyer et al 2005(71)	II	Denmark, 2 centres	N= 22, 19 LAPC, 3 recurrence post-surgery	45Gy/3# (except 2 patients given 30Gy/3# and 45Gy/6#) Radiotherapy BED ₁₀ = 112.5Gy	Local control rate at 6 months: 57% Median OS: 5.4 months Toxicity: marked acute deterioration in performance status, increased nausea and increased pain 79% ≥G2 toxicity. High rates of drop out make late toxicity difficult to define

Koong et al 2005(72)	II	USA, single centre	N=19 all LAPC	Conventional CRT (45Gy/25# with 5FU) followed by stereotactic boost 25Gy single fraction Radiotherapy boost BED ₁₀ = 87.5Gy	Toxicity: ≥G3 acute GI 12.5%, late toxicity not reported FFLP: 94% Median OS: 8.3 months
---------------------------------	----	--------------------------	------------------	---	---

LPFS= local progression free survival, FFLP= freedom from local progression.

Table of prospective trials using SBRT for the treatment of LAPC, adapted from Palta et al (58) ASTRO Pancreatic Guideline Full Evidence Table. Palta et al performed a systematic review of pancreatic cancer SBRT trials (with ≥20 patients) published between May 2007-June 2017. Additional studies added as per table of prospective studies from Comito et al (57) and from Pubmed search carried out by me (January 2020, using search terms pancreatic cancer, stereotactic, SBRT, SABR, hypofractionated) to cover the time between June-2017-January 2020.

To date there have been no randomized control trials comparing SBRT to CRT (or indeed chemotherapy alone) and given SBRT's increasing use and appeal to patients in terms of shorter treatment times it is unlikely that a phase 3 trial directly comparing conventional dose CRT with SBRT ever will be performed. However, there is a likely appetite within the field for trials looking at the optimal dose and fractionation schedules for stereotactic treatments (and indeed other hypofractionated schedules) as currently there is no consensus on the best regimens to use to maximise patient outcomes. In particular the role of dose escalated treatment warrants further investigation as at present 'standard dose' SBRT does not offer much of a survival benefit over CRT.

1.3.4 Role of Dose Escalation in Locally Advanced Pancreatic Cancer

Conventionally fractionated regimens for LAPC such as those used in the SCALOP (50.4Gy/28#) and LAP 07 (54Gy/30#) trials have a biological equivalent dose (BED₁₀) of 59.47Gy and 63.72Gy respectively, calculated using the following formula:

$$BED = nd \left[1 + \frac{d}{\alpha/\beta} \right]$$

Where n is the number of fractions, d is the dose per fraction and α/β for tumour is 10.

The SBRT dose used in Herman et al's (64) phase II multi-institutional study (the most commonly adopted SBRT fractionation at present) of 33Gy/5# gives a BED₁₀ of 54.78 Gy, and although this does not include the potential benefit of reduced time factor, the similarity in BED₁₀ may explain why this type of SBRT has failed to show a survival benefit over contemporary CRT trials (such as LAP 07 and SCALOP). Perhaps the doses being given are not high enough to impact on survival?

In 2016, a retrospective review published by MD Anderson Cancer Centre of 200 patients suggested that increasing the dose delivered to the tumour GTV above standard levels to a BED₁₀ of >70Gy could lead to an improvement in OS compared to non-escalated treatment. For the 47 patients selected for dose-escalation, 2 year OS was 36% versus 19% in the non-escalated group, while median survival was increased to 17.8 months versus 15 months ($p=0.03$) figure 1.3 (73). In order to achieve this degree of dose escalation without excessive toxicity, the team used IMRT with a two dose level or simultaneous integrated boost technique to dose escalate the GTV whilst maintaining a lower dose to a larger planning target volume (PTV). Exact fractionation schedules were tailored to the patient's anatomy (ranging between 50-70.4Gy/ 5-39#) and OAR constraints were given planning priority. Only those patients with favourable anatomy (tumours >1cm from GI OARs) were eligible for dose escalation. Patients were generally treated in breath-hold with daily CT-on-rails or cone-beam CT for position verification. Dose escalation in this manner appeared to not only improve survival but as a follow up paper suggests (74) it is also well tolerated with rates of toxicity below that of a comparable non-dose escalated cohort.

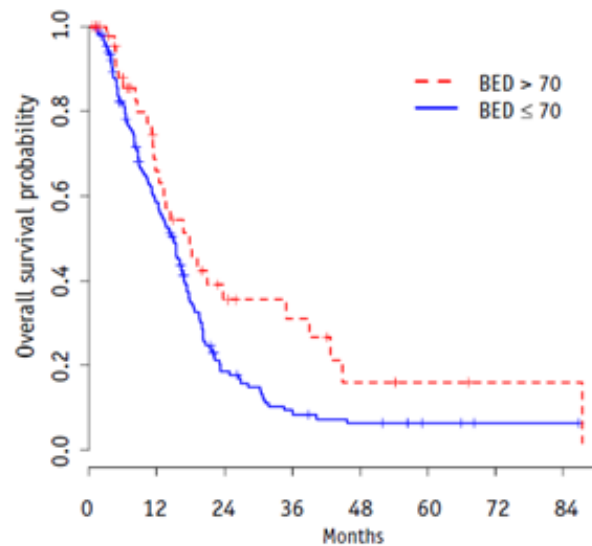


Figure 1.3 Kaplan Meier plot from Krishnan et al (73)

A similar dose-response relationship has also been suggested by Chung et al (75), who found that (based on a retrospective analysis) total dose (EQD2 <61Gy vs ≥ 61 Gy, cut off equivalent to BED₁₀ of 73.2Gy) was statistically significant for survival benefit, HR 0.47 (0.28-0.79) (75). As in the MD Anderson study, IMRT was used in all dose-escalated patients. Patients were planned so that 99% of the GTV received at least 95% of the prescription dose and again strict OAR dose constraints were maintained.

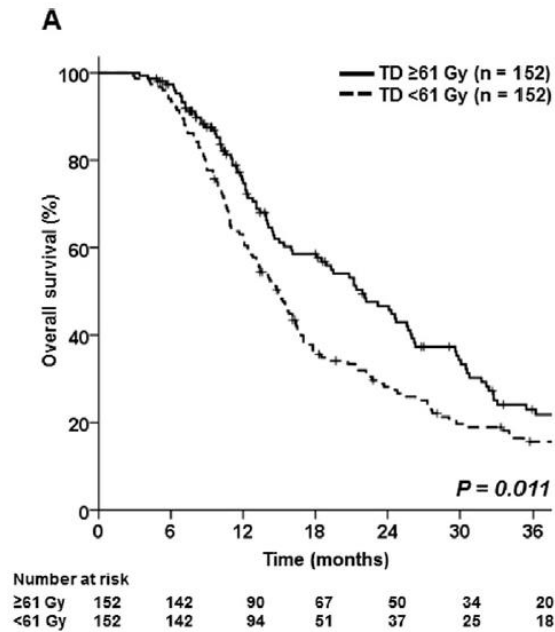


Figure 1.4 Kaplan Meier plot from Chung et al (75)

In addition, a National Cancer Database study by Ma et al (76) suggests a benefit of dose escalation above standard doses, with those receiving an EQD2 of ≥ 55 Gy and receiving induction chemotherapy having an OS benefit compared to those receiving <55Gy, HR 0.77 (0.64-0.95). Indeed, biophysical modelling by Moraru et al looking at the dose response curve for locally advanced pancreatic cancer would suggest that response rates continue to improve with higher doses (i.e. BED₁₀ of >90Gy) (77), although they note the lack of safety data available for these levels of dose escalation.

For the vast majority of patients with LAPC, due to the close proximity of dose-sensitive OARs, safe dose escalation of this kind is a real technical challenge and is not possible using standard techniques. Indeed, in the MD Anderson cohort only those patients whose tumour was >1cm from a hollow GI OAR were considered for dose escalation.

It should also be noted that the BED₁₀ cut off of > 70Gy assumes an alpha/beta ratio for pancreatic cancer of 10. This is the value which has been historically used for rapidly dividing tumours but the exact alpha/beta for pancreatic cancer

is not known and data is limited. When performing a review of the literature I was able to find only one publication, published in abstract form, which estimated the α/β ratio for locally advanced pancreatic cancer to be 9.5 (78). If the value is lower than this then dose escalation may have a greater effect on the biologically effective dose received, however, if in fact it is higher then the biological effective dose increase of dose escalation will be less.

It is also likely that any benefit of dose escalation will not be equal for all patients. The challenge will therefore be selecting those that are most likely to benefit. It is understood that many with LAPC actually have occult metastatic disease at presentation and as a result, if fit enough, patients are commonly offered upfront chemotherapy in the first instance followed by radiotherapy if their disease remains localised. Despite this 'trial of biology' the majority still go on to develop metastatic disease after a relatively short time period and die from distant metastatic progression. For these patients focus would be better spent on optimisation of systemic treatment in the first instance as least until their local disease becomes a more pressing issue.

However, one third of LAPC patients will go on to die from predominantly local disease (43). It is this group of patients who are therefore most likely to benefit from the improvements in local control offered by dose escalation. Unfortunately, identification of these differing subgroups at the time of diagnosis is challenging and prognostic and predictive biomarkers of response are needed to help personalize treatment decisions. The current interest in dose escalation studies offers an excellent opportunity to incorporate biomarker identification into study design. The role of genetic biomarkers in prognosis and treatment response prediction is currently being examined by the Precision Panc umbrella study (NCT04161417) which aims to improve pancreatic cancer outcomes by tailoring treatment based on genomic analysis of individual patients and their tumours. If gene signatures which predict for predominantly localised disease can be identified, then it may be possible to study the effects of dose escalation in this group as well as the wider LAPC population.

Similarly, if genetic analysis and tailored drug treatments can push more LAPC patients away from developing metastatic disease, ablation of the primary site may have a greater impact on overall survival. Ensuring the patients have access to personalised systemic therapy if available is therefore important. Finally, advances in imaging technology may make identification of occult disease at diagnosis more accurate and the development of novel imaging biomarkers may help identify those most likely to respond to radiotherapy or where dose escalation would be of benefit.

1.4 Magnetic resonance guided online adaptive radiotherapy

Adaptive radiotherapy (ART) refers to a group of techniques which enable adjustment of radiotherapy treatment plans based on changes occurring to the target volume or OARs during the treatment pathway. Variation in target and OAR shape/position during and between fractions is recognised as a potential cause of target miss and increased treatment toxicity. Historically it has mandated wide treatment margins and limited the potential for dose escalation. ART aims to compensate for these deformations with the ultimate goal of improved treatment accuracy enabling smaller treatment margins, optimal dose to the target volume and avoidance of healthy structures. Clinically this should lead to improved patient outcomes with better tumour control rates and minimal toxicity.

In its simpler forms (for example couch shifts), ART has been used in clinical practice for some time. More recently, techniques such as the 'library of plans' approach have also been used, particularly in the pelvis. However, with improvements in computing power and technology, more advanced forms of ART such as online adaptive replanning are now becoming a clinical reality.

Online adaptive replanning (see Figure 1.5) enables a patient's radiotherapy plan to be re-optimised at each fraction based on the anatomy of the day. This adaption means that inter-fraction size, shape and position changes, to both the target and organs at risk can be accounted for and a new re-optimised plan produced on a daily basis. Theoretically, this should lead to better target coverage and reduced normal tissue irradiation. In the online workflow, re-contouring and replanning takes place while the patient remains on the treatment couch.

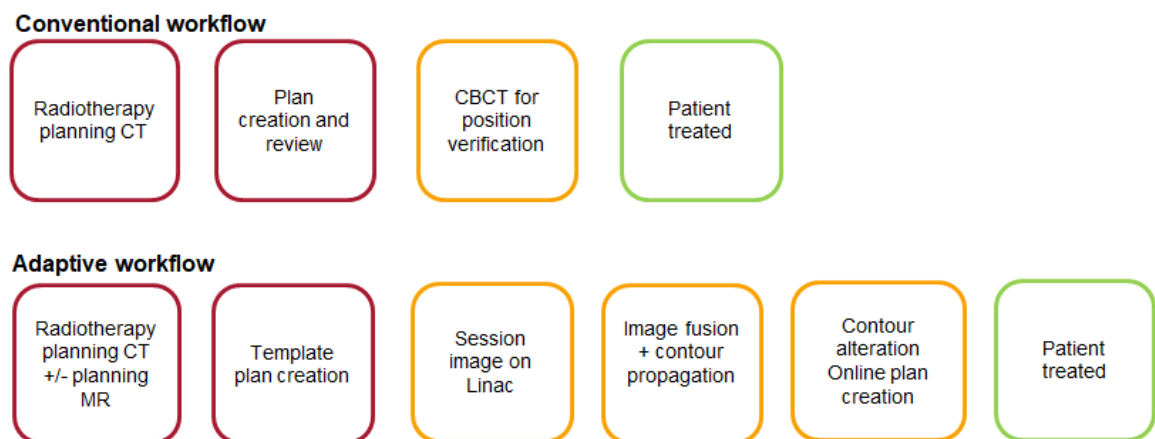


Figure 1.5 Online adaptive workflow

At the heart of this adaptive strategy is high quality, online imaging. Images need to be acquired quickly, with high geometric and temporal accuracy. They must have good soft tissue contrast, cause minimal side effects to the patient and ideally they should be able to detect anatomical and functional changes which occur both between and during a treatment fraction. Compared to x-ray based imaging, MR offers superior soft tissue definition with no associated ionising radiation risk (79). It has been shown to improve inter and intra observer contouring variation (80) and to reduce target volumes (81) in some tumour sites. The development of ‘functional’ imaging sequences also holds promise, enabling adaptation of treatment based on an individual’s differential response to treatment (82, 83). Traditionally, MR’s role had been limited by technical difficulties in integrating a MR scanner with a radiotherapy delivery system. However, this problem has now been overcome with integrated platforms such as the MRIdian platform (ViewRay Inc., Oakwood Village, OH) and the Elekta Unity (Elekta AB, Stockholm, Sweden) now available for commercial use (84).

1.4.1 MR guided online adaptation for LAPC and MIBC

MR guided online adaptive replanning encompasses various techniques whereby a patient’s plan is re-optimised based upon information provided by daily online MR imaging. In order to be successful, this necessitates the bringing together of MR image guidance, plan evaluation, plan re-optimisation and quality assurance all while the patient is on the treatment couch(85). Although still in its relative

infancy, this form of treatment has now been shown to be not only feasible but crucially dosimetrically beneficial in certain tumour sites (85-88). Acharya et al (85) using the MRIdian platform have demonstrated that their MR guided replanning protocol with gated motion management in various abdominal sites resulted in 30.6% (52/170) of eligible fractions being re-optimised with 54.1% of fractions benefitting from an online adapted or previously adapted plan. Similarly, a phase 1 trial of stereotactic radiotherapy for abdominal tumours which utilised online adaptive replanning, found the technique to be feasible and potentially dosimetrically beneficial with increased PTV coverage in 64/97 fractions. Dose escalated was possible in 20/97 fractions and had a reduction in OAR violations was seen in 61/97 fractions compared to a standard treatment (89). In the setting of LAPC, use of MR guided treatments to facilitate dose escalation has been used by Rudra et al (90). In their multi-institutional, retrospective series, 44 patients with LAPC were treated using MR guided radiotherapy using the MRIdian device. Various dose/fractionation schedules were used, with patients receiving 15 fractions or less undergoing online adaptation. These adaptive plans used 5mm margins and prioritised strict OAR constraints over PTV coverage. On days of 'good' anatomy, dose escalation to the PTV (above the prescription dose) was permitted. Similar to Krishnan et al, they found that those with dose escalation above a BED₁₀ of 70 (N= 24) appeared to have a 2 year survival advantage over others treated to a lower dose (2-year OS (49% vs 30% p =0.03)). Their work is now being extended to a phase II multi-institutional trial (NCT03621644) using prescription of 50Gy in 5 fractions.

Within the pelvis where variations in bladder and rectal filling along with uterine movements can cause significant inter-fraction variations, the potential dosimetric benefit of MR guided adaptive replanning in bladder cancer patients undergoing hypofractionated treatment has also been shown in a planning study (91). By performing adaptive replanning, the PTV volume could be reduced by the initial bladder volume plus an additional 170cc compared to the volume treated using a plan selection technique (when a library of 3 plans is assessed and the best fitting plan selected), this was achieved whilst maintaining target coverage. In this often frail patient cohort, PTV reduction and hence OAR sparing is an attractive proposal and opens up the potential for more accurate dose escalation. It should

be noted however, that the intra-fraction planning margins used in this study were only 5mm, in clinical reality these may need to be extended due to the duration of an MR guided fraction, which will be discussed in further detail in subsequent chapters.

Based on the above, it would appear that MR-guided adaptive radiotherapy offers exciting potential benefits. However as with any new technology, robust preclinical and early-stage workflow studies are needed to achieve this potential (92). In addition, it is important to note the differences in the 2 commercially available MR Linacs which mean that workflows which are suitable for one device are not compatible with the other. This is particularly important in the case of LAPC where differences in device capabilities such as the availability of treatment gating, mean that it is not possible to take the exact workflows developed by the MRIdian teams and convert them to the Elekta Unity.

1.5 The Elekta Unity MR Linac



Figure 1.6 The Elekta Unity

The Elekta Unity (Elekta AB, Stockholm, Sweden) is a new radiotherapy treatment platform combining a modern linear accelerator with a 1.5T MR

scanner. The Royal Marsden is currently one of two NHS centres in the UK with this device and, in collaboration with The Institute of Cancer Research, it is one of the founding members of the Elekta MR Linac Consortium, which aims to facilitate the evidence based introduction of this technology into clinical practice (92, 93). Compared to ViewRay's MRIdian, it has been in clinical use for a shorter period of time, with the first clinical use occurring in May 2017 at The University Medical Centre Utrecht.

At the start of my thesis (in January 2018) the Elekta Unity was not yet in clinical use in the UK although its potential to deliver significant gains to patients had been much discussed (84, 94, 95). This represented an excellent opportunity for me to be at the forefront of a cutting-edge technology. However, in order to deliver safe and effective treatment, we needed to think carefully about the potential challenges of this new type of treatment delivery. For example, to maximise the benefit of MR guidance and plan adaptation, it is important to ensure that inter-observer contouring variability on MR has been assessed and optimised. The quality of images produced by the MR Linac must be assessed and their suitability for use in treatment established. Equally, in order to develop appropriate workflows, knowledge of inter- and intra-fraction variability is essential in informing the need/benefit of daily adaptation, the size of intra-fraction (PTV) margins and the optimal advanced motion management strategies. Finally, practical matters concerning the delivery of treatment on the MR Linac need to be considered, such as capacity and work force limitations. The focus of this thesis is therefore finding solutions to some of these challenges to enable Elekta Unity MR-guided adaptive radiotherapy for bladder and pancreatic cancer to become a clinical reality.

1.6 Key issues to be addressed in this thesis- with reference to relevant chapters

1.6.1 MR based contouring assessment and MR sequence development.

Online target and/or OAR re-contouring on MR images is a requirement of the online MR guided adaptive radiotherapy workflow. To undertake this task, clinicians need to correctly interpret MR images and have access to MR Linac images of sufficient clarity to enable key structure visualisation.

In bladder cancer, unlike in other pelvic tumour sites (96), there is no consensus guidance for the use of MR in the radiotherapy pathway. Consensus is important to help minimise inter-observer contouring variation, which can impact on trial outcomes (97). Therefore, I aimed to establish the current inter-observer variability in target delineation using MR and, with the help of participating clinicians, I developed consensus guidance on its use. This work will be discussed in Chapter 2.

For pancreatic cancer, I focused on MR sequence development in both the online and offline setting. This was because, unlike in MIBC, the sequences provided by Elekta were felt to be suboptimal for use within a fully adaptive workflow due to poor visualisation of key structures. This development work will be discussed in Chapter 5.

1.6.2 Management of intra-fraction motion

The Elekta Unity can perform online adaptive replanning enabling a re-optimised plan to be created for each fraction. However, this procedure takes time, ~ 40 minutes from the patient having their initial online scan to the completion of treatment. As a result, while this online adaptive replanning diminishes the impact of inter-fraction motion, intra-fraction motion becomes a more pressing issue.

For bladder cancer patients, whilst replanning is taking place, intra-fraction bladder filling will occur. There are several studies looking at intra-fraction bladder filling (31, 98-102) however, the majority of these record filling over a shorter time period and are therefore of limited use in this scenario. For the study which did report filling over a 28 minute time period (100), the impact of this filling on plan coverage was not assessed. Using scans already obtained from a previous institutional study I have therefore modelled the impact on filling on plan coverage using different margins in order to determine the most appropriate intra-fraction margin to use in our online workflow. I have also assessed the need for bowel re-contouring during online adaption. Both these pieces of work will be discussed in Chapter 3.

In pancreatic cancer, respiratory motion results in target motion of between 5-15mm (103). This motion necessitates the use of larger treatment margins and

impacts on MR image clarity. Abdominal compression can be used to try to reduce this motion but the integration and practicalities of compression within a MR guided radiotherapy workflow needs to be carefully considered. This work is discussed in Chapter 6.

1.6.3 Development of hypofractionated workflows and protocols

Due to workflow constraints, it is not practical to treat patients using standard fractionation regimens on the MR Linac, instead hypofractionated regimens are needed. For MIBC, hypofractionated treatment (36Gy in 6 fractions) is an accepted regimen for patients not fit enough to tolerate standard length protocols(104). This patient group was therefore selected as the initial cohort for treatment on the MR Linac as a way of building our experience of this new technology. In Chapter 4 I will discuss our experience of treating the first 5 MIBC patients on the Elekta Unity Linac.

In comparison, at the start of my thesis, there were no NHS commissioned hypofractionated regimens in use for LAPC patients. Although the ultimate goal will be to offer a hypofractionated dose escalated treatment (i.e. BED₁₀ >70Gy) on the MR Linac, for safety reasons we felt it was prudent to start with a non dose escalated regimen. As a result, I have developed a non-dose escalated hypofractionated protocol using 45Gy/15#. The rationale and details for this will be discussed further in Chapter 7.

1.7 References

1. CRUK. <https://www.cancerresearchuk.org/health-professional/cancer-statistics/statistics-by-cancer-type/bladder-cancer>. Accessed December 2018.
2. Miyazaki J, Nishiyama H. Epidemiology of urothelial carcinoma. International journal of urology : official journal of the Japanese Urological Association. 2017;24(10):730-4.
3. Ploussard G, Daneshmand S, Efstathiou JA, Herr HW, James ND, Rodel CM, et al. Critical analysis of bladder sparing with trimodal therapy in muscle-invasive bladder cancer: a systematic review. European urology. 2014;66(1):120-37.

4. NICE. Bladder cancer: diagnosis and management. <https://www.nice.org.uk/guidance/ng2> Accessed December 2018.
5. Alfred Witjes J, Lebre T, Comperat EM, Cowan NC, De Santis M, Bruins HM, et al. Updated 2016 EAU Guidelines on Muscle-invasive and Metastatic Bladder Cancer. *European urology*. 2017;71(3):462-75.
6. Hindson BR, Turner SL, Millar JL, Foroudi F, Gogna NK, Skala M, et al. Australian & New Zealand Faculty of Radiation Oncology Genito-Urinary Group: 2011 consensus guidelines for curative radiotherapy for urothelial carcinoma of the bladder. *Journal of medical imaging and radiation oncology*. 2012;56(1):18-30.
7. Spiess PE, Agarwal N, Bangs R, Boorjian SA, Buyyounouski MK, Clark PE, et al. Bladder Cancer, Version 5.2017, NCCN Clinical Practice Guidelines in Oncology. *Journal of the National Comprehensive Cancer Network : JNCCN*. 2017;15(10):1240-67.
8. Kulkarni GS, Hermanns T, Wei Y, Bhindi B, Satkunasivam R, Athanasopoulos P, et al. Propensity Score Analysis of Radical Cystectomy Versus Bladder-Sparing Trimodal Therapy in the Setting of a Multidisciplinary Bladder Cancer Clinic. *Journal of clinical oncology : official journal of the American Society of Clinical Oncology*. 2017;35(20):2299-305.
9. CRUK. <https://www.cancerresearchuk.org/health-professional/cancer-statistics/statistics-by-cancer-type/pancreatic-cancer>. Accessed December 2018.
10. Hidalgo M. Pancreatic Cancer. *New England Journal of Medicine*. 2010;362(17):1605-17.
11. NICE. Pancreatic cancer in adults: diagnosis and management. <https://www.nice.org.uk/guidance/ng85/evidence/full-guideline-pdf-170091398525> Accessed December 2018.
12. Hammel P, Huguet F, van Laethem JL, Goldstein D, Glimelius B, Artru P, et al. Effect of Chemoradiotherapy vs Chemotherapy on Survival in Patients With Locally Advanced Pancreatic Cancer Controlled After 4 Months of Gemcitabine With or Without Erlotinib: The LAP07 Randomized Clinical Trial. *Jama*. 2016;315(17):1844-53.
13. Suker M, Beumer BR, Sadot E, Marthey L, Faris JE, Mellon EA, et al. FOLFIRINOX for locally advanced pancreatic cancer: a systematic review and patient-level meta-analysis. *The Lancet Oncology*. 2016;17(6):801-10.
14. Boustead GB, Fowler S, Swamy R, Kocklebergh R, Hounscome L. Stage, grade and pathological characteristics of bladder cancer in the UK: British Association of Urological Surgeons (BAUS) urological tumour registry. *BJU international*. 2014;113(6):924-30.
15. Bochner BH, Dalbagni G, Sjoberg DD, Silberstein J, Keren Paz GE, Donat SM, et al. Comparing Open Radical Cystectomy and Robot-assisted Laparoscopic Radical Cystectomy: A Randomized Clinical Trial. *European urology*. 2015;67(6):1042-50.
16. James ND, Hussain SA, Hall E, Jenkins P, Tremlett J, Rawlings C, et al. Radiotherapy with or without chemotherapy in muscle-invasive bladder cancer. *The New England journal of medicine*. 2012;366(16):1477-88.
17. Hoskin PJ, Rojas AM, Bentzen SM, Saunders MI. Radiotherapy with concurrent carbogen and nicotinamide in bladder carcinoma. *Journal of clinical oncology : official journal of the American Society of Clinical Oncology*. 2010;28(33):4912-8.

18. Huddart RA, Birtle A, Maynard L, Beresford M, Blazeby J, Donovan J, et al. Clinical and patient-reported outcomes of SPARE - a randomised feasibility study of selective bladder preservation versus radical cystectomy. *BJU international*. 2017;120(5):639-50.
19. Ritch CR, Balise R, Prakash NS, Alonzo D, Almengo K, Alameddine M, et al. Propensity matched comparative analysis of survival following chemoradiation or radical cystectomy for muscle-invasive bladder cancer. *BJU international*. 2018;121(5):745-51.
20. Cahn DB, Handorf EA, Ghiraldi EM, Ristau BT, Geynisman DM, Churilla TM, et al. Contemporary use trends and survival outcomes in patients undergoing radical cystectomy or bladder-preservation therapy for muscle-invasive bladder cancer. *Cancer*. 2017;123(22):4337-45.
21. Seisen T, Sun M, Lipsitz SR, Abdollah F, Leow JJ, Menon M, et al. Comparative Effectiveness of Trimodal Therapy Versus Radical Cystectomy for Localized Muscle-invasive Urothelial Carcinoma of the Bladder. *European urology*. 2017;72(4):483-7.
22. Mak RH, Hunt D, Shipley WU, Efstathiou JA, Tester WJ, Hagan MP, et al. Long-term outcomes in patients with muscle-invasive bladder cancer after selective bladder-preserving combined-modality therapy: a pooled analysis of Radiation Therapy Oncology Group protocols 8802, 8903, 9506, 9706, 9906, and 0233. *Journal of clinical oncology : official journal of the American Society of Clinical Oncology*. 2014;32(34):3801-9.
23. Fahmy O, Khairul-Asri MG, Schubert T, Renninger M, Malek R, Kubler H, et al. A systematic review and meta-analysis on the oncological long-term outcomes after trimodality therapy and radical cystectomy with or without neoadjuvant chemotherapy for muscle-invasive bladder cancer. *Urologic oncology*. 2018;36(2):43-53.
24. Giacalone NJ, Shipley WU, Clayman RH, Niemierko A, Drumm M, Heney NM, et al. Long-term Outcomes After Bladder-preserving Tri-modality Therapy for Patients with Muscle-invasive Bladder Cancer: An Updated Analysis of the Massachusetts General Hospital Experience. *European urology*. 2017;71(6):952-60.
25. Efstathiou JA, Bae K, Shipley WU, Kaufman DS, Hagan MP, Heney NM, et al. Late pelvic toxicity after bladder-sparing therapy in patients with invasive bladder cancer: RTOG 89-03, 95-06, 97-06, 99-06. *Journal of clinical oncology : official journal of the American Society of Clinical Oncology*. 2009;27(25):4055-61.
26. Mak KS, Smith AB, Eidelman A, Clayman R, Niemierko A, Cheng JS, et al. Quality of Life in Long-term Survivors of Muscle-Invasive Bladder Cancer. *International journal of radiation oncology, biology, physics*. 2016;96(5):1028-36.
27. Hafeez S, McDonald F, Lalondrelle S, McNair H, Warren-Oseni K, Jones K, et al. Clinical Outcomes of Image Guided Adaptive Hypofractionated Weekly Radiation Therapy for Bladder Cancer in Patients Unsuitable for Radical Treatment. *International journal of radiation oncology, biology, physics*. 2017;98(1):115-22.
28. Huddart R, Hafeez S, Lewis R, McNair H, Syndikus I, Henry A, et al. Clinical Outcomes of a Randomized Trial of Adaptive Plan-of-the-Day Treatment in Patients Receiving Ultra-hypofractionated Weekly Radiation Therapy for Bladder Cancer. *International journal of radiation oncology, biology, physics*. 2021;110(2):412-24.

29. Muren LP, Smaaland R, Dahl O. Organ motion, set-up variation and treatment margins in radical radiotherapy of urinary bladder cancer. *Radiotherapy and oncology : journal of the European Society for Therapeutic Radiology and Oncology*. 2003;69(3):291-304.
30. Pos FJ, Koedooder K, Hulshof MC, van Tienhoven G, Gonzalez Gonzalez D. Influence of bladder and rectal volume on spatial variability of a bladder tumor during radical radiotherapy. *International journal of radiation oncology, biology, physics*. 2003;55(3):835-41.
31. Dees-Ribbers HM, Betgen A, Pos FJ, Witteveen T, Remeijer P, van Herk M. Inter- and intra-fractional bladder motion during radiotherapy for bladder cancer: a comparison of full and empty bladders. *Radiotherapy and oncology : journal of the European Society for Therapeutic Radiology and Oncology*. 2014;113(2):254-9.
32. Vestergaard A, Sondergaard J, Petersen JB, Hoyer M, Muren LP. A comparison of three different adaptive strategies in image-guided radiotherapy of bladder cancer. *Acta oncologica (Stockholm, Sweden)*. 2010;49(7):1069-76.
33. Lalondrelle S, Huddart R, Warren-Oseni K, Hansen VN, McNair H, Thomas K, et al. Adaptive-Predictive Organ Localization Using Cone-Beam Computed Tomography for Improved Accuracy in External Beam Radiotherapy for Bladder Cancer. *International Journal of Radiation Oncology*Biography*Physics*. 2011;79(3):705-12.
34. McDonald F, Lalondrelle S, Taylor H, Warren-Oseni K, Khoo V, McNair HA, et al. Clinical implementation of adaptive hypofractionated bladder radiotherapy for improvement in normal tissue irradiation. *Clinical oncology (Royal College of Radiologists (Great Britain))*. 2013;25(9):549-56.
35. Burrige N, Amer A, Marchant T, Sykes J, Stratford J, Henry A, et al. Online adaptive radiotherapy of the bladder: small bowel irradiated-volume reduction. *International journal of radiation oncology, biology, physics*. 2006;66(3):892-7.
36. Vestergaard A, Muren LP, Lindberg H, Jakobsen KL, Petersen JB, Elstrom UV, et al. Normal tissue sparing in a phase II trial on daily adaptive plan selection in radiotherapy for urinary bladder cancer. *Acta oncologica (Stockholm, Sweden)*. 2014;53(8):997-1004.
37. Varughese M, Treece S, Drinkwater KJ. Radiotherapy Management of Muscle Invasive Bladder Cancer: Evaluation of a National Cohort. *Clinical oncology (Royal College of Radiologists (Great Britain))*. 2019;31(9):637-45.
38. Zietman AL, Grocela J, Zehr E, Kaufman DS, Young RH, Althausen AF, et al. Selective bladder conservation using transurethral resection, chemotherapy, and radiation: management and consequences of Ta, T1, and Tis recurrence within the retained bladder. *Urology*. 2001;58(3):380-5.
39. Majewski W, Maciejewski B, Majewski S, Suwinski R, Miszczyk L, Tarnawski R. Clinical radiobiology of stage T2-T3 bladder cancer. *International journal of radiation oncology, biology, physics*. 2004;60(1):60-70.
40. Hafeez S, Warren-Oseni K, McNair HA, Hansen VN, Jones K, Tan M, et al. Prospective Study Delivering Simultaneous Integrated High-dose Tumor Boost (≤ 70 Gy) With Image Guided Adaptive Radiation Therapy for Radical Treatment of Localized Muscle-Invasive Bladder Cancer. *International journal of radiation oncology, biology, physics*. 2016;94(5):1022-30.
41. Pos F, Moonen L. Brachytherapy in the treatment of invasive bladder cancer. *Seminars in radiation oncology*. 2005;15(1):49-54.

42. Pos FJ, Hart G, Schneider C, Sminia P. Radical radiotherapy for invasive bladder cancer: What dose and fractionation schedule to choose? *International journal of radiation oncology, biology, physics*. 2006;64(4):1168-73.
43. van Leeuwen CM, Oei AL, Crezee J, Bel A, Franken NAP, Stalpers LJA, et al. The alfa and beta of tumours: a review of parameters of the linear-quadratic model, derived from clinical radiotherapy studies. *Radiation oncology (London, England)*. 2018;13(1):96.
44. Choudhury A, Porta N, Hall E, Song YP, Owen R, MacKay R, et al. Hypofractionated radiotherapy in locally advanced bladder cancer: an individual patient data meta-analysis of the BC2001 and BCON trials. *The Lancet Oncology*. 2021;22(2):246-55.
45. Song YP, McWilliam A, Hoskin PJ, Choudhury A. Organ preservation in bladder cancer: an opportunity for truly personalized treatment. *Nature reviews Urology*. 2019;16(9):511-22.
46. Yoshida S, Koga F, Kobayashi S, Ishii C, Tanaka H, Tanaka H, et al. Role of diffusion-weighted magnetic resonance imaging in predicting sensitivity to chemoradiotherapy in muscle-invasive bladder cancer. *International journal of radiation oncology, biology, physics*. 2012;83(1):e21-7.
47. Hafeez S, Koh M, Jones K, El Ghzal A, D'Arcy J, Kumar P, et al. Assessing Bladder Radiotherapy Response With Quantitative Diffusion-Weighted Magnetic Resonance Imaging Analysis. *Clinical oncology (Royal College of Radiologists (Great Britain))*. 2022.
48. O'Connor JPB, Robinson SP, Waterton JC. Imaging tumour hypoxia with oxygen-enhanced MRI and BOLD MRI. *The British journal of radiology*. 2019;92(1095):20180642.
49. Woo S, Suh CH, Kim SY, Cho JY, Kim SH. Diagnostic performance of MRI for prediction of muscle-invasiveness of bladder cancer: A systematic review and meta-analysis. *European journal of radiology*. 2017;95:46-55.
50. Gandhi N, Krishna S, Booth CM, Breau RH, Flood TA, Morgan SC, et al. Diagnostic accuracy of magnetic resonance imaging for tumour staging of bladder cancer: systematic review and meta-analysis. *BJU international*. 2018;122(5):744-53.
51. Huang L, Kong Q, Liu Z, Wang J, Kang Z, Zhu Y. The Diagnostic Value of MR Imaging in Differentiating T Staging of Bladder Cancer: A Meta-Analysis. *Radiology*. 2018;286(2):502-11.
52. Katz MH, Marsh R, Herman JM, Shi Q, Collison E, Venook AP, et al. Borderline resectable pancreatic cancer: need for standardization and methods for optimal clinical trial design. *Annals of surgical oncology*. 2013;20(8):2787-95.
53. Versteijne E, Suker M, Punt CJA, Groothuis KB, Beukema JC, Bruynzeel A, et al. Preoperative Chemoradiotherapy Potentially Improves Outcome for (Borderline) Resectable Pancreatic Cancer: Preliminary Results of the Dutch Randomized Phase III PREOPANC Trial. *International Journal of Radiation Oncology • Biology • Physics*. 2018;102(5):1606-7.
54. Tempero MA, Malafa MP, Al-Hawary M, Asbun H, Bain A, Behrman SW, et al. Pancreatic Adenocarcinoma, Version 2.2017, NCCN Clinical Practice Guidelines in Oncology. *Journal of the National Comprehensive Cancer Network : JNCCN*. 2017;15(8):1028-61.
55. Iacobuzio-Donahue CA, Fu B, Yachida S, Luo M, Abe H, Henderson CM, et al. DPC4 gene status of the primary carcinoma correlates with patterns of failure in patients with pancreatic cancer. *Journal of clinical oncology : official journal of the American Society of Clinical Oncology*. 2009;27(11):1806-13.

56. Chauffert B, Mornex F, Bonnetain F, Rougier P, Mariette C, Bouche O, et al. Phase III trial comparing intensive induction chemoradiotherapy (60 Gy, infusional 5-FU and intermittent cisplatin) followed by maintenance gemcitabine with gemcitabine alone for locally advanced unresectable pancreatic cancer. Definitive results of the 2000-01 FFCD/SFRO study. *Annals of oncology : official journal of the European Society for Medical Oncology*. 2008;19(9):1592-9.
57. Loehrer PJ, Sr., Feng Y, Cardenes H, Wagner L, Brell JM, Cella D, et al. Gemcitabine alone versus gemcitabine plus radiotherapy in patients with locally advanced pancreatic cancer: an Eastern Cooperative Oncology Group trial. *Journal of clinical oncology : official journal of the American Society of Clinical Oncology*. 2011;29(31):4105-12.
58. Palta M, Godfrey D, Goodman KA, Hoffe S, Dawson LA, Dessert D, et al. Radiation Therapy for Pancreatic Cancer: Executive Summary of an ASTRO Clinical Practice Guideline. *Practical radiation oncology*. 2019;9(5):322-32.
59. Mukherjee S, Hurt CN, Bridgewater J, Falk S, Cummins S, Wasan H, et al. Gemcitabine-based or capecitabine-based chemoradiotherapy for locally advanced pancreatic cancer (SCALOP): a multicentre, randomised, phase 2 trial. *The Lancet Oncology*. 2013;14(4):317-26.
60. Fujimoto K, Shiinoki T, Yuasa Y, Onizuka R, Yamane M. Evaluation of the effects of motion mitigation strategies on respiration-induced motion in each pancreatic region using cine-magnetic resonance imaging. *Journal of applied clinical medical physics*. 2019;20(9):42-50.
61. Hall WA, Heerkens HD, Paulson ES, Meijer GJ, Kotte AN, Knechtges P, et al. Pancreatic gross tumor volume contouring on computed tomography (CT) compared with magnetic resonance imaging (MRI): Results of an international contouring conference. *Practical radiation oncology*. 2018;8(2):107-15.
62. Tree AC, Khoo VS, Eeles RA, Ahmed M, Dearnaley DP, Hawkins MA, et al. Stereotactic body radiotherapy for oligometastases. *The Lancet Oncology*. 2013;14(1):e28-37.
63. Quan K, Sutera P, Xu K, Bernard ME, Burton SA, Wegner RE, et al. Results of a prospective phase 2 clinical trial of induction gemcitabine/capecitabine followed by stereotactic ablative radiation therapy in borderline resectable or locally advanced pancreatic adenocarcinoma. *Practical radiation oncology*. 2018;8(2):95-106.
64. Herman JM, Chang DT, Goodman KA, Dholakia AS, Raman SP, Hacker-Prietz A, et al. Phase 2 multi-institutional trial evaluating gemcitabine and stereotactic body radiotherapy for patients with locally advanced unresectable pancreatic adenocarcinoma. *Cancer*. 2015;121(7):1128-37.
65. Gurka MK, Collins SP, Slack R, Tse G, Charabaty A, Ley L, et al. Stereotactic body radiation therapy with concurrent full-dose gemcitabine for locally advanced pancreatic cancer: a pilot trial demonstrating safety. *Radiation oncology (London, England)*. 2013;8:44.
66. Tozzi A, Comito T, Alongi F, Navarria P, Iftode C, Mancosu P, et al. SBRT in unresectable advanced pancreatic cancer: preliminary results of a mono-institutional experience. *Radiation oncology (London, England)*. 2013;8:148.
67. Schellenberg D, Kim J, Christman-Skieller C, Chun CL, Columbo LA, Ford JM, et al. Single-fraction stereotactic body radiation therapy and sequential gemcitabine for the treatment of locally advanced pancreatic cancer. *International journal of radiation oncology, biology, physics*. 2011;81(1):181-8.
68. Polistina F, Costantin G, Casamassima F, Francescon P, Guglielmi R, Panizzoni G, et al. Unresectable locally advanced pancreatic cancer: a

multimodal treatment using neoadjuvant chemoradiotherapy (gemcitabine plus stereotactic radiosurgery) and subsequent surgical exploration. *Annals of surgical oncology*. 2010;17(8):2092-101.

69. Comito T, Cozzi L, Clerici E, Franzese C, Tozzi A, Iftode C, et al. Can Stereotactic Body Radiation Therapy Be a Viable and Efficient Therapeutic Option for Unresectable Locally Advanced Pancreatic Adenocarcinoma? Results of a Phase 2 Study. *Technology in cancer research & treatment*. 2017;16(3):295-301.

70. Petrelli F, Comito T, Ghidini A, Torri V, Scorsetti M, Barni S. Stereotactic Body Radiation Therapy for Locally Advanced Pancreatic Cancer: A Systematic Review and Pooled Analysis of 19 Trials. *International journal of radiation oncology, biology, physics*. 2017;97(2):313-22.

71. Hoyer M, Roed H, Sengelov L, Traberg A, Ohlhuis L, Pedersen J, et al. Phase-II study on stereotactic radiotherapy of locally advanced pancreatic carcinoma. *Radiotherapy and oncology : journal of the European Society for Therapeutic Radiology and Oncology*. 2005;76(1):48-53.

72. Koong AC, Christofferson E, Le QT, Goodman KA, Ho A, Kuo T, et al. Phase II study to assess the efficacy of conventionally fractionated radiotherapy followed by a stereotactic radiosurgery boost in patients with locally advanced pancreatic cancer. *International journal of radiation oncology, biology, physics*. 2005;63(2):320-3.

73. Krishnan S, Chadha AS, Suh Y, Chen HC, Rao A, Das P, et al. Focal Radiation Therapy Dose Escalation Improves Overall Survival in Locally Advanced Pancreatic Cancer Patients Receiving Induction Chemotherapy and Consolidative Chemoradiation. *International journal of radiation oncology, biology, physics*. 2016;94(4):755-65.

74. Colbert LE, Moningi S, Chadha A, Amer A, Lee Y, Wolff RA, et al. Dose escalation with an IMRT technique in 15 to 28 fractions is better tolerated than standard doses of 3DCRT for LAPC. *Advances in radiation oncology*. 2017;2(3):403-15.

75. Chung SY, Chang JS, Lee BM, Kim KH, Lee KJ, Seong J. Dose escalation in locally advanced pancreatic cancer patients receiving chemoradiotherapy. *Radiotherapy and oncology : journal of the European Society for Therapeutic Radiology and Oncology*. 2017;123(3):438-45.

76. Ma SJ, Prezzano KM, Hermann GM, Singh AK. Dose escalation of radiation therapy with or without induction chemotherapy for unresectable locally advanced pancreatic cancer. *Radiation oncology (London, England)*. 2018;13(1):214.

77. Moraru IC, Tai A, Erickson B, Li XA. Radiation dose responses for chemoradiation therapy of pancreatic cancer: an analysis of compiled clinical data using biophysical models. *Practical radiation oncology*. 2014;4(1):13-9.

78. Prior PW, Chen X, Hall WA, Erickson BA, Li A. Estimation of the Alpha-beta Ratio for Chemoradiation of Locally Advanced Pancreatic Cancer. *Int J Radiat Oncol Biol Phys*. 2018;102(3):S97-S.

79. Noel CE, Parikh PJ, Spencer CR, Green OL, Hu Y, Mutic S, et al. Comparison of onboard low-field magnetic resonance imaging versus onboard computed tomography for anatomy visualization in radiotherapy. *Acta oncologica (Stockholm, Sweden)*. 2015;54(9):1474-82.

80. Rasch C, Barillot I, Remeijer P, Touw A, van Herk M, Lebesque JV. Definition of the prostate in CT and MRI: a multi-observer study. *International journal of radiation oncology, biology, physics*. 1999;43(1):57-66.

81. O'Neill BD, Salerno G, Thomas K, Tait DM, Brown G. MR vs CT imaging: low rectal cancer tumour delineation for three-dimensional conformal radiotherapy. *The British journal of radiology*. 2009;82(978):509-13.
82. Meng J, Zhu L, Zhu L, Xie L, Wang H, Liu S, et al. Whole-lesion ADC histogram and texture analysis in predicting recurrence of cervical cancer treated with CCRT. *Oncotarget*. 2017;8(54):92442-53.
83. Wong KH, Panek R, Dunlop A, McQuaid D, Riddell A, Welsh LC, et al. Changes in multimodality functional imaging parameters early during chemoradiation predict treatment response in patients with locally advanced head and neck cancer. *European journal of nuclear medicine and molecular imaging*. 2018;45(5):759-67.
84. Pathmanathan AU, van As NJ, Kerkmeijer LGW, Christodouleas J, Lawton CAF, Vesprini D, et al. Magnetic Resonance Imaging-Guided Adaptive Radiation Therapy: A 'Game Changer' for Prostate Treatment? *International Journal of Radiation Oncology • Biology • Physics*. 2018;100(2):361-73.
85. Acharya S, Fischer-Valuck BW, Kashani R, Parikh P, Yang D, Zhao T, et al. Online Magnetic Resonance Image Guided Adaptive Radiation Therapy: First Clinical Applications. *International journal of radiation oncology, biology, physics*. 2016;94(2):394-403.
86. Fischer-Valuck BW, Henke L, Green O, Kashani R, Acharya S, Bradley JD, et al. Two-and-a-half-year clinical experience with the world's first magnetic resonance image guided radiation therapy system. *Advances in radiation oncology*. 2017;2(3):485-93.
87. Raaymakers BW, Jurgensliemk-Schulz IM, Bol GH, Glitzner M, Kotte A, van Asselen B, et al. First patients treated with a 1.5 T MRI-Linac: clinical proof of concept of a high-precision, high-field MRI guided radiotherapy treatment. *Physics in medicine and biology*. 2017;62(23):L41-L50.
88. Bohoudi O, Bruynzeel AME, Senan S, Cuijpers JP, Slotman BJ, Lagerwaard FJ, et al. Fast and robust online adaptive planning in stereotactic MR-guided adaptive radiation therapy (SMART) for pancreatic cancer. *Radiotherapy and oncology : journal of the European Society for Therapeutic Radiology and Oncology*. 2017;125(3):439-44.
89. Henke L, Kashani R, Robinson C, Curcuru A, DeWees T, Bradley J, et al. Phase I trial of stereotactic MR-guided online adaptive radiation therapy (SMART) for the treatment of oligometastatic or unresectable primary malignancies of the abdomen. *Radiotherapy and oncology : journal of the European Society for Therapeutic Radiology and Oncology*. 2018;126(3):519-26.
90. Rudra S, Jiang N, Rosenberg SA, Olsen JR, Roach MC, Wan L, et al. Using adaptive magnetic resonance image-guided radiation therapy for treatment of inoperable pancreatic cancer. *Cancer medicine*. 2019;8(5):2123-32.
91. Vestergaard A, Hafeez S, Muren LP, Nill S, Hoyer M, Hansen VN, et al. The potential of MRI-guided online adaptive re-optimisation in radiotherapy of urinary bladder cancer. *Radiotherapy and oncology : journal of the European Society for Therapeutic Radiology and Oncology*. 2016;118(1):154-9.
92. Verkooijen HM, Kerkmeijer LGW, Fuller CD, Huddart R, Faivre-Finn C, Verheij M, et al. R-IDEAL: A Framework for Systematic Clinical Evaluation of Technical Innovations in Radiation Oncology. *Frontiers in oncology*. 2017;7:59.
93. Kerkmeijer LG, Fuller CD, Verkooijen HM, Verheij M, Choudhury A, Harrington KJ, et al. The MRI-Linear Accelerator Consortium: Evidence-Based Clinical Introduction of an Innovation in Radiation Oncology Connecting

Researchers, Methodology, Data Collection, Quality Assurance, and Technical Development. *Frontiers in oncology*. 2016;6:215.

94. Kupelian P, Sonke JJ. Magnetic resonance-guided adaptive radiotherapy: a solution to the future. *Seminars in radiation oncology*. 2014;24(3):227-32.

95. Choudhury A, Budgell G, MacKay R, Falk S, Faivre-Finn C, Dubec M, et al. The Future of Image-guided Radiotherapy. *Clinical Oncology*. 2017;29(10):662-6.

96. Salembier C, Villeirs G, De Bari B, Hoskin P, Pieters BR, Van Vulpen M, et al. ESTRO ACROP consensus guideline on CT- and MRI-based target volume delineation for primary radiation therapy of localized prostate cancer. *Radiotherapy and oncology : journal of the European Society for Therapeutic Radiology and Oncology*. 2018;127(1):49-61.

97. Peters LJ, O'Sullivan B, Giralt J, Fitzgerald TJ, Trotti A, Bernier J, et al. Critical impact of radiotherapy protocol compliance and quality in the treatment of advanced head and neck cancer: results from TROG 02.02. *Journal of clinical oncology : official journal of the American Society of Clinical Oncology*. 2010;28(18):2996-3001.

98. Nishioka K, Shimizu S, Shinohara N, Ito YM, Abe T, Maruyama S, et al. Analysis of inter- and intra fractional partial bladder wall movement using implanted fiducial markers. *Radiation oncology (London, England)*. 2017;12(1):44.

99. Gronborg C, Vestergaard A, Hoyer M, Sohn M, Pedersen EM, Petersen JB, et al. Intra-fractional bladder motion and margins in adaptive radiotherapy for urinary bladder cancer. *Acta oncologica (Stockholm, Sweden)*. 2015;54(9):1461-6.

100. McBain CA, Khoo VS, Buckley DL, Sykes JS, Green MM, Cowan RA, et al. Assessment of bladder motion for clinical radiotherapy practice using cine-magnetic resonance imaging. *International journal of radiation oncology, biology, physics*. 2009;75(3):664-71.

101. Mangar SA, Scurr E, Huddart RA, Sohaib SA, Horwich A, Dearnaley DP, et al. Assessing intra-fractional bladder motion using cine-MRI as initial methodology for Predictive Organ Localization (POLO) in radiotherapy for bladder cancer. *Radiotherapy and oncology : journal of the European Society for Therapeutic Radiology and Oncology*. 2007;85(2):207-14.

102. Foroudi F, Pham D, Bressel M, Gill S, Kron T. Intrafraction bladder motion in radiation therapy estimated from pretreatment and posttreatment volumetric imaging. *International journal of radiation oncology, biology, physics*. 2013;86(1):77-82.

103. Lens E, van der Horst A, Kroon PS, van Hooft JE, Davila Fajardo R, Fockens P, et al. Differences in respiratory-induced pancreatic tumor motion between 4D treatment planning CT and daily cone beam CT, measured using intratumoral fiducials. *Acta oncologica (Stockholm, Sweden)*. 2014;53(9):1257-64.

104. radiologists Rco. Radiotherapy dose fractionation. https://www.rcr.ac.uk/system/files/publication/field_publication_files/bfco16_bladder_corrected.pdf Accessed December 2018.

Chapter 2

MRI based inter-observer contouring variability in bladder cancer radiotherapy and consensus guidance generation

Sections of this chapter have been published:

Abstracts:

A Hunt, A Sohaib, M Serra, M Koh, R Huddart, S Hafeez. Multidisciplinary Inter-observer Variation using Magnetic Resonance Imaging (MRI) for Muscle Invasive Bladder Cancer (MIBC) Radiotherapy Target Definition. Clinical oncology (Royal College of Radiologists (Great Britain)). 2019;31(2),e25-e26

Hunt A, Chan A, Delacroix L, Dysager L, Edwards A, Frew J, et al. EP-1589 Establishing international variation in target delineation using MRI for bladder radiotherapy. Radiotherapy and Oncology. 2019;133:S857-S8.

Chapter 2 MRI based inter-observer contouring variability in bladder cancer radiotherapy and consensus guidance generation.

2.1 Introduction

Interest in the use of MRI in the bladder cancer radiotherapy treatment pathway is increasing thanks to its superior soft tissue definition and its high diagnostic performance (1-4). However, compared to CT, radiation oncologists have less experience using MRI for radiotherapy contouring and at the start of my thesis there was no guidance available on its use in radiotherapy target delineation for bladder cancer. For MRgRT to be a success, clinicians must be able to correctly identify and define the target and OARs on MRI. As MRI is increasingly utilised in the diagnostic setting, a working knowledge of bladder MRI is becoming more important for the radiation oncologist even when a conventional CT based radiotherapy workflow is followed. Whilst MRI interpretation skills can be learnt through MDT interactions with radiologists or self-directed learning, knowledge should not be regarded as innate especially as many radiation oncologists will have had limited exposure to MRI during their training. Inter-observer contouring variability is well documented (5-10) and failure to accurately define the radiotherapy target has been shown to negatively impact patient outcomes (11-13). Consensus guidance generation has been used to help standardise CT based contouring across many different tumour sites (14-17). In acknowledgment of the differences in CT interpretation compared to MRI, MRI specific contouring guidance has also been produced for sites such as the prostate (18). However, at the start of my thesis no similar guidance existed in bladder cancer². The work described in this chapter aims to address this.

² Since writing this chapter recommendations for planning and delivery of radiotherapy for bladder cancer have been published (June 2021) in Radiotherapy & Oncology, they do not however focus purely on MRI 19. Khalifa J, Supiot S, Pignot G, Hennequin C, Blanchard P, Pasquier D, et al. Recommendations for planning and delivery of radical radiotherapy for localized urothelial carcinoma of the bladder. Radiotherapy and Oncology.,

I will discuss the results of two pieces of work I have undertaken in relation to MRI based contouring for bladder cancer. Firstly, I will report on the inter-observer contouring variability seen between members of the bladder radiotherapy multi-disciplinary team and how this can be altered through the development of consensus guidance (discussed in Part 1). Secondly, I will discuss the process of guidance generation (discussed in Part 2).

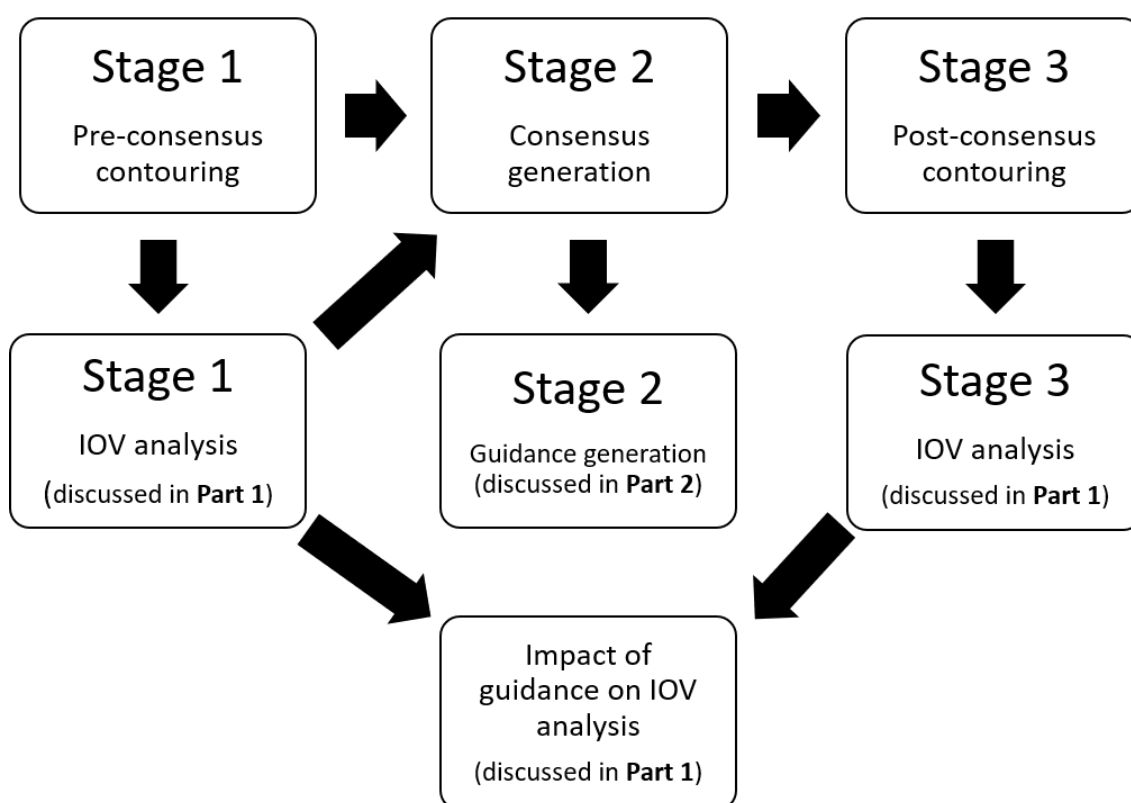


Figure 2.1 Flow chart of study stages and their relevant chapter parts.

IOV= interobserver variability

2.2 Part 1: Interobserver contouring variation and the impact of consensus guidance generation- Methods

This part of the study is divided into three stages, figure 2.1. Stage 1 involved establishing baseline inter-observer contouring variability within the radiation oncology community. Stage 2 involved consensus guidance generation, which

included agreement on target delineation, along with education on correct MRI interpretation. The consensus was then used to facilitate a second contouring exercise (stage 3) enabling a comparison of inter-observer variability (IOV) pre and post consensus guidance. Stages 1 and 3 will be discussed in this part of the chapter with stage 2 discussed in greater detail in Part 2.

2.2.1 Participant selection

The aim of this work was to develop a consensus guideline for MRI based contouring which could be used by the international radiation oncology community. We therefore included participants from within our local department, the wider UK community (by inviting participants already contributing to UK based bladder radiotherapy trials) and participants from outside the UK (mainly focussing on those who were part of the Elekta MR Linac consortium). Involvement in the study was voluntary and although we encouraged participants to be involved in all 3 stages those who could only contribute in part were still included. Recruitment for stage 1 began in spring 2018. Stage 3 was completed in January 2020. Dr Hafeez made initial contact with prospective participants, I followed up with those who expressed an interest in participating.

2.2.2 Contouring case selection

Contouring cases were selected by myself and agreed with Dr Hafeez. Stage 1 included three MRI based cases and one CT based case (as a comparator). Stage 3 included 3 MRI based cases only. One case in stage 3 was a repeat from stage 1. MRI based cases were selected from a cohort of patients with MIBC who had undergone diagnostic MRIs within the IDEAL MRI sub study trial (NCT01124682), these patients had consented for their MRIs to be used for research purposes. Cases were selected to include a variety of tumour positions and appearances. MRIs were acquired on a 1.5T Siemens Aera (Erlangen, Germany). The CT based case was a radiotherapy planning CT from a patient who had consented for their radiotherapy imaging to be used for research.

2.2.3 Contouring method

Cases were anonymised prior to contouring. Contouring was completed in one of two ways. For staff local to The Royal Marsden Sutton, contouring occurred

directly onto the Royal Marsden Research Monaco treatment planning system (TPS). Other participants used an identical online version of Research Monaco TPS with their contours subsequently downloaded to the Royal Marsden research platform. Participants were blinded to the contours of others. Information sheets detailing the rationale behind the study, its aims and objectives and the tasks to be completed for each stage were provided (see appendix 2.1).

The information sheets included case vignettes with information on patient characteristics, relevant cystoscopy and histology findings and an abbreviated MRI report. Participants contoured a GTV and CTV on the T2 weighted sequence and an outer bladder wall structure on a T1W sequence. Advice was given on structure delineation, based on the radiotherapy planning guidance for the RAIDER bladder radiotherapy trial (NCT02447549), table 2.1. In bladder radiotherapy, outside of the trial setting, the GTV is a less commonly contoured structure compared to the CTV. However, we wanted to assess variation in contouring of this structure as interest in partial bladder+/- tumour boost techniques is increasing so accurate delineation of the GTV is likely to become more important in the future. For the MRI based cases, participants were given access to T1, T2 and diffusion weighted imaging to help guide their contouring. In stage 3, participants were given updated contouring guidance (as developed during Stage 2 and tabulated by Dr Hafeez) along with general guidance on MRI interpretation, (appendix 2.2).

Table 2.1 Stage 1 contouring guidance

Structure	Delineation advice	Image set to use
GTV	Visible tumour/tumour bed Ignore any potentially positive lymph nodes, concentrate instead on the tumour related to the bladder itself.	T2W
CTV	GTV plus the whole bladder plus any areas of extravesical spread.	T2W

	<p>If the tumour is at the base of the bladder or distant CIS was/is present, the CTV should include 1.5cm of the prostatic urethra in males or 1cm of the urethra in females.</p> <p>Ignore any lymph node disease.</p>	
Outer bladder wall	Contour as you would the bladder as an OAR	T1W

2.2.4 Additional tasks completed by participants

In addition to the contouring itself, in stage 1 consultant radiation oncologists were asked to complete an experience questionnaire (appendix 2.3) in order to understand their prior experience of MRI within the radiotherapy pathway.

2.2.5 Determining inter-observer contouring variability

In order to facilitate inter-observer comparisons, once all contours were complete I created reference ‘gold standard’ structure sets for each of the cases. These ‘gold standard’ structures were developed using a 2 stage process. Firstly, based on the work of Warfield et al (20) and using a computer algorithm written by Jennifer Kieselmann (PhD student, ICR physics department), I created a ‘simultaneous truth and performance level estimation’ (STAPLE) structure of the GTV, CTV and outer bladder wall contours for each of the cases. The STAPLE structure concept has been previously used to assess inter-observer contouring variability (5, 21-23). The STAPLE structure is formed by using a computer algorithm which analyses each participant’s contours and computes a probabilistic estimate of the ground truth contour by weighting each contour depending on its estimated performance level. The end result is a computer-generated structure which should represent the ‘true’ or correct contour. This can then be used to compare each of the participant’s contours against.

A weakness of this approach is that misplaced contours still have some impact on the overall STAPLE structure produced. This can cause the STAPLE structure to deviate from the ground truth. To overcome this problem, the second stage of our gold standard structure generation involved adapting the GTV and CTV STAPLE structures for each MRI based case to better reflect ground truth. Adaptation was undertaken by myself, Dr Hafeez and Dr Sohaib (consultant

radiologist) working together to identify areas where misinterpretation of the MRI had affected the STAPLE or where the STAPLE structure did not conform to a valid anatomical contour. This reference structure was labelled the 'gold standard' structure and was used alongside the STAPLE structure in inter-observer analyses. This step was not carried out for the CT based case or the outer bladder wall structure sets due to time constraints. In the majority of cases, the STAPLE closely resembled the gold standard. A comparison of the variability between the STAPLE and the reference gold standard for each case is included in the discussion.

2.2.6 Analysis of inter-observer variation

Qualitative analysis of inter-observer variation was carried out using visual inspection of each case.

Quantitative analysis included assessment of the maximum variability ratio (MVR) for each structure set and assessment of the geometric inter-observer variation by calculating the DICE similarity coefficient (DCE), Cohen-Kappa ($C\kappa$), mean distance to agreement (MDA) and Hausdorff Distance (HD).

MVR is the ratio of the maximum and minimum volumes within each structure set (24). The closer the ratio to one, the less variation in size between participants' volumes. DCE and $C\kappa$ are overlap metrics providing an assessment of the degree of geometric overlap between two structures, with a value of 1 equalling perfect overlap.

$DCE = \frac{2(X \cap Y)}{(X + Y)}$ where \cap represents the area of overlap of two structures

$C\kappa = \frac{P_0 - P_e}{1 - P_e}$ where P_0 represents the probability of agreement and P_e represents the probability of random agreement

MDA and HD are surface similarity metrics. MDA provides an average of the distance between all points on surface A versus surface B, while HD describes the maximum distance between two comparable points. Numbers closer to zero therefore indicate better agreement, see figure 2.2. Assessment of the geometric

inter-observer variability was carried out using Monaco ADMIRE software v2.0 (research version, Elekta AB, Stockholm, Sweden).

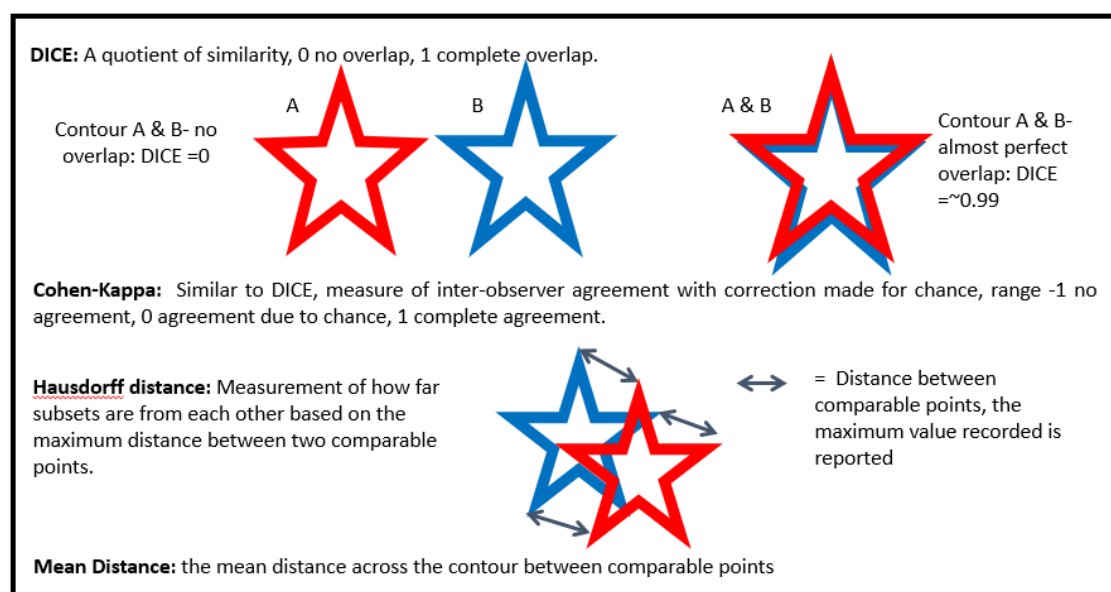


Figure 2.2 Geometric inter-observer comparison metrics

2.2.7 Assessment of the impact of consensus guidance on inter-observer variability

For each participant who fully completed Stage 1 and Stage 3, mean scores pre and post consensus guidance generation were compared in order to assess the impact of this intervention on inter-observer variability.

2.2.8 Exploratory assessment of effect of consensus generation on simulated target coverage

While the geometric variability metrics described above give an assessment of the variability seen between individuals they do not provide information on the clinical impact of this variation. I therefore performed an additional exploratory analysis on the simulated dosimetric effect of inter-observer variability on the reference gold standard target coverage.

To do this I used the delineations provided for case 3 (contoured pre and post consensus guidance). Firstly, I calculated the percentage of the gold standard

GTV (GTV_{GS}) and CTV (CTV_{GS}) covered by each participant's volume (figure 2.3, A). Then, taking each participant's contours individually, I created PTVs based on the contours drawn:

PTV_{1_participant_small} = participant GTV + small margin

PTV_{1_participant_medium} = participant GTV + medium margin

PTV_{2_participant_small} = participant CTV + small margin

PTV_{2_participant_medium} = participant CTV + medium margin

The margin dimensions used were taken from the RAIDER trial, see table 2.2.

Table 2.2 Margin sizes

Structure	Small margin	Medium margin	Corresponding PTV
GTV	0.5 cm isotropic	1.5 cm anterior/superior 1.0 cm posterior 0.5 cm inferior/lateral	PTV ₁
CTV	0.5 cm isotropic	1.5 cm anterior/superior 1.0 cm posterior 0.5 cm inferior/lateral	PTV ₂

I then calculated the percentage of GTV_{GS} and CTV_{GS} covered by each of the participant's PTVs, (Figure 2.3, B). Assuming that in the optimal planning scenario, the PTV contour edge would match the 95% isodose line (i.e. a plan conformity index of 1), this provided an estimate for the percentage of gold standard structure covered by the 95% isodose if the participant's PTVs had been used to drive the plan optimiser. I then looked at overlap between each participant's PTV and the corresponding gold standard PTV₁ and PTV₂ (PTV_{1_GS} and PTV_{2_GS}) which were created using the same margin formulae as above. This enabled an assessment of gold standard PTV coverage, figure 2.3, C.

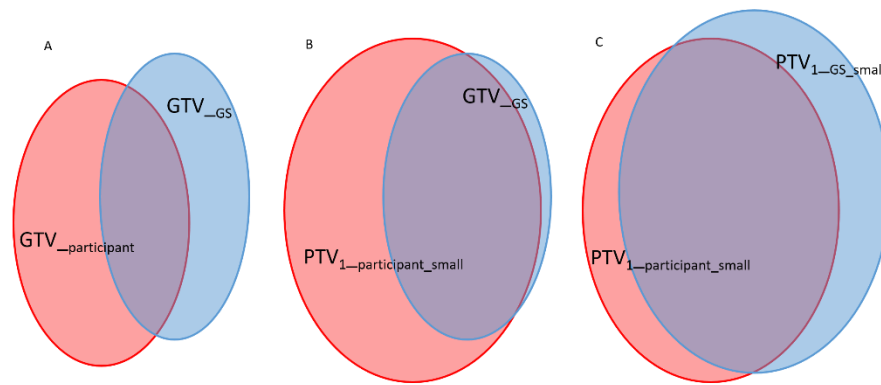


Figure 2.3 Assessment of gold standard PTV coverage.

A: By calculating the volume of GTV_{GS} within the overlapping region the percentage of GTV_{GS} covered by each $GTV_{participant}$ was calculated. B: Using a similar method the percentage of GTV_{GS} covered by $PTV1_{participant_small}$ was also calculated. C: Similarly, the percentage of $PTV1_{GS_small}$ covered by $PTV1_{participant_small}$ was also assessed. This process was repeated using $PTV1_{medium}$ and $PTV2$ structures.

Using the same conformity assumption as above, for each participant it was also possible to estimate the volume of gold standard non-target tissue which would have received $> 95\%$ of planned dose. I calculated this by calculating the volume of $PTV_{participant}$ falling outside of the corresponding PTV_{GS} . This represents a surrogate for excess normal tissue irradiation.

2.2.9 Statistical analysis

The primary end-point of this study was the difference in mean MRI GTV DCE pre and post consensus guidance generation. This was calculated by comparing the mean MRI GTV DCE scores for each participant who completed a full set of contours pre and post consensus guidance generation. Based on an initial sample (participants from within the RMH/ICR), the mean DCE before guidance generation was 0.7 (standard deviation 0.13). Assuming equal standard deviation pre and post guidance, and using a paired t-test with 5% significance and 80% power, 24 participants would be needed to detect a difference in DCE of 0.08 (i.e. DCE going from 0.70 to 0.78). If 29 participants were recruited then a difference of 0.07 could be detected. Based on these numbers I aimed to recruit approximately 30 participants to allow for drop out during the study. There is no clinical rationale for using an improvement in DICE of 0.07 as a cut off for

significance. This was instead a pragmatic decision taking into account the number of participants I thought I would be able to recruit and the degree of improvement I thought we were likely to see.

On review of the final data it became apparent that the dataset was non-parametric. As a result, the Wilcoxon signed ranks test was used in place of a paired T-test to test for a statistical significance difference in pre and post consensus MRI GTV DCE scores.

Statistical testing was carried out using IBM SPSS Statistics for Windows V27.0 (IBM Corp., Armonk, N.Y., USA).

My thanks to Mercy Ofuya and Charlotte Emery (ICR CTSU) for their help with the statistical plan.

2.3 Part 1: Results

2.3.1 Participant Characteristics

A total of 31 participants were involved in this study. 30 participants completed stage 1; 28 participants completed stage 3 (this included one participant who did not complete stage 1). A total of 26 completed all 6 MRI based cases and were therefore included in the pre and post guidance inter-observer contouring analysis.

Participants were from 6 different countries, UK (N=22), Netherlands (N=2), Denmark (N=2), Canada (N=2), Australia (N=2) and India (N=1). They included 24 radiation oncology consultants, 2 radiation oncology fellows (from RMH), 3 therapeutic radiographers (2 from RMH, one from Canada) and 2 radiologists (from RMH). A breakdown of participants in the relevant stages is given in Table 2.3.

Table 2.3 Participant Characteristics

	Stage 1	Stage 3
Total participants	30	28
Professional Group		
Consultant Radiation Oncologist	23	22
Radiation Oncology Fellow	2	2
Therapeutic radiographer	3	3
Consultant radiologist	2	1
Country of Residence		
UK	22	21
Canada	2	2
Australia	2	2
Netherlands	1	1
Denmark	2	2
India	1	0
Participants completing all MRI based cases	29	27
Participants partially completing MRI based cases	1	1

96% (22/23) of consultant radiation oncologists participating in stage 1 completed an experience questionnaire. Consultants had a median of 10 years' experience in bladder radiotherapy (range 4-30). Use of MRI in the radiotherapy pathway was mixed, 64% (14/22) had access to diagnostic MRI in some capacity (usually only for radical cases), 14% (3/22) had access to a radiotherapy planning MRI, while 32% (7/22) did not routinely use any MRI in their radiotherapy pathway.

2.3.2 Case Characteristics

Details of the patient case characteristics are shown in Table 2.4, example images depicting the gold standard GTV and CTV from each case are shown in figure 2.4. Case 3 was included in both stage 1 and 3. Case 6 was a CT based case, used as a comparator.

Table 2.4 Case Characteristics

	Case 1	Case 2	Case 3	Case 4	Case 5	Case 6 (CT based)
Age	78	82	78	70	60	68
Sex	M	F	M	M	M	M
Tumour staging	G3 T3 N0 TCC	G3 T3 N0 TCC	G3 T3b N0 TCC	G3 T3 N0 TCC	G3 T3 N0 TCC	G3 T3 N0
Tumour position*	Anterior- Superior	Right Anterior- Lateral	Left Anterior- Lateral involving Left VUJ	Anterior- Superior	Right Lateral	Anterior- Left Lateral
Imaging parameters T2w	2d TSE, Axial view 25 slices 3mm thick	2d TSE, Axial view 20 slices 4mm thick	2d TSE, Axial view 43 slices 5mm thick	2d TSE, Axial view 22 slices 4mm thick	2d TSE, Axial view 25 slices 4mm thick	CT based case 129 slices 2.5mm thick
T1w	2d TSE, Axial view 43 slices 5mm thick	2d TSE, Axial view 20 slices 4mm thick	2d TSE, Axial view 43 slices 5mm thick	2d TSE, Axial view 22 slices 4mm thick	2d TSE, Axial view 20 slices 4mm thick	
Study stage	1	1	1 & 3	3	3	1

* All cases had visible tumour

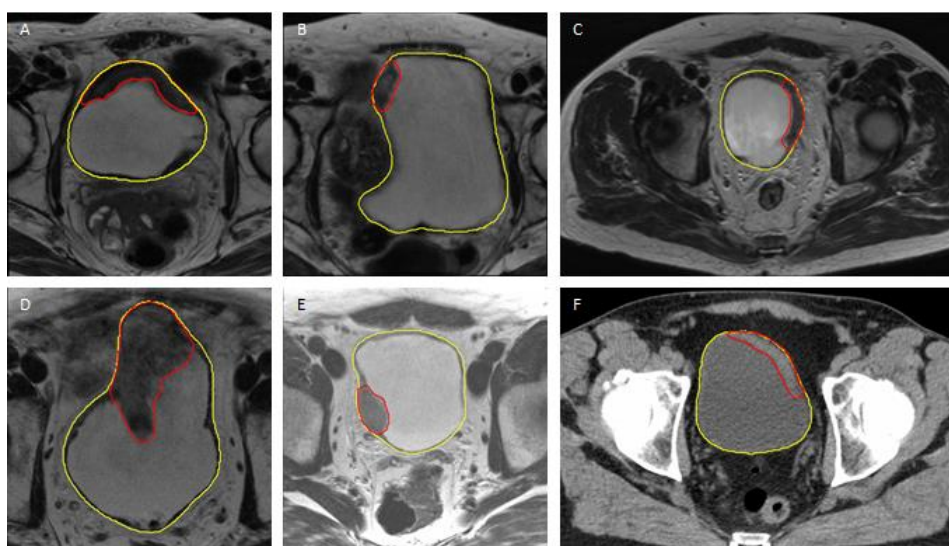


Figure 2.4 Representative axial slices of the 6 cases.

A= case 1, B= case 2, C= case 3, D= case 4, E= case 5, F= case 6. Yellow = CTV contour, Red= GTV contour

2.3.3 Contours completed

In total, 575 contours, 330 in stage 1 and 245 in stage 3 were completed. 2 contours in stage 1 were not suitable for analysis due to technical reasons (contours drawn on wrong image set). In Stage 3, one participant only completed the GTV and CTV for case 3.

2.3.4 Analysis of inter-observer variation

Stage 1 Pre-consensus guidance generation contouring

GTV variation

A breakdown of the variation metrics for the pre-consensus (Stage 1) GTVs is shown in Table 2.5.

Table 2.5 Stage 1 GTV variation.

The all-encompassing volume is the composite volume when all participant volumes are added together, MVR= maximum variability ratio, DCE= DICE similarity coefficient, Cκ= Cohen-Kappa, HD= Hausdorff Distance, MDA= mean distance to agreement

GTV	Case 1	Case 2	Case 3	Case 6 (CT)
Median participant volume (range), cc	18.6 (11.4-35.5)	5.3 (2.8- 50.0)	18.0 (7.0- 53.1)	10.6 (3.9-19.9)
MVR	3.1	17.9	7.6	5.1
All-encompassing volume, cc	50.0	64.2	103.9	34.8
STAPLE volume, cc	26.3	9.8	44.7	17.6
Gold Standard volume, cc	21.3	9.3	17.1	-
Median DCE (range) Compared to GTV_STAPLE	0.78 (0.52-0.89)	0.64 (0- 0.79)	0.54 (0.26- 0.86)	0.7 (0.35- 0.88)
Compared to GTV_Gold Standard	0.79 (0.56-0.85)	0.67 (0- 0.8)	0.61 (0.43-0.75)	-
Median Cκ (range) Compared to GTV_STAPLE	0.74 (0.48-0.87)	0.60 (-0.02- 0.77)	0.51 (0.23- 0.84)	0.67 (0.32- 0.87)
Compared to GTV_Gold Standard	0.75 (0.52-0.82)	0.63 (-0.02- 0.77)	0.57 (0.4- 0.71)	-
Median HD (range), mm Compared to GTV_STAPLE	12.2 (6.2- 20.9)	15.6 (7.1- 60.2)	32.9 (13.5- 55.3)	12.0 (6.6-20.5)

Compared to GTV_Gold Standard	10.4 (6.8- 17.0)	15.7 (7.1- 60.2)	26.8 (7.3-51.7)	-
Median MDA (range), mm Compared to GTV_STAPLE	2.1 (0.8- 5.9)	3.2 (1.0- 32.8)	8.1 (0.8- 20.6)	2.2 (0.6- 6.9)
Compared to GTV_Gold Standard	1.4 (0.8- 4.2)	3.0 (1.0- 32.5)	1.7 (1.2- 7.0)	-

Case 3 showed the greatest degree of GTV inter-observer contouring variability. It had the lowest median DCE and C_x scores and largest median HD. Although the median overall contour volume size was similar to the gold standard volume (18 vs 17 cc), this case showed the second highest MVR and the highest inter-quartile volume range (13.8 cc for case 3 versus 6.6 cc for case 1 and 2.8 cc for case 2).

Examples of the GTV contouring variation seen for case 3 are shown in Figure 2.5. Variation at the superior and inferior aspect of the contour was evident as was variation in the anterior and posterior extent of the contours. There was inconsistency surrounding the inclusion of the prostate with some participants incorrectly extending their volume to include part of the uninvolved prostate.

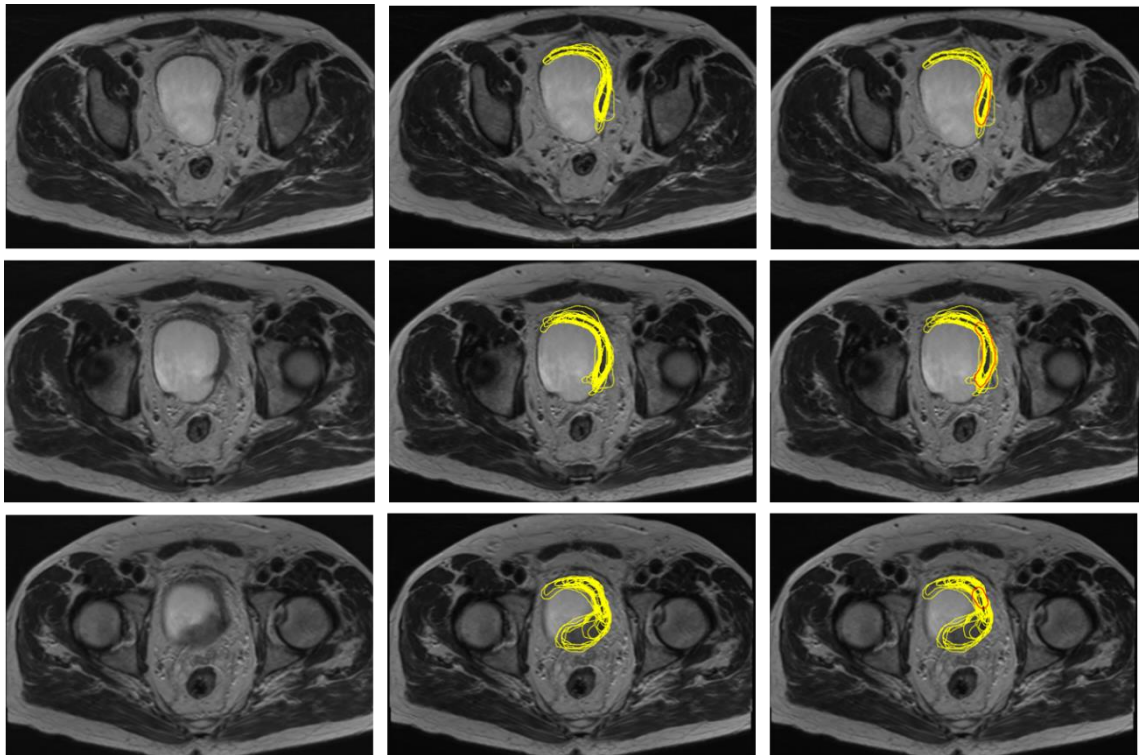


Figure 2.5 Inter-observer contouring variability for case 3.

Top row- superior portion of GTV, middle row- mid section of GTV, bottom row- inferior section of GTV. Each row shows (L-R) the same axial slice without contours, with participants' contours (yellow lines) and with participants' and gold standard contour for that slice (red line). Note the wide variation in the anterior/posterior extent of the contour especially when compared to the gold standard structure. Note also the incorrect inclusion of part of the prostate by some participants (inferior slice).

Case 1 showed the least GTV inter-observer variation, with a median DCE exceeding that of the CT based case. Inter-observer variation in volume size was less marked than Case 3 with a MVR of 3.1. On visual inspection, contours were well matched in the mid portion of the volume, with most variation seen in the superior and inferior extent of the contours. Variability in the lateral extent of the disease was seen particularly in the inferior section, although less so than case 3, Figure 2.6.

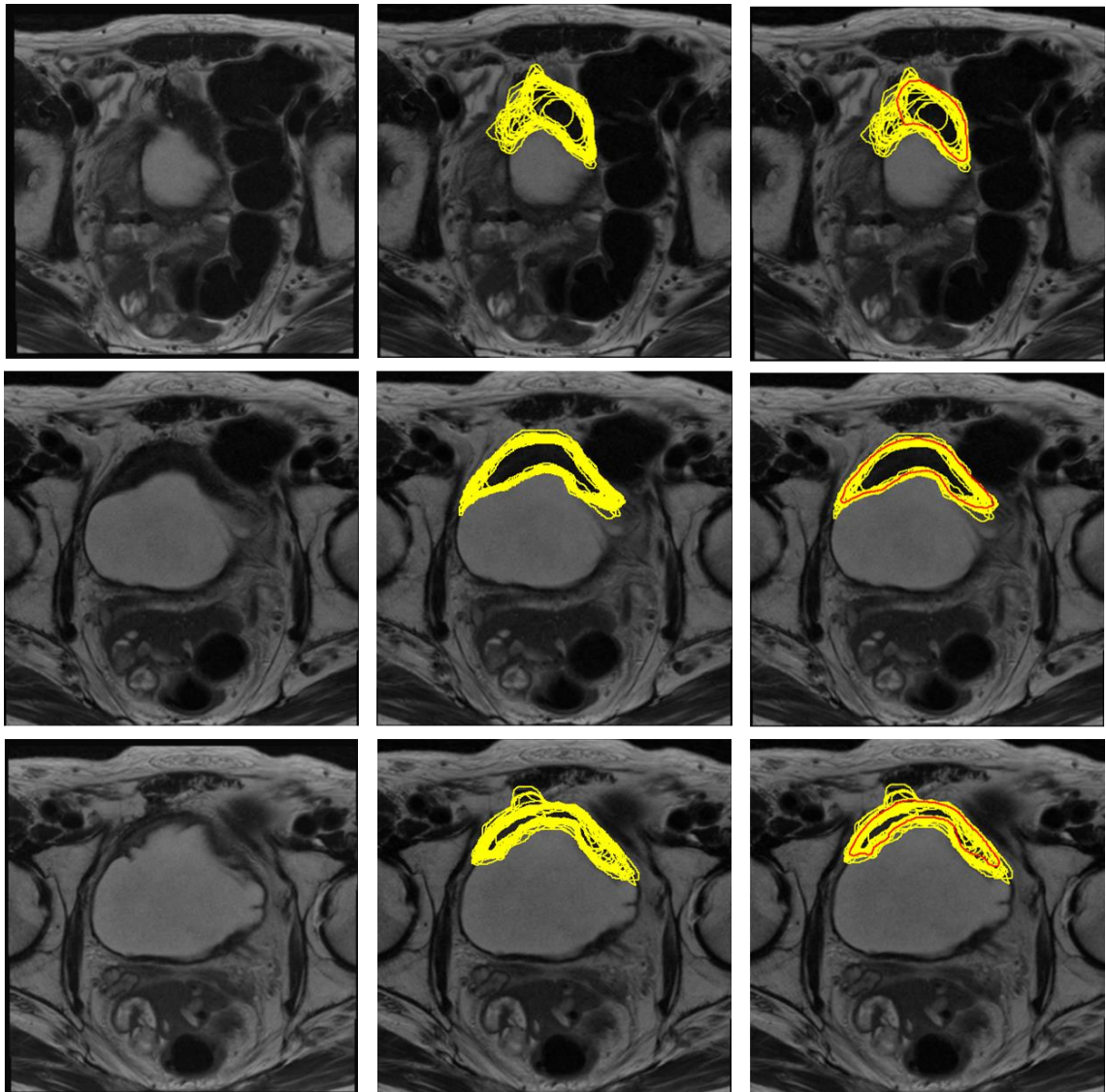


Figure 2.6 Inter-observer GTV contouring variability for case 1

Top row- superior portion of GTV, middle row- mid section of GTV, bottom row- inferior section of GTV. Contour colours as per previous figure. Compared to case 3 note the reduced variability in participants' contours particularly in the mid-section.

Case 2 showed the largest MVR and the largest range for DCE, $C\chi$, HD and MDA. This is because two participants failed to identify the correct position of the tumour resulting in a DCE of zero (i.e. no overlap with the gold standard) and large MDA and HD values. This error was due to misidentification of adjacent bowel. However, the majority successfully identified the target, resulting in a median DCE of 0.64. As with the other cases, variation superiorly and inferiorly still occurred, Figure 2.7.

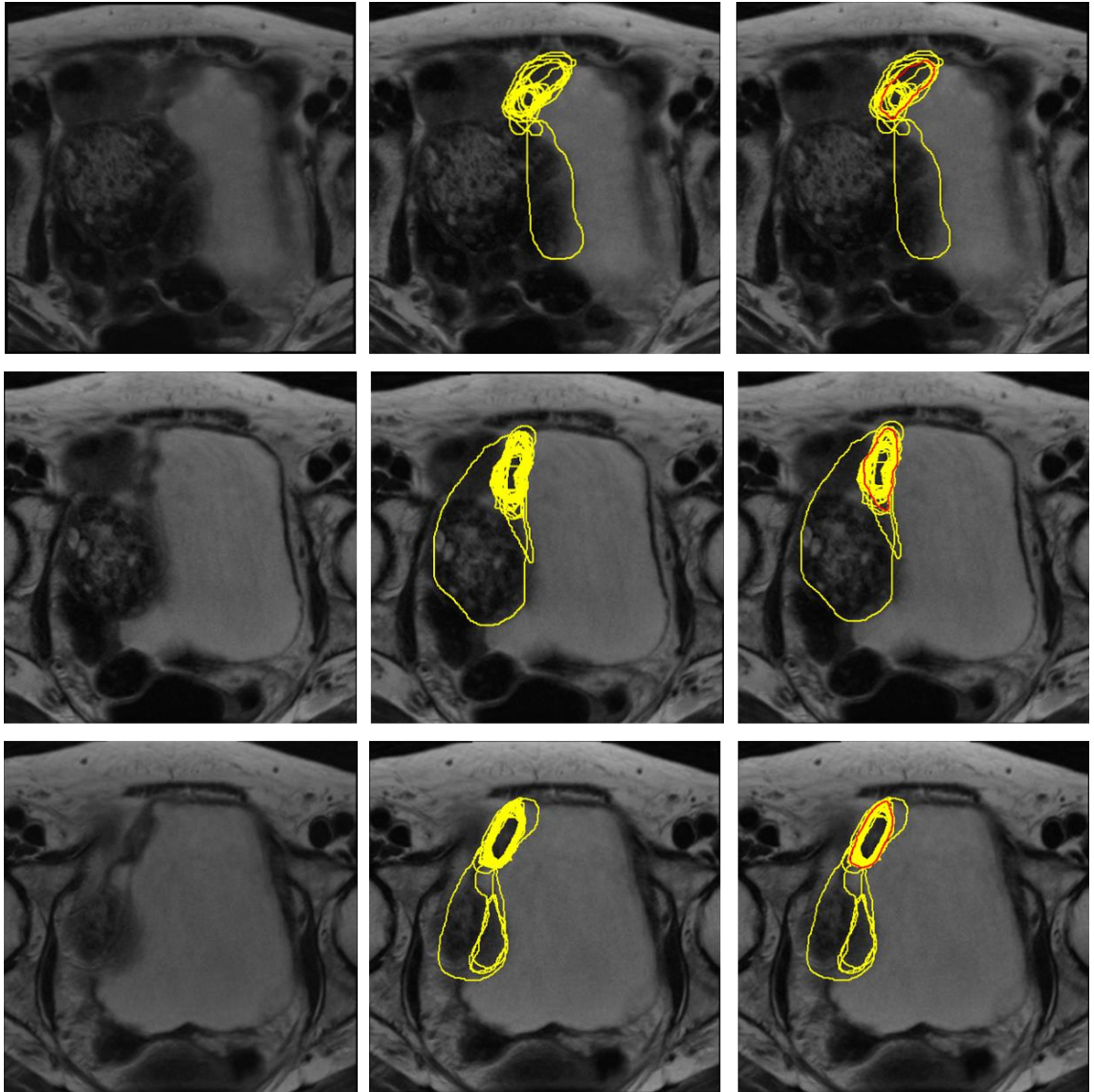


Figure 2.7 Inter-observer GTV contouring variability for case 2.

Top row- superior portion of GTV, middle row- mid section of GTV, bottom row- inferior section of GTV. Contour colours as per previously. Note the misidentification of tumour by some participants and the incorrect inclusion of adjacent bowel.

CTV variation

A breakdown of the variation metrics for pre-consensus CTVs is shown in Table 2.6.

Table 2.6 Stage 1 CTV variation.

Abbreviations as per previously.

CTV	Case 1	Case 2	Case 3	Case 6 (CT)
Median participant volume (range), cc	161.3 (142.0-175.1)	260.2 (237.7-286.2)	262.7 (221.3-315.2)	197.8 (182.6-230.0)
MVR	1.2	1.2	1.4	1.3
All-encompassing volume , cc	217.1	382.0	398.7	250.0
STAPLE volume , cc	163.3	264.9	276.1	203.4
Gold Standard volume , cc	159.1	263	267.4	-
Median DCE (range) Compared to CTV_STAPLE Compared to CTV_Gold Standard	0.95 (0.92-0.96) 0.94 (0.92- 0.96)	0.94 (0.87-0.96) 0.95 (0.86- 0.97)	0.95 (0.89-0.97) 0.95 (0.89- 0.97)	0.97 (0.94- 0.98) -
Median Cx (range) Compared to CTV_STAPLE Compared to CTV_Gold Standard	0.91 (0.87- 0.94) 0.91 (0.87- 0.93)	0.90 (0.81- 0.93) 0.93 (0.79-0.95)	0.92 (0.82- 0.95) 0.92 (0.82- 0.95)	0.95 (0.90- 0.97) -
Median HD (range), mm Compared to CTV_STAPLE Compared to CTV_Gold Standard	6.2 (3.7- 15.1) 6.4 (4.2- 14.1)	7.6 (5.5- 23.7) 6.7 (5.4- 24.3)	12.4 (5.8- 25.7) 12.1 (6.8- 23.9)	4.3 (2.9- 12.8) -
Median MDA (range), mm Compared to CTV_STAPLE Compared to CTV_Gold Standard	1.1 (0.8- 1.8) 1.2 (0.9- 1.7)	1.3 (1.0-2.5) 1.0 (0.7- 2.7)	1.3 (0.9- 3.3) 1.3 (0.7- 2.8)	0.6 (0.4- 1.3) -

Compared to the GTV, variation in CTV contouring was less marked. Agreement levels were high and there was less variation between cases.

Examples of the variation seen for case 1 are shown on Figure 2.8. Compared to the case 1 GTV there was less variation between participants in the most superior and inferior slices contoured, varying over 2 slices (6 mm) and 3 slices (9 mm) respectively compared to 21mm and 18mm for the GTV. On visual inspection, contours in the mid-zone were well aligned. Inferiorly, there was some variation in prostatic urethra inclusion, although the vast majority did not extend their contour into the prostate. This was in line with the CTV contouring guidance for the case.

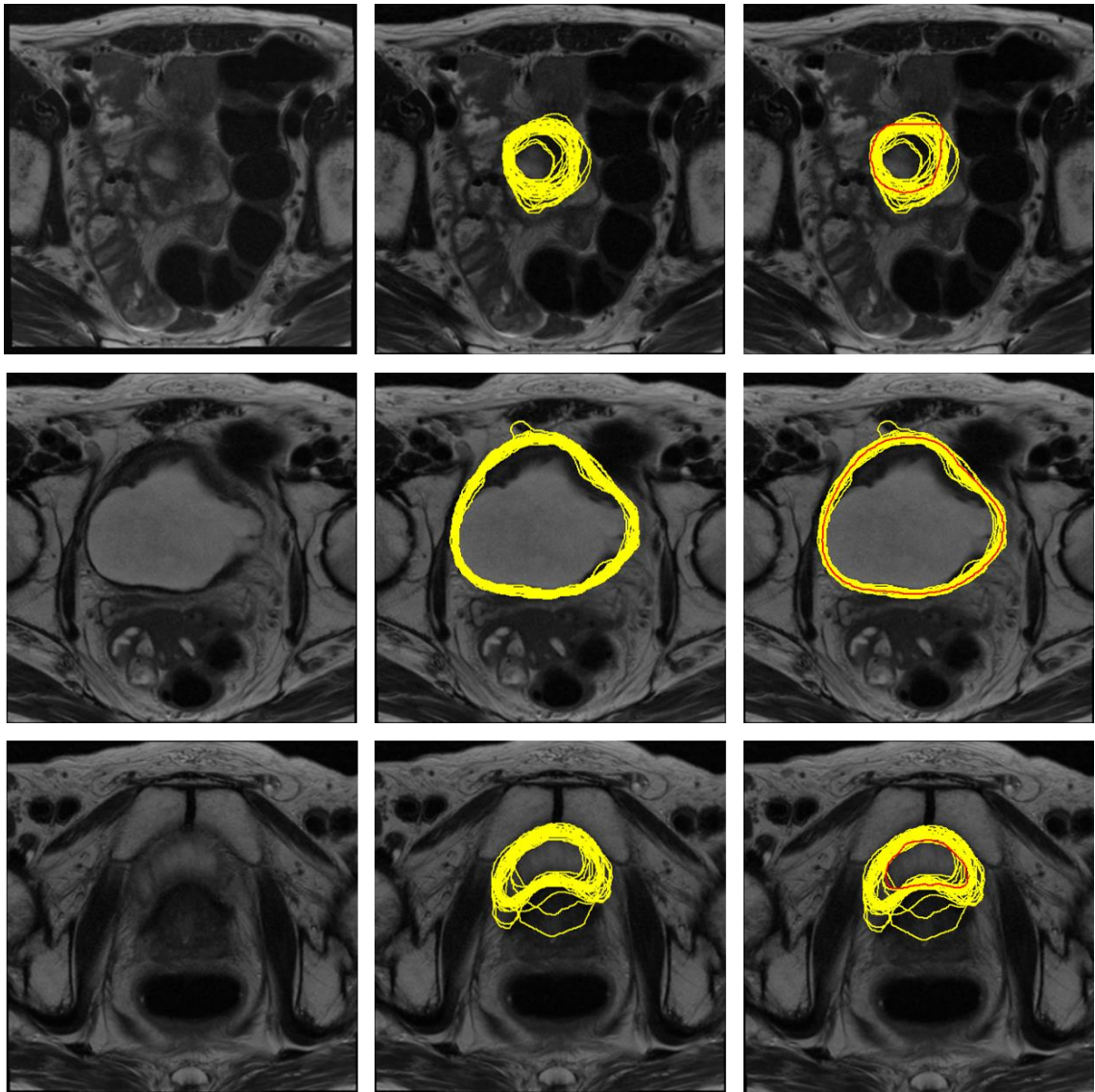


Figure 2.8 Inter-observer CTV contouring variability for case 1.

Top row- superior portion of CTV, middle row- mid section of CTV, bottom row- inferior section of CTV. Contouring colours as per previous figures. Note the reduced variability compared to GTV. Inferiorly, participants' contours tended to be more generous than the gold standard while superiorly this difference was less marked.

In Case 2, as with Case 1, variation between participants in the superior and inferior extent of the CTV was less than for the GTV, occurring over 6mm and 9mm respectively (compared to 24mm and 16mm). However, as with the GTV, the adjacent bowel caused problems for some participants, with their contour incorrectly extending into this region, see Figure 2.9. MRI interpretation inferiorly

was also challenging with a number of participants incorrectly including part of the vagina.

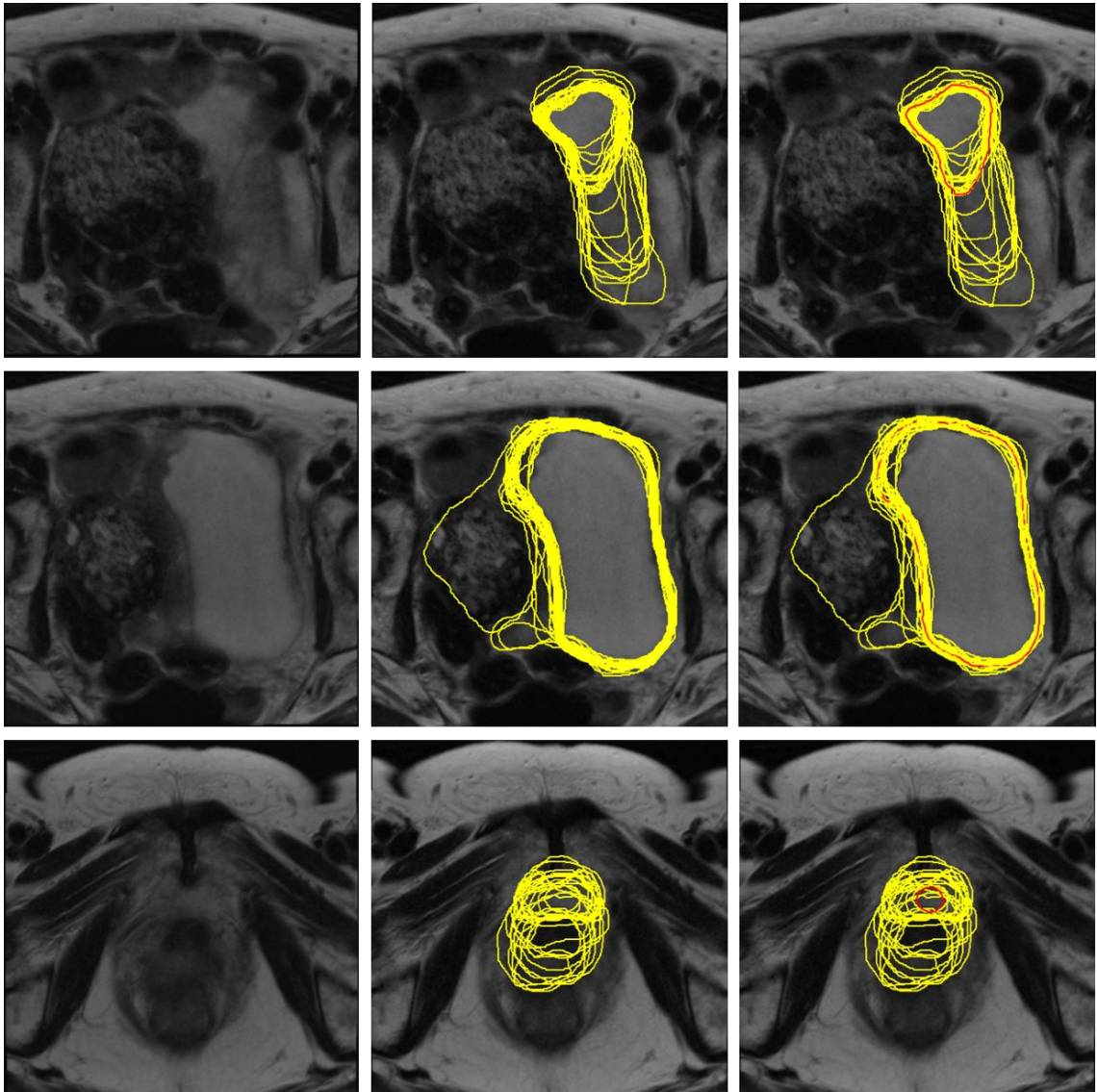


Figure 2.9 Inter-observer CTV contouring variability for case 2.

Top row- superior portion of CTV, middle row- mid section of CTV, bottom row- inferior section of CTV. Contouring colours as per previous figures. Note the variation in the anterior/posterior extent of the contour superiorly due to partial voluming of the bowel. Inferiorly, incorrect inclusion of the vagina was also noted.

In case 3, the contouring guidance called for the CTV to be extended into the prostatic urethra. There was marked variation in if/how this was achieved, Figure 2.10. The most inferior slice contoured ranged over 4 slices (20mm). The middle

portion of the CTV showed good agreement bar some incorrect inclusion of perivesical tissue. Superiorly, variation was minimal, with the most superior slice varying over 2 slices only, with 93% (27/29) starting on the same slice as the gold standard.

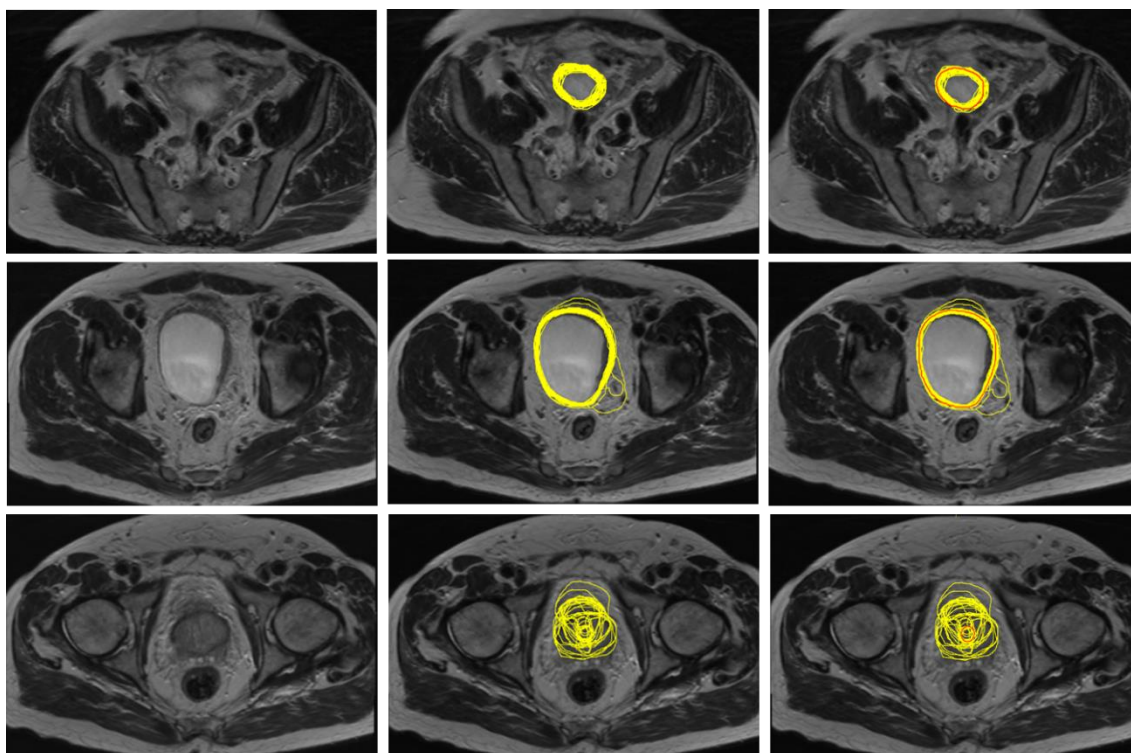


Figure 2.10 Inter-observer CTV contouring variability for case 3.

Top row- superior portion of CTV, middle row- mid section of CTV, bottom row- inferior section of CTV. Contouring colours as per previous figures. Agreement was good superiorly but inferiorly there was significant variation in how to include the prostatic urethra.

Outer bladder wall variation

Outer bladder wall contouring was completed on T1W imaging. This structure was included to evaluate participant's proficiency in T1W image interpretation and bladder wall identification.

Across the 3 MRI based cases, inter-observer contouring variability was similar, with metric scores similar to those obtained for CTVs, see Table 2.7.

Table 2.7 Stage 1 Outer bladder wall variation.

Abbreviations as pre previously

Outer bladder wall	Case 1	Case 2	Case 3
Median participant volume (range), cc	184.4 (155.3- 199.4)	443.8 (403.2- 596.1)	255.1 (230.6- 277.6)
MVR	1.3	1.5	1.2
All-encompassing volume, cc	249.4	716.7	319.7
STAPLE volume, cc	197.5	462.2	265.0
Median DCE (range) Compared to outer bladder wall_STAPLE	0.94 (0.88- 0.97)	0.94 (0.86-0.96)	0.96 (0.93- 0.98)
Median Cx (range) Compared to outer bladder wall_STAPLE	0.90 (0.81- 0.95)	0.90 (0.77- 0.93)	0.93 (0.87- 0.96)
Median HD (range), mm Compared to outer bladder wall_STAPLE	7.1 (4.5- 13.4)	10.4 (6.0- 24.8)	6.9 (4.1- 14.9)
Median MDA (range), mm Compared to outer bladder wall_STAPLE	1.4 (0.7- 2.7)	1.7 (1.2- 3.3)	1.0 (0.6- 2.3)

In case 1, in comparison to the CTV, there was more variation in the boundary between bladder and adjacent bowel. The middle section of the contour however showed excellent agreement. Inferiorly, there was occasional extension of the contour into the prostate, Figure 2.11.

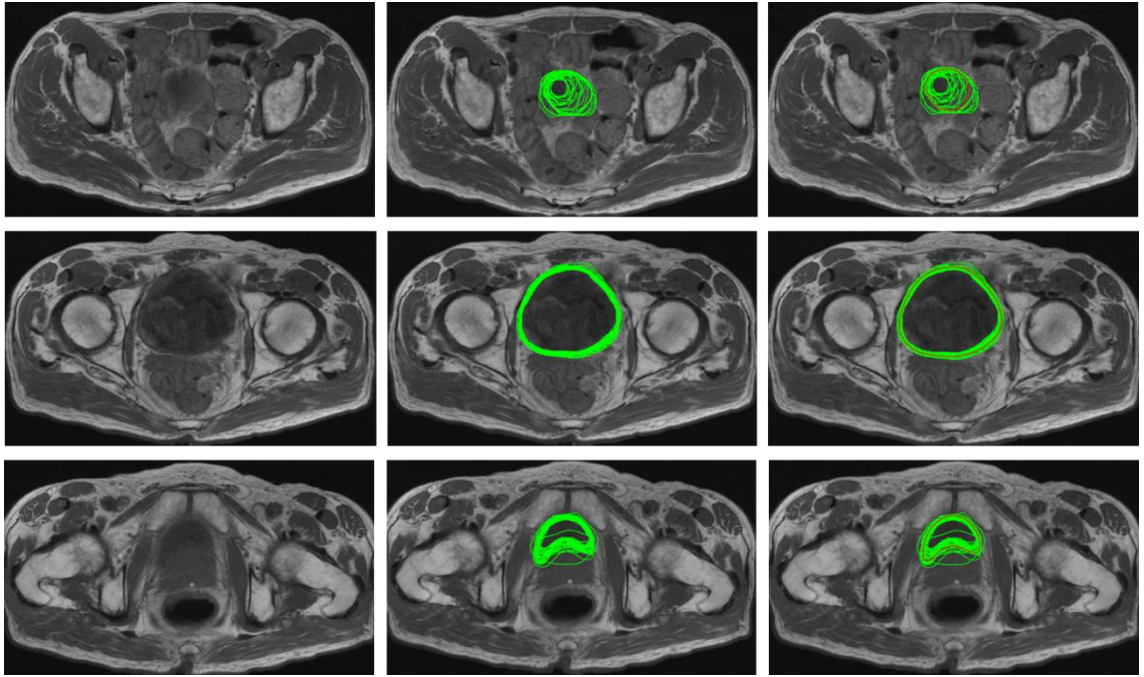


Figure 2.11 Inter-observer outer bladder wall contouring variability for case 1.

Top row- superior portion of outer bladder wall, middle row- mid section of outer bladder wall, bottom row- inferior section of outer bladder wall. Participants' contours in green, STAPLE contour in red.

In case 2, as with the CTV, defining the boundary between bladder and bowel was challenging. In the mid-section of the contour, less variation was seen. Inferiorly, homogeneity of the image intensity made distinguishing the boundaries between anatomical structures more difficult causing a wider range of anterior/posterior contour positioning, Figure 2.12.

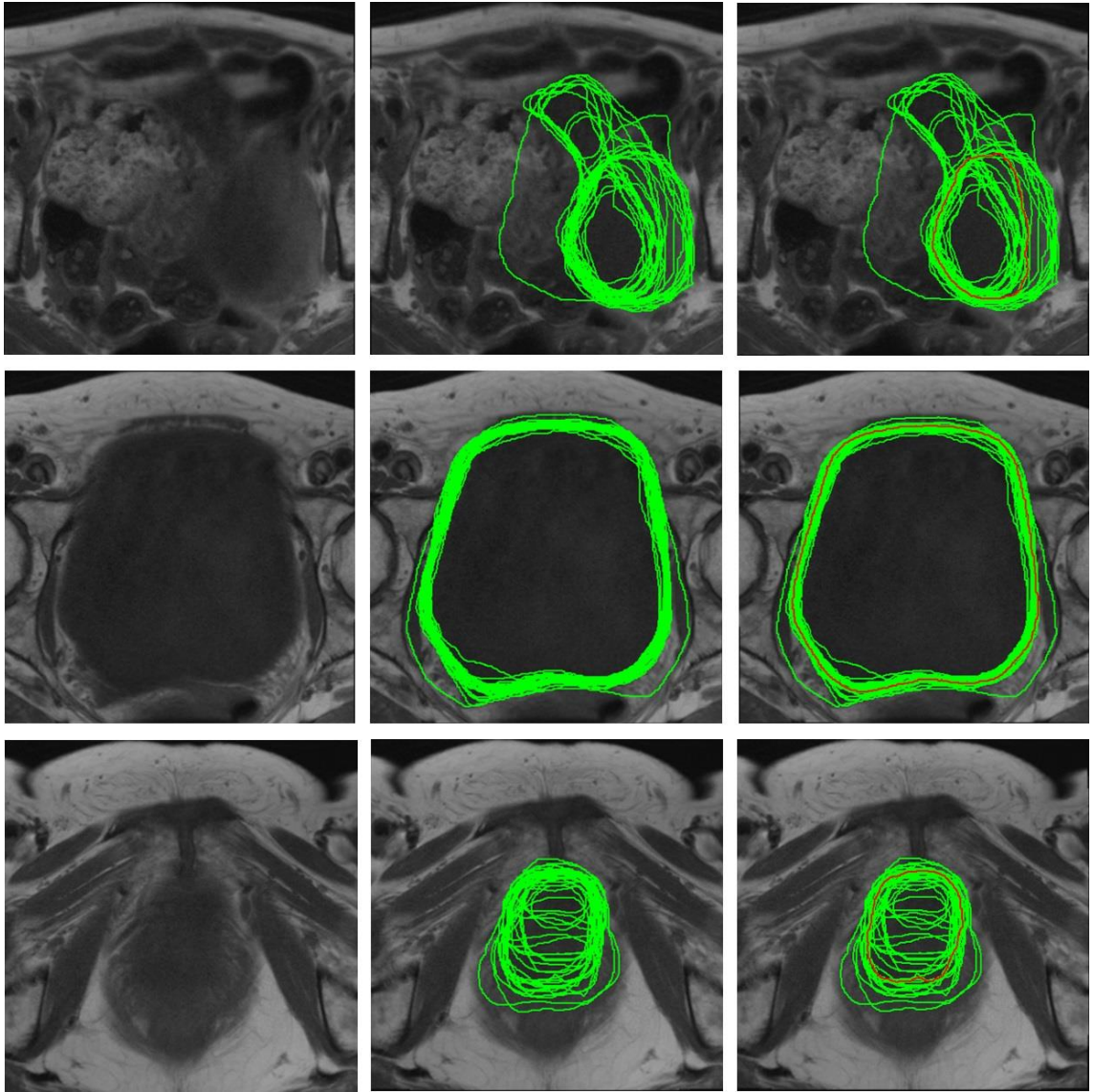


Figure 2.12 Inter-observer outer bladder wall contouring variability for case 2.

Top row- superior portion of outer bladder wall, middle row- mid section of outer bladder wall, bottom row- inferior section of outer bladder wall. Participants' contours in green, STAPLE contour in red

Case 3 had the highest DCE for outer bladder wall of all MRI based structures sets (0.96). There was good agreement superiorly with 93% (28/30) of participants beginning the superior aspect of their contour on the same slice. In the mid-section, as with the other cases, contouring variability was limited. Inferiorly, there was good agreement on the most inferior slice (varying over 2 slices), however, variability with respect to inclusion of the prostate was again noted, Figure 2.13.

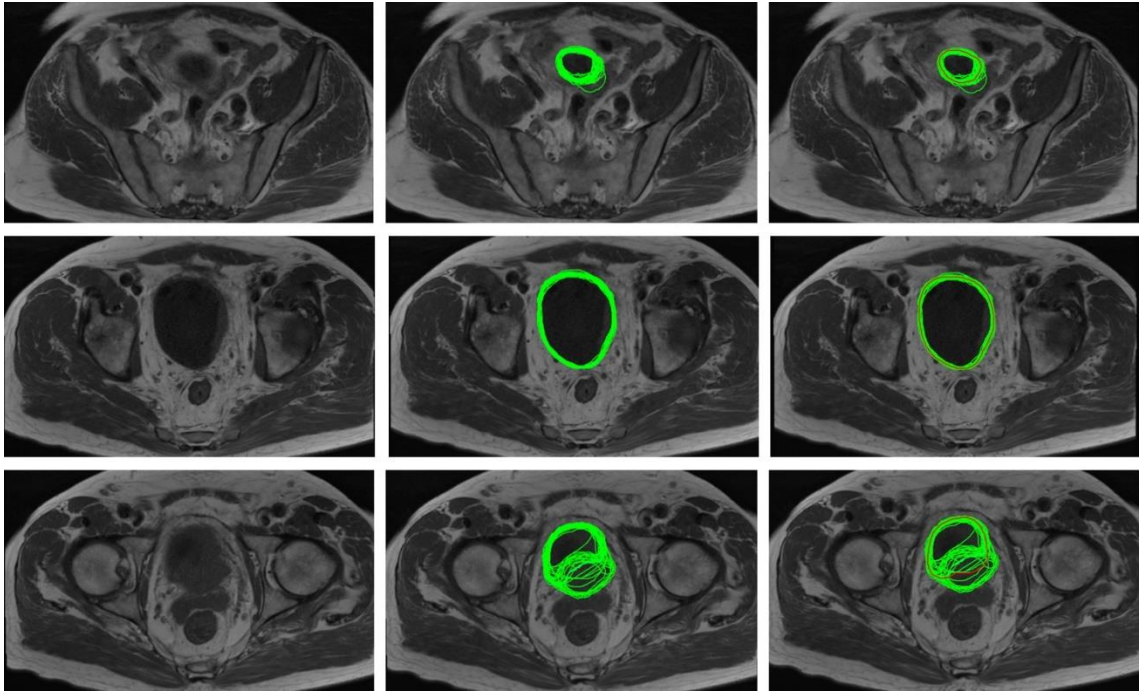


Figure 2.13 Inter-observer outer bladder wall contouring variability for case 3.

Top row- superior portion of outer bladder wall, middle row- mid section of outer bladder wall, bottom row- inferior section of outer bladder wall. Participants' contours in green, STAPLE contour in red.

22/23 consultants participating in stage 1 completed an experience questionnaire of which 21 documented the number of years' experience they had. Consultants had a median of 10 years' experience in bladder radiotherapy (range 4-30).

When divided into two groups, those with 10 years or less experience (n=12) compared to those with greater than 10 years' experience (n=9), there was no statistical difference between the groups with respect to median MRI GTV or CTV DICE scores, (Mann-Whitney U 395, $p=0.21$ and U 401, $p=0.22$ respectively), Table 2.8.

Table 2.8 Table of median DICE scores depending on years of bladder radiotherapy experience.

Years of experience	Median MRI GTV DCE	Median MRI CTV DCE
≤ 10 years' experience	0.73	0.95
> 10 years' experience	0.64	0.95

Stage 3 Post-consensus guidance generation contouring

This stage included 2 new and one repeat (case 3) MRI based cases. A CT based case was not included in this stage. 28 participants participated in this part of the study although one participant only completed the GTV and CTV for case 3 and did not contour case 4 and 5.

GTV variation

The inter-observer GTV contouring variation in stage 3 is summarised in Table 2.9.

Table 2.9 Stage 3 GTV variation

Abbreviations as per previously

GTV	Case 3	Case 4	Case 5
Median participant volume (range), cc	16.3 (8.3- 38.1)	90.4 (76.8- 106.6)	17.1 (14.1- 20.3)
MVR	4.6	1.4	1.4
All-encompassing volume, cc	76.2	151.1	30.1
STAPLE volume, cc	35.5	102.2	18.8
Gold Standard volume, cc	17.1	101.3	18.3

Median DCE (range) Compared to GTV_STAPLE	0.59 (0.33- 0.84)	0.91 (0.83- 0.96)	0.91 (0.85- 0.96)
Compared to GTV_Gold Standard	0.67 (0.42- 0.81)	0.91 (0.84- 0.96)	0.91 (0.86- 0.96)
Median Cx (range) Compared to GTV_STAPLE	0.55 (0.3- 0.8)	0.88 (0.78- 0.94)	0.88 (0.80- 0.94)
Compared to GTV_Gold Standard	0.62 (0.39- 0.78)	0.88 (0.78- 0.94)	0.88 (0.81- 0.94)
Median HD (range), mm Compared to GTV_STAPLE	31.3 (12.8- 43.9)	12.2 (5.6- 41.2)	5.7 (4.2- 14.9)
Compared to GTV_Gold Standard	18.8 (7.1- 55.7)	10.6 (5.62- 41.2)	6.1 (2.9- 20.0)
Median MDA (range), mm Compared to GTV_STAPLE	6.6 (1.1- 14.8)	1.4 (0.7- 2.9)	0.9 (0.5- 1.6)
Compared to GTV_Gold Standard	1.7 (1.1- 3.8)	1.4 (0.6- 2.8)	0.9 (0.4- 1.4)

Case 3 showed the lowest levels of GTV contour agreement of the post-consensus cases, however, compared to the pre-consensus contouring an improvement was seen (Table 2.12). The DCE improved from 0.61 to 0.67 and the HD and MDA both decreased. The variability in contour size also decreased (MVR 4.6 versus 7.6). Superiorly, there was less variation in the lateral extent of the contour and a higher proportion of participants began their contouring on the same slice as the gold standard (71% versus 59%). However, inferiorly variation was still seen with some participants continuing to include prostate within their volume.

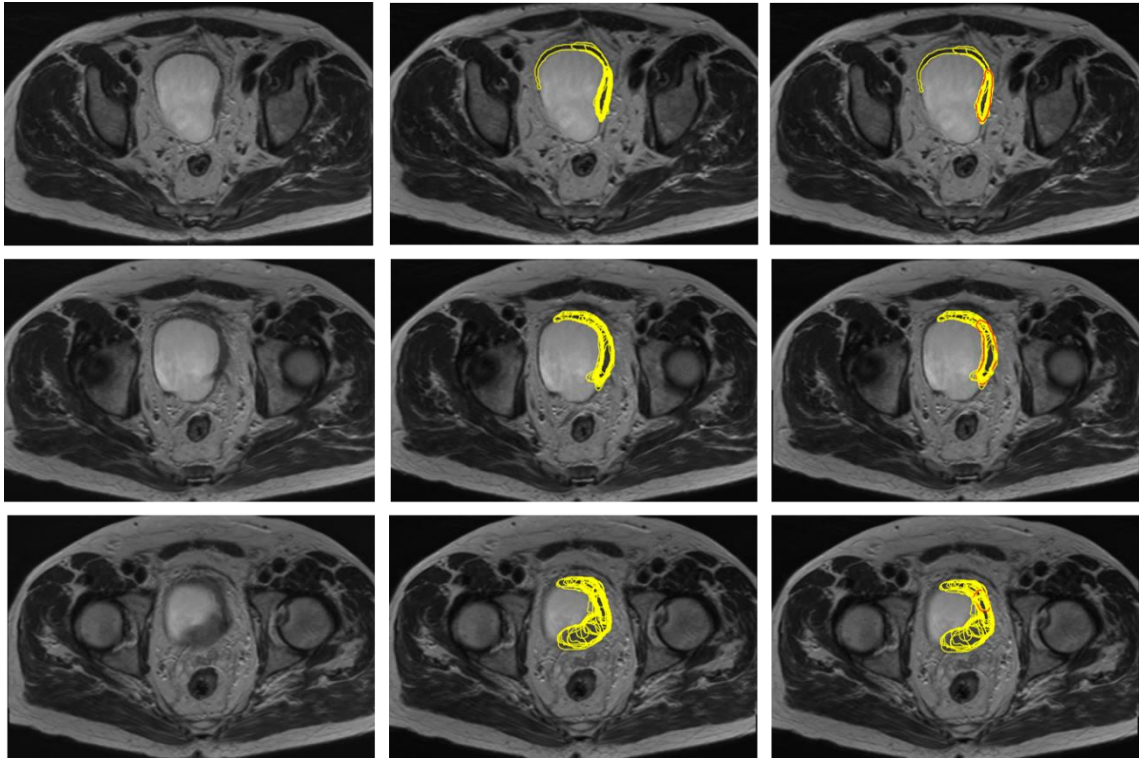


Figure 2.14 Inter-observer contouring variability for case 3 post consensus.

Top row- superior portion of GTV, middle row- mid section of GTV, bottom row- inferior section of GTV. Contouring colours as per previously.

In comparison, Case 4 had a GTV median DCE of 0.91, the joint highest of the MRI based cases. Participants correctly distinguished bladder tumour from adjacent bowel. In the mid-section of the contour, a minority extended their contour to the right, but the majority were aligned with the gold standard contour. Inferiorly, there was more variation in participant contours, with the most inferior slice extending over 20mm, see Figure 2.15.

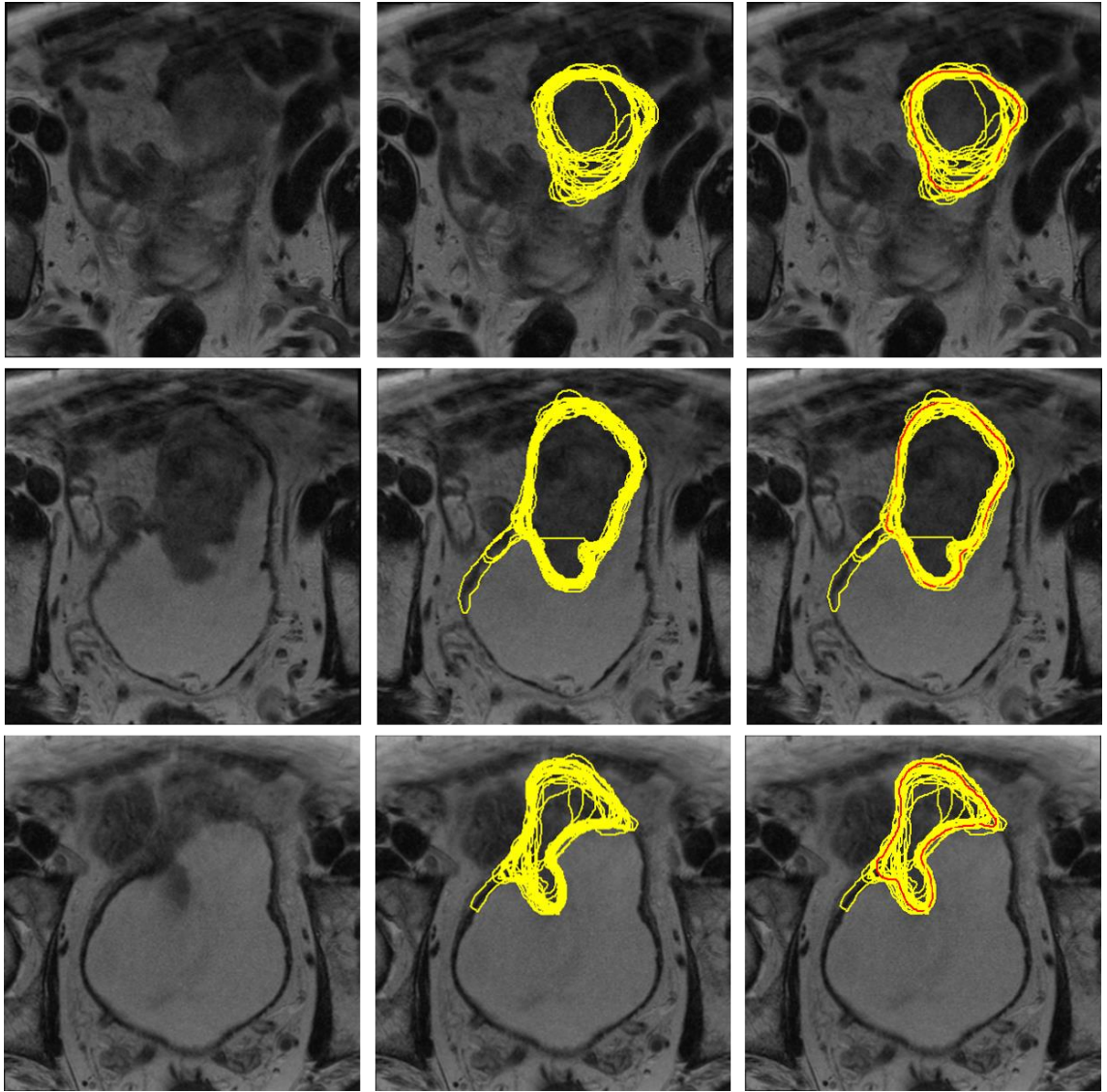


Figure 2.15 Inter-observer contouring variability for case 4.

Top row- superior portion of GTV, middle row- mid section of GTV, bottom row- inferior section of GTV. Contouring colours as per previously.

The median DCE for case 5 was also 0.91, and the HD and MDA were the lowest of all the MRI cases (both pre and post consensus). Throughout the volume, contours generally closely matched the gold standard in the left/right, anterior/posterior directions, as per previously most variation was seen at the superior and inferior aspects of the contour, Figure 2.16.

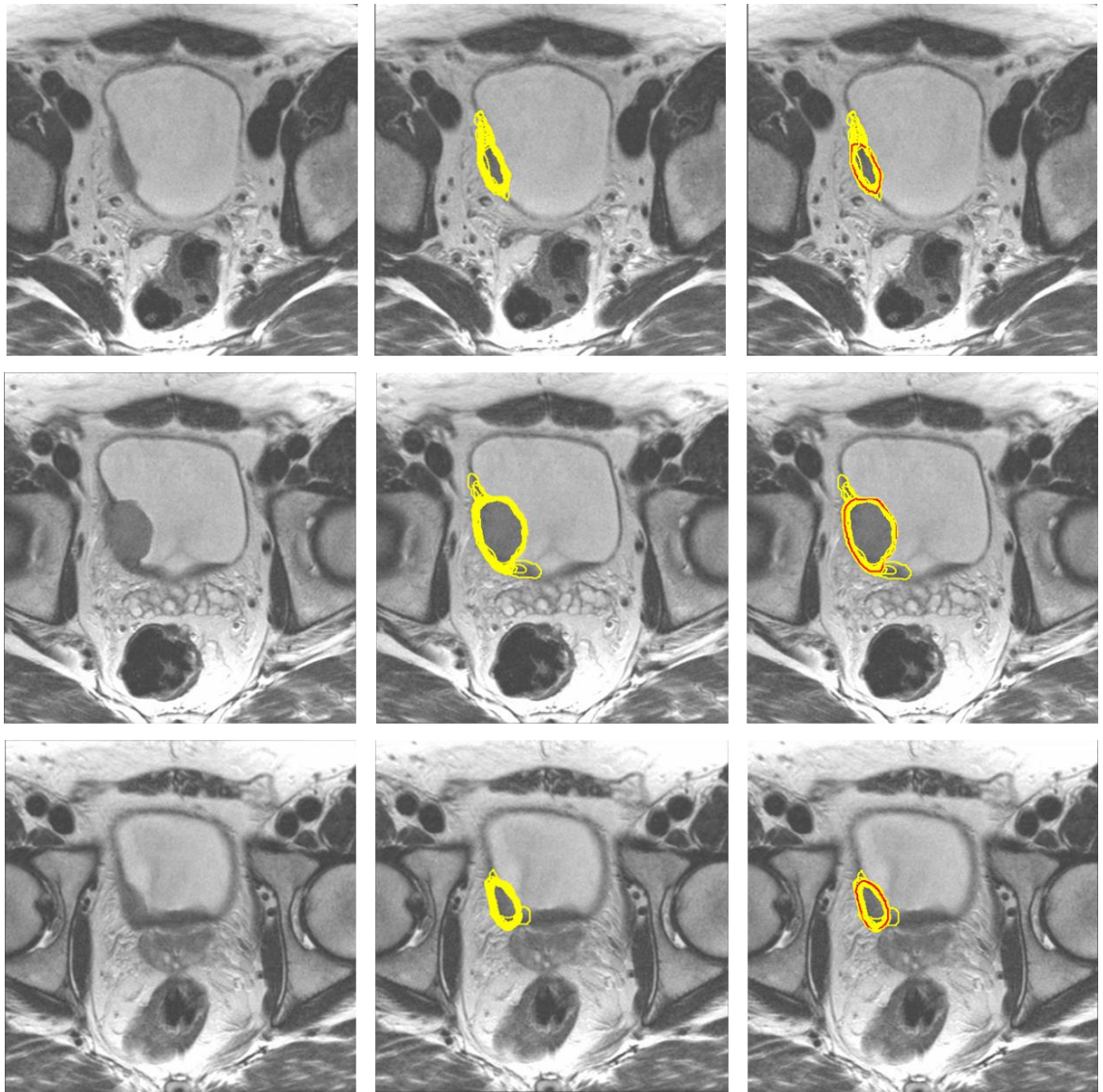


Figure 2.16 Inter-observer contouring variability for case 5.

Top row- superior portion of GTV, middle row- mid section of GTV, bottom row- inferior section of GTV. Contouring colours as per previously.

CTV variation

As seen pre-consensus, CTV variation was less than the variation seen for GTVs, Table 2.10.

Table 2.10 Stage 3 CTV variation

CTV	Case 3	Case 4	Case 5
Median participant volume (range), cc	260.9 (242.0- 288.5)	376.5 (346.3- 407.9)	260.4 (247.7- 273.3)
MVR	1.2	1.2	1.1
All-encompassing volume, cc	356.5	490.3	315.8
STAPLE volume, cc	270.4	386.2	265.2
Gold Standard volume, cc	267.4	384.6	263.0
Median DCE (range) Compared to CTV_STAPLE	0.96 (0.92- 0.98)	0.96 (0.93- 0.97)	0.97 (0.95- 0.98)
Compared to CTV_Gold Standard	0.96 (0.91- 0.97)	0.96 (0.93- 0.98)	0.97 (0.95-0.98)
Median Cx (range) Compared to CTV_STAPLE	0.93 (0.87- 0.96)	0.94 (0.90- 0.96)	0.95 (0.92- 0.97)
Compared to CTV_Gold Standard	0.93 (0.87- 0.96)	0.94 (0.90- 0.96)	0.94 (0.9- 0.96)
Median HD (range), mm Compared to CTV_STAPLE	8.8 (6.0- 25.1)	7.3 (5.4- 26.5)	5.4 (3.5- 22.2)
Compared to CTV_Gold Standard	9.6 (5.4- 31.2)	8.9 (5.5- 26.5)	6.1 (4.1-23.2)
Median MDA (range), mm Compared to CTV_STAPLE	1.1 (0.7- 1.9)	1.0 (0.7- 1.6)	0.7 (0.4- 1.1)
Compared to CTV_Gold Standard	1.1 (0.7- 2.0)	1.0 (0.7-1.6)	0.8 (0.6- 1.3)

Participants' contours continued to closely match those of the gold standard. However, as per previously, the variation that did occur happened in the superior and inferior aspects of the contour.

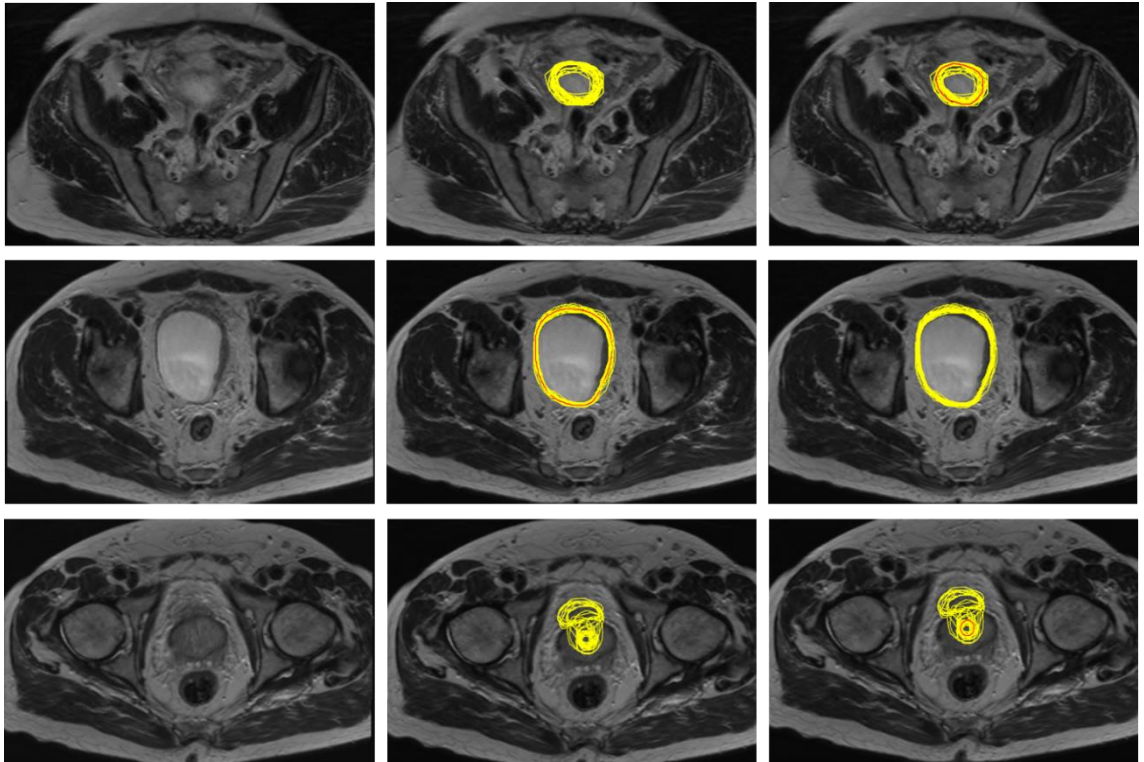


Figure 2.17 Inter-observer contouring variability for case 3.

Top row- superior portion of CTV, middle row- mid section of CTV, bottom row- inferior section of CTV. Contouring colours as per previously.

In case 3, there was less variation in the inferior aspect of the contour compared to Stage 1, Figure 2.17.

In case 4 and 5, variation was minimal in the mid portion of the contour but more noticeable in the superior and inferior aspects, Figures 2.18 and 2.19 respectively.

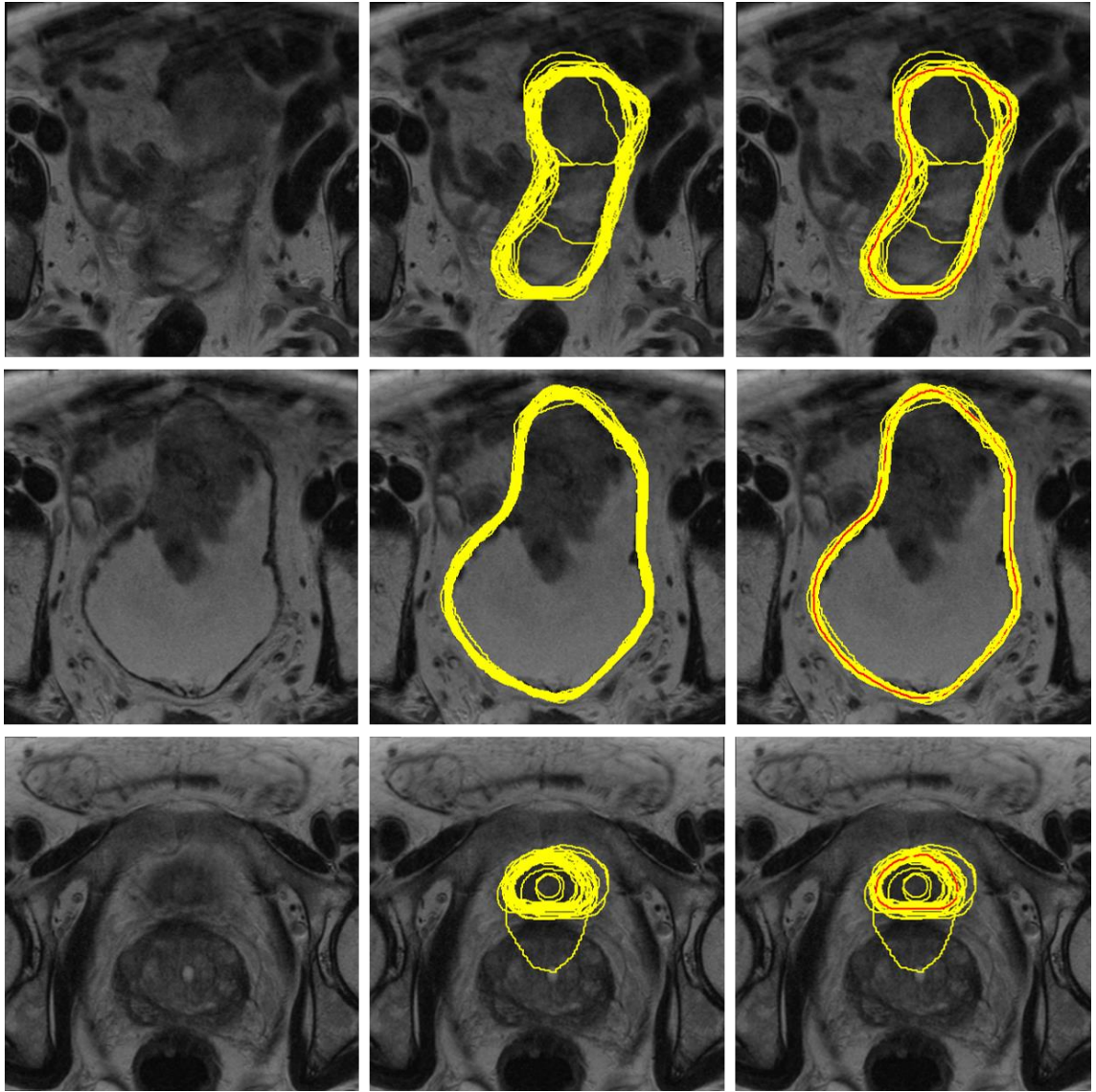


Figure 2.18 Inter-observer contouring variability for case 4.

Top row- superior portion of CTV, middle row- mid section of CTV, bottom row- inferior section of CTV. Contouring colours as per previously.

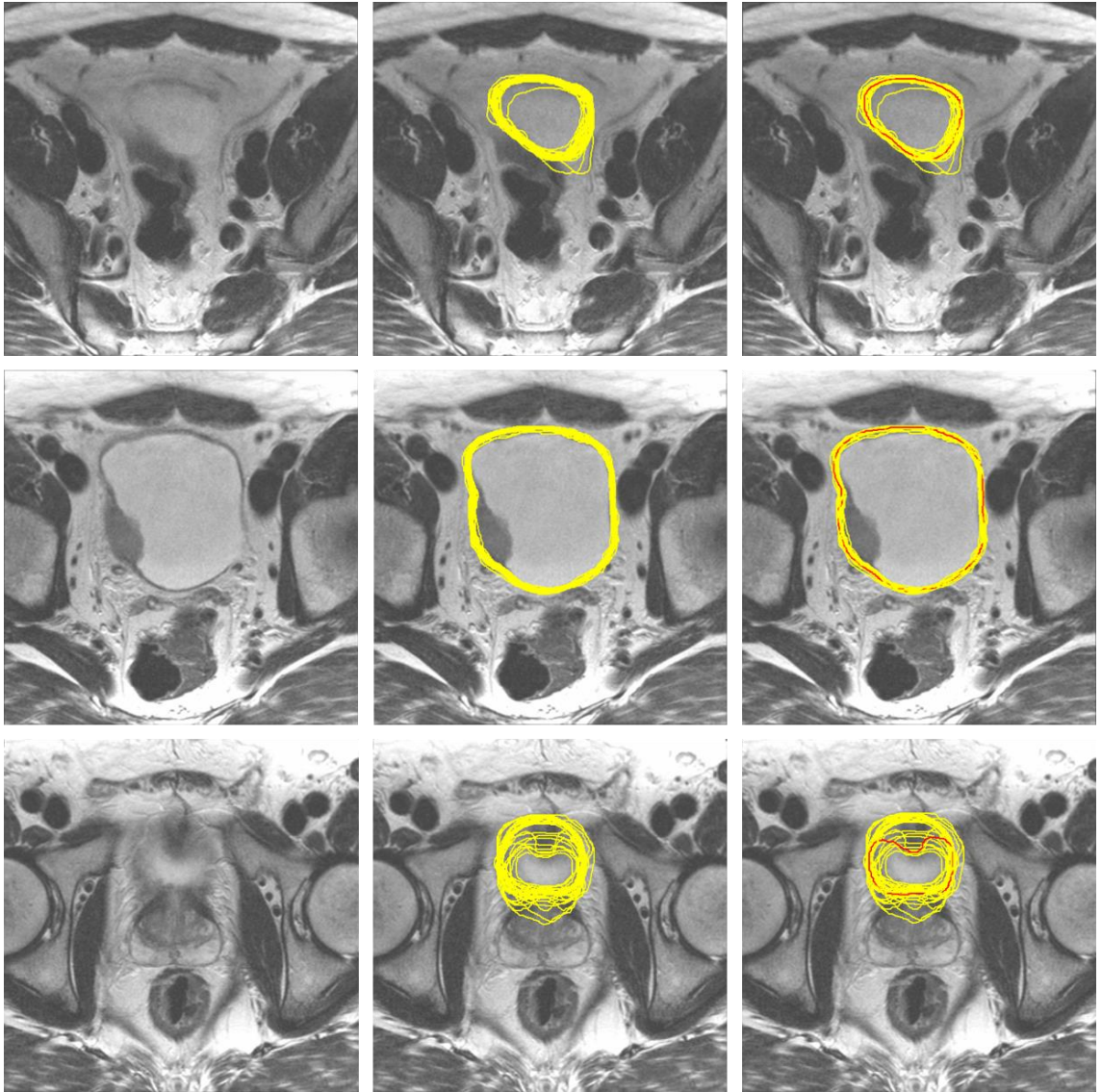


Figure 2.19 Inter-observer contouring variability for case 5.

Top row- superior portion of CTV, middle row- mid section of CTV, bottom row- inferior section of CTV. Contouring colours as per previously. Note inferiorly the incorrect inclusion of the symphysis pubis by some participants.

Outer bladder wall variation

As in Stage 1, variation in outer bladder wall contouring was similar to that observed for the CTV. Close agreement was seen between participants in all three cases.

Table 2.11 Stage 3 Outer bladder wall variation

Outer bladder wall	Case 3	Case 4	Case 5
Median participant volume (range), cc	256.3 (227.5- 279.2)	436.3 (409.0- 455.8)	401.6 (380.1- 410.1)
MVR	1.2	1.1	1.1
All-encompassing volume, cc	318.3	523.6	456.6
STAPLE volume, cc	265.2	446.2	404.5
Median DCE (range) Compared to outer bladder wall_STAPLE	0.96 (0.92- 0.98)	0.97 (0.95-0.98)	0.98 (0.97- 0.99)
Median C₁ (range) Compared to outer bladder wall_STAPLE	0.94 (0.87- 0.96)	0.95 (0.92- 0.97)	0.96 (0.94- 0.98)
Median HD (range), mm Compared to outer bladder wall_STAPLE	6.9 (3.3- 13.4)	6.7 (5.0- 11.7)	4.4 (2.9- 6.3)
Median MDA (range), mm Compared to outer bladder wall_STAPLE	0.9 (0.7- 2.1)	0.9 (0.5- 1.5)	0.6 (0.4- 1.0)

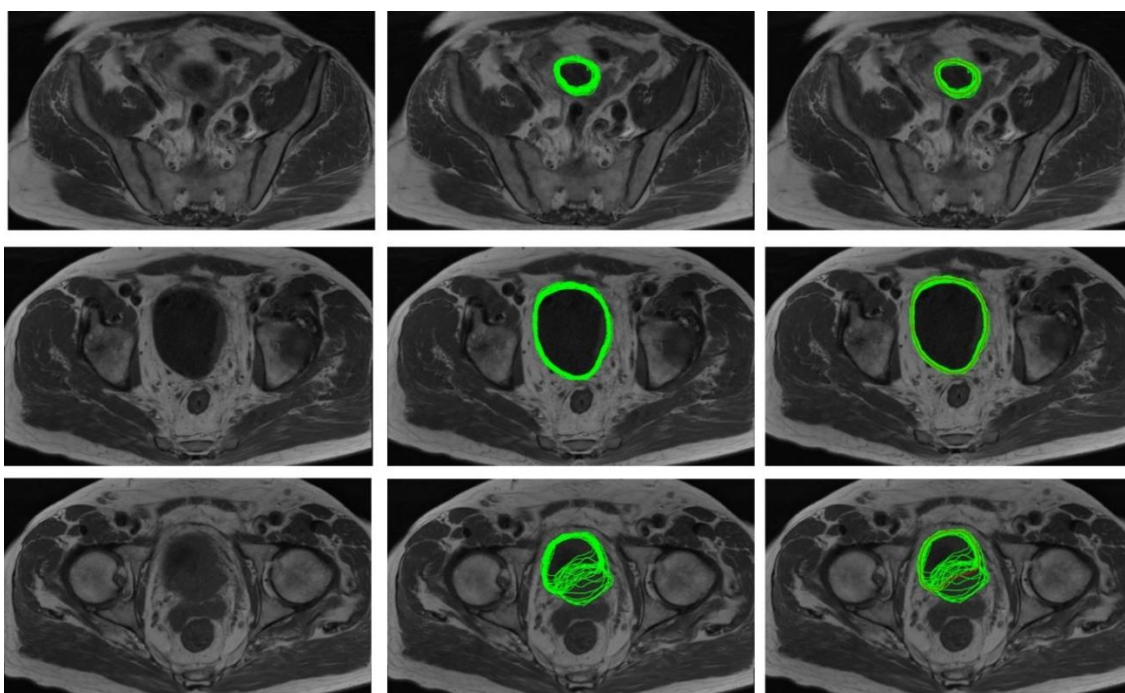


Figure 2.20 Inter-observer contouring variability for case 3.

Top row- superior portion of outer bladder wall, middle row- mid section of outer bladder wall, bottom row- inferior section of outer bladder wall. Contouring colours as per previously.

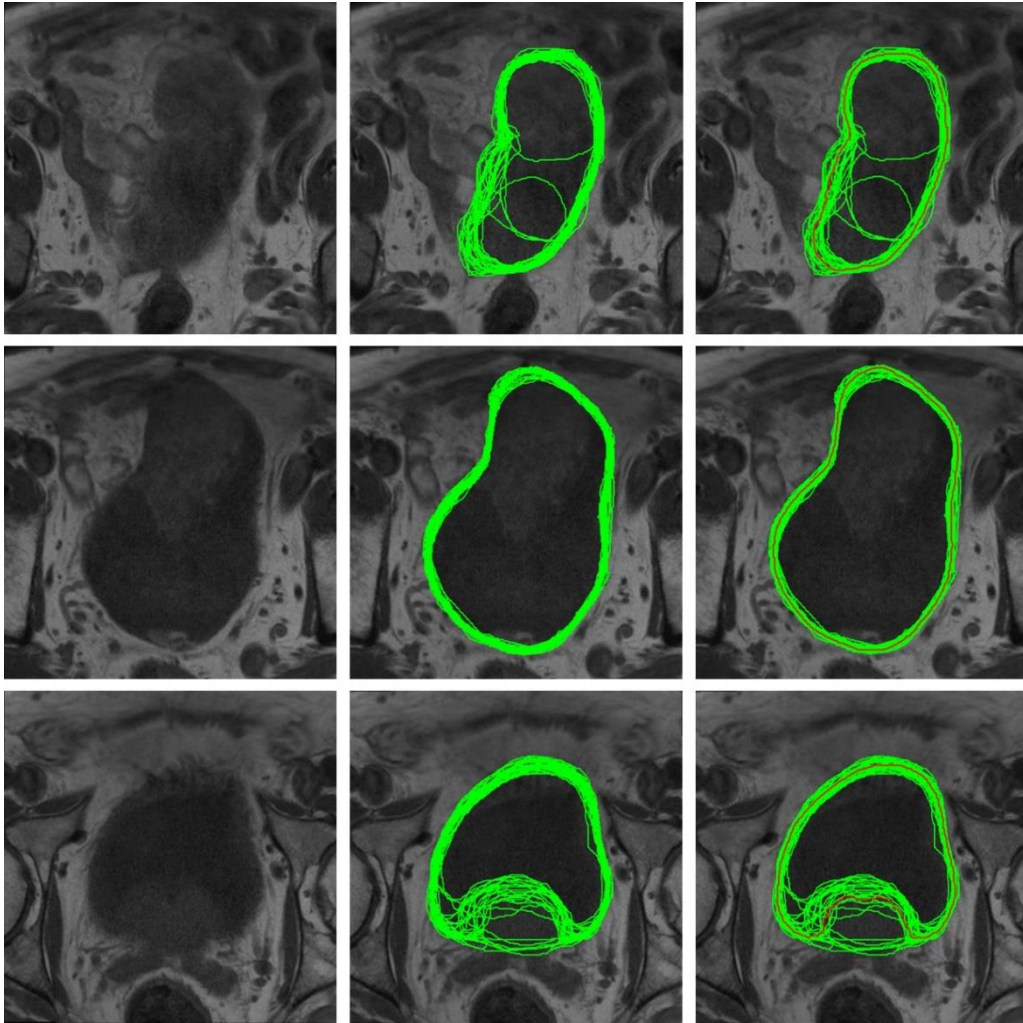


Figure 2.21 Inter-observer contouring variability for case 4.

Top row- superior portion of outer bladder wall, middle row- mid section of outer bladder wall, bottom row- inferior section of outer bladder wall. Contouring colours as per previously.

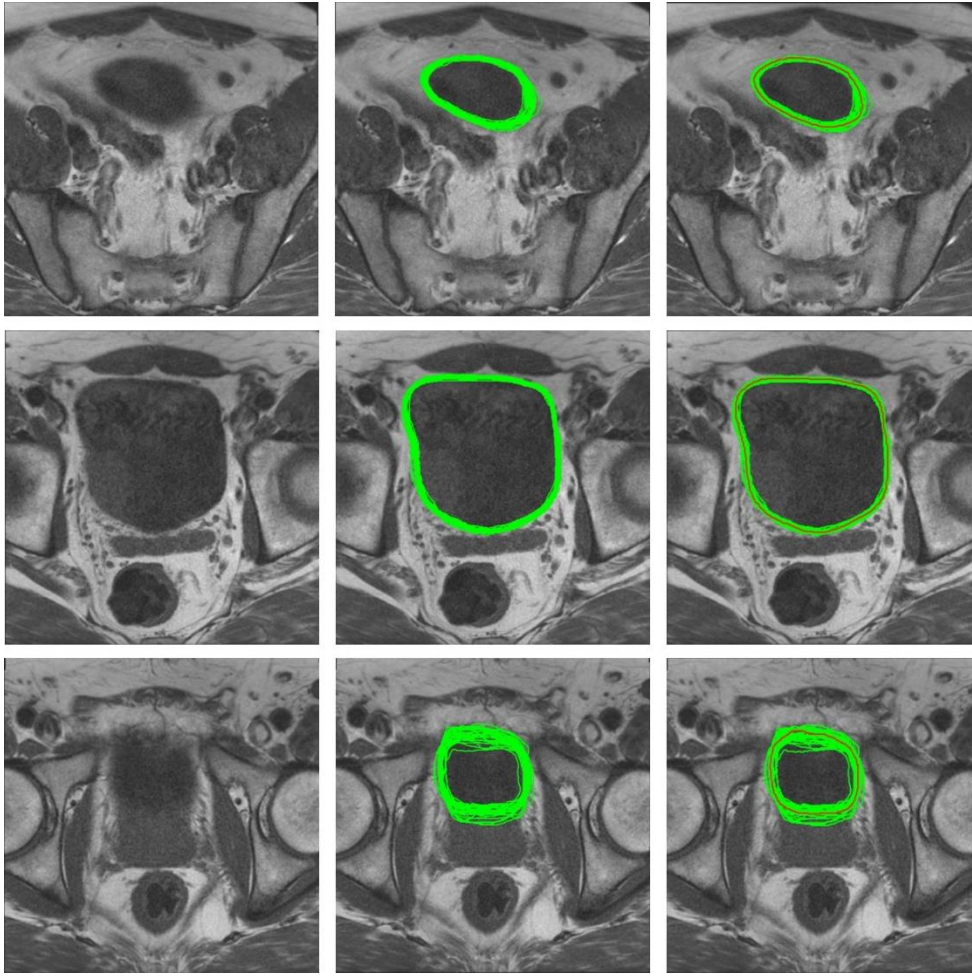


Figure 2.22 Inter-observer contouring variability for case 5.

Top row- superior portion of outer bladder wall, middle row- mid section of outer bladder wall, bottom row- inferior section of outer bladder wall. Contouring colours as per previously.

2.3.5 Impact of consensus guidance generation on interobserver variation

The contours of 26 participants were suitable for this analysis.

Consensus guidance generation resulted in an improvement across all comparison metrics as shown in Table 2.12. A statistically significant improvement in the study's pre-defined primary endpoint (MRI GTV DCE) was observed from 0.68 pre consensus to 0.83 post consensus ($Z = -4.46$, $p < 0.001$). Post consensus MRI metrics compared favourably compared to the more familiar CT based comparator.

Table 2.12 Effect of consensus guidance generation on interobserver variability.

	MRI GTV		MRI CTV		MRI Bladder wall		CT GTV	CT CTV
	Pre	Post	Pre	Post	Pre	Post		
Mean MVR	9.5	2.5	1.3	1.2	1.3	1.1	3.7	1.3
Median DCE	0.68	0.83 [‡]	0.95	0.96	0.95	0.97	0.7	0.97
Median Cκ	0.64	0.79	0.92	0.94	0.91	0.95	0.67	0.95
Median MDA (mm)	2.2	1.4	1.2	1.0	1.4	0.8	2.2	0.6
Median HD (mm)	19.4	13.6	9.5	7.7	8.7	6.0	12.0	4.4

[‡]Consensus guidance generation produced a statistically significant improvement in GTV DICE similarity coefficient, $p < 0.001$. Interobserver metrics calculated using the gold standard structure as ground truth for MRI GTV and CTV comparisons, un-modified STAPLE structure for bladder wall and CT GTV and CTV comparisons. The CT columns show the interobserver variability scores for the CT based case and are included to enable comparison between the values obtained on MRI versus a more familiar CT dataset. Pre = pre consensus guidance generation i.e. Stage 1 results, Post = post consensus i.e. Stage 3 results.

If the results of case 3 alone (repeated pre and post guidance generation) are analysed, again a statistically significant improvement in the study's pre-defined primary endpoint (MRI GTV DCE) is observed from 0.60 pre consensus to 0.66 post consensus ($Z = -2.57$, $p = 0.01$), Table 2.13.

Table 2.13 Effect of consensus guidance generation on interobserver variability, case 3 alone.

	MRI GTV		MRI CTV		MRI Bladder wall	
	Pre	Post	Pre	Post	Pre	Post
MVR	7.6	4.6	1.4	1.2	1.2	1.2
Median DCE	0.60	0.66 [‡]	0.95	0.96	0.96	0.97
Median Cκ	0.56	0.61	0.92	0.93	0.93	0.94
Median MDA (mm)	1.8	1.8	1.3	1.0	1.0	0.9
Median HD (mm)	27.3	18.8	12.2	9.3	6.9	6.9

[‡]Consensus guidance generation produced a statistically significant improvement in GTV DICE similarity coefficient, $p = 0.01$. Abbreviations as above.

2.3.6 Effect of consensus guidance generation on simulated target coverage.

The results of simulated coverage are provided in table 2.14. As expected, given the reduced IOV seen in the CTV structure compared to the GTV structure, coverage of the CTV__gold standard by participants' CTV was better than the coverage seen for GTV__gold standard.

Median coverage of PTV₂__gold standard by the participants' PTV₂ was >95% both pre and post consensus for both margins scenarios. In comparison, coverage of PTV₁__gold standard was less than 95% in all scenarios.

No statistically significant difference in GTV__gold standard, CTV__gold standard or PTV__gold standard coverage was seen pre and post consensus guidance generation. However, the volume of 'non-target' tissue within the participants' PTVs did show a statistically significant improvement in 3 out of the 4 scenarios tested, Table 2.14.

Table 2.14 Results of simulated target coverage

Parameter	Pre-consensus		Post-consensus		p-value
	median	IQR	median	IQR	
GTV_ _{GS} covered by GTV_ _{participant} (%)	66.4	54.5-73.8	67.5	58.5-72.5	0.99
CTV_ _{GS} covered by CTV_ _{participant} (%)	94.6	92.6-96.1	94.9	92.5-96.3	0.47
% of GTV_ _{GS} covered by PTV _{1participant_small}	99.4	94.6-100	98.5	95.2-100	0.96
% of GTV_ _{GS} covered by PTV _{1participant_medium}	100	99.4-100	100	98.2-100	0.70
% of CTV_ _{GS} covered by PTV _{2participant_small}	100	100-100	100	100-100	0.50
% of CTV_ _{GS} covered by PTV _{2participant_medium}	100	100-100	100	100-100	0.79
% of PTV _{1small_GS} covered by PTV _{1participant_small}	81.6	71.2-87.8	78.9	74.9-85.7	0.70
% of PTV _{1GS_medium} covered by PTV _{1participant_medium}	85.8	78.0-91.1	87.3	84.3-92.6	0.10
% of PTV _{2L_GS_small} covered by PTV _{2participant_small}	95.6	94.0-97.0	95.9	93.7-97.4	0.42
% of PTV _{2GS_medium} covered by PTV _{2participant_medium}	96.0	94.6-97.3	96.5	94.5-97.7	0.49
Non-target tissue within PTV _{1participant_small} (cc)	24.1	14.8-46.4	18.3	8.4-29.2	0.03*
Non-target tissue within PTV _{1participant_medium} (cc)	43.6	29.0-77.2	37.2	14.0-58.4	0.52
Non-target tissue within PTV _{2participant_small} (cc)	16.6	9.6-33.4	12.7	7.8-20.4	0.04*
Non-target tissue within PTV _{2participant_medium} (cc)	21.9	12.0-41.1	14.6	9.6-29.1	0.04*

GS= gold standard, * = statistically significant result

2.4 Part 1: Discussion

In Part 1 I evaluated the impact of an MRI specific consensus guideline on inter-observer contouring variability in the context of bladder cancer radiotherapy. This is the first study to undertake such an evaluation in this context.

I found that the development and use of a consensus guideline, which included education on MRI interpretation, resulted in a statically significant improvement in MRI GTV DCE, the study's primary endpoint. Improvement in all other MRI GTV IOV metrics was also seen. Post introduction of the consensus guideline, MRI GTV IOV metrics outperformed those of the more familiar CT dataset in all bar one domain. This improvement in GTV variability is especially encouraging as this structure demonstrated relatively low levels of inter-observer agreement in stage 1.

Improvements to IOV metrics for CTV and outer bladder wall structure sets were also noted but to a lesser degree. This is likely due to the fact that contouring concordance was already high pre-consensus generation despite the relative unfamiliarity of MRI, reducing the scope for further improvement. On visual inspection, variation was most marked at the superior and inferior portions of the contour, and at the interfaces with bladder and bowel, and bladder and prostate suggesting that these areas should be targeted by further educational resources.

The lower rates of concordance seen in the GTV compared to CTV are likely due to three main reasons. Firstly, contouring of the GTV is more technically challenging as the boundary between involved and uninvolved bladder wall is not always clear. In comparison, for the CTV, the dividing line between outer bladder wall and perivesical structures is usually more pronounced. Secondly, the GTV structure is less commonly delineated in standard radiotherapy protocols (particularly in the UK), this means that participants may have less experience in delineating the tumour/tumour bed in day-to-day practice. Thirdly, as the GTV is a smaller structure, the impact of individual variation is magnified when calculating metrics which rely on a ratio (MVR, DCE and $C\lambda$), this makes variations between individuals more pronounced compared to a larger structure such as the CTV.

2.4.1 Choice of IOV metrics used

Although inter-observer variability studies are commonplace in the literature there is wide variation in the IOV metrics used and no consensus on which metrics provide the 'best' method of comparison (25, 26). I chose to evaluate geometric inter-observer variability using five comparison metrics, reporting on volume (including MVR), overlap (DCE and $C\chi$) and surface variation (HD and MDA). This in line with published guidance, as no singular metric provides a complete description of variation (25, 27-29). MVR has been used in previous bladder contouring studies (24, 30) and allows for an appreciation of the variation in contour size amongst participants. It does not however give any indication as to the positional similarity of the structures. DCE and $C\chi$ are overlap metrics and are useful in providing the positional component to a comparison providing an appreciation on the degree of overlap between two structures. However, they are ratios and therefore give no information as to the absolute distance between the two analysed contours. Use of surface measures such as HD and MDA are therefore an important addition, providing information on the actual distance between comparable points.

Compared to other studies investigating IOV in bladder cancer radiotherapy our participants performed favourably. Foroudi et al (24) compared the MVR of 4 radiation oncologists contouring a whole bladder CTV on 4 CT based radiotherapy planning scans, values ranged between 1.06-1.38 with a mean of 1.23 (compared to a mean of 1.2 in this study). A GTV was not contoured. Logue et al (30) asked 8 radiation oncologists to contour a GTV on 2 cases and a CTV on 2 additional cases using radiotherapy planning CTs. Mean MVR was 2.6 for GTV (compared to 2.5 post-consensus in this study) and 1.3 for CTV. Neither study reported on DCE, $C\chi$, HD or MDA making further inter-study comparisons impossible.

There is currently no consensus in the literature as to what exactly defines a 'good' DCE, $C\chi$, HD or MDA score. Cacicedo et al (31), in a systematic review of educational interventions designed to improve contouring in radiotherapy, suggest that a DCE of >0.7 is considered good especially when it is associated with an intervention which results in a DCE improving from <0.7 pre-intervention

to >0.7 post-intervention. Our MRI GTV DCE would fulfil this criterion. A study investigating the use of multimodality imaging in MR-guided radiotherapy for prostate cancer (21), found DCE, C_x and MDA values similar to our own when evaluating prostate CTV contours on T2w MRI (0.93, 0.89 and 1.0mm respectively). Their HD was slightly better than ours at 5.2mm (c.f. 7.7mm). It should be noted however that differences in CTV size in bladder versus prostate radiotherapy make direct comparisons difficult. They did not evaluate a GTV structure.

2.4.2 Use of gold standard structures

In order to carry out IOV comparisons it is necessary to define a reference structure to make comparisons against. Ideally this should represent the 'ground truth' for each structure. Use of a consensus structure based on the opinion of 'experts' is common in the literature. However, defining an expert in this scenario is challenging. Some studies have used the contours of radiologists to define their consensus structure however, studies have shown that radiologist contours often differ from radiation oncologists, as radiation oncologists are more concerned with avoiding target miss (30). Other studies use the contours of more experienced colleagues as the basis for evaluation. However, when incorporating newer imaging modalities into the radiotherapy pathway, years of contouring experience on standard imaging modalities does not necessarily correlate with more accurate contours on a new imaging modality. Indeed, in this study, the contours of participants with greater experience in bladder radiotherapy were not shown to have improved concordance with the gold standard compared to their less experienced colleagues.

Use of a STAPLE structure allows the contours of the whole group to inform the comparison structure. Its probabilistic nature means that outlier contours have less weight in deciding the STAPLE compared to those closer to the mean contour. However, in this study we were concerned that lack of familiarity in MRI interpretation might result in STAPLE structures that were anatomically incorrect, especially if participants' contours converged on an area of MRI misinterpretation. For example, in case 5, a number of participants incorrectly included the symphysis pubis in their CTV contour, this meant that the STAPLE structure also

included the symphysis pubis which is against the contouring guidance. In order to overcome this issue, the STAPLE contour was amended to create a reference 'gold standard' STAPLE. With the help of Dr Sohaib (Consultant Radiologist), myself and Dr Hafeez adapted the STAPLE structures for the MRI CTV and GTV structures to better reflect the anatomical ground truth. For the majority of cases, the changes required to the STAPLE to create the gold standard were minimal. Table 2.15 shows the variability metrics for when the STAPLE is compared to the corresponding gold standard structure. Agreement is generally good apart from the GTV for case 3 which required more adjustments compared to the other cases.

Table 2.15 Comparison between STAPLE contour and Gold standard STAPLE contour.

STAPLE vs Gold standard comparison	DCE	C κ	MDA (mm)	HD (mm)
Case 1 GTV	0.86	0.84	0.8	11.8
Case 1 CTV	0.97	0.95	0.6	3.2
Case 2 GTV	0.9	0.88	0.6	2.95
Case 2 CTV	0.96	0.94	0.8	5.0
Case 3 GTV- Stage 1	0.53	0.49	1.3	40.7
Case 3 CTV- Stage 1	0.98	0.96	0.6	10.2
Case 3 GTV- Stage 3	0.64	0.6	1.0	29.4
Case 3 CTV- Stage 3	0.99	0.99	0.1	6.9
Case 4 GTV	0.99	0.99	0.1	5.0
Case 4 CTV	1	0.99	0.1	9.2
Case 5 GTV	0.97	0.96	0.3	5.9
Case 5 CTV	0.99	0.97	0.4	4.5

2.4.3 Impact of case selection

When selecting cases for this study I considered a variety of factors. Firstly, the quality of the images and the visibility of the tumour was important. I selected cases where tumour was still evident thereby excluding patients who had undergone a complete TURBT. This was to test whether participants could distinguish healthy bladder wall from visible disease. Secondly, all cases needed

to have diffusion weighted imaging available, along with T1W and T2W sequences. This is because multiparametric MRI images improve the diagnostic accuracy of bladder MRIs, providing valuable additional information on tumour extent. Thirdly, case mix was important, I aimed to include at least one female patient and chose patients with tumour in a variety of positions. At least one case required the CTV to be extended into the urethra to test how participants approached this situation.

The decision to use 2 new cases for stage 3 rather than repeating the same cases for Stage 1 and 3 was discussed extensively between myself, Dr Hafeez and Prof Huddart. Due to the design of this study, where the cases and contours from Stage 1 were used as an educational resource in Stage 2, it was felt that if all cases were simply repeated for Stage 3 we would only be testing the participants recall of the correct contours as discussed at the teaching/contour development session rather than a true improvement in their MRI interpretation skills. By introducing new cases we felt that this risk was reduced. We elected to keep case 3 in both stages for 2 reasons. Firstly, this case tested the participants' approach to extending the CTV into the prostatic urethra. At the time the study was developed I had access to a limited pool of MRIs. Very few had a visible tumour and a large enough field of view to enable the contour to be extended the required distance into the prostate and as a result there was no suitable alternatives available. Any recall bias was minimised by ensuring there was an extended time period (>9 months) between the education/consensus session and Stage 3 contouring. Images of case 3 GTV were also not included in the circulated guidance document. Secondly, by keeping this case the same it was possible to undertake my exploratory dosimetric analysis which required the exact same case in Stage 1 and 3.

The weakness of this approach is that case complexity varies across patients and by introducing new cases for Stage 3 it is possible that any improvement in interobserver variability is simply due to easier cases being selected. I tried to mitigate this risk by selecting new cases I deemed to be of similar complexity, with tumour in a similar position to previously. I also took the mean values across all 3 cases in each stage when performing the pre and post consensus analysis.

It should be noted that the GTV in case 4 was considerably bigger than the other GTVs, measuring 101 cc compared to an average of 16 cc for the other cases. This large size may have masked the IOV seen due to the ratio nature of DCE, Cx and MVR. However, the non ratio metrics MDA and HD also showed improvement pre and post consensus generation suggesting the improvement seen was genuine. This is backed up by the fact that, when analysed separately, a statistically significant difference was also seen in the DICE for the MRI GTV for case 3 which was repeated in both stages.

Finally, it would have been preferable to use dedicated planning MRIs in this study rather than diagnostic MRIs as this would more accurately reflect the image sets used for radiotherapy planning. Diagnostic MRIs from our centre tend to use small field of views on their T2W images which makes dosimetric comparisons difficult. In addition, diagnostic MRIs are acquired using different bladder filling protocols which makes direct comparisons between volumes drawn on MRI and those drawn on radiotherapy planning CTs impossible. Unfortunately, at the time of this study's development such MRI planning scans were not available. However, I still believe this study has value as its purpose was to increase participants' confidence in contouring on MRI and to enable consensus generation which can then be used by the wider radiation oncology community. The principles of MRI interpretation are the same regardless of whether the scan is for diagnostic or planning purposes.

2.4.4 Examples of others using consensus guidance to improve contouring variability.

Inter-observer contouring variation has been described as the weak link in the radiotherapy treatment pathway (32). Within the literature, interventions to improve inter-observer contouring variability can be broken down into four main categories: imaging interventions such as the introduction of new imaging modalities to the radiotherapy pathway, radiotherapy guideline or protocol development, teaching or educational interventions, and the use of auto contouring technology. There is currently no consensus as to which of these interventions is the most successful (33). In this study we used guideline development interwoven with education to improve the variability of participants'

contours. I am not aware of any similar studies investigating the effect of guidance generation in bladder cancer contouring however, a similar technique was deployed by Nijkamp et al (9) for early stage rectal cancer delineation. Here, 11 radiation oncologists contoured CTVs for 8 patients before and after guidance generation. They found a significant improvement in target delineation variation. Indeed, in a review of the literature, Vinod et al (33) found that in seven out of the nine identified studies, a statistically significant improvement in IOV occurred with the development of guidelines.

In our study it is likely that both the guideline generation and the education given on MRI interpretation helped to improve the IOV seen. In the case of the GTV, guidance on what should be included in this structure did not change between Stage 1 and Stage 3 however, an improvement in variation was seen. This suggests that it was the educational element of our intervention which helped improve variability. In the case of the CTV, advice was given on how best to contour the prostatic urethra, this resulted in decreased variation in this region of visual inspection, highlighting the benefit of our consensus guidance.

2.4.5 Statistical testing

Analysis of multiple structures and use of multiple metrics made sample size calculation for this study a challenge. For simplicity, I therefore chose to base my sample size calculation on the change in MRI GTV DCE only. The reason for this was two-fold. Firstly, based on an initial pilot cohort it was clear that the GTV structure had the lowest concordance of all the analysed structures. This structure was therefore most in need of improvement. The low level of concordance also meant that there was scope to detect a larger difference pre and post consensus generation keeping the sample size within a manageable target. Secondly, I felt that if it was only possible to select one metric, an overlap metric provided the most useful measure of the variation as a whole accepting its limitations as discussed above. By preselecting a single analysis it was also possible to avoid the need for a Bonferroni correction allowing statistical significance to be set at $p=0.05$.

Whilst this study resulted in a statically significant improvement in DCE, the clinical significance of this improvement is not known. Clinical significance is dependent on where the discrepancy lies, and the margins added during planning. For example, variations in GTV contour may not have a clinical impact as long as the true target remains covered and OAR dose is not exceeded during the planning process.

In order to address this weakness in the study, I performed an exploratory analysis on the estimated dosimetric impact on IOV. It was only possible to perform this analysis on case 3 as only this case had a large enough field of view to accommodate the planning margins used.

2.4.6 Impact of guidance on simulated dosimetry

The development of consensus guidance failed to produce a statistically significant improvement in gold standard target coverage. This could be for a variety of reasons. Firstly, this analysis only included case 3, which of all the cases was the most technically challenging. The boundary between healthy and diseased bladder wall was difficult to appreciate and diffusion weighted imaging only provided limited additional benefit. Even our expert radiologist struggled to consistently define the tumour edge. This means that even with consensus guidance, participants were likely to struggle with this case. Secondly, the improvement in DCE may have been more heavily influenced by changes to participants GTV's in areas away from the gold standard position. For example, the volume of 'non target' tissue receiving 95% of planned dose (defined as the areas of a participant's PTV falling outside of the gold standard PTV) did significantly decrease after consensus generation suggesting that participants contours decreased in size and included less normal tissue. The clinical impact of this is hard to gauge as further OAR analysis was not performed.

It should be noted that the IOV seen in CTV delineation appeared to have a minimal impact on simulated target coverage. The median coverage of the gold standard PTV₂ using participants' PTVs was greater than >95% pre and post consensus. This is encouraging as it suggests that despite the reduced familiarity of contouring on MRI, participants CTV contours produced PTVs which would

have adequately covered the gold standard PTVs. In comparison, coverage of PTV₁ was below this threshold. This suggests that although IOV improved after consensus generation the variability seen in GTV delineation would still have a dosimetric impact on gold standard PTV₁ coverage particularly when the smaller planning margin was used. It does raise the question as to what planning margins would be needed to ensure adequate coverage of the GTV. If a 5mm margin was used to account for inter-observer variability alone then the gold standard GTV would have been well covered. However, to this would then need to be added all the other components of the planning margin e.g. set up error in order to give an overall CTV to PTV margin. Future work should involve investigation into the margin needed to encompass the contouring variability seen so that this can be incorporated into our overall planning margins. It is likely that the margin needed to account for GTV variation would be greater than that needed for CTV variation, and this would only be needed for treatments using two or more dose levels e.g. tumour boost or partial bladder protocols.

2.5 Part 1: Conclusion

This study has shown that development of a consensus guideline with interwoven education can improve MRI based inter-observer contouring variability. This improvement was statistically significant for GTV delineation, however as residual variation is still present further work should be undertaken to establish the clinical impact this may have. This is particularly important when considering appropriate planning margins for partial bladder or tumour boost radiotherapy techniques where accurate GTV delineation becomes more important. Pleasingly, the more commonly contoured CTV structure showed minimal IOV despite the relative unfamiliarity of MRI.

2.6 Part 1 References

1. Gandhi N, Krishna S, Booth CM, Breau RH, Flood TA, Morgan SC, et al. Diagnostic accuracy of magnetic resonance imaging for tumour staging of bladder cancer: systematic review and meta-analysis. *BJU international*. 2018;122(5):744-53.

2. Huang L, Kong Q, Liu Z, Wang J, Kang Z, Zhu Y. The Diagnostic Value of MR Imaging in Differentiating T Staging of Bladder Cancer: A Meta-Analysis. *Radiology*. 2018;286(2):502-11.
3. Woo S, Suh CH, Kim SY, Cho JY, Kim SH. Diagnostic performance of MRI for prediction of muscle-invasiveness of bladder cancer: A systematic review and meta-analysis. *European journal of radiology*. 2017;95:46-55.
4. Crozier J, Papa N, Perera M, Ngo B, Bolton D, Sengupta S, et al. Comparative sensitivity and specificity of imaging modalities in staging bladder cancer prior to radical cystectomy: a systematic review and meta-analysis. *World journal of urology*. 2018.
5. Cloak K, Jameson MG, Paneghel A, Wiltshire K, Kneebone A, Pearse M, et al. Contour variation is a primary source of error when delivering post prostatectomy radiotherapy: Results of the Trans-Tasman Radiation Oncology Group 08.03 Radiotherapy Adjuvant Versus Early Salvage (RAVES) benchmarking exercise. *Journal of medical imaging and radiation oncology*. 2019;63(3):390-8.
6. Roach D, Holloway LC, Jameson MG, Dowling JA, Kennedy A, Greer PB, et al. Multi-observer contouring of male pelvic anatomy: Highly variable agreement across conventional and emerging structures of interest. *Journal of medical imaging and radiation oncology*. 2019;63(2):264-71.
7. Louie AV, Rodrigues G, Olsthoorn J, Palma D, Yu E, Yaremko B, et al. Inter-observer and intra-observer reliability for lung cancer target volume delineation in the 4D-CT era. *Radiotherapy and oncology : journal of the European Society for Therapeutic Radiology and Oncology*. 2010;95(2):166-71.
8. Caravatta L, Macchia G, Mattiucci GC, Sainato A, Cernusco NL, Mantello G, et al. Inter-observer variability of clinical target volume delineation in radiotherapy treatment of pancreatic cancer: a multi-institutional contouring experience. *Radiation oncology (London, England)*. 2014;9:198.
9. Nijkamp J, de Haas-Kock DF, Beukema JC, Neelis KJ, Woutersen D, Ceha H, et al. Target volume delineation variation in radiotherapy for early stage rectal cancer in the Netherlands. *Radiotherapy and oncology : journal of the European Society for Therapeutic Radiology and Oncology*. 2012;102(1):14-21.
10. Petrič P, Hudej R, Rogelj P, Blas M, Tanderup K, Fidarova E, et al. Uncertainties of target volume delineation in MRI guided adaptive brachytherapy of cervix cancer: a multi-institutional study. *Radiotherapy and oncology : journal of the European Society for Therapeutic Radiology and Oncology*. 2013;107(1):6-12.
11. Peters LJ, O'Sullivan B, Giralt J, Fitzgerald TJ, Trotti A, Bernier J, et al. Critical impact of radiotherapy protocol compliance and quality in the treatment of advanced head and neck cancer: results from TROG 02.02. *Journal of clinical oncology : official journal of the American Society of Clinical Oncology*. 2010;28(18):2996-3001.
12. Wuthrick EJ, Zhang Q, Machtay M, Rosenthal DI, Nguyen-Tan PF, Fortin A, et al. Institutional clinical trial accrual volume and survival of patients with head and neck cancer. *Journal of clinical oncology : official journal of the American Society of Clinical Oncology*. 2015;33(2):156-64.
13. Crane CH, Winter K, Regine WF, Safran H, Rich TA, Curran W, et al. Phase II study of bevacizumab with concurrent capecitabine and radiation followed by maintenance gemcitabine and bevacizumab for locally advanced pancreatic cancer: Radiation Therapy Oncology Group RTOG 0411. *Journal of*

clinical oncology : official journal of the American Society of Clinical Oncology. 2009;27(25):4096-102.

14. Valentini V, Gambacorta MA, Barbaro B, Chiloiri G, Coco C, Das P, et al. International consensus guidelines on Clinical Target Volume delineation in rectal cancer. *Radiotherapy and oncology : journal of the European Society for Therapeutic Radiology and Oncology*. 2016;120(2):195-201.

15. Wu AJ, Bosch WR, Chang DT, Hong TS, Jabbour SK, Kleinberg LR, et al. Expert Consensus Contouring Guidelines for Intensity Modulated Radiation Therapy in Esophageal and Gastroesophageal Junction Cancer. *International journal of radiation oncology, biology, physics*. 2015;92(4):911-20.

16. Harris VA, Staffurth J, Naismith O, Esmail A, Gulliford S, Khoo V, et al. Consensus Guidelines and Contouring Atlas for Pelvic Node Delineation in Prostate and Pelvic Node Intensity Modulated Radiation Therapy. *International journal of radiation oncology, biology, physics*. 2015;92(4):874-83.

17. Gregoire V, Ang K, Budach W, Grau C, Hamoir M, Langendijk JA, et al. Delineation of the neck node levels for head and neck tumors: a 2013 update. DAHANCA, EORTC, HKNPCSG, NCIC CTG, NCRI, RTOG, TROG consensus guidelines. *Radiotherapy and oncology : journal of the European Society for Therapeutic Radiology and Oncology*. 2014;110(1):172-81.

18. Salembier C, Villeirs G, De Bari B, Hoskin P, Pieters BR, Van Vulpen M, et al. ESTRO ACROP consensus guideline on CT- and MRI-based target volume delineation for primary radiation therapy of localized prostate cancer. *Radiotherapy and oncology : journal of the European Society for Therapeutic Radiology and Oncology*. 2018;127(1):49-61.

19. Khalifa J, Supiot S, Pignot G, Hennequin C, Blanchard P, Pasquier D, et al. Recommendations for planning and delivery of radical radiotherapy for localized urothelial carcinoma of the bladder. *Radiotherapy and Oncology*.

20. Warfield SK, Zou KH, Wells WM. Simultaneous truth and performance level estimation (STAPLE): an algorithm for the validation of image segmentation. *IEEE transactions on medical imaging*. 2004;23(7):903-21.

21. Pathmanathan AU, McNair HA, Schmidt MA, Brand DH, Delacroix L, Eccles CL, et al. Comparison of prostate delineation on multimodality imaging for MR-guided radiotherapy. *The British journal of radiology*. 2019;92(1095):20180948.

22. Leung E, D'Souza D, Bachand F, Han K, Alfieri J, Huang F, et al. MRI-based interstitial brachytherapy for vaginal tumors: A multi-institutional study on practice patterns, contouring, and consensus definitions of target volumes. *Brachytherapy*. 2019;18(5):598-605.

23. Raman S, Chin L, Erler D, Atenafu EG, Cheung P, Chu W, et al. Impact of Magnetic Resonance Imaging on Gross Tumor Volume Delineation in Non-spine Bony Metastasis Treated With Stereotactic Body Radiation Therapy. *International journal of radiation oncology, biology, physics*. 2018;102(4):735-43.e1.

24. Foroudi F, Haworth A, Pangehel A, Wong J, Roxby P, Duchesne G, et al. Inter-observer variability of clinical target volume delineation for bladder cancer using CT and cone beam CT. *Journal of medical imaging and radiation oncology*. 2009;53(1):100-6.

25. Hanna GG, Hounsell AR, O'Sullivan JM. Geometrical analysis of radiotherapy target volume delineation: a systematic review of reported comparison methods. *Clinical oncology (Royal College of Radiologists (Great Britain))*. 2010;22(7):515-25.

26. Fotina I, Lütgendorf-Caucig C, Stock M, Pötter R, Georg D. Critical discussion of evaluation parameters for inter-observer variability in target definition for radiation therapy. *Strahlentherapie und Onkologie : Organ der Deutschen Röntgengesellschaft [et al]*. 2012;188(2):160-7.
27. Vinod SK, Jameson MG, Min M, Holloway LC. Uncertainties in volume delineation in radiation oncology: A systematic review and recommendations for future studies. *Radiotherapy and Oncology*. 2016;121(2):169-79.
28. Jameson MG, Holloway LC, Vial PJ, Vinod SK, Metcalfe PE. A review of methods of analysis in contouring studies for radiation oncology. *Journal of medical imaging and radiation oncology*. 2010;54(5):401-10.
29. Kottner J, Audigé L, Brorson S, Donner A, Gajewski BJ, Hróbjartsson A, et al. Guidelines for Reporting Reliability and Agreement Studies (GRRAS) were proposed. *Journal of clinical epidemiology*. 2011;64(1):96-106.
30. Logue JP, Sharrock CL, Cowan RA, Read G, Marrs J, Mott D. Clinical variability of target volume description in conformal radiotherapy planning. *International journal of radiation oncology, biology, physics*. 1998;41(4):929-31.
31. Cacicedo J, Navarro-Martin A, Gonzalez-Larragan S, De Bari B, Salem A, Dahele M. Systematic review of educational interventions to improve contouring in radiotherapy. *Radiotherapy and oncology : journal of the European Society for Therapeutic Radiology and Oncology*. 2020;144:86-92.
32. Roques TW. Patient selection and radiotherapy volume definition - can we improve the weakest links in the treatment chain? *Clinical oncology (Royal College of Radiologists (Great Britain))*. 2014;26(6):353-5.
33. Vinod SK, Min M, Jameson MG, Holloway LC. A review of interventions to reduce inter-observer variability in volume delineation in radiation oncology. *Journal of medical imaging and radiation oncology*. 2016;60(3):393-406.

2.7 Part 2: Consensus guidance generation- Method

After completion of Stage 1, participants were invited to participate in an interactive webinar led by myself, Dr Hafeez and Dr Sohaib. The webinar was held on 30th January 2019. During this webinar inter-observer contouring variations were discussed. Common pitfalls in MRI interpretation were highlighted by Dr Sohaib and preliminary structure definition statements for contouring were suggested based on those from the RAIDER clinical trial.

Using the preliminary structure definition statements as a starting point I performed a literature review of existing bladder cancer contouring guidelines. A search of MEDLINE PubMed was carried out using the following search term: “Urinary Bladder Neoplasms/radiotherapy” [MeSH] AND (contour* OR delineat* OR guideline*). In January 2019 this yielded 72 results. After abstract screening (English only), 3 relevant articles were found of which 2 (1, 2) were used in guideline development along with relevant articles from their reference sections. The third paper was not included as it was published in 1986 and radiotherapy techniques have changed considerably since then (3). In addition, papers from key bladder trials were reviewed for information on their defined target volumes (4-8).

Guidance statements were then evaluated using a Delphi survey (9) to assess the level of agreement for each of the statements among participating clinical/radiation oncologists. Participants were asked to rate the strength of their agreement for each of the statements on a scale of 1 (strongly disagree) to 9 (strongly agree), they were also given the option of “unable to score” if they felt unable to give a recommendation due to insufficient expertise.

The results of the survey were summarised in descriptive statistics. The percentage of participants who scored each statement as 1-3 (disagree), 4-6 (equivocal), 7-9 (agree) was recorded. Consensus was defined *a priori* as any statement which scored agree (7-9) by $\geq 70\%$ participants.

2.8 Part 2: Results

Sixteen preliminary consensus statements were developed and assessed as part of the Delphi process. An elective nodal volume was not included as there is no conclusive evidence that this improves patient outcomes (4, 10).

In total 26 clinicians participated in the Delphi survey.

The results from the Delphi survey are tabulated in table 2.16. In total 13 statements reached consensus agreement (highlighted in green in table 2.16).

2.8.1 Agreed consensus statements

2.8.1.1 Delineation of the gross tumour volume (GTV)

Agreed consensus statements:

Prior to outlining, diagnostic images and surgical bladder map should be referred to where available in order to assist tumour localisation.

All extravesical tumour and pathological bladder wall thickening due to cancer should be included in the GTV.

Initial pre-treatment disease should be included in the GTV.

If no tumour is visible (i.e. post transurethral resection of the bladder tumour, TURBT and, or following chemotherapy), the tumour bed is reconstructed at the appropriate bladder wall position using available diagnostic imaging, surgical bladder map, or fiducial markers.

2.8.1.2 Delineation of the clinical target volume (CTV)

Agreed consensus statement:

The CTV should encompass the entire tumour, (or tumour bed where appropriate), the whole bladder and any area of extravesical spread

2.8.1.3 Inclusion of the urethra and prostate within the CTV

Agreed consensus statements:

If GTV is at the base of bladder or if distant CIS is present the CTV should also include 1.5cm of prostatic urethra in males or 1cm of urethra in females.

The urethra is difficult to visualise without catheterisation therefore in the male pelvis using a 1cm roller ball (diameter) begin at bladder neck extending the contouring caudally to the start of penile urethra so total length is 1.5cm.

In the female pelvis begin contouring using a 1cm roller ball at the internal urethral orifice extending the structure caudally to the perineum along the anterior wall of the vagina so total length is 1cm.

2.8.1.4 Delineation of the Rectum

Agreed consensus statements:

The rectum is outlined to include the full circumference and rectal contents. Outlining should extend from the lowest level of ischial tuberosities to the recto-sigmoid junction.

The recto-sigmoid junction will be defined by the point at which the rectum loses its round shape in the axial plane and turns anteriorly into the sigmoid colon (often best appreciated on the sagittal image).

2.8.1.5 Delineation of other bowel

Agreed consensus statement:

The small and large bowel (including sigmoid colon) will be outlined as a single solid structure. The entire small and large bowel visible on relevant levels of the planning scan will be outlined as individual bowel loops. The superior extent of outlining should be 2cm beyond the superior extent of PTV.

2.8.1.6 Delineation of Femoral Heads

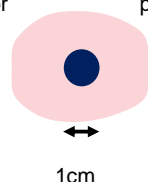
Agreed consensus statement:

Both the femoral heads are outlined to the bottom of the curvature of their heads (femoral necks are not included).

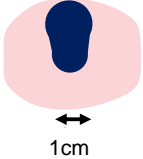
Table 2.16 Results of Delphi consensus.

Statements highlighted in green are those which met the pre-defined threshold for agreement³.

Structure	Statement	Agreement score, % of participants			
		Disagree (1-3)	Equivocal (4-6)	Agree (7-9)	Unable to comment
Gross tumour volume (GTV)	Prior to outlining, diagnostic images and surgical bladder map should be referred to where available in order to assist tumour localisation.	0	0	100	0
	All extravesical tumour and pathological bladder wall thickening due to cancer should be included in the GTV.	0	8	92	0
	Initial pre-treatment disease should be included in the GTV.	0	15	85	0
	If no tumour is visible (i.e. post transurethral resection of the bladder tumour, TURBT and, or following chemotherapy), the tumour bed is reconstructed at the appropriate bladder wall position using available diagnostic imaging, surgical bladder map, or fiducial markers.	0	8	92	0
Clinical target volume (CTV)	This should encompass the entire tumour, (or tumour bed where appropriate), the whole bladder and any area of extravesical spread.	4	0	96	0
	If GTV is at the base of bladder or if distant CIS is present the CTV should also include 1.5cm of prostatic urethra in males or 1cm of urethra in females.	0	4	96	0
	The urethra is difficult to visualise without catheterisation: In the male pelvis using a 1cm roller ball (diameter) begin at bladder neck extending the contouring caudally to the start of penile urethra so total length is 1.5cm.	4	8	88	0
	If prostatic urethra is not visible within the prostate gland, central positioning of the roller ball within the prostate gland on axial slice is acceptable surrogate for true position as shown in Figure 1.	12	19	69	0
	Figure 1. Acceptable surrogate for prostatic urethra contour (dark) on axial representation through prostate (light).				



³ Table and figures developed by Dr Shaista Hafeez

	<p>Figure 2. Acceptable variation is extension of prostatic urethra volume anteriorly.</p>  <p>1cm</p>	0	12	88	0
	In the female pelvis begin contouring using a 1cm roller ball at the internal urethral orifice extending the structure caudally to the perineum along the anterior wall of the vagina so total length is 1cm.	4	4	88	4
Rectum	The rectum is outlined to include the full circumference and rectal contents. Outlining should extend from the lowest level of ischial tuberosities to the recto-sigmoid junction	4	4	92	0
	The recto-sigmoid junction will be defined by the most inferior of the following three landmarks				
	i) the point at which the rectum loses its round shape in the axial plane and turns anteriorly into the sigmoid colon (often best appreciated on the sagittal image);	0	0	100	0
	ii) the bifurcation of the inferior mesenteric artery into the sigmoid and superior rectal arteries;	15	38	35	12
	iii) the S2/S3 junction.	23	19	54	4
Other bowel	The small and large bowel (including sigmoid colon) will be outlined as a single solid structure. The entire small and large bowel visible on relevant levels of the planning scan will be outlined as individual bowel loops. The superior extent of outlining should be 2cm beyond the superior extent of PTV.	8	4	85	4
Femoral Heads	Both the femoral heads are outlined to the bottom of the curvature of their heads (femoral necks are not included).	0	4	96	0

2.9 Part 2: Discussion

The Delphi process is a well-established methodology for consensus generation (9). In this study, we adapted the process by using the webinar as an informal first round. The second round was completed around the time of the second contouring session. A formal third round was not undertaken due to the high level of agreement seen but participants had a window of opportunity to provide feedback if they wanted. While the contouring exercise concentrated on CTV, GTV and bladder wall delineation, the consensus guidance also included statements about organs at risk. This is because consensus on these structures is also necessary if there is to be consistency in contouring across centres.

2.9.1 GTV delineation

Delineation of the bladder GTV is not standard practice in the UK outside of a clinical trial. However, as interest in multi-dose level radiotherapy is increasing, we believe it is helpful to provide guidance on what the GTV should entail if delineation is required. We recommend that the GTV should contain all sites of initial pre-treatment disease (as defined by imaging and cystoscopy), therefore we advocate the inclusion of a tumour bed even if this is not clearly visible on MRI/CT. This is in line with the RAIDER trial (NCT02447549). This approach differs slightly from the guidance of Hindson's group (1) which states that if there has been a maximal TURBT with no extravesical spread there will be no definable GTV. Our rationale behind this deviation is that localised recurrences post bladder preserving therapy tend to occur at the site of initial disease (11) and if a boost region is to be defined it should take into account all known sites of pre-treatment disease. In addition, there is evidence to suggest that the absence of tumour on repeat TURBT after neoadjuvant treatment does not predict for pathological absence of tumour at radical cystectomy (12, 13). It should also be remembered that with respect to MRI, tumours of <1cm and areas of CIS may not be apparent on imaging.

Technically speaking if there is no tumour visible then there is no 'gross tumour volume' to define and so in this case it would be more accurate to describe this area as a CTV_{boost} or CTV_{high dose} structure. However, 92% of participants in the consensus survey agreed with the statement that the GTV should include the

tumour bed if no visible tumour was present, with no participants disagreeing and 8% being equivocal. This is perhaps due to the fact that a large number of the participants had participated in the RAIDER trial which includes the tumour bed in the GTV structure and they are therefore familiar and comfortable with this definition.

2.9.2 CTV delineation

We recommend that the CTV should incorporate the GTV and areas at risk of harbouring microscopic disease. Outside of the trial setting, we recommend the inclusion of the whole bladder (to the edge of the outer bladder wall) along with any extravesical tumour extension. This recommendation is in line with the RAIDER trial control arm (14) and the previous BCON (5), BC2001 (4), and TROG (6) trials. Inclusion of the whole bladder is recommended as urothelial cancer often occurs as a result of field change to the urothelium.

In cases where imaging or cystoscopy confirms the presence of direct invasion of the bladder tumour into the prostate we would recommend the inclusion of the whole prostate within the CTV. For cases where this is not seen, we recommend that the urethra is included within the CTV when tumour is present at the base of the bladder or distant CIS is found at cystoscopy. This recommendation is based on the findings of surgical cystectomy series. In male patients, concomitant involvement of the prostatic urethra with transitional cell carcinoma ranged between 15.6-48% (15-26) based on histopathological reviews of cystectomy specimens, whilst in women, involvement occurs in approximately 12% (calculated from a weighted average of 378 patients from 7 studies) (27). It should be noted that the rates of stromal involvement (which is known to negatively impact on survival outcomes (22, 25, 26)) are lower (ranging between 5.2-18.2% (15-22, 26)). Many of the above studies carried out multivariate analysis to identify risk factors of urethral involvement. Tumour at the base of the bladder was found to be statistically significant in 9 studies (16-19, 21, 22, 24, 28, 29), while the presence of CIS was statistically significant in 7 (15-17, 19, 21, 22, 24). In addition, 3 studies found multifocality to be significant (15, 22, 24). Revelo et al (23) in their analysis of 121 consecutive samples found that disease within the prostate tended to spread in the proximal to distal direction leading to their

recommendation that sparing of the apical prostate was possible during cystectomy. This concept has been replicated in our recommendation to include the proximal 1.5cm (in males) and proximal 1cm (in females) rather than the full length of the urethra. We feel that by using a rollerball of 1cm diameter around the urethra a sufficient volume of prostate will be included (especially once this volume is expanded by a CTV to PTV margin) whilst avoiding an increase in dose to the rectum.

Distinguishing between the base of the bladder and the prostate can at times prove difficult. On T2W MRI the prostate capsule is usually seen as a distinct dark rim which is most clearly seen at the prostate's posterior-lateral border (30). By following the structure superiorly, the dividing line between the prostate and bladder can be better appreciated. Defining the prostatic urethra on MRI can be challenging. We recommend beginning on slices where visibility is better and then interpolating to create a volume contiguous with the base of the bladder. Eighty-eight percent of participants agreed that when the urethra was difficult to visualise the volume could extend anteriorly (see diagram in table 2.14), whilst sixty-nine percent felt a roller ball placed in the central prostate alone was sufficient (just below the cut off for agreement).

2.9.3 Delineation of Organs at risk

Rectal delineation recommendations are in line with those of the RAIDER and HYBRID bladder radiotherapy trial protocols. They also match the recommendations made in ESTRO and RTOG guidance on prostate radiotherapy (30, 31) and the delineation recommendations made in the CHHip radiotherapy trial (32). It is also broadly in line with the Global Quality Assurance of Radiation Therapy Clinical Trials Harmonization Group (GHG) recommendations (33). Similarly, delineation recommendations for 'other bowel' and 'femoral head' structures match the recommendations made in RAIDER and HYBRID radiotherapy trials. The GHG recommendations for bowel also match our own although they advocate the inclusion of the femoral necks in a combined femoral head and neck structure. An alternative to 'other bowel' contouring found in the literature is the use of a bowel bag for example as recommended by

Baumann et al (34) in their guidance on post cystectomy radiotherapy. This was mentioned as a preferred technique by one of our participants.

2.10 Part 2 Conclusion

This part of the study describes the development of consensus guidance for MRI based bladder radiotherapy. The consensus was developed and validated by an international group of bladder radiotherapy specialists, and it is hoped that it can be used as a means to improve contouring variability across the wider bladder radiotherapy community. Moving forward, I plan to publish the consensus alongside general education on MRI bladder interpretation so that more people with an interest in bladder radiotherapy can benefit from the work we have undertaken. It is also hoped that this consensus can be incorporated into future bladder radiotherapy trials particularly those looking into the use of MR guided workflows.

2.11 Part 2 References

1. Hindson BR, Turner SL, Millar JL, Foroudi F, Gogna NK, Skala M, et al. Australian & New Zealand Faculty of Radiation Oncology Genito-Urinary Group: 2011 consensus guidelines for curative radiotherapy for urothelial carcinoma of the bladder. *Journal of medical imaging and radiation oncology*. 2012;56(1):18-30.
2. Pieters BR, van der Steen-Banasik E, Smits GA, De Brabandere M, Bossi A, Van Limbergen E. GEC-ESTRO/ACROP recommendations for performing bladder-sparing treatment with brachytherapy for muscle-invasive bladder carcinoma. *Radiotherapy and oncology : journal of the European Society for Therapeutic Radiology and Oncology*. 2017;122(3):340-6.
3. Shipley WU, Van der Schueren E, Kitagawa T, Gospodarowicz MK, Frommhold H, Magno L, et al. Guidelines for radiation therapy in clinical research on bladder cancer. *Progress in clinical and biological research*. 1986;221:109-21.
4. Huddart RA, Hall E, Hussain SA, Jenkins P, Rawlings C, Tremlett J, et al. Randomized noninferiority trial of reduced high-dose volume versus standard volume radiation therapy for muscle-invasive bladder cancer: results of the BC2001 trial (CRUK/01/004). *International journal of radiation oncology, biology, physics*. 2013;87(2):261-9.
5. Hoskin PJ, Rojas AM, Bentzen SM, Saunders MI. Radiotherapy with concurrent carbogen and nicotinamide in bladder carcinoma. *Journal of clinical oncology : official journal of the American Society of Clinical Oncology*. 2010;28(33):4912-8.
6. Gogna NK, Matthews JH, Turner SL, Mameghan H, Duchesne GM, Spry N, et al. Efficacy and tolerability of concurrent weekly low dose cisplatin during radiation treatment of localised muscle invasive bladder transitional cell carcinoma: a report of two sequential Phase II studies from the Trans Tasman

Radiation Oncology Group. Radiotherapy and oncology : journal of the European Society for Therapeutic Radiology and Oncology. 2006;81(1):9-17.

7. Hagan MP, Winter KA, Kaufman DS, Wajsbman Z, Zietman AL, Heney NM, et al. RTOG 97-06: initial report of a phase I-II trial of selective bladder conservation using TURBT, twice-daily accelerated irradiation sensitized with cisplatin, and adjuvant MCV combination chemotherapy. International journal of radiation oncology, biology, physics. 2003;57(3):665-72.

8. Cowan RA, McBain CA, Ryder WD, Wylie JP, Logue JP, Turner SL, et al. Radiotherapy for muscle-invasive carcinoma of the bladder: results of a randomized trial comparing conventional whole bladder with dose-escalated partial bladder radiotherapy. International journal of radiation oncology, biology, physics. 2004;59(1):197-207.

9. Hasson F, Keeney S, McKenna H. Research guidelines for the Delphi survey technique. Journal of advanced nursing. 2000;32(4):1008-15.

10. Tunio MA, Hashmi A, Qayyum A, Mohsin R, Zaeem A. Whole-pelvis or bladder-only chemoradiation for lymph node-negative invasive bladder cancer: single-institution experience. International journal of radiation oncology, biology, physics. 2012;82(3):e457-62.

11. Zietman AL, Grocela J, Zehr E, Kaufman DS, Young RH, Althausen AF, et al. Selective bladder conservation using transurethral resection, chemotherapy, and radiation: management and consequences of Ta, T1, and Tis recurrence within the retained bladder. Urology. 2001;58(3):380-5.

12. Kukreja JB, Porten S, Golla V, Ho PL, Noguera-Gonzalez G, Navai N, et al. Absence of Tumor on Repeat Transurethral Resection of Bladder Tumor Does Not Predict Final Pathologic T0 Stage in Bladder Cancer Treated with Radical Cystectomy. European urology focus. 2018;4(5):720-4.

13. Zibelman M, Asghar AM, Parker DC, O'Neill J, Wei S, Greenberg RE, et al. Cystoscopy and Systematic Bladder Tissue Sampling in Predicting pT0 Bladder Cancer: A Prospective Trial. Journal of Urology. 2021;205(6):1605-11.

14. Hafeez S, Webster A, Hansen VN, McNair HA, Warren-Oseni K, Patel E, et al. Protocol for tumour-focused dose-escalated adaptive radiotherapy for the radical treatment of bladder cancer in a multicentre phase II randomised controlled trial (RAIDER): radiotherapy planning and delivery guidance. BMJ open. 2020;10(12):e041005.

15. Nixon RG, Chang SS, Lafleur BJ, Smith JA, Cookson MS. CARCINOMA IN SITU AND TUMOR MULTIFOCALITY PREDICT THE RISK OF PROSTATIC URETHRAL INVOLVEMENT AT RADICAL CYSTECTOMY IN MEN WITH TRANSITIONAL CELL CARCINOMA OF THE BLADDER. The Journal of Urology. 2002;167(2, Part 1):502-5.

16. Arce J, Gaya JM, Huguet J, Rodriguez O, Palou J, Villavicencio H. Can we identify those patients who will benefit from prostate-sparing surgery? Predictive factors for invasive prostatic involvement by transitional cell carcinoma. Can J Urol. 2011;18(1):5529-36.

17. Patel SG, Cookson MS, Barocas DA, Clark PE, Smith JA, Chang SS. Risk factors for urothelial carcinoma of the prostate in patients undergoing radical cystoprostatectomy for bladder cancer. BJU international. 2009;104(7):934-7.

18. Tabibi A, Simforoosh N, Parvin M, Abdi H, Javaherforooshzadeh A, Farrokhi F, et al. Predictive Factors for Prostatic Involvement by Transitional Cell Carcinoma of the Bladder. Urol J. 2011;8(1):43-7.

19. Richards KA, Parks GE, Badlani GH, Kader AK, Hemal AK, Pettus JA. Developing selection criteria for prostate-sparing cystectomy: a review of cystoprostatectomy specimens. *Urology*. 2010;75(5):1116-20.
20. von Rundstedt FC, Lerner SP, Godoy G, Amiel G, Wheeler TM, Truong LD, et al. Usefulness of transurethral biopsy for staging the prostatic urethra before radical cystectomy. *J Urol*. 2015;193(1):58-63.
21. Pettus JA, Al-Ahmadie H, Barocas DA, Koppie TM, Herr H, Donat SM, et al. Risk assessment of prostatic pathology in patients undergoing radical cystoprostatectomy. *European urology*. 2008;53(2):370-5.
22. Bruins HM, Djaladat H, Ahmadi H, Sherrod A, Cai J, Miranda G, et al. Incidental prostate cancer in patients with bladder urothelial carcinoma: comprehensive analysis of 1,476 radical cystoprostatectomy specimens. *J Urol*. 2013;190(5):1704-9.
23. Revelo MP, Cookson MS, Chang SS, Shook MF, Smith JA, Jr., Shappell SB. Incidence and location of prostate and urothelial carcinoma in prostates from cystoprostatectomies: implications for possible apical sparing surgery. *J Urol*. 2008;179(5 Suppl):S27-32.
24. Kefer JC, Voelzke BB, Flanigan RC, Wojcik EM, Waters WB, Campbell SC. Risk assessment for occult malignancy in the prostate before radical cystectomy. *Urology*. 2005;66(6):1251-5.
25. Ayyathurai R, Gomez P, Luongo T, Soloway MS, Manoharan M. Prostatic involvement by urothelial carcinoma of the bladder: clinicopathological features and outcome after radical cystectomy. *BJU international*. 2007;100(5):1021-5.
26. Shen SS, Lerner SP, Muezzinoglu B, Truong LD, Amiel G, Wheeler TM. Prostatic involvement by transitional cell carcinoma in patients with bladder cancer and its prognostic significance. *Human pathology*. 2006;37(6):726-34.
27. Stein JP, Penson DF, Wu SD, Skinner DG. Pathological guidelines for orthotopic urinary diversion in women with bladder cancer: a review of the literature. *J Urol*. 2007;178(3 Pt 1):756-60.
28. Stein JP, Esrig D, Freeman JA, Grossfeld GD, Ginsberg DA, Cote RJ, et al. Prospective pathologic analysis of female cystectomy specimens: risk factors for orthotopic diversion in women. *Urology*. 1998;51(6):951-5.
29. Chen ME, Pisters LL, Malpica A, Pettaway CA, Dinney CP. Risk of urethral, vaginal and cervical involvement in patients undergoing radical cystectomy for bladder cancer: results of a contemporary cystectomy series from M. D. Anderson Cancer Center. *J Urol*. 1997;157(6):2120-3.
30. Salembier C, Villeirs G, De Bari B, Hoskin P, Pieters BR, Van Vulpen M, et al. ESTRO ACROP consensus guideline on CT- and MRI-based target volume delineation for primary radiation therapy of localized prostate cancer. *Radiotherapy and oncology : journal of the European Society for Therapeutic Radiology and Oncology*. 2018;127(1):49-61.
31. Lawton CA, Michalski J, El-Naqa I, Buyyounouski MK, Lee WR, Menard C, et al. RTOG GU Radiation oncology specialists reach consensus on pelvic lymph node volumes for high-risk prostate cancer. *International journal of radiation oncology, biology, physics*. 2009;74(2):383-7.
32. Dearnaley D, Syndikus I, Mossop H, Khoo V, Birtle A, Bloomfield D, et al. Conventional versus hypofractionated high-dose intensity-modulated radiotherapy for prostate cancer: 5-year outcomes of the randomised, non-inferiority, phase 3 CHHiP trial. *The Lancet Oncology*. 2016;17(8):1047-60.
33. Mir R, Kelly SM, Xiao Y, Moore A, Clark CH, Clementel E, et al. Organ at risk delineation for radiation therapy clinical trials: Global Harmonization Group

consensus guidelines. *Radiotherapy and oncology : journal of the European Society for Therapeutic Radiology and Oncology*. 2020;150:30-9.

34. Baumann BC, Bosch WR, Bahl A, Birtle AJ, Breau RH, Challapalli A, et al. Development and Validation of Consensus Contouring Guidelines for Adjuvant Radiation Therapy for Bladder Cancer After Radical Cystectomy. *International journal of radiation oncology, biology, physics*. 2016;96(1):78-86.

Chapter 3

Workflow development for the treatment of bladder cancer on the Elekta Unity

Chapter 3 Workflow development for the treatment of bladder cancer on the Elekta Unity.

3.1 Introduction

Successful treatment of patients with MIBC on the Elekta Unity required the development of a treatment workflow. This was a multi-disciplinary effort, with involvement of clinicians, therapeutic radiographers, MR and medical physicists. The final workflow will be discussed in more detail in Chapter 4. In this Chapter I will discuss two aspects of the workflow which I contributed significantly to.

As a team we chose to develop an online 'adapt to shape' (ATS) workflow. This type of workflow allows daily re-contouring and full plan re-optimisation based on the anatomy of the day. This is in contrast to an 'adapt to position' (ATP) workflow where contours remain unchanged with only an isocentre shift performed prior to plan re-optimisation (1). An example of the ATS workflow is summarised in Figure 3.1. We chose to pursue an ATS approach as bladders are known to alter significantly in size and shape on a fraction by fraction basis (2, 3). It was anticipated that by using such a workflow we would therefore be able to improve treatment conformality compared to standard bladder radiotherapy as the impact of inter-fraction bladder variation would be reduced.

However, an ATS workflow takes time to complete, and was predicted to be in the region of 40 minutes per fraction (4). As a result, intra-fraction bladder filling is likely to be greater than for a standard fraction. It was therefore hypothesised that our current intra-fraction treatment margin of 3mm (developed for a mean intra-fraction filling time of ~ 10mins (2) on a conventional linac) was unlikely to be sufficient to maintain target coverage. I therefore undertook a piece of work to investigate what treatment margin would ensure adequate target coverage. This work informed the planning margins taken forward into our clinical workflow.

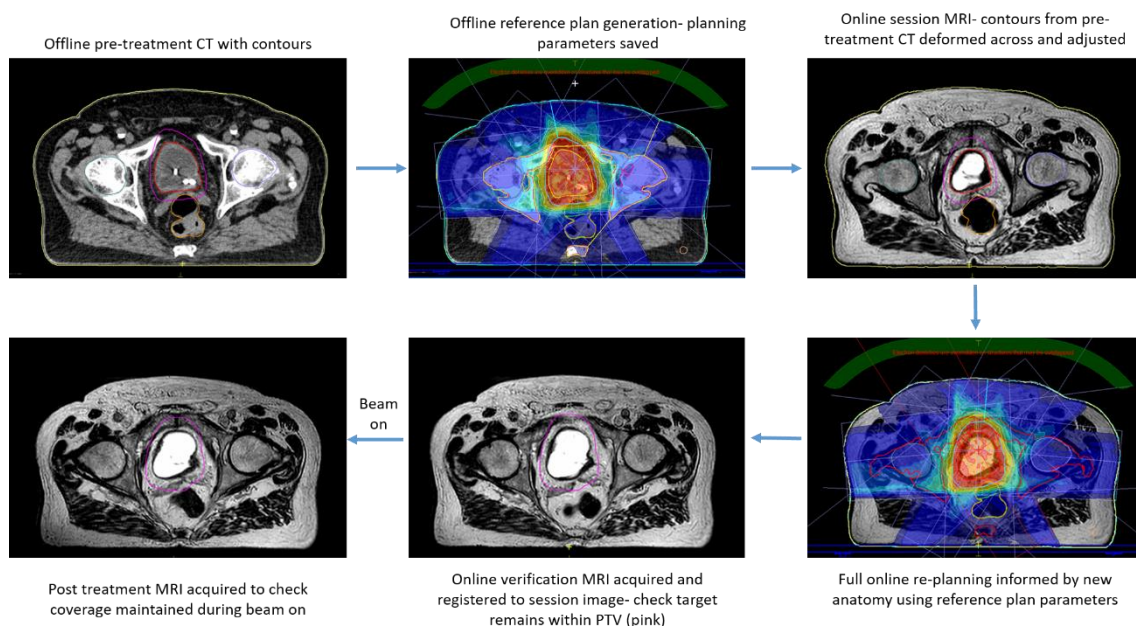


Figure 3.1 Adapt to shape workflow

Another aspect of the workflow which needed consideration was the time spent on daily online re-contouring. As part of the ATS workflow, contours from the planning scan are deformed to the first MRI of the day, known as the ‘session’ MRI (MRI_{session}). While the deformation of structures such as the external contour is relatively reliable (based on visual inspection of test cases), the quality of the deformable image registration (DIR) is less good for the bladder (target) and rectal and other bowel (bowel excluding rectum) OARs particularly when deforming from a CT to MRI, Figure 3.2.

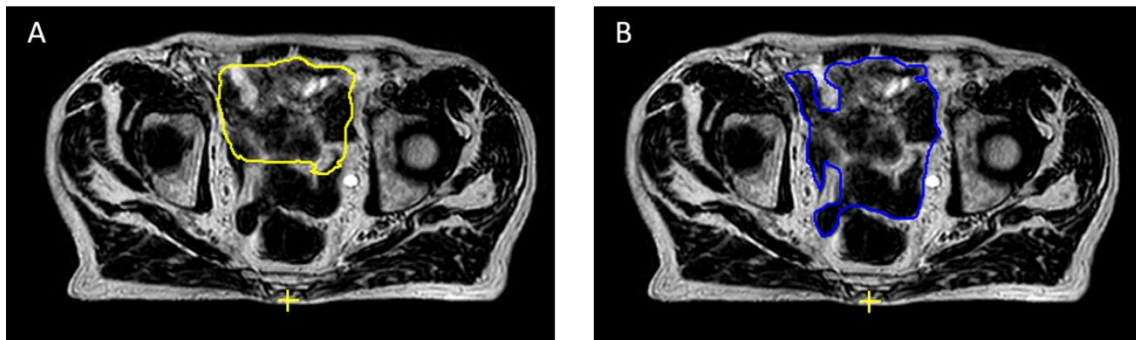


Figure 3.2 Demonstration of deformable image registration (DIR) performance for bowel.

Panel A: Bowel contour (yellow) as produced using DIR from planning CT to session MRI. Panel B: Clinician drawn bowel contour (blue) for comparison.

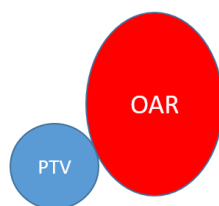
If time is not an issue, one would manually adjust the deformed contours of all planning structures to optimise the accuracy and performance of the re-optimised plan and ensure the validity of the dose volume histogram (DVH). However, ATS workflows need to be kept as short as possible. This is because the target volume increases in size with bladder filling. Logically, the longer the filling time, the larger the planning margins that are needed to ensure target coverage is maintained and thus the potential for higher dose to normal tissues. Prolonged treatment times are also less tolerable to patients. Additionally, workforce and machine time constraints require streamlined treatments to maximise the number of patients treated.

While spending time re-contouring the target was deemed important review of other structures where re-contouring time could be minimised was important. In practice cases, DIR for the other bowel and rectum structure sets was often poor necessitating time consuming alteration in order to match the anatomy of the day. To reduce the time needed for re-contouring, a planning ‘class solution’ was developed which used a dose gradient based planning method as opposed to a standard DVH based planning system. In this scenario, the plan optimisation parameters focus on quick dose fall off around the target, achieved through the use of shrink margins applied to the external contour. Avoidance of OARs is achieved by using similar or slightly stricter dose fall off objectives to areas of the OAR close to the PTV. This results in a sharper dose fall off at OAR/PTV interfaces and less conformity in areas away from vulnerable organs.

Therefore, optimisation of the plan is only dependent on accurate contouring at the PTV/OAR interface allowing re-contouring to be focussed on these areas rather than the whole OAR. Dr Ian Hanson (Medical Physicist) developed such a solution for use in our workflow. Figure 3.3 and 3.4 illustrate this planning method in contrast to a standard DVH based planning system, my thanks to Dr Ian Hanson for the use of his adapted illustrations.

Standard DVH based planning

Offline:

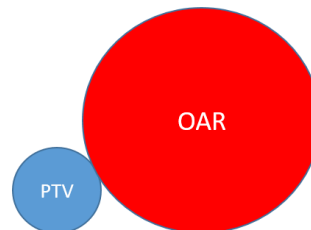


Planning goals:

1. Define minimum dose to PTV
2. Define mean dose to OAR- used to conform dose to PTV

Generates a plan which covers target and optimally spares OAR

Online:



OAR has increased in size

Mean dose OAR objective no longer optimal

Suboptimal plan produced

Figure 3.3 Standard DVH based planning approach.

Changes to OAR size/shape in the online setting effect the robustness of the online plan

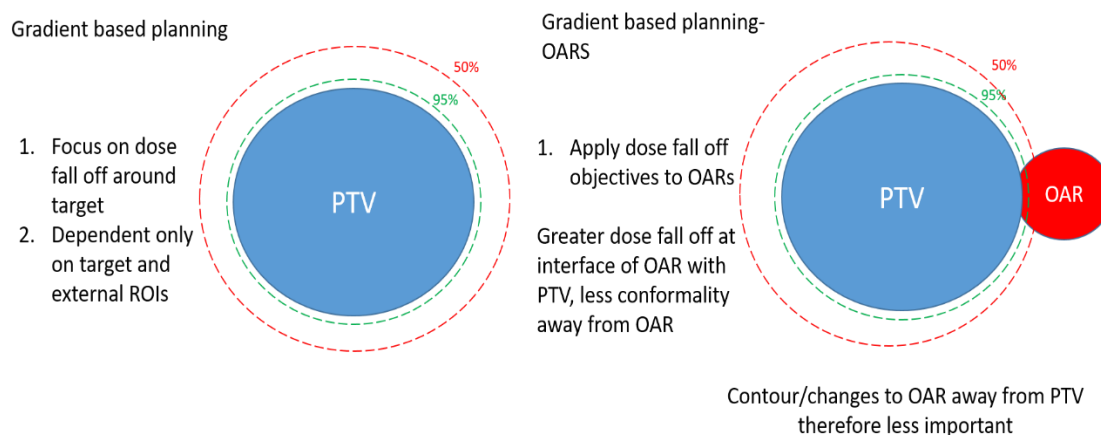


Figure 3.4 Gradient based planning approach.

Less susceptible to OAR changes enabling more robust online re-planning and limiting the need for full OAR re-contouring. ROI= region of interest.

The impact of this approach with respect to the need for full re-contouring of OARs was tested. Focussing on the other bowel structure (the most time consuming structure to re-contour) I hypothesised that full online re-contouring of the other bowel structure would not result in a clinically meaningful improvement in plan dosimetry compared to using automatically propagated structures and as a result full re-contouring of this structure would not be necessary within our MRgRT 36Gy in 6 fraction protocol.

3.2 Methods

3.2.1 Development of intra-fraction treatment margins

To gain an understanding of the degree of bladder filling expected over 40 minutes a literature search was performed. Although there are several studies looking at intra-fraction bladder filling in bladder cancer patients (5-10), the majority covered shorter time periods and were therefore of limited utility in this setting. One study reported filling over a 28 minute time period (8) but this was in a cohort of 10 patients and the effect on planned target coverage was not assessed.

I therefore looked for other sources of information which might inform our intra-fraction margin size. I was granted access to radiotherapy planning scans from two previous clinical trials undertaken at my institution where bladder cancer patients undergoing radiotherapy to the bladder had undergone two CT planning scans 30 minutes apart. Whilst acknowledging that this time period fell slightly short of our projected 'on couch' filling time of 40 minutes I was able to use these datasets to model the impact of bladder filling on target coverage using different treatment planning margins.

I undertook a retrospective analysis of the radiotherapy CT planning scan datasets acquired as part of the APPLY (NCT01000129) (11) and IDEAL (NCT01124682) (12) trials. These trials investigated the feasibility of a 'plan library' approach for MIBC patients undergoing radiotherapy. The APPLY trial treated patients with a hypofractionated once weekly schedule, whilst IDEAL focussed on patients undergoing daily fractionation. We planned to treat hypofractionated patients in our initial MRL cohort so I focused predominantly on the APPLY dataset with the smaller IDEAL cohort included in the exploratory setting.

For those enrolled in APPLY, during treatment planning, patients underwent two CT planning scans, one at time 0 (CT_0) and one ~30 minutes later (CT_{30}). Patients were asked to empty their bladders just before CT_0 and to not drink anything for 30 minutes prior. They remained on the treatment couch between CT_0 and CT_{30} , voiding during this time was prohibited. The two scans were rigidly fused and CTVs (CTV_0 and CTV_{30}) were delineated on the respective CT scans. The CTV included the whole bladder plus extravesical spread +/- a portion of the urethra depending on disease state. In this trial the CTV_{30} was used to identify patients with >50cc of filling between the scans as this effected the PTVs produced. PTVs were grown for this analysis are as per Table 3.1.

In IDEAL, patients were asked to empty their bladders and then drink 350mls of water. They then underwent a CT planning scan at 30 minutes (CT_{30}) and a further scan at 60 minutes (CT_{60}). As in APPLY, these scans were then rigidly

fused and CTVs (CTV₃₀ and CTV₆₀) delineated. PTVs grown for this analysis as in Table 3.1.

Table 3.1 PTV expansions

PTV	APPLY CTV ₀ expansion	IDEAL CTV ₃₀ expansion
Small	0.5cm isotropically	0.5cm isotropically
Medium	0.5cm laterally and inferiorly 1cm posteriorly 1.5cm superiorly and anteriorly	0.5cm laterally and inferiorly 1cm posteriorly 1.5cm superiorly and anteriorly
Standard	0.75cm laterally and inferiorly 1cm posteriorly 1.5cm superiorly and anteriorly	N/A

The small and medium PTV margins are the same as with those used in APPLY and IDEAL. The standard margin is the margin used at my institution when 'plan of the day' is not deployed.

55 patients were enrolled in APPLY. The datasets for 4 patients could not be recovered from the treatment planning system and were therefore not included in this analysis. To limit the impact of inter-observer contouring variability, the clinical CTV₀ were used without alteration. In 6 cases, I made slight alterations to CTV₃₀ to maintain consistency between the CTV₀ and the CTV₃₀. In 4 cases, the CTV₃₀ had not been acquired or varied significantly from the CTV₀ so I felt it best to exclude these cases from the analysis. I excluded a further 3 cases where PTVs were missing and changes to the computing software made it difficult to recreate the missing structure sets. 44 APPLY cases were therefore suitable for analysis. 20 patients, with available datasets, from the IDEAL study (12) were included in the IDEAL analysis.

By comparing the volume of the two CTVs for each patient dataset, it was possible to estimate the degree of intra-fraction volume change which might be expected had these patients undergone an online adaptive radiotherapy fraction.

3.2.1.1 Assessment of CTV₃₀ or CTV₆₀ contour coverage by initial PTVs in order to establish suitable intra-fraction margin

In the original trials, the patients' scans were rigidly registered. It was therefore possible to assess the later scan's CTV coverage (either CTV₃₀ or CTV₆₀ depending on the trial) by each of the PTVs created from the initial CTV, see figure 3.5. Assuming all clinical plans met ICRU 83/50 criteria, the 95% isodose would closely adhere to the PTV outline. I therefore classified a significant geographical miss (indicating a too small intra-fraction margin) as one where < 95% of the later CTV was covered by a PTV. For cases with a significant miss I then used visual inspection to identify the predominant geographical area of this target miss.

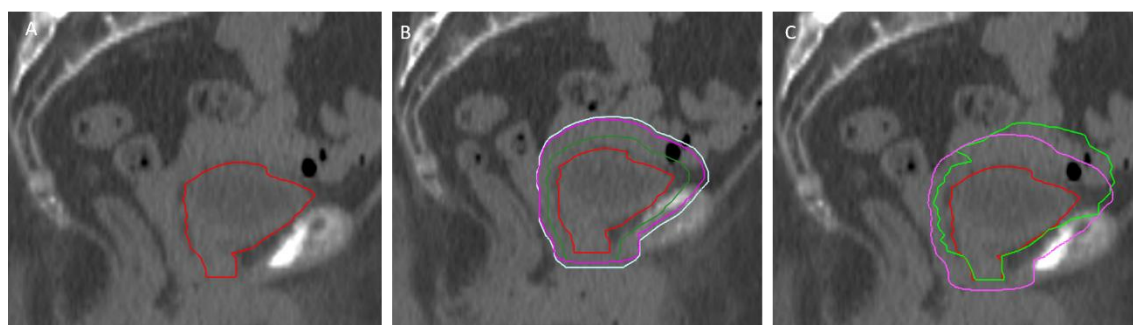


Figure 3.5 Steps involved in margin analysis, using an APPLY patient scan.

Panel A; sagittal CT₀ image with CTV₀ outlined in red. Panel B; sagittal CT₀ image with PTV margins applied to CTV₀, PTV_{small} in light green, PTV_{medium} in purple, PTV_{standard} in light blue. Panel C; sagittal CT₀ image with CTV₃₀ superimposed (bright green), PTV_{medium} shown (purple), note how CTV₃₀ extends outside of the PTV_{medium} predominantly in the anterior/superior direction. This case was therefore classed as a significant miss for a medium intra-fraction margin as <95% of CTV₃₀ was covered by the PTV_{medium}.

3.2.1.2 Assessment of CTV₃₀ coverage by 95% isodose line

Acknowledging that in reality the planned 95% isodose line does not conform exactly to the PTV I extended this work by performing a planning study using the

APPLY dataset and 2 of the PTV margins (small and medium). The APPLY dataset was used as these patients were similar to the patients due to be treated in our first cohort on the MRL. I transferred the datasets from their original treatment planning system to Monaco TPS (version 5.5, Elekta AB, Stockholm, Sweden). Using the CT₀ as my session image and the 'class solution' as developed by Dr Ian Hanson (adapted as needed) I created 2 plans per patient, one with a small PTV margin and one with a medium PTV margin (planning dose constraints in Table 3.2, planning parameters included in table 4.2 of Chapter 4).

Table 3.2 Planning dose constraints used

Organ	Constraint		
CTV	D95%	>95%	
	D98%	>95%	
	D99%	>90%	
Rectum (including anus)		Optimal	Mandatory
	V17Gy	50%	80%
	V28Gy	20%	60%
	V33Gy	15%	50%
	V36Gy	5%	30%
Other Bowel (including small and large bowel as single structure)	V25Gy	139cc	208cc
	V28Gy	122cc	183cc
	V31Gy	105cc	157cc
	V33Gy	84cc	126cc
	V36Gy	26cc	39cc
Femoral Heads	V28Gy	<50%	
Normal Tissue (External –PTV)	D1cc	≤ 105% prescribed dose	≤ 110% prescribed dose

I then overlaid the corresponding CTV₃₀ structure onto those plans to assess the extent to which the CTV₃₀ was covered by the 95% isodose line, see Figure 3.6. Coverage of <95% of CTV₃₀ by the 95% isodose line was deemed a target miss.

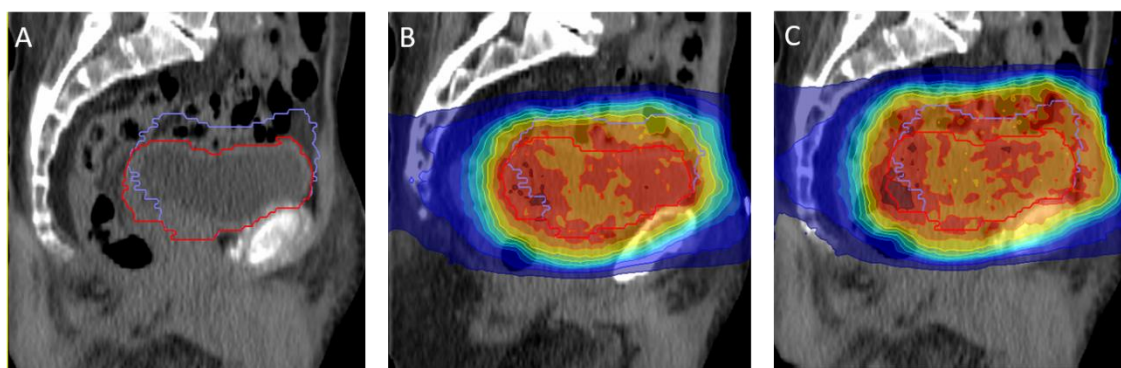


Figure 3.6 Planning study for APPLY dataset.

Panel A: CT planning scan with CTV0 (red) and superimposed CTV30 (purple). Panel B: Same planning scan with isodoses from plan optimised using a small PTV margin around CTV0. Note how CTV30 partly falls outside of the 95% isodose (orange) particularly in the anterior/superior region. Panel C: same planning scan with isodoses from plan optimised using medium PTV margin around CTV0. Note how CTV30 now adequately covered by 95% isodose line.

This analysis included 34 patients, 10 patients were excluded due to the presence of metal hips (n=9) or a body habitus too large for the MRL bore (n=1). In 11 patients, when using the medium margins, it was not possible to meet the mandatory OAR planning constraints due to the anatomy at CT₀, see table 3.3 for further details. In these instances, plans were optimised to ensure D95% >95% for target coverage, with OAR doses kept as low as possible. These cases were still included in the analysis as it was anticipated that as the bladder filled over the intra-fraction period, the volume of OAR receiving these higher doses would decrease (as the OARs were moved away from the high dose region by the enlarging bladder) and so the ‘true’ OAR dose would be less. This is in line with our centre’s standard ‘plan of the day’ practice, where in cases where OAR constraints are missed by a moderate degree on a medium plan a patient may still be treated and watched carefully for toxicity, with their treatment stopped one fraction early if necessary. All cases which missed the dose constraints in my study also missed their dose constraints in the medium clinical plan used for their treatment. When using the small margin, all OAR constraints were met.

Table 3.3 Patients where OAR dose constraints were missed when using medium margin.

There were no violations involving the femoral head or normal tissue constraints.

Patient	Extent to which OAR constraint missed									
	Rectum					Other Bowel				
	V36Gy %	V33Gy %	V28Gy %	V17Gy %		V36Gy cc	V33Gy cc	V31Gy cc	V28Gy cc	V25Gy cc
Apply 3	-	-	-	6		35	1	-	-	-
Apply 8	-	-	-	-		7	-	-	-	-
Apply 18	-	-	-	-		12	-	-	-	-
Apply 19	-	-	-	-		11	-	-	-	-
Apply 27	-	-	-	5		32	18	10	14	22
Apply 28	-	-	-	-		7	-	-	-	-
Apply 33	-	-	-	-		35	36	30	39	54
Apply 44	-	-	-	-		15	-	-	-	-
Apply 47	-	-	-	-		10	-	-	-	-
Apply 50	-	-	-	-		4	-	-	-	-
Apply 56	-	-	10	5		25	9	4	12	24

3.2.1.3 Development of receiver operating characteristic curve.

As an exploratory analysis, I also looked at whether volume change over 30 minutes could be used as a predictor for planned target miss when using the small margin. I hypothesised that those who fill more are more likely to experience target miss than those who fill less. The small margin was chosen as the numbers experiencing a target miss using a medium margin was low in this cohort. To do this I took the true filling rate of each patient from the APPLY dataset (calculated by taking the volume change seen across the 2 CT planning scans divided by the true number of minutes between scans, ~ 30 minutes) and multiplied this by 30 to give the expected volume change over a 30 minute period. IBM SPSS statistics (version 23, IBM, Armonk, USA) was used to create a receiver operating characteristic (ROC) curve from which the area under the curve (AUC) was calculated and an optimal threshold determined.

3.2.2 Impact of other bowel re-contouring

I recruited bladder cancer patients to an MR linac imaging study (PRIMER, CCR4576) and simulated an online fraction with differing degrees OAR re-contouring to assess the impact this might have on estimated delivered dose to the target and OARs.

This work was undertaken using datasets of 5 patients recruited to the MRL imaging study PRIMER. The aim of the work was to investigate the degree of 'other bowel' (bowel excluding rectum) re-contouring required during an online fraction. The other bowel structure was selected as DIR for this structure is often sub-optimal and re-contouring is time consuming (more so than the rectal contour). Patients undergoing radiotherapy to the bladder on a standard linac were asked to undertake additional imaging sessions on the MRL. Patients were asked to empty their bladders and then underwent imaging in the form of four T2W scans at 10 minute intervals. These images, along with the patient's original radiotherapy planning scan were then uploaded onto research Monaco TPS (model as per previously) and used to simulate an online fraction in the offline setting. The steps involved in this process are shown in Figure 3.7 and discussed further below.

Firstly, I transferred the patient's radiotherapy CT scan and associated contours to research Monaco TPS. Using the 'class solution' developed by Dr Ian Hanson, I then created a plan based on this image and structure set. The resulting plan was then adjusted until all mandatory dose constraints were met (as detailed in the table 4.1 of chapter 4). This plan, along with its associated planning parameters, were used as the reference plan in the simulated online 'ATS' pathway. Using Monaco's deformable image registration functionality, I adapted the planning structure sets from the planning CT onto the 'session MRI' i.e. the first T2W MRI of the patient's PRIMER session. I re-contoured the CTV and grew the PTV (using a medium margin as used in the APPLY/IDEAL analysis) before copying the scan and structures to create 3 identical datasets. One of these datasets was left unaltered, for one dataset I spent 3 minutes⁴ correcting the other bowel structure focussing my efforts within an isotropic 2cm of the PTV and for the final dataset I re-contoured the other bowel in its entirety without time constraints. Using the planning parameters as defined in the reference plan I then re-optimised the plans based on the contoured anatomy on the 3 session MRIs. In order to assess the estimated dose that each of these plans would deliver to the patient's anatomy 30 minutes later (i.e. at the end of an adapted fraction), I contoured a CTV₃₀, rectum and other bowel structure on the MRI acquired at 30 minutes. I then 'overlaid' each plan onto this MRI by using Monaco's ATS original segments function allowing for a '30 minute' anatomy DVH to be produced. By comparing DVHs I was then able to establish whether alterations to the bowel contour had a clinically significant impact, defined as CTV₃₀ coverage falling below V95% <95% prescription or an increase in estimated dose to the other bowel at 30 minutes such that mandatory dose constraints were no longer met, see Table 3.2. My thanks to medical physicist Dr Alex Dunlop for his help with the development of this offline simulation.

⁴ 3 minutes was chosen as compromise time period which would allow some re-contouring around critical areas whilst not extending the total workflow excessively.

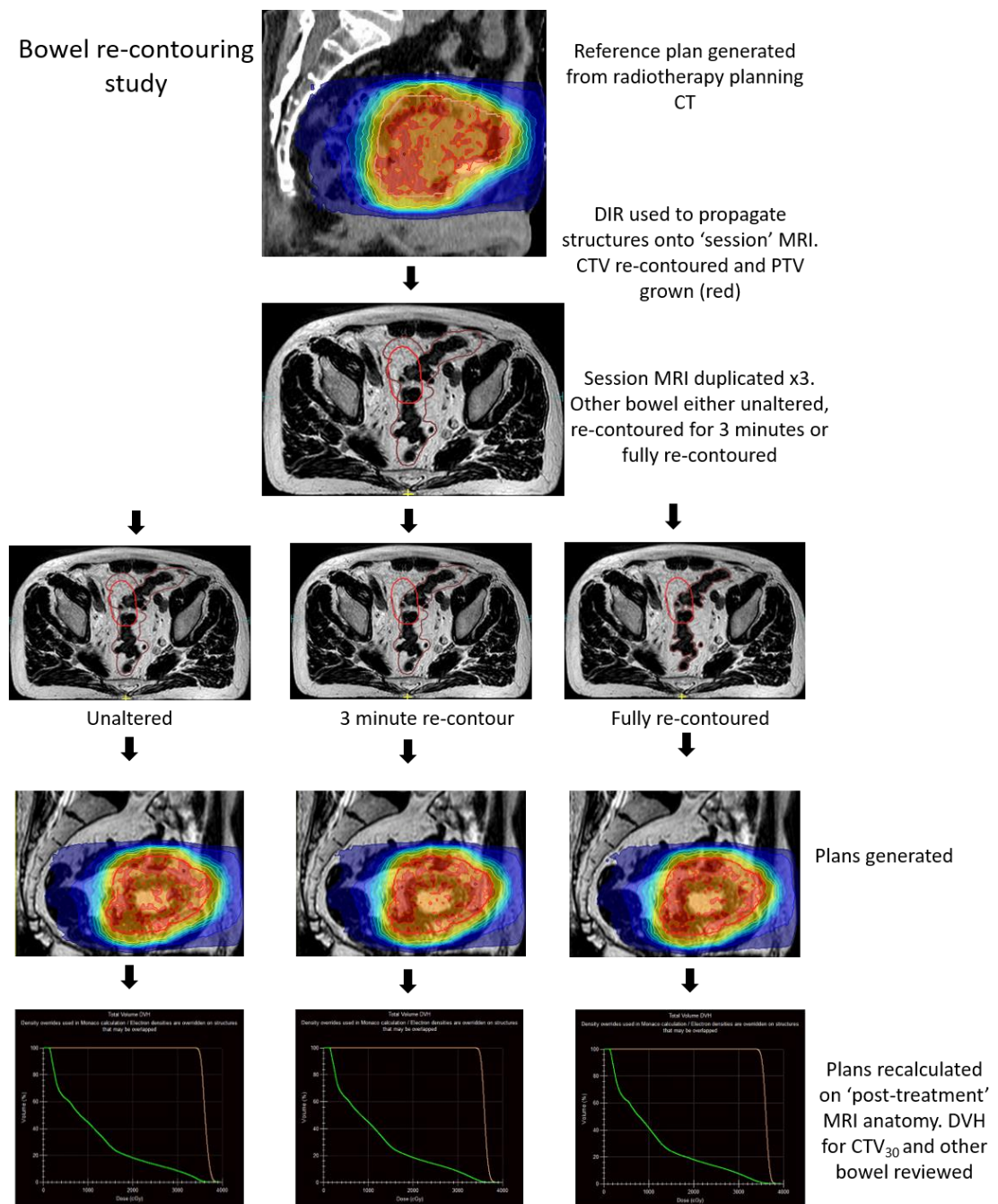


Figure 3.7 Bowel re-contouring study pathway.

Note the varying degree of other bowel re-contouring (brown), with a focus around the PTV (red). DVHs show coverage of CTV₃₀ (beige) and other bowel (green).

3.3 Results

3.3.1 Development of intra-fraction treatment margins

44 patients were included in the APPLY intra-fraction margins analysis.

Table 3.4 Characteristics of APPLY patients n=44

Mean Volume of CTV ₀	156 cc (SD 93, range 46-489 cc)
Mean Volume of CTV ₃₀	188 cc (SD 95, range 63-489 cc)
Mean Volume Change	32 cc (SD 29, range -0.6-131 cc)
Mean Rate of Change	1.17 cc/min (SD 1.1, range -0.02-4.67 cc/min)

20 patients were included from the IDEAL dataset. The mean CTV₃₀ size was 184cc, with a mean filling of 64cc, and a mean rate of change of 2.13cc/min, Table 3.5.

Table 3.5 Characteristics of IDEAL n=20

Mean Volume of CTV ₃₀	184 cc (SD 130, range 90-697 cc)
Mean Volume of CTV ₆₀	247 cc (SD 160, range 128-845 cc)
Mean Volume Change	64 cc (SD 61, range 2-252 cc)
Mean Rate of Change	2.13 cc/min (SD 2.02, range 0.06-8.41 cc/min)

3.3.1.1 Assessment of CTV₃₀ or CTV₆₀ contour coverage by initial PTVs
For APPLY patients, using a small PTV margin around CTV₀ resulted in a geographical miss of the CTV₃₀ contour in 39% of cases (Table 3.6). The medium and standard margins achieved better coverage, with 9% experiencing a geographical miss.

Table 3.6 APPLY patients coverage of CTV₃₀ by differing PTV margins around CTV₀

	PTV margin applied to CTV ₀		
	Small	Medium	Standard
Number of patients where CTV ₃₀ contour not completely covered by PTV	42 (95%)	18 (41%)	16 (36%)
Number of patients where < 95% of CTV ₃₀ contour covered by PTV (defined as geographical miss)	17 (39%)	4 (9%)	4 (9%)

In APPLY, for all PTV margins, the predominant location of geographical miss (<95% contour coverage) was in the superior/anterior direction, Figure 3.8

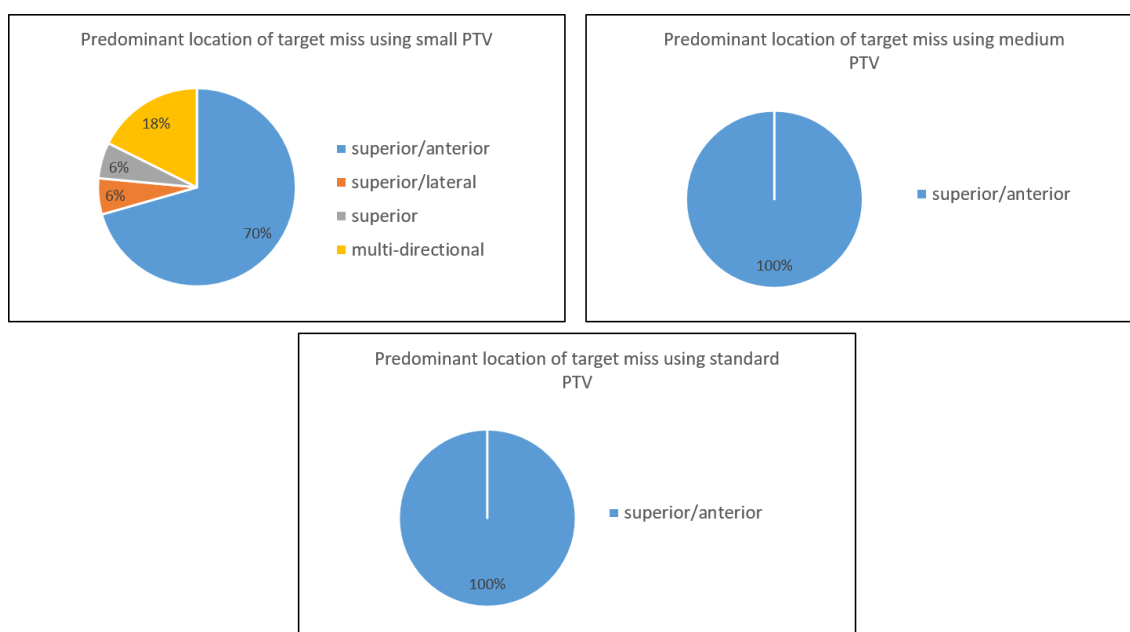


Figure 3.8 Predominant direction of target miss for APPLY cohort

For the IDEAL patients, the small margin resulted in a geographical miss in 45% of cases. The medium PTV resulted in a geographical miss in 10% of cases. The standard margin was not assessed as based on the APPLY data, this margin was not felt to provide additional benefit over the medium margin (Table 3.7).

Table 3.7 Coverage of CTV₆₀ by differing PTV margins around CTV₃₀

	PTV margin applied to CTV ₃₀	
	Small	Medium
Number of patients where CTV ₆₀ contour not completely covered by PTV	20 (100%)	7 (35%)
Number of patients where < 95% of CTV ₆₀ contour covered by PTV (defined as geographical miss)	9 (45%)	2 (10%)

In this cohort, the predominant direction of geographical miss was more varied, however misses in the superior and anterior directions were still more common than inferiorly and laterally, see Figure 3.9.

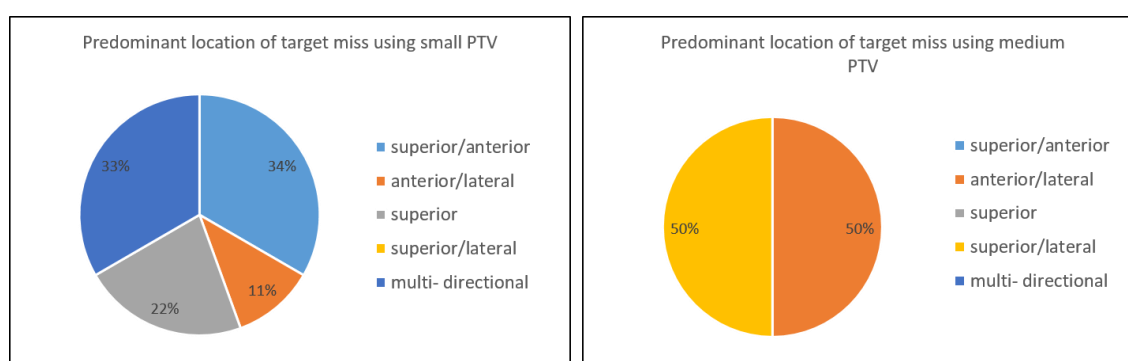


Figure 3.9 Predominant direction of target miss for IDEAL cohort

3.3.1.2 Assessment of CTV₃₀ coverage by 95% isodose line

Using the 34 suitable APPLY patient datasets, a total of 68 plans were generated (2 plans per patient). 32% of generated plans using a small PTV failed to cover 95% of the CTV₃₀ with the 95% isodose. 9% of plans using the medium margin failed to cover 95% of CTV₃₀ by the 95% isodose (Table 3.8).

Table 3.8 Coverage of CTV₃₀ by 95% isodose, n=34

	PTV margin applied to CTV ₀	
	Small	Medium
Number of patients where < 95% of CTV ₃₀ covered by 95% isodose	11 (32%)	3 (9%)

3.3.1.3 Development of ROC curve

Using the data from the APPLY small plan analysis, I looked at the predictive value of volume change over 30 minutes with respect to >95% coverage of CTV₃₀ by the 95% isodose line when using a small margin. The ROC curve (Figure 3.10) shows that volume change can be used as a predictor for maintaining target coverage, with an area under the curve (AUC) score of 0.91. A volume change of >27.8 cc over 30 minutes has a 91% sensitivity and 83% specificity for predicting target miss when deploying a small margin.

ROC Curve

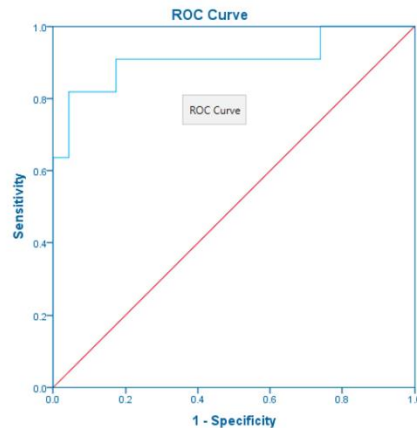
ROC Curve - Area Under the Curve - October 23, 2020

Area Under the Curve				
filling				
Area	Std. Error ^a	Asymptotic Sig. ^b	Asymptotic 95% Confidence Interval	
			Lower Bound	Upper Bound
.909	.067	.000	.778	1.000

a. Under the nonparametric assumption
b. Null hypothesis: true area = 0.5

ROC Curve

ROC Curve - ROC Curve - October 23, 2020



ROC Curve

ROC Curve - Coordinates of the Curve - October 23, 2020

Coordinates of the Curve			
filling			
Positive if Greater Than or Equal To ^a	Sensitivity	1 - Specificity	
-1.6375	1.000	1.000	
-.1356	1.000	.957	
.9276	1.000	.913	
3.4465	1.000	.870	
6.8291	1.000	.826	
8.3221	1.000	.783	
9.1100	1.000	.739	
10.6450	.909	.739	
11.5391	.909	.696	
11.6991	.909	.652	
12.2329	.909	.609	
14.7169	.909	.565	
17.4001	.909	.522	
19.1431	.909	.478	
21.5646	.909	.435	
23.0826	.909	.391	
23.6932	.909	.348	
24.9030	.909	.304	
25.8343	.909	.261	
26.4491	.909	.217	
27.8179	.909	.174	
30.7549	.818	.174	
33.9871	.818	.130	
39.3189	.818	.087	
44.3880	.818	.043	
50.2597	.727	.043	
55.6327	.636	.043	
59.9413	.636	.000	
64.7149	.545	.000	
65.8699	.455	.000	
67.4199	.364	.000	
74.0094	.273	.000	
95.4219	.182	.000	
125.8150	.091	.000	
141.0925	.000	.000	

Figure 3.10 ROC curve results using small margins.

In the coordinates of the curve data, ^a the smallest cut off value is the minimum observed test value minus 1, the largest cut off value is the maximum observed test value plus 1. All the other cut off values are the averages of two consecutive ordered observed test values.

3.3.2 Impact of other bowel re-contouring

3.3.2.1 Variability in other bowel volume

Figure 3.11 shows the variability in other bowel volume across the 5 patients enrolled in this study and the impact on bowel volume of contour adjustment.

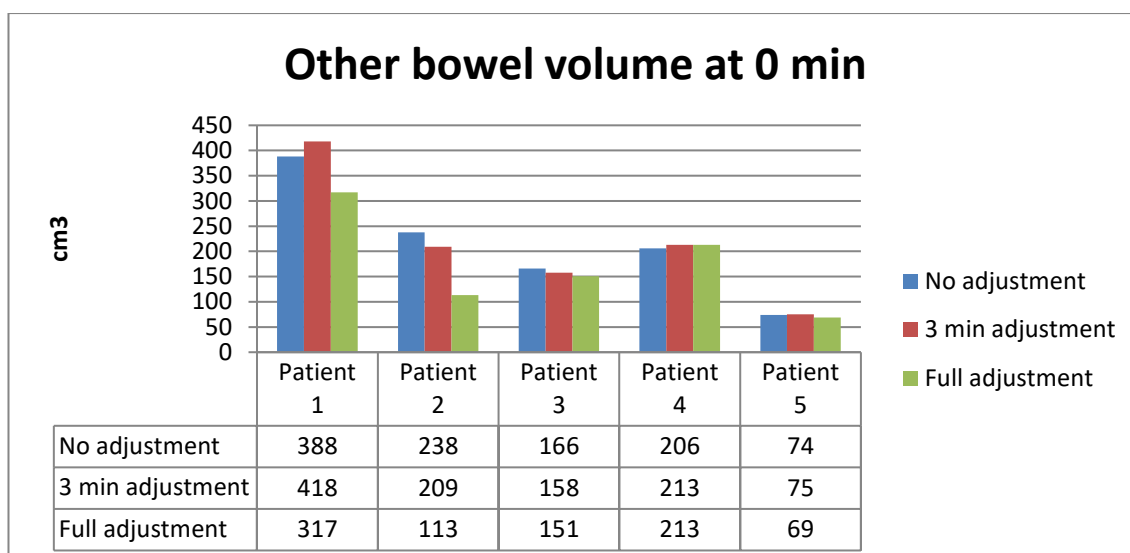


Figure 3.11 Variability of other bowel volume across 5 patients

Note the variability in volume of other bowel for each patient, with patient 1 having considerably more other bowel within the area of interest (defined as all other bowel within 2cm of the superior extent of the PTV) compared to patient 5. Note also how full adjustment generally leads to a decrease in other bowel volume while 3 minutes of adjustment can lead to an increase in volume. This is because when only having 3 minutes to re-contour I would focus around the PTV edge, often adding in other bowel which was missed by the DIR propagated structure but not then having time to remove incorrectly place additional other bowel further away from the PTV.

3.3.2.2 Impact on CTV₃₀ coverage

There was no difference in CTV₃₀ coverage when comparing the three different re-contouring methods, Figure 3.12.

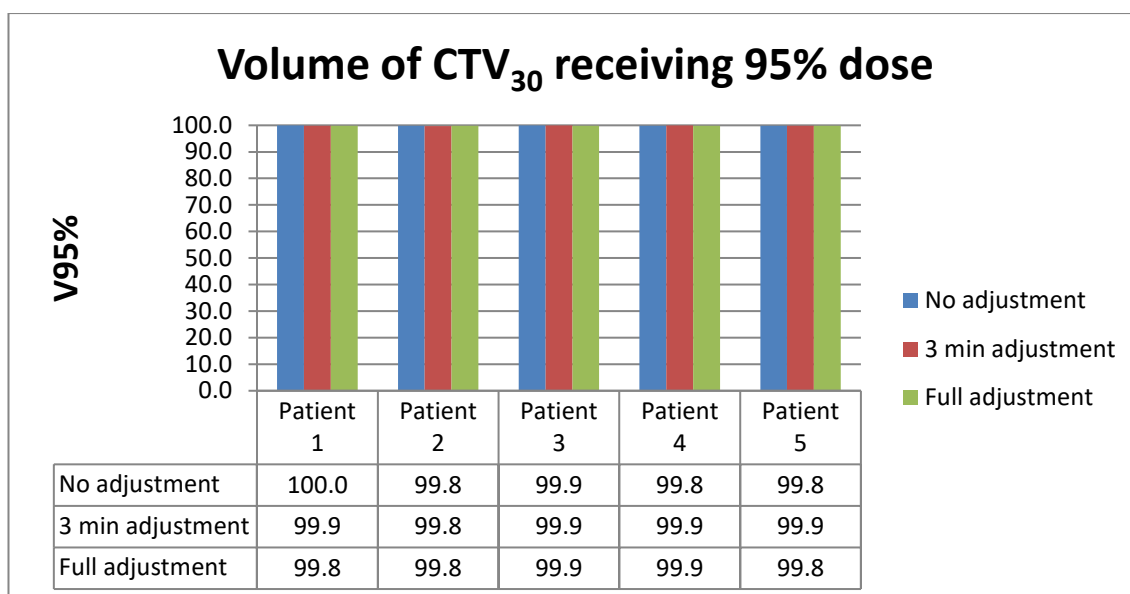


Figure 3.12 CTV₃₀ V95% coverage

3.3.2.3 Impact on dose to other bowel at 30 minutes

All plans remained within the other bowel dose optimal constraints tolerances, Figures 3.13-3.3.17.

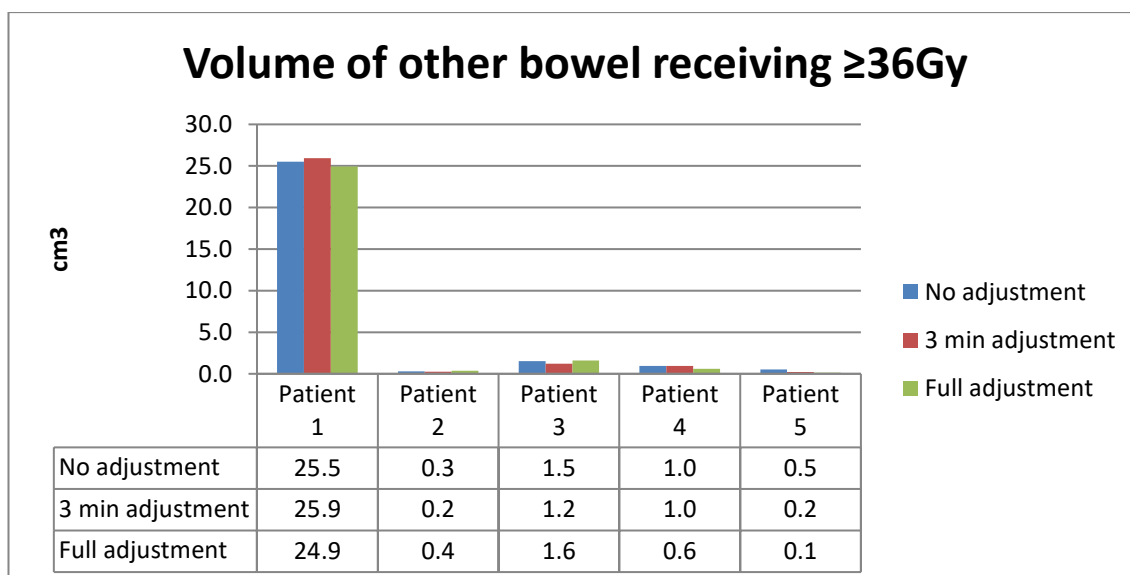


Figure 3.13 Volume of other bowel receiving ≥ 36 Gy.

Optimal dose constraint $< 26\text{cm}^3$, mandatory $< 39\text{cm}^3$.

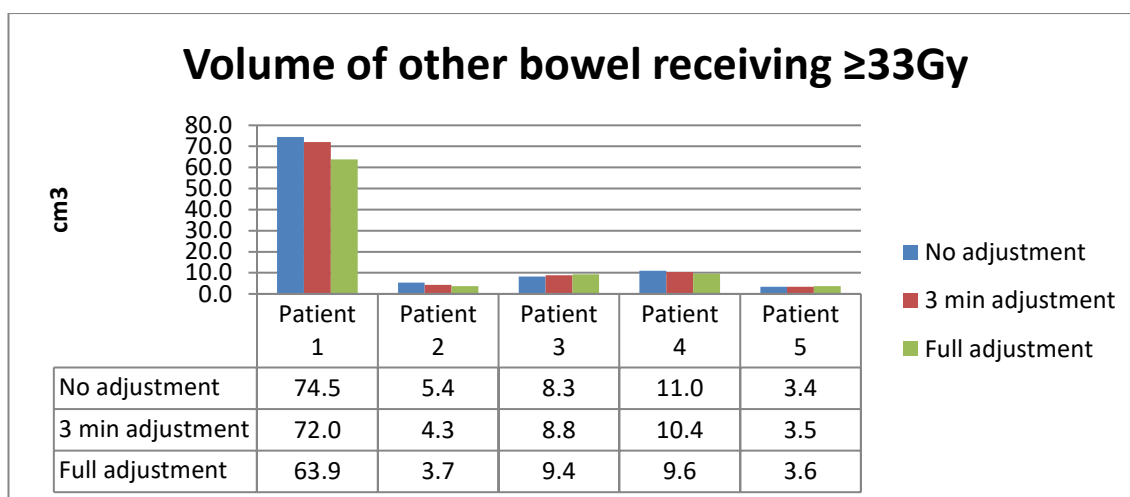


Figure 3.14 Volume of other bowel receiving $\geq 33\text{Gy}$.

Optimal dose constraint 84 cm^3 , mandatory 126 cm^3 .

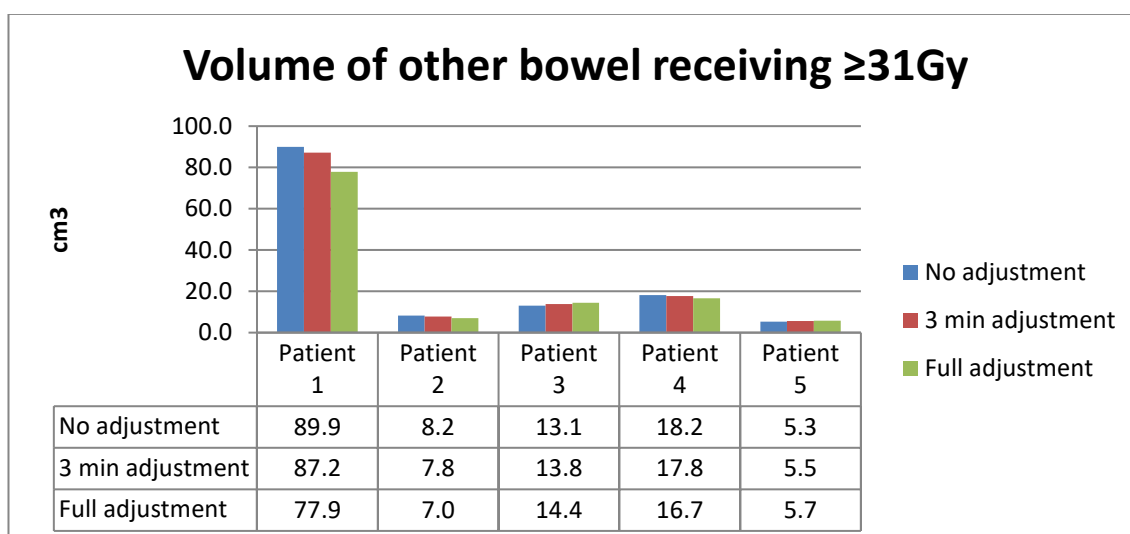


Figure 3.15 Volume of other bowel receiving $\geq 31\text{Gy}$.

Optimal dose constraint 105 cm^3 , mandatory 157 cm^3 .

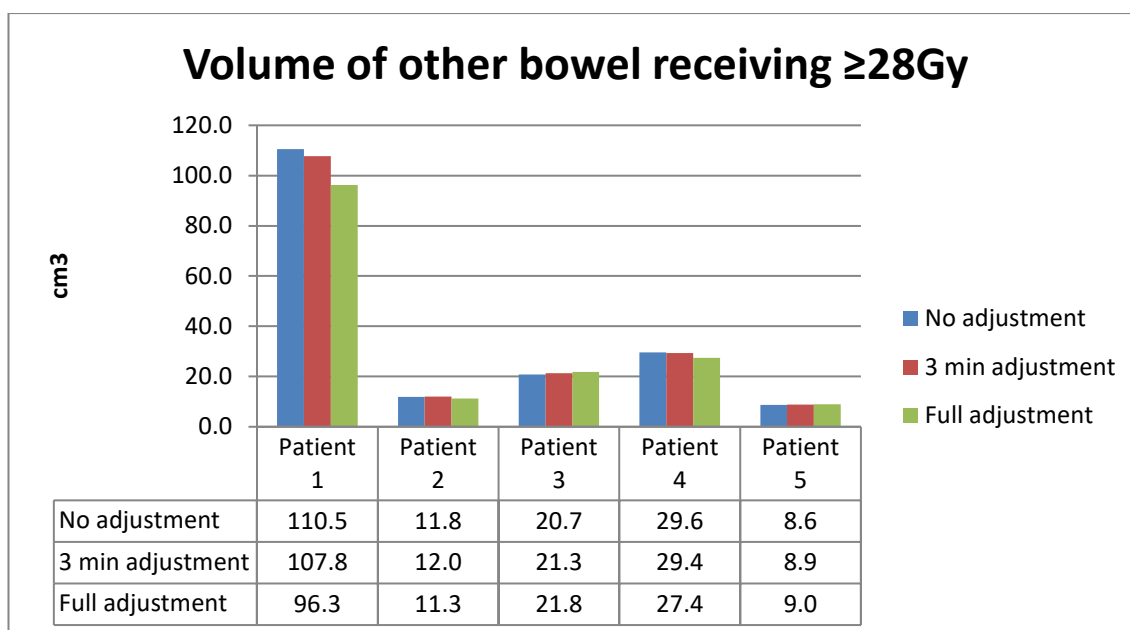


Figure 3.16 Volume of other bowel receiving $\geq 28\text{Gy}$.

Optimal dose constraint 122 cm^3 , mandatory 183 cm^3 .

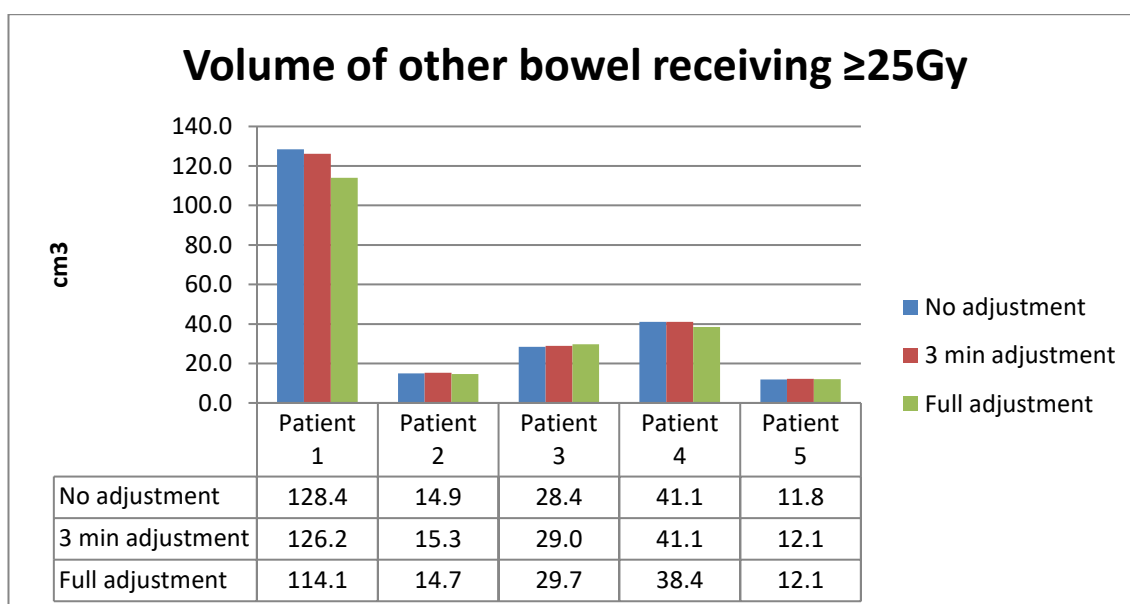


Figure 3.17 Volume of other bowel receiving $\geq 25\text{Gy}$.

Optimal dose constraint 139 cm^3 , mandatory 208 cm^3 .

3.4 Discussion

3.4.1 Development of intra-fraction treatment margins

Based on the results of this intra-fraction treatment margin study, the anisotropic medium margin was selected to take forward into our clinical workflow. This margin allowed target coverage after 30 minutes of filling to be maintained at an acceptable level in $\geq 90\%$ of cases (when combined with drinking and voiding instructions as used in APPLY/IDEAL). In comparison, use of the small margin resulted in unsatisfactory target coverage in 39% and 45% of patients respectively depending on the drinking/voiding protocol, (APPLY vs IDEAL). The standard margin offered little benefit over the medium in terms of target coverage, but if used would result in higher normal tissue doses due to its larger size inferiorly and laterally and was therefore not taken forward into the clinical workflow.

Previous studies have shown that bladder filling/expansion is the predominant cause of intra-fraction bladder motion (13) and this filling is known to be non-uniform (2, 8, 9), predominantly occurring in the anterior/superior direction. This study confirms this finding. The anisotropic nature of the medium margin allows for this non-uniformity of filling enabling coverage to be maintained superiorly/anteriorly for the majority of patients. The ROC curve also confirmed that CTV volume change over 30 minutes can be used as a predictor for target miss when using a small margin, confirming the dominant role of bladder filling as opposed to other deformation, in intra-fraction bladder motion. It also raises that possibility that personalisation of margins may be possible, with those filling less, and in particular < 27 cc perhaps benefitting from use of the small margin to avoid unnecessary normal tissue dose. Due to the small numbers of patients involved in this study, this observation requires validation with a larger dataset.

A potential issue with the uniform use of the medium margin for all patients is that this margin size sometimes violates OAR constraints based on the anatomy seen at planning/ on the session MRI, in particular when there is a large volume of small bowel lying within the PTV itself. In the planning portion of this study this was the case for 11 patients. However, it is expected that as the bladder fills, the OARs will be pushed out of this higher dose area and so the true dose received

to the OARs will be less than the initial DVH suggests. This is dependent on the bladder actually filling during the intra-fraction period but with a mean filling of 35 cc expected over 30mins, and 80% of patients experiencing at least 10 cc of filling, some movement of OARs out of the high risk area is likely to occur. In some rare instances where this does not occur patients should be watched carefully for acute bowel toxicity and it might be necessary to stop treatment at 5 rather than 6 fractions. It should also be noted that the dose constraints used in this study are based on those used in the APPLY trial which showed relatively low rates of acute bowel toxicity (grade 2, 38%, grade 3, 4%), with no episodes of \geq grade 3 late bowel toxicity and a rate of 4.3% late grade 2 bowel toxicity at 12 months (11). In cases where there is still concern about bowel toxicity, consideration could be given to the use of an indwelling catheter on free drainage for the duration of treatment and or a switch to a small PTV margin.

A weakness of this study is that although plans were used to evaluate the validity of the planning margin in terms of target coverage, I did not look at OAR coverage at this later time. This was due to time constraints, as in order to get an accurate appreciation of the true OAR dose, further contouring and additional steps in the ATS workflow would have been needed (as done in the bowel contouring exercise), which takes a considerable time. As the margins are now in clinical use in our MRL workflow, patients with close/ exceeded OAR constraints on the initial CT planning scan will need to be monitored carefully, and ideally should undergo offline assessment of the degree of bladder filling seen during the intra-fraction period to check the assumption that high dose OAR dose constraints improve during the intra-fraction period.

While this work has shown that the medium margin is likely to be acceptable for the majority of patients, the next step in margin definition would be personalisation of the intra-fraction margin to the individual patient. However, predicting how an individual will fill on a day-to-day basis is a challenge.

The level of hydration and drinking instructions given to a patient before treatment are an important factor in determining a patient's fill rate, as demonstrated by the greater fill rates seen in the IDEAL cohort versus the APPLY cohort. However, as

shown in the data presented in Chapter 4, even with consistent drinking and voiding instructions intra-patient fill rates vary on a fraction by fraction basis. This is not surprising as a patient's hydration status is multifactorial and influenced by the volume of liquid consumed in the immediate preceding time period and also other factors such as co-morbidity, drug history and time of day.

Another factor which is more consistent on a fraction by fraction basis but also likely to have an impact on filling and target coverage is the position of the tumour within the bladder itself. In this study, tumour visibility on CT imaging was not sufficient to analyse this in detail. However, work by McBain et al (8) suggests that in a group of 10 patients with bladder cancer who underwent cine MRI imaging, intra-fraction filling tended to occur away from the diseased wall. It should be noted however that diseased bladders were noted to have considerable variation in the maximum wall displacement seen compared to their healthy bladder comparators. As more patients undergo treatment on our MRL we will be able to build up a better picture of the impact of tumour position on intra-fraction motion. This will require well curated datasets and I have set up a research imaging protocol which is now carried out at each bladder MRL fraction which enables images to be collected for future analysis.

A final factor which will influence intra-fraction filling is the total time taken for each online fraction. This analysis assumes that an online fraction will be in the region of 30-40 minutes. Anything significantly longer or shorter than this would potentially invalidate the use of a medium margin. It is hoped that with advances in computing power, MRI acquisition speed and auto-contouring, the total intra-fraction time can be reduced. In this case use of a smaller margin should be re-considered. This should be an area of active research as reductions in the intrafraction margin required will improve the treatment conformality that can be achieved with adaptive replanning and increase the likely benefit of MRgRT. At the other extreme, if a fraction takes significantly longer to deliver the medium margin is unlikely to be sufficient. This is unlikely to be a frequent occurrence as our workflow has been shown to be relatively robust (see Chapter 4). However, to mitigate against this risk as part of our workflow we always re-image prior to

beam on to check target coverage and if deemed to be unsatisfactory we have the option of halting the fraction and asking the patient to void.

3.4.2 Impact of other bowel re-contouring

Although limited by the small number of datasets analysed, there was no clear benefit to support the need for full re-contouring of other bowel either in terms of target coverage at 30 minutes or dose to other bowel at 30 minutes. This fits with the hypothesis that when using a 'dose gradient' approach to planning, the exact position of the OARs is less important in optimising target coverage. In the online workflow, OAR re-contouring time will be limited to less than 3 minutes, with attention focussed at the PTV/OAR interface (within a 2cm radius of the PTV). Allowing 3 minutes of re-contouring will enable more accurate DVHs to be produced which are used as part of the online plan assessment and approval process. By focussing recontouring within 2cm of the PTV and the PTV/OAR interface, hotspots to OARs will be limited whilst still maintaining target coverage. The clinician must bear in mind however, that if full re-contouring has not taken place, the DVHs produced will not be accurate, especially for those constraints looking at percentage of total volumes. If other bowel or rectal constraints are tight at the time of reference planning (or anatomy appears to have change significantly since reference plan generation), an early offline review of estimated delivered dose is recommended.

A strength of this work is that the effect of other bowel re-contouring was measured on the anatomy as seen 30 minutes later i.e. roughly at the time the treatment beam would have been turned on, giving an estimate of the real dose delivered to the target and OARs. This is important as intra-fraction changes in rectum and other bowel position can occur resulting in the planned dose differing from that which is actually delivered. However, analysis of this kind is time consuming and as a result I was only able to study a small number of datasets. If time had allowed, it would have been beneficial to extend this work to a larger patient dataset particularly focusing on patients with challenging anatomy such as large volumes of bowel in the pelvis where dose constraints are more likely to be violated. It would also be helpful to repeat the process looking at the rectal structure set.

It should be noted that this more relaxed approach to re-contouring may be less optimal if a dose-escalated treatment is being trialled. In this case violation of the higher dose constraints is more likely and could have more significant clinical consequences and so the accuracy of DVHs is more important. I would recommend repeating aspects of this study when dose-escalated treatments are adopted.

A way to improve this aspect of our workflow is with the use of MRI to MRI DIR propagation. The quality of DIR appears to be better between MRIs than between CT and MRI. This is particularly true of the external body contour which sometimes requires MRI to MRI propagation to obtain a reliable outline in the online setting. Initially we did not use MRI to MRI propagation as our default as it required an additional offline plan to be produced. Instead, this option was reserved for those patients where CT to MRI DIR was felt to be suboptimal. In recent times however, we have now moved to MRI to MRI DIR for all bladder patients in an attempt to reduce the time needed for re-contouring and to improve the accuracy of online DVHs.

There is no published data available regarding other centres approach to OAR re-contouring with respect to MRgRT for bladder cancer. However, in the context of MRgRT to the pancreas delivered on the ViewRay MRIdian using a SBRT planning technique and daily online adaption, online OAR re-contouring is focussed to within 3mm of the PTV rather than the whole organ (14). The smaller 3mm margin is possible due to the use of SBRT and the resulting sharp dose fall off from the PTV. As we are using IMRT for our bladder cancer patients we felt a focus within 2cm for the PTV was more appropriate for our situation.

3.5 Conclusion

The work discussed in this chapter has helped to shape our current online adaptive radiotherapy workflow. I have shown that a medium margin maintains target coverage across the intra-fraction period in the majority of patients and that full re-contouring of the other bowel OAR is not required in the online setting. As we gain further experience in the use of MRgRT for bladder cancer, I believe this work will serve as a steppingstone to further optimisation of our online workflow

with the ultimate goal of being able to offer a truly personalised approach to each patient.

3.6 References

1. Winkel D, Bol GH, Kroon PS, van Asselen B, Hackett SS, Werensteijn-Honingh AM, et al. Adaptive radiotherapy: The Elekta Unity MR-linac concept. *Clinical and translational radiation oncology*. 2019;18:54-9.
2. Lalondrelle S, Huddart R, Warren-Oseni K, Hansen VN, McNair H, Thomas K, et al. Adaptive-Predictive Organ Localization Using Cone-Beam Computed Tomography for Improved Accuracy in External Beam Radiotherapy for Bladder Cancer. *International Journal of Radiation Oncology*Biology*Physics*. 2011;79(3):705-12.
3. McDonald F, Lalondrelle S, Taylor H, Warren-Oseni K, Khoo V, McNair HA, et al. Clinical implementation of adaptive hypofractionated bladder radiotherapy for improvement in normal tissue irradiation. *Clinical oncology (Royal College of Radiologists (Great Britain))*. 2013;25(9):549-56.
4. Werensteijn-Honingh AM, Kroon PS, Winkel D, Aalbers EM, van Asselen B, Bol GH, et al. Feasibility of stereotactic radiotherapy using a 1.5T MR-linac: Multi-fraction treatment of pelvic lymph node oligometastases. *Radiotherapy and oncology : journal of the European Society for Therapeutic Radiology and Oncology*. 2019;134:50-4.
5. Dees-Ribbers HM, Betgen A, Pos FJ, Witteveen T, Remeijer P, van Herk M. Inter- and intra-fractional bladder motion during radiotherapy for bladder cancer: a comparison of full and empty bladders. *Radiotherapy and oncology : journal of the European Society for Therapeutic Radiology and Oncology*. 2014;113(2):254-9.
6. Nishioka K, Shimizu S, Shinohara N, Ito YM, Abe T, Maruyama S, et al. Analysis of inter- and intra fractional partial bladder wall movement using implanted fiducial markers. *Radiation oncology (London, England)*. 2017;12(1):44.
7. Gronborg C, Vestergaard A, Hoyer M, Sohn M, Pedersen EM, Petersen JB, et al. Intra-fractional bladder motion and margins in adaptive radiotherapy for urinary bladder cancer. *Acta oncologica (Stockholm, Sweden)*. 2015;54(9):1461-6.
8. McBain CA, Khoo VS, Buckley DL, Sykes JS, Green MM, Cowan RA, et al. Assessment of bladder motion for clinical radiotherapy practice using cine-magnetic resonance imaging. *International journal of radiation oncology, biology, physics*. 2009;75(3):664-71.
9. Mangar SA, Scurr E, Huddart RA, Sohaib SA, Horwich A, Dearnaley DP, et al. Assessing intra-fractional bladder motion using cine-MRI as initial methodology for Predictive Organ Localization (POLO) in radiotherapy for bladder cancer. *Radiotherapy and oncology : journal of the European Society for Therapeutic Radiology and Oncology*. 2007;85(2):207-14.
10. Foroudi F, Pham D, Bressel M, Gill S, Kron T. Intrafraction bladder motion in radiation therapy estimated from pretreatment and posttreatment volumetric imaging. *International journal of radiation oncology, biology, physics*. 2013;86(1):77-82.
11. Hafeez S, McDonald F, Lalondrelle S, McNair H, Warren-Oseni K, Jones K, et al. Clinical Outcomes of Image Guided Adaptive Hypofractionated Weekly

Radiation Therapy for Bladder Cancer in Patients Unsuitable for Radical Treatment. International journal of radiation oncology, biology, physics. 2017;98(1):115-22.

12. Hafeez S, Warren-Oseni K, McNair HA, Hansen VN, Jones K, Tan M, et al. Prospective Study Delivering Simultaneous Integrated High-dose Tumor Boost (≤ 70 Gy) With Image Guided Adaptive Radiation Therapy for Radical Treatment of Localized Muscle-Invasive Bladder Cancer. International journal of radiation oncology, biology, physics. 2016;94(5):1022-30.

13. Lotz HT, van Herk M, Betgen A, Pos F, Lebesque JV, Remeijer P. Reproducibility of the bladder shape and bladder shape changes during filling. Medical physics. 2005;32(8):2590-7.

14. Reyngold M, Parikh P, Crane CH. Ablative radiation therapy for locally advanced pancreatic cancer: techniques and results. Radiation oncology (London, England). 2019;14(1):95.

Chapter 4

Feasibility of Magnetic Resonance Guided Radiotherapy for the Treatment of Muscle-Invasive Bladder Cancer.

Sections of this chapter have been published

Abstract:

Hunt A, Hanson I, Dunlop A, Bower L, Barnes H, Chick J, et al. OC-0469: MR-guided online adaptive radiotherapy for muscle invasive bladder cancer: First UK experience. *Radiotherapy and Oncology*. 2020;152:S262-S3

Original article:

Hunt A, Hanson I, Dunlop A, Barnes H, Bower L, Chick J, et al. Feasibility of magnetic resonance guided radiotherapy for the treatment of bladder cancer. *Clinical and translational radiation oncology*. 2020;25:46-51.

Chapter 4 Feasibility of Magnetic Resonance Guided Radiotherapy for the Treatment of Muscle-Invasive Bladder Cancer.

4.1 Introduction

As discussed in the introduction chapter, one of the challenges of bladder radiotherapy is the large inter-fraction variation in target position, shape and size secondary to variable urinary filling and nearby organ motion (1-3). Historically, this has necessitated large population based treatment margins to ensure acceptable target coverage. However, this approach is often over-generous resulting in excessive normal tissue irradiation (4) and is still prone to target miss (5).

Use of daily adaptive replanning aims to reduce the impact of inter-fraction variation by re-optimising the plan based on the anatomy of the day. On the Elekta Unity 1.5T MR linac system, this 'adapt to shape' approach (6, 7) has been tested in clinical feasibility studies, for example in the treatment of the pelvic oligometastases (8) and other pelvic sites (9) however, at the time of writing, there have been no similar reports specifically for bladder radiotherapy. A crucial difference between the treatment of the bladder versus other pelvic sites is the impact of intra-fraction bladder filling causing an increase in CTV size as the patient lies on the treatment couch. As MR guided radiotherapy fractions are typically longer than conventional treatments, this volume change may be more pronounced and must be accounted for to ensure continual target coverage as the bladder fills.

At The Royal Marsden/ICR, our 1.5T MR linac went live clinically in September 2018. The first tumour site to be treated was the prostate representing the first use of online adaptive MRgRT (using any platform) in the UK. Additional tumour sites were brought online in a stepwise manner. We treated our first patient with bladder cancer in April 2019. This represented the first use of online adaptive MRgRT for the treatment of bladder cancer in the UK.

At the local level, the development of the RMH/ICR bladder cancer MR linac workflow was a multi-disciplinary effort, with involvement of clinicians, therapeutic radiographers, medical and MR physicists. My involvement in workflow development included recruitment of volunteer patients to an imaging study on the MR linac, development of an imaging protocol to evaluate bladder filling during a simulated intra-fraction time period, validation of appropriate treatment margins and the development of an online re-contouring strategy in collaboration with our physics team and Dr Hafeez and Prof Huddart.

We aimed to show that it would be feasible to deliver MR guided online adaptive radiotherapy to patients with MIBC. We hypothesised that it would be possible to deliver the treatment in a timely manner (<1 hour), that the treatment would be tolerable for the patient and that target coverage would be maintained throughout delivery (>95% of CTV covered by 95% isodose) despite the increase in fraction time.

4.2 Methods

4.2.1 Patient eligibility

Between April 2019 and December 2019, 5 patients with MIBC who were suitable for hypofractionated weekly radiation therapy but unsuitable for radical treatment with either cystectomy or daily radiation therapy due to either cancer stage or comorbidity, were prospectively recruited to PERMIT, an institutional Clinical Research and Ethics Committee approved protocol for MRgRT (NCT03727698). Patients with a contra-indication to MRI, prosthetic hips or an inability to lie flat for the anticipated duration of an MRgRT fraction (~45 minutes) were excluded.

This patient group was selected for feasibility testing for pragmatic reasons. Firstly, their weekly fraction schedule enabled any inter-fraction technical issues to be resolved without delays to the radiotherapy schedule. Secondly, the workforce implications of delivering a radical 32 fraction schedule were felt to be too great and at the time this was our only radical treatment schedule. Subsequently, a 20 fraction regimen has been approved which will be used for the next stage of our workflow development. Finally, the majority of the data behind the development of our intra-fraction margin was based on patients

undergoing weekly fractionation, it therefore made sense to test the suitability of our margin on this group in the first instance.

4.2.2 Reference plan generation

Patients underwent a non-contrast planning CT scan (CT_{planning}) with an empty bladder. For patients with a urinary catheter in situ this was placed on free flow. In addition, all patients underwent a 'day 0' imaging session on the MR Linac, this enabled us to check patient tolerability and image quality.

The Clinical Target Volume (CTV) was defined as the whole bladder plus extravesical spread. In patients with involvement of the prostate (direct invasion or concurrent prostate adenocarcinoma) the whole prostate was included. For multifocal disease or distant carcinoma in situ, 1.5cm of the prostatic urethra (in males) or 1cm of urethra (in females) was included as per our institutional practice. Defined OARs were the rectum (including the anus), other bowel (including small and large bowel as a single structure) and femoral heads.

I contoured all bar one of the cases with my volumes checked by Dr Hafeez.

Additional reference structures to help guide reproducibility of online contouring, such as base of bladder/prostatic urethra were also contoured.

Once contours were complete, image sets were transferred to the Monaco treatment planning system (version 5.4, Elekta AB, Stockholm, Sweden).

In Monaco, a planning target volume (PTV) was created using an anisotropic margin of 1.5cm anterior/superior, 1cm posterior and 0.5cm lateral/inferior. This margin was to account for on couch intra-fraction bladder filling and was based on my work on intra-fraction filling as described in Chapter 3.

The relative electron densities of 3 key structures (bones, CTV and external density) were calculated and assigned to the relevant planning structures, this technique, along with the use of bulk density layering, enabled the calculation of dose on daily MRIs.

Using the dose constraints detailed in Table 4.1, a 7 field IMRT ‘step and shoot’ treatment plan was produced based on a previously developed ‘class solution’ (see Table 4.2 for the template settings). This class solution was designed by Dr Ian Hanson (Medical Physicist) to produce robust plans which once personalised to an individual patient’s anatomy were designed to require minimal/no additional changes to optimisation parameters during online adaption. The impact of the magnetic field was accounted for in dose calculations.

Table 4.1 Dose constraints

As per our institutional standard and published in Hafeez et al (10)

Organ	Constraint		
PTV	D95%	>95% mandatory	
	D98%	>95% optimal	
	D99%	>90% mandatory	
Rectum (including anus)		Optimal	Mandatory
	V17Gy	50%	80%
	V28Gy	20%	60%
	V33Gy	15%	50%
	V36Gy	5%	30%
Other Bowel	V25Gy	139cc	208cc
	V28Gy	122cc	183cc
	V31Gy	105cc	157cc
	V33Gy	84cc	126cc
	V36Gy	26cc	39cc
Femoral Heads	V28Gy	<50%	
Normal Tissue (External –PTV)	D1cc	≤ 105% prescribed dose	≤ 110% prescribed dose

Once a suitable reference plan was produced this served as a template for online replanning.

The prescription dose was 30-36Gy in 5-6 weekly fractions, with a dose of 30Gy used in cases of metastatic disease.

Table 4.2 Template Settings

Developed by Dr Ian Hanson and adapted from Mr-Linac: PERMIT Bladder Offline Planning Isodocument

Setting	Value
Number of beams	7
Grid spacing	0.3cm
Statistical uncertainty	2% per plan
Fluence smoothing	Medium
Maximum segments	80
Minimum segment width	0.5cm
Minimum segment area	4cm ²
Minimum segment monitor unit	3MU
IMRT constraints	PTV_3600, Rectum, RectumSpare, Other_Bowel, BowelSpare and External_reduced
Bulk density ROIs	Bones_reduced (density taken from the bone ROI limited to superior and inferior extent of target), CTV, External_reduced (density taken from the External_reduced ROI limited to superior and inferior extent of target)
SSO loops	10*

*once online this changes to 5. RectumSpare = Rectum – (PTV +1.5cm), planning structure to aid optimisation; BowelSpare = Other Bowel – (PTV+1.5cm), planning structure to aid optimisation; External_reduced = reduced volume external ROI to facilitate reduced treatment planning time;

Bones_reduced = reduced volume bones ROI to facilitate reduced treatment planning times.

4.2.3 Online adaptive workflow

Patients were asked to void prior to set up. All underwent an online 'adapt to shape' (ATS) adaptive workflow with daily re-contouring and plan re-optimisation (6, 7).

The workflow steps are as follows, see also Figure 4.1

1. A transverse 3D T2W MRI (2 minute acquisition time) (MRI_{session}) was obtained, exported to online Monaco TPS, and registered to the CT_{planning} using soft tissue matching. Contours were propagated from CT_{planning} to MRI_{session} using rigid and deformable image registration (DIR). Rigid registration was used for stable structures such as bones while deformable registration was used for structures with a higher degree of variance such as the bowel and CTV. Contours were manually altered as needed. Generally, this included a complete re-contour of the CTV. Re-contours of the rectum and other bowel structure (within 2cm of PTV) were also undertaken. See Panel C in Figure 4.1.
2. Once contouring was complete, a new radiotherapy plan informed by the MRI_{session} contours was optimised using the reference plan parameters. The dose distribution and DVH was reviewed by the clinician. An independent plan check was carried out by a physicist. Panel D in Figure 4.1
3. Prior to beam on, a further T2W MRI was acquired ($MRI_{\text{verification}}$) to confirm patient positioning and to ensure appropriate target coverage was maintained. Panel E.
4. If the new CTV was not completely within the planned PTV a subsequent adapt-to-position workflow was performed (7). Based on rigid registration between MRI_{session} and $MRI_{\text{verification}}$, the segments from the ATS plan were shifted relative to the isocentre. The dose was then recalculated on the

MRI_{session} optimising the weights of the segments based on the new position. No actual couch shift was performed.

5. If this shift was still deemed to be insufficient due to intra-fraction bladder filling exceeding the boundary of the PTV, we planned to halt the workflow to enable the patient to void prior to performing an additional re-optimisation, in reality this step was never required.
6. A final post treatment T2W MRI (MRI_{post}) was acquired to enable offline assessment of intra-fractional CTV change and coverage. Panel F.

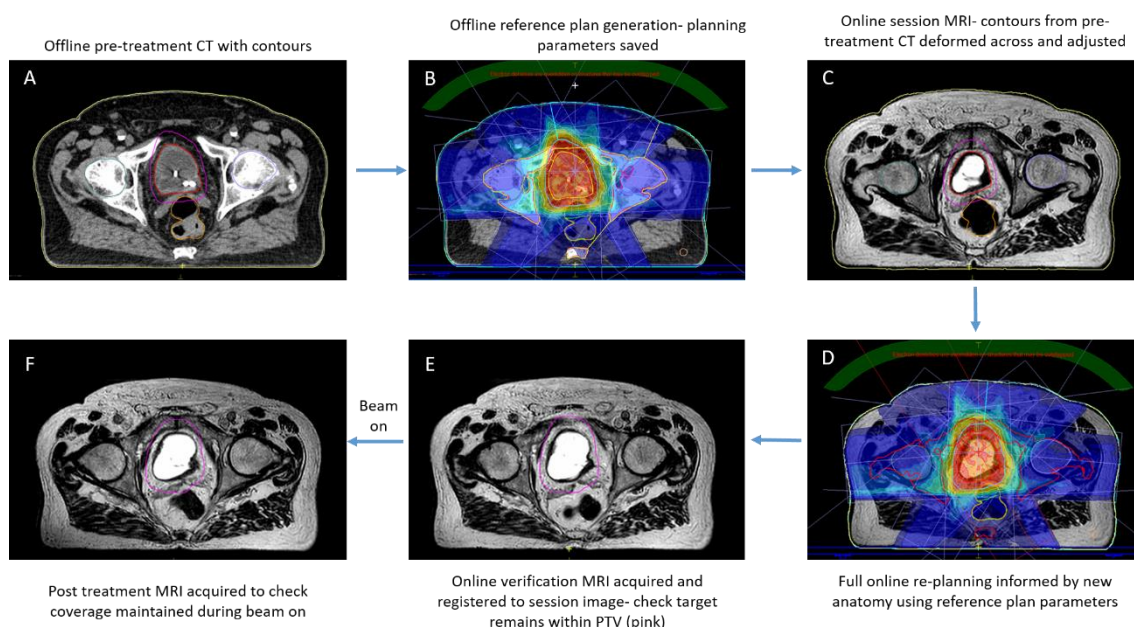


Figure 4.1 Flow chart of adaptive workflow

4.2.4 Workflow feasibility

During each fraction a stopwatch was used to time the key stages of the online workflow. I analysed this data in order to gain an understanding of our average on couch, re-contouring, plan re-optimisation and beam on times across the cohort.

4.2.5 Offline assessment

Post treatment, I re-contoured the CTV, rectum, and other bowel on the MRI_{verification}, and MRI_{post} images. In addition, I corrected the CTV on the MRI_{session} whenever I felt that the session CTV had inadvertently been drawn bigger or smaller than I would have expected. This can occur (usually on a limited number of slices) due to the time pressured scenario of online re-contouring and/or the use of interpolation. The changes I made were small⁵ and unlikely to be clinically significant in the context of fixed field IMRT but without them a bias in the volume change calculation would have been introduced as these errors would have been difficult to replicate when contouring on the verification and post treatment images, see Figure 4.2.

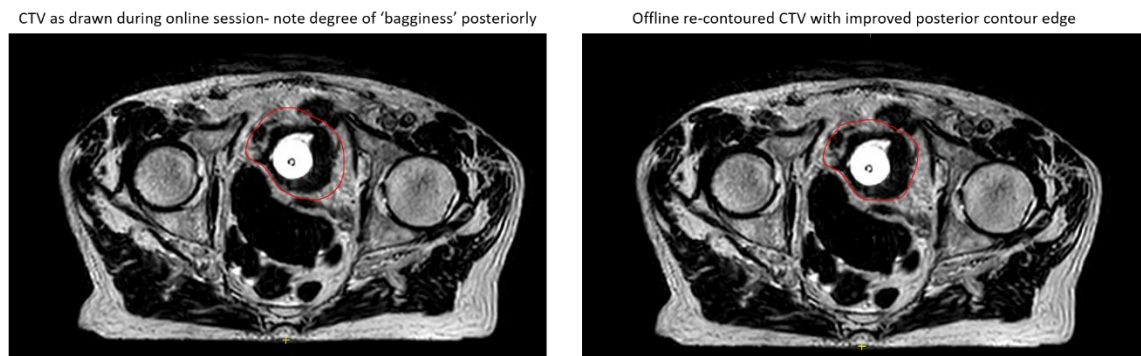


Figure 4.2 example of offline CTV re-contouring

I carried out the offline re-contouring as a single observer in order to minimise inter-observer contouring variability. The intra-fractional CTV change was calculated for each fraction. In addition, estimated delivered dose to the CTV and organs at risk was re-calculated on the MRI_{verification}, and MRI_{post} anatomy. Acceptable CTV coverage was defined as 95% of CTV receiving $\geq 95\%$ prescribed dose.

Plan conformity index (CI_{RTOG}), the proportion of total volume receiving $>95\%$ dose compared to CTV was used as a surrogate for the dose received by normal-tissue (11).

⁵ Median difference between clinical CTV and re-contoured CTV 1.9cc (range 0-18.5cc), for context median re-contoured CTV 107cc.

$$CI_{\text{RTOG}} = \text{Volume within 95\% isodose} \div CTV$$

Here, the higher the CI_{RTOG} the more normal tissue receives >95% planned dose and a $CI_{\text{RTOG}} = 1$ means no normal tissue received this dose.

In this calculation, I used the treatment CTV_{session} (rather than my amended version). This was because, in order to have a read off for the volume receiving 95% prescription dose a calculated plan was needed. However, due to Monaco's software it was not possible to add structures to pre-existing plans (i.e. the plans used clinically) without invalidating the dose calculations on those plans. Invalidating of the clinical plan would have caused issues in other parts of this analysis (such as CTV coverage) so I did not deem this appropriate.

OAR re-contouring on $MRI_{\text{verification}}$, and MRI_{post} was completed by performing an 'adapt to anatomy' command available in Monaco, where the contours from the MRI_{session} are deformed across to the $MRI_{\text{verification}}$, and MRI_{post} images. I left the femoral heads, bone and external structure sets unchanged as the DIR was of acceptable quality but altered the other bowel and rectum structures (named Other_bowel_offline_reviewAH and Rectum_offline_reviewAH respectively) to enable better assessment of the dose received by these structures. By using the same margin formulas and layering priorities as used in the original plan, I then recreated the planning structures needed to calculate the estimated dose delivered on the new anatomy. These steps were needed to enable the treatment planning system to calculate dose. Once these planning structures were in place, using the 'adapt to shape' command in Monaco and utilising the original segments option, I calculated the estimated dose delivered to the anatomy at verification and post treatment by using the same segments and monitor units as used for that online fraction.

All offline assessments were carried out on research Monaco TPS. Patients' data was transferred from the clinical system with preservation of the clinically used image registration.

4.2.6 Patient experience

Patients completed a tolerability assessment after fractions 1-3 and for the final fraction. This consisted of questions related to the patient's environment, comfort, coping and informational needs during treatment. It was scored on a 4-part Likert scale from 0- 3. The questionnaire was adapted from Olausson et al (12) by Dr Helen McNair (Therapeutic Radiographer) and was finalised during the recruitment period. Patients 1-4 completed a questionnaire with 11 questions, while patient 5 completed a questionnaire with 18 questions. Following a discussion with Dr McNair, it was felt that for the purpose of reporting tolerability depending on whether the question had negative or positive connotations, scores between 0-1 and 2-3 were considered noteworthy. A copy of the final questionnaire is included in appendix 4.1.

I was involved with the recruitment, consent, treatment (including online re-contouring) and follow up of patients on our study. I also carried out the analysis of the workflow duration, tolerability of treatment and the success of our treatment with respect to target coverage for the first 5 patients (as detailed below).

4.3 Results

Patient characteristics are summarised in Table 4.3. The median age at start of treatment was 86 years (range 73-88). All patients had transitional cell carcinoma in the bladder, 2 patients also had adenocarcinoma of the prostate and one patient had metastatic disease. Patient 2 had a long-term urinary catheter in situ. 3 patients had both the bladder and prostate included in the CTV.

Table 4.3 Patient Characteristics

	Patient 1	Patient 2	Patient 3	Patient 4	Patient 5
Age	86	86	86	73	88
Sex	Male	Male	Male	Female	Male
Performance status (KPS)	90	70	80	80	80
Cancer staging	T3N0M0 bladder	T4aN0M0 bladder	T4bN1M0 bladder T2N0M0 prostate	T2N0Mx bladder T4N3M1 ureter	T2N2M0 bladder T2N1M0 prostate Ca
Structures included within the CTV	Whole bladder 1.5cm urethra	Whole bladder Prostate	Whole bladder Pelvic sidewall Prostate	Whole bladder 1cm urethra	Whole bladder Prostate
Volume of CTV as on CT _{planning} (cc)	106	134	175	87	334
Prescription Dose	36Gy in 6 fractions	36Gy in 6 fractions	36Gy in 6 fractions	30Gy in 5 fractions	36Gy in 6 fractions
Clinical Notes	-	Long term urinary catheter in situ	-	Metastatic upper tract cancer, bladder radiotherapy given for haemostasis	-

4.3.1 Online adaptive workflow

All patients completed their planned course of treatment on the MR linac. A total of 29 online adaptive fractions were delivered. 4 fractions required an additional ATP after ATS due to a shift in patient position (2 occasions) or bladder filling. No fractions were halted to enable the patient to void.

Figure 4.3 summarises the time taken for key parts of the online adaptive workflow. The median time on treatment couch was 39 minutes (range 33-48), median time spent re-contouring was 7 minutes (range 4-11), median plan re-optimisation was 5 minutes (range 3-6) and treatment delivery lasted for a median of 9 minutes (range 8-12).

For Patient 1, technical issues resulted in premature beam termination during fraction 4. The missed dose (15% of that fraction's planned dose) was compensated for in subsequent fractions. Patient 5 experienced a one week delay prior to fraction 3 due to a non-treatment related admission to hospital, this was compensated for by extending total treatment time by one week.

In patients 2&4, the CT_{planning} to MRI DIR based external ROI propagation performed poorly with ≥ 1 cm difference seen from the true external contour position and the propagated contour. Differences of this magnitude were felt to potentially impact clinically on the dose calculations. To correct for this, from fraction 3 and 2 respectively, the MRI_{session} from fraction 1 was fully re-contoured offline and used to create a new reference plan. This improved External ROI propagation in subsequent fractions.

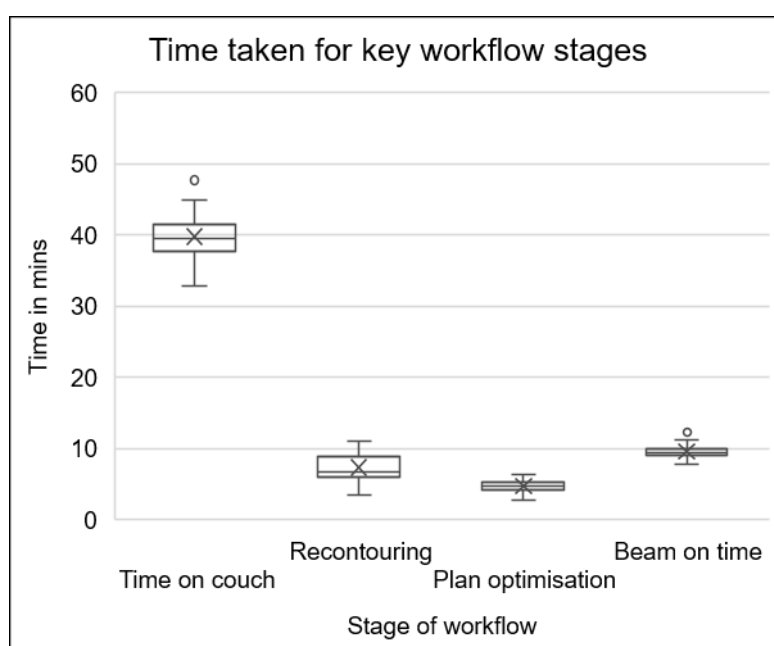


Figure 4.3 Time taken for online adaptive workflow stages.

Note that some stages, for example, online image acquisition are not included in this graph so total time of couch is more than the sum of re-contouring, plan optimisation and beam on time. In this box and whisker plot x= mean value, horizontal line median value, box edges inter-quartile range, whiskers maximum and minimum values and circles outliers.

4.3.2 Inter- and intra-fraction CTV variation

Inter- and intra-fraction CTV variation is shown in figure 4.4. The median CTV⁶ as determined on MRI_{session} was 107cc (range 60-243cc). Patient 1 showed the widest variation of CTV size, range 72cc-106cc. Patient 4 showed the least.

⁶ Refers to my amended CTV

Median intra-fraction CTV change (which represents a surrogate for bladder filling determined by change in volume between MRI_{session} and MRI_{post}) was 30cc, range between -2-82cc. Patient 1 demonstrated the greatest filling with a median of 64cc (range 25-82cc), Table 4.4.

As expected, patient 2 (urinary catheter in situ) showed the least, and in some cases negative filling. However, there were also instances where the CTV increased in size by up to 30cc (fraction 3), likely due to the position of the catheter allowing urine to pool temporarily.

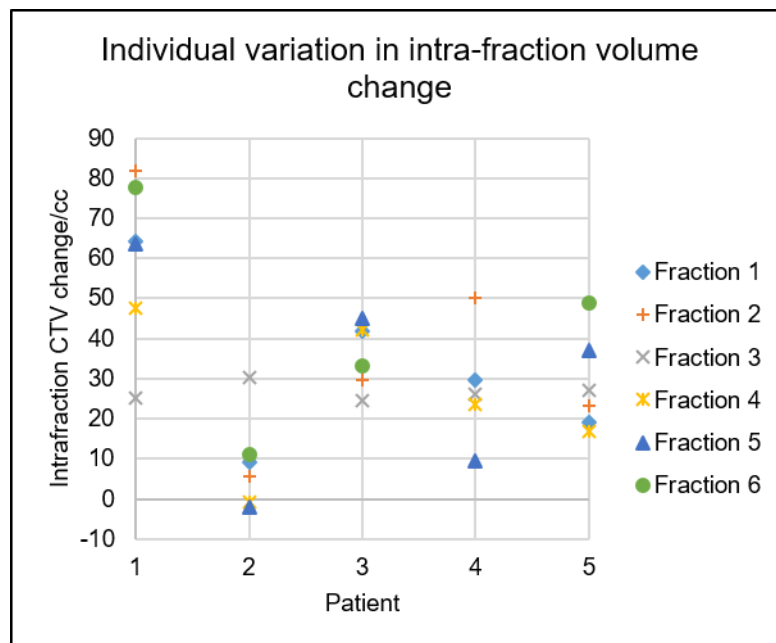
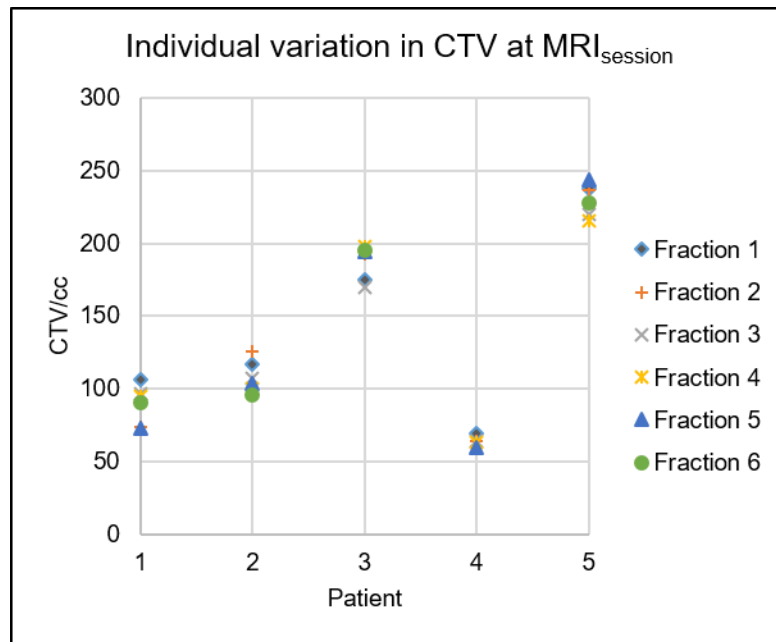


Figure 4.4 Variation in CTV at MRI_{session} (top graph), Variation in intra-fraction volume change, (bottom graph).

Table 4.4 Intra-fraction CTV change

	Patient 1	Patient 2	Patient 3	Patient 4	Patient 5
Median CTV change	64 cc	8 cc	38 cc	26 cc	25 cc
Range	25-82 cc	-2-30 cc	25-45 cc	10-50 cc	17-49 cc

On an intra-patient basis, there does not seem to be any clear pattern of a change to fill rate as the fractions progressed, Figure 4.5.

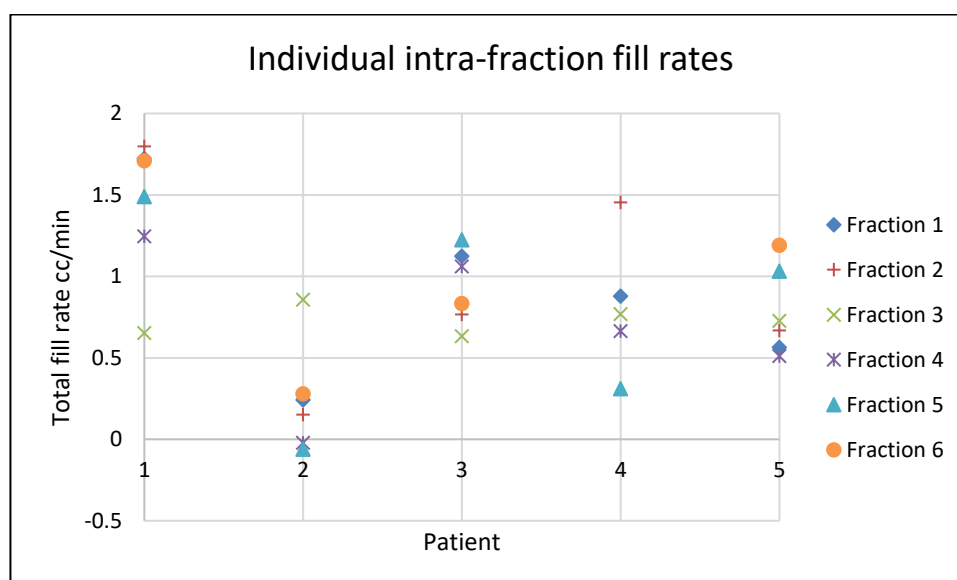


Figure 4.5 Intra-fraction fill rates

4.3.3 Target coverage and Conformity Index

CTV coverage based on anatomy from MRI_{verification} and MRI_{post} (V95% prescribed dose >95% CTV) was maintained for 28/29 fractions; with 1 fraction having post treatment coverage of 94.5% (patient 1), estimated dose remained above 95% on verification for this fraction, see Figure 4.6. For patients 2-5, the CTV was adequately covered throughout treatment.

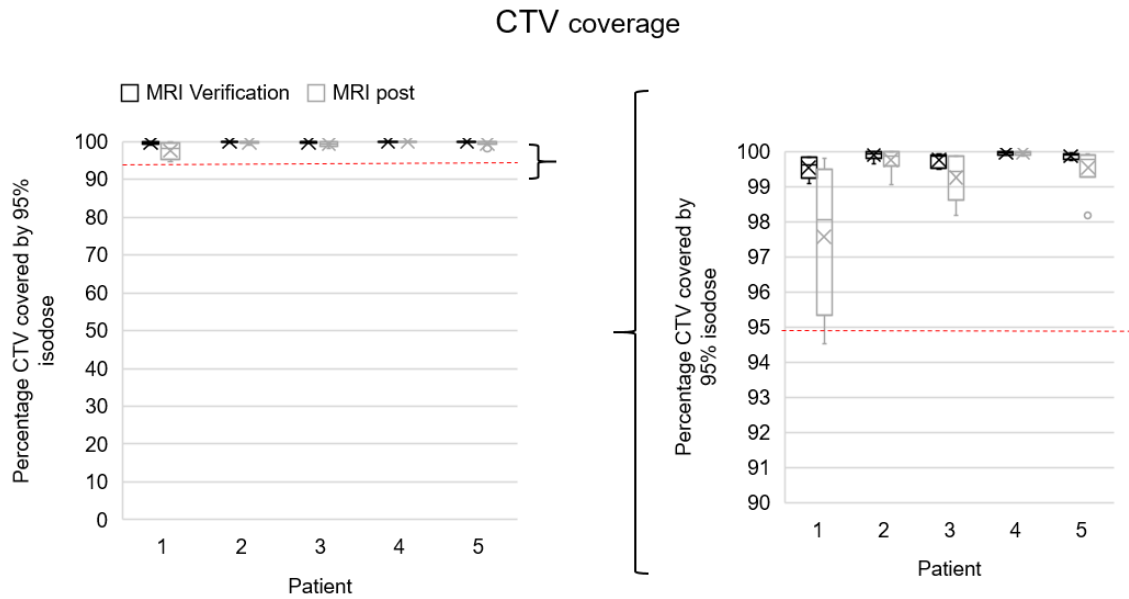


Figure 4.6 Box and Whisker plot (as per figure 4.3) depicting CTV coverage by 95% isodose on verification and post treatment MRIs.

Insert plot shows the same data with Y axis rescaled to start at 90% to better visualise the data. Dotted line indicates 95%. There were no data points below 90%.

In 27/29 fractions, the delivered plan resulted in estimated dose to OARs within the mandatory dose constraints, based on the anatomy seen on the verification and post treatment MRI. For patient 2 fraction 1, the V36Gy for other bowel exceeded tolerance on the verification image (by 15 cc) but was within tolerance on the post treatment image and subsequent fractions. For patient 5, rectal dose constraints were missed in fraction 2 (by up to 12%) but were within tolerance for subsequent fractions. This violation in rectal dose constraints occurred due to a gas bubble passing through the rectum pushing the rectum anteriorly, see Figure 4.7.

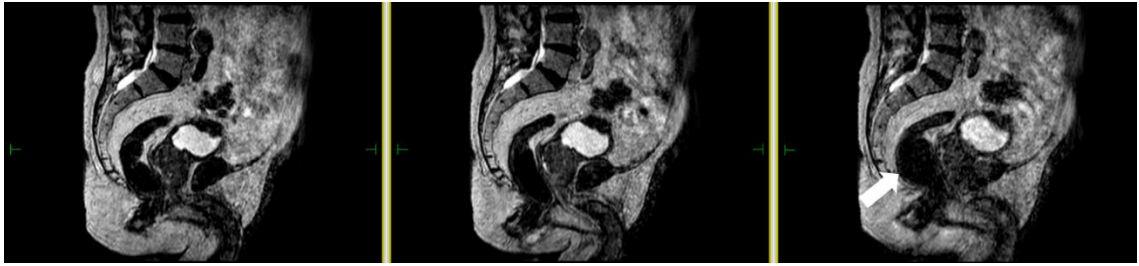


Figure 4.7 Intra-fraction changes to rectal shape.

L-R session MRI, verification MRI and post treatment MRI. See how the rectum enlarges between the session and post treatment image (white arrow)

The Conformity Index (CI_{RTOG}) on MRI_{post} improved compared to the corresponding $\text{MRI}_{\text{session}}$, except for the patient with a urinary catheter or in cases with minimal intra-fraction filling, such as patient 4 fraction 5, see Figure 4.8. The mean CI_{RTOG} on MRI_{post} was 2.44, when the patient with the catheter was excluded this improved further to 2.28.

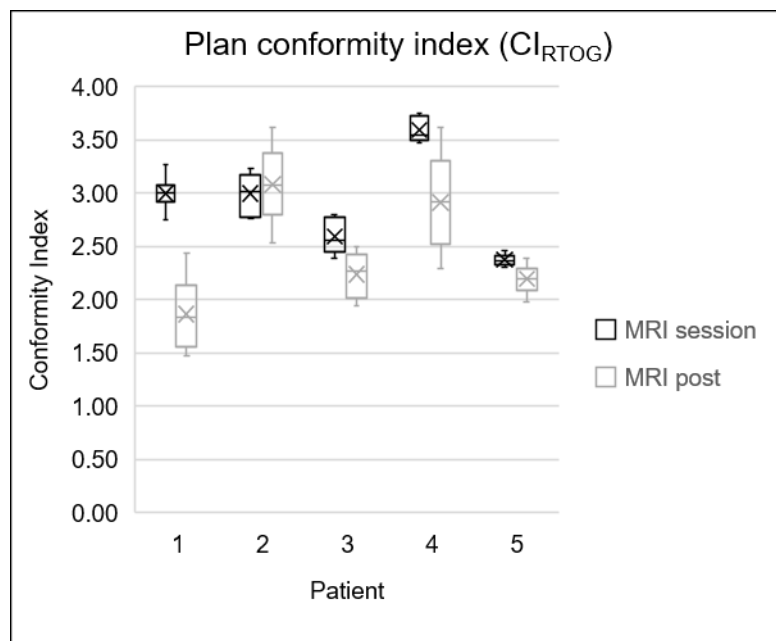


Figure 4.8 Conformity index based on session anatomy versus post treatment anatomy.

A value closer to 1 indicates less normal tissue receiving 95% planned dose. Box and Whisker interpretation as per previously.

4.3.4 Patient tolerability

Experience questionnaires were completed by all patients at ≥ 3 time points. A total of 19/20 experience questionnaires were returned. Questionnaires for patients 1-4 had 11 questions, questionnaires for patient 5 had 18 questions (as the questionnaire was updated during the study). One questionnaire from patient 3 (fraction 3) was missing/not completed. Patient 1 failed to answer one question (fraction 1). A total of 235 questions were therefore answered.

Of these 235 questions, 99.1% of responses reflected acceptable/favourable treatment experience. Two responses were given a 'noteworthy' score which was classified as a score of 0 or 1 for a positive statement and 2 or 3 for a negative statement. One noteworthy score was in the situational coping theme with the question "Did you feel calm during your session" scored as 0 "not at all" by patient 1 for fraction 1. The other was in the environmental theme, with the question "I found the noise in the room easy to tolerate" scored as 0 "not at all" by patient 5 for fraction 2. In both instances preceding or subsequent questionnaires did not highlight an ongoing problem.

4.4 Discussion

This is the first report on the clinical use of the Elekta Unity 1.5T MR linac for the treatment of bladder cancer. Indeed, from review of the literature, details on the clinical use of MRgRT in bladder cancer is sparse across both commercially available MR linac platforms. One prior report mentioned treatment of the bladder on ViewRay's MRIdian, but it is unclear what treatment margins were used, whether these patients underwent daily adaption and what CTV coverage was achieved (13).

We successfully demonstrated that full online adaption using the Elekta Unity was technically and clinically feasible. We achieved our aim of completing each fraction within 1 hour. In comparison to other centres using the Elekta Unity system, our workflow was of a comparable length. Bertelsen et al (9) reported a median on couch time of 45 minutes when treating patients with a variety of pelvic cancers with an ATS approach. This is compared to our median on couch time of 39 minutes using the same technique which was achieved despite the large

fraction size used which would have increased beam on time. Of note, their case series did not include any patients with the bladder as the target. Fractions which required an additional ATP step had a longer on couch time (median 45 minutes vs 39 minutes), but they were still all completed in a timely manner.

There was variation seen in our re-contouring time with a range across all fractions of 4-11 minutes. This variation is due to a variety of reasons. Firstly, the complexity and size of the CTV varied across patients. For example, patients 1&4 had smaller CTVs compared to the other cases (mean of 76.6cc vs 175.4cc). The smaller size is likely to have contributed to the shorter median re-contouring time (6 minutes for patients 1&4) compared to a median in excess of 7 minutes for the other cases. Secondly, total re-contouring time was impacted by the need to re-contour additional structures such as the rectum or other bowel. For example, patient 5 fraction 6 required re-contouring of structures other than the CTV and took a total of 9 minutes to re-contour while for fraction 5, the CTV alone was re-contoured with total time of 8 minutes. Finally, 3 different clinicians were involved in online re-contouring and there are likely differences in the speed of contouring due to influences such as familiarity with the case and contouring programme and the day-to-day variation in anatomy the interpretation of this.

Plan re-optimisation and beam on times were relatively consistent across the fractions.

Treatment was well tolerated with no sessions terminated due to patient discomfort. In the patient questionnaire, 0.85% (2/235) of questions answered gave a response which we would consider of noteworthy concern with respect to unfavourable/poor tolerability. These were within the situational coping and environmental coping themes. Other questions answered on the same day within these themes did not reflect similar concerns. Patients were not asked about their responses upon completion of the questionnaire, so it is impossible to know whether these answers reflect a true concern of whether this was a misinterpretation in the question or scale. However, for all patients the vast majority of answers did not raise concerns with respect to treatment tolerability.

Further work on treatment tolerability for a wider group of patients having treatment on the MR linac to a variety of tumour sites is ongoing.

Intra-patient inter-fraction variation in CTV size on MRI_{session} was noted, this was despite the patients being asked to empty their bladder prior to getting on the treatment couch. This is consistent with other bladder radiotherapy studies. Lalondrelle et al reported a similar finding following an analysis of pre-treatment cone beam CTs (CBCT_{pre}) for 15 patients (5). The CTV volume was within +/- 20cc of the CTV at planning (CTV0) for 3 patients while in 10 patients the CBCT_{pre} was greater than CTV0 for more than 50% of fractions. This variation in CTV size highlights the importance of adaptive techniques for bladder cancer radiotherapy. A benefit of online adaptive replanning over other techniques such as a library of plans, is that the impact of this inter-fraction variation can essentially be removed.

However, while inter-fraction variation can be mitigated against using online adaption and re-optimisation, intra-fraction variability becomes more of an issue due to the increased time taken to deliver each fraction. In a conventional treatment, the time between the cone beam of the day and beam off is in the region of 14 minutes (14) whilst in our study the time from first image to beam off was 39 minutes. It was therefore expected that in patients without a catheter some degree of bladder filling and hence CTV increase will occur. In a study by McDonald et al (14) in a similar cohort of patients, bladder filling over a 30 minute period averaged 26cc (standard deviation 18, range 5-71), with 8% experiencing filling more than 50cc. In our study, median filling was 30cc increasing to 33cc when the patient 2 was excluded. Two patients (1&4) had filling of >50cc in at least one of their fractions. It should also be noted that the intra-patient intra-fraction variation was marked as shown in figure 4.4 and Table 4.4. There did not appear to be any pattern to the variability seen. This is in contrast to Hafeez et al (15) who found that the rate of bladder filling decreased over the course of treatment although this was for patients receiving a radical course of treatment. With such a small cohort, it is not possible to draw any firm conclusions as to whether the variability seen in this study can be extrapolated to the wider population. Future work will aim to explore this issue further.

Despite the variation in intra-fraction filling seen, coverage of the post treatment CTV by the 95% isodose remained above our 95% goal in 28/29 fractions. For the one fraction where it dipped below this threshold, the 95% goal was missed by 0.5% and so unlikely to be clinically significant. My method of analysis used the 'isotoxicity' approach as described by Green et al (16). I evaluated each plan *de novo* rather than attempting dose summation. This means no adjustments were made to dose constraints based on the dose previously delivered. I acknowledge that this form of dose analysis is crude and likely to be more conservative than other methods which attempt to accumulate dose through deformable image registration and displacement vector fields (17) but given my time and resource constraints I consider this a reasonable compromise.

While maintenance of target coverage is clearly a priority, it should not come at the expense of excessive dose to normal tissue and OARs. The analysis of estimated delivered dose to OARs suggested that in the majority of fractions, all mandatory dose constraints were met. These dose constraints were met despite the fact that full online re-contouring of the bowel and rectum was not carried out. As a continuation of the work detailed in Chapter 3, I attempted to look further into the value of full re-contouring for this patient cohort, in particular looking at whether full re-contouring improved the dose received by OARs. However, due to differences in the clinical and research Monaco platforms a reliable comparison was not possible.

In addition to OAR constraints we used the CI_{RTOG} as a measure of dose to normal tissue. This conformity index metric has been previously used by Hafeez et al (15) when examining the impact of the 'plan of the day' approach on normal tissue dose during bladder radiotherapy. Our mean conformity index compares favourably with the conformity achieved in this study, with a mean CI_{RTOG} on post treatment cone beam CT of 3.5 compared to a mean post treatment CI_{RTOG} in our study of 2.4. When the patient with the urinary catheter is excluded (as was the case for Hafeez et al) our CI_{RTOG} improves still further to a value of 2.28. This suggests that while our intra-fraction margin may seem generous at first glance, it performs well compared to other adaptive strategies.

In the literature, other centres have used planning studies to model the impact of online plan re-optimisation on dose to normal tissue and found a similar improvement over standard treatment techniques (18, 19). However, these studies assumed a shorter intra-fraction treatment time and therefore utilised smaller treatment margins. Given the work presented in Chapter 3, I feel that use of such margins in our workflow would likely result in target miss. However, I acknowledge that optimisation of our intra-fraction margin is warranted. The ultimate goal would be to truly personalise the margin to the individual. Unfortunately, due to the variability in intra-fraction filling seen on an intra-patient basis this will be challenging as it does not appear that you can predict the degree of filling that will occur on subsequent fractions. The clear exception to this is patients with a urinary catheter where margin reduction is likely possible. Another issue is the impact of nearby organ motion, for example, there was several occasions where a rectal gas bubble pushed the target volume anteriorly, our margin was able to account for this but smaller margins would be less able to accommodate such random displacement. Future work will focus on this issue and is likely to include more advanced adaptive radiotherapy techniques such as MR guided real time target tracking (20).

4.5 Conclusions and future directions

I have shown that delivery of online adaptive MRgRT is feasible in the context of muscle invasive bladder cancer. Treatment was delivered in a timely manner, was well tolerated and target coverage was maintained without excessive dose to normal tissue. Further work will include continued recruitment into the 36Gy/6# cohort along with an expansion into the radical 20# treatment paradigm.

Future work should investigate the potential to predict intra-fraction filling to better personalise intra-fraction treatment margins. In addition, steps to reduce the total time needed to treat a patient should be explored which will have a positive impact on both margin size and patient throughput. The role of dose escalation will also be investigated using the MR Linac.

In the longer term, studies comparing MRgRT to more conventional radiotherapy treatment should be considered to ensure that patients receive the optimal radiotherapy for their clinical situation.

4.6 References

1. Muren LP, Smaaland R, Dahl O. Organ motion, set-up variation and treatment margins in radical radiotherapy of urinary bladder cancer. *Radiotherapy and oncology : journal of the European Society for Therapeutic Radiology and Oncology*. 2003;69(3):291-304.
2. Pos FJ, Koedooder K, Hulshof MC, van Tienhoven G, Gonzalez Gonzalez D. Influence of bladder and rectal volume on spatial variability of a bladder tumor during radical radiotherapy. *International journal of radiation oncology, biology, physics*. 2003;55(3):835-41.
3. Dees-Ribbers HM, Betgen A, Pos FJ, Witteveen T, Remeijer P, van Herk M. Inter- and intra-fractional bladder motion during radiotherapy for bladder cancer: a comparison of full and empty bladders. *Radiotherapy and oncology : journal of the European Society for Therapeutic Radiology and Oncology*. 2014;113(2):254-9.
4. Vestergaard A, Sondergaard J, Petersen JB, Hoyer M, Muren LP. A comparison of three different adaptive strategies in image-guided radiotherapy of bladder cancer. *Acta oncologica (Stockholm, Sweden)*. 2010;49(7):1069-76.
5. Lalondrelle S, Huddart R, Warren-Oseni K, Hansen VN, McNair H, Thomas K, et al. Adaptive-Predictive Organ Localization Using Cone-Beam Computed Tomography for Improved Accuracy in External Beam Radiotherapy for Bladder Cancer. *International Journal of Radiation Oncology*Biology*Physics*. 2011;79(3):705-12.
6. Winkel D, Bol GH, Kiekebosch IH, Van Asselen B, Kroon PS, Jurgenliemk-Schulz IM, et al. Evaluation of Online Plan Adaptation Strategies for the 1.5T MR-linac Based on "First-In-Man" Treatments. *Cureus*. 2018;10(4):e2431.
7. Winkel D, Bol GH, Kroon PS, van Asselen B, Hackett SS, Werensteijn-Honingh AM, et al. Adaptive radiotherapy: The Elekta Unity MR-linac concept. *Clinical and translational radiation oncology*. 2019;18:54-9.
8. Werensteijn-Honingh AM, Kroon PS, Winkel D, Aalbers EM, van Asselen B, Bol GH, et al. Feasibility of stereotactic radiotherapy using a 1.5T MR-linac: Multi-fraction treatment of pelvic lymph node oligometastases. *Radiotherapy and oncology : journal of the European Society for Therapeutic Radiology and Oncology*. 2019;134:50-4.
9. Bertelsen AS, Schytte T, Moller PK, Mahmood F, Riis HL, Gottlieb KL, et al. First clinical experiences with a high field 1.5 T MR linac. *Acta oncologica (Stockholm, Sweden)*. 2019;58(10):1352-7.
10. Hafeez S, Patel E, Webster A, Warren-Oseni K, Hansen V, McNair H, et al. Protocol for hypofractionated adaptive radiotherapy to the bladder within a multicentre phase II randomised trial: radiotherapy planning and delivery guidance. *BMJ open*. 2020;10(5):e037134.
11. ICoRUa: M. ICRU Report 62, Prescribing, Recording and Reporting Photon

Beam Therapy (Supplement to ICRU Report 50):. Nuclear Technology Publishing; 1999.

12. Olausson K, Holst Hansson A, Zackrisson B, Edvardsson D, Ostlund U, Nyholm T. Development and psychometric testing of an instrument to measure the patient's experience of external radiotherapy: The Radiotherapy Experience Questionnaire (RTEQ). *Technical innovations & patient support in radiation oncology*. 2017;3-4:7-12.
13. Henke LE, Contreras JA, Green OL, Cai B, Kim H, Roach MC, et al. Magnetic Resonance Image-Guided Radiotherapy (MRIGRT): A 4.5-Year Clinical Experience. *Clinical oncology (Royal College of Radiologists (Great Britain))*. 2018;30(11):720-7.
14. McDonald F, Lalondrelle S, Taylor H, Warren-Oseni K, Khoo V, McNair HA, et al. Clinical implementation of adaptive hypofractionated bladder radiotherapy for improvement in normal tissue irradiation. *Clinical oncology (Royal College of Radiologists (Great Britain))*. 2013;25(9):549-56.
15. Hafeez S, Warren-Oseni K, McNair HA, Hansen VN, Jones K, Tan M, et al. Prospective Study Delivering Simultaneous Integrated High-dose Tumor Boost (≤ 70 Gy) With Image Guided Adaptive Radiation Therapy for Radical Treatment of Localized Muscle-Invasive Bladder Cancer. *International journal of radiation oncology, biology, physics*. 2016;94(5):1022-30.
16. Green OL, Henke LE, Hugo GD. Practical Clinical Workflows for Online and Offline Adaptive Radiation Therapy. *Seminars in radiation oncology*. 2019;29(3):219-27.
17. Chetty IJ, Rosu-Bubulac M. Deformable Registration for Dose Accumulation. *Seminars in radiation oncology*. 2019;29(3):198-208.
18. Vestergaard A, Hafeez S, Muren LP, Nill S, Hoyer M, Hansen VN, et al. The potential of MRI-guided online adaptive re-optimisation in radiotherapy of urinary bladder cancer. *Radiotherapy and oncology : journal of the European Society for Therapeutic Radiology and Oncology*. 2016;118(1):154-9.
19. Vestergaard A, Muren LP, Sondergaard J, Elstrom UV, Hoyer M, Petersen JB. Adaptive plan selection vs. re-optimisation in radiotherapy for bladder cancer: a dose accumulation comparison. *Radiotherapy and oncology : journal of the European Society for Therapeutic Radiology and Oncology*. 2013;109(3):457-62.
20. Menten MJ, Fast MF, Nill S, Kamerling CP, McDonald F, Oelfke U. Lung stereotactic body radiotherapy with an MR-linac - Quantifying the impact of the magnetic field and real-time tumor tracking. *Radiotherapy and oncology : journal of the European Society for Therapeutic Radiology and Oncology*. 2016;119(3):461-6.

Chapter 5

MRI sequence optimisation for pancreatic MR guided radiotherapy.

Sections of this chapter/ preliminary work have been published/presented:

Presentation:

Magnetic resonance imaging sequence evaluation for stereotactic MR-guided online adaptive radiotherapy for pancreatic cancer. Oral presentation by myself at SABR UK Consortium Meeting 2019

Original articles:

Eccles CL, Adair Smith G, Bower L, Hafeez S, Herbert T, Hunt A, et al. Magnetic resonance imaging sequence evaluation of an MR Linac system; early clinical experience. Technical innovations & patient support in radiation oncology. 2019;12:56-63

Chapter 5 MRI sequence optimisation for pancreatic MR guided radiotherapy.

5.1 Introduction

As previously discussed in the thesis introduction, online adaptive dose escalated MRgRT for pancreatic cancer has many postulated benefits over conventional radiotherapy. However, realisation of this potential is reliant on the development of suitable MRI sequences which can be successfully integrated into the online adaptive workflow.

5.1.1 Use of MRI in radiotherapy workflows

Integration of MRI into radiotherapy workflows can occur in many ways. In its simplest form, this involves the use of unfused diagnostic MRI to aid delineation on CT planning scans. This requires little in the way of extra resources but relies on ‘cognitive fusion’ by the contouring clinician and does not take into account differences in patient or OAR or tumour positioning between the scans. It also does not allow for online adaption.

The next level of complexity involves the use of dedicated planning MRIs or ‘MR simulation’ scans. Here an MRI can either be fused to the planning CT (the primary dataset for planning purposes) or as is being trialled at some centres (1, 2), the MRI can be used offline as a standalone planning scan (i.e. a MR only workflow). In order to avoid the introduction of geometric uncertainty, diagnostic MRIs must be modified to reduce geometric distortion and MRI/CT fusion accuracy must be checked (3). The MRI should be performed in the radiotherapy position, ideally on the same day as the planning CT, with similar motion control and scan slice thickness. Dedicated MRI radiotherapy protocols are therefore required (4). At the start of my thesis no such protocols were available at my institution for pancreas radiotherapy.

In the *online* setting, which is the predominant area of interest for my thesis, the advent of MR Linacs has made MRgRT possible, however, hardware differences between diagnostic scanners and MR Linacs mean that optimised diagnostic

scanner sequences will not necessarily produce the same image quality when run on the MRL. Instead, dedicated MRL sequences are required.

My institution's MRL came with 3, CE marked sequences for use in online MRgRT for the upper abdomen. Whilst these sequences were geometrically valid and integrated within the MRL system, their image clarity was suboptimal. Visualisation of key OARs was limited making online delineation challenging thereby reducing our ability to perform a fully adaptive online workflow and in turn limiting the scope for dose escalation.

Therefore, at the start of my thesis, there was no access to suitable MRI sequences for use in either an offline 'MR simulation' capacity or in an online fully adaptive radiotherapy pathway.

5.1.2 Challenges of developing offline and online radiotherapy planning MRI sequences for pancreatic cancer

Although used less frequently than CT, MRI is established in the pancreatic cancer diagnostic pathway especially in cases of diagnostic uncertainty (5) (6). Imaging protocols typically involve a variety of sequences, each optimised to provide additional diagnostic information (see Table 5.1).

Table 5.1 Typical imaging protocol for pancreatic cancer.

Adapted from Royal College of Radiology Recommendations for cross-sectional imaging in cancer management, Second Edition.

Sequence	Plane	Slice thickness	Field of view
T1W with fat suppression	Axial	4 +/- 1mm	Large
T1W with contrast	Dependent on tumour position	4 +/- 1mm	Large
T1W with contrast	Axial	5 +/- 2mm	Small
T2W	Dependent on tumour position	4 +/- 1mm	Large
T2W	Axial	5 +/- 2mm	Small

Unfortunately, optimised diagnostic sequences are not necessarily suitable for use in radiotherapy due to the differing demands of these two scenarios (7-10). In general terms, these differences include parameters such as couch type and patient positioning, along with factors such as geometric distortion mitigation, 2D versus 3D imaging, field of view coverage and slice thickness. More specifically in the case of pancreatic cancer workflows, management of respiratory motion and the role of IV contrast needs to be considered. In the online setting, workflow time constraints are more pressing, limiting the type and number of sequences which can be acquired. These differences are further summarised in Table 5.2.

Table 5.2 Differences between diagnostic and radiotherapy planning MRIs for pancreatic cancer.

Adapted from White et al (8) with additional parameters added.

Parameter	MRI for diagnosis	MRI for use within MR sim/ online MRgRT
Couch	Maximised for patient comfort, soft and often concave, concave feature improves SNR(10)	Flat couch required for RT but this can reduce SNR impacting on image quality
Patient positioning	Supine, maximised for patient comfort	Supine, position dependent on planning technique Dedicated immobilisation devices needed, position reproducibility paramount
Field strength	Increasing field strength preferred as SNR improved	Increasing field strength increases geometric distortion, max. recommended 1.5T (7)
Coverage	FOV limited to area immediately around tumour improving SNR	Larger FOV required to ensure margin for PTV and external body contour imaged to enable planning
Preferred sequence(s)	Multiple sequences to maximise diagnostic information, 2D or 3D acceptable. Slice thickness can vary to facilitate optimisation	Ideally single sequence for contouring, planning and position verification. Must be 3D. Slice thickness as thin as possible to facilitate planning Limited acquisition time if used in online setting
Geometric accuracy	Relative rather than true position of tumour important	True physical position in space vital to enable safe dose delivery

Use of IV contrast agent	Used to improve diagnostic quality	Challenge of use over multiple fractions
Motion management	<p>Intramuscular buscopan to reduce peristaltic motion</p> <p>Breath-hold and/or abdominal compression to reduce respiratory motion: geometric and inter-scan reproducibility less important</p>	<p>Challenge of multiple intramuscular injections</p> <p>If used, reproducible breath-hold and/or abdominal compression required across treatment course.</p>

5.1.3 Sequence optimisation

Without access to pre-optimised offline or online MRI, development of optimised sequences became the first priority for the pancreatic component of my thesis. The majority of my time was focussed on the development of online sequences, but I also investigated, to a lesser degree, how MRI might be integrated into our current offline planning process.

Despite initial optimism about the extent of optimisation that could be achieved, during my research time I was constrained by two important factors. Firstly, at my institution, it is mandated that all patients who are treated on the MRL are treated within a clinical trial. The trial relevant to pancreas patients is the PERMIT trial whose ethical approval mandates that the MRL is used within its CE marking. In-house developed sequences must therefore be approved by Elekta to be used in treatment. However, despite initial encouragement, approval by Elekta was not forthcoming and promised timelines with respect to approvals or sequence upgrades slipped considerably during this period. This meant that some of the optimised sequences discussed below could not be used to treat patients without a major trial protocol amendment, which itself took time to be initiated. Secondly, elements of optimisation and sequence development require advanced computing software and many hours of specialised technical support particularly with respect to image post-processing. While other institutions within the Elekta consortium (such as Wisconsin) had access to these resources I did not.

Therefore, development of certain sequences such as a dedicated 4D MRI on the MRL (which is Wisconsin's preferred sequence) was not an option within my period of research.

Despite these limitations, I believe there is still value in the work presented below as it has helped to refine our decision making with respect to preferred sequences for use within our treatment protocol.

The aims of this part of my thesis were:

1. Primary aim: To optimise and evaluate suitable sequences for use in an online pancreatic MRgRT workflow
2. Secondary aim: To identify suitable candidate sequences for use as an offline MR radiotherapy simulation scan

5.2 Methods

5.2.1 Development of radiotherapy simulation MRIs

At our centre, MRI is not routinely used for locally advanced pancreatic cancer patients. Therefore, in order to gain experience of MRI in this setting, I recruited patients due to undergo radiotherapy for borderline resectable/ locally advanced pancreatic cancer to the ethically approved Library study (CCR4477). This study aims to establish a MRI library of cases to facilitate MRgRT workflow development.

All patients undergoing chemoradiotherapy to the pancreas with no contra-indication to MRI were eligible for recruitment. The protocol limited the number of pancreatic cancer patients to 10.

Each patient underwent one 'MR simulation' session around the time of their radiotherapy planning CT.

The aims of this 'MR simulation' session were as follows:

1. To gain experience of patient setup and scanning parameters, using a diagnostic protocol as a starting point but adapting aspects such as couch type to better fit a radiotherapy workflow.
2. To trial different sequences to establish which sequence would be most useful as a 'primary' MR simulation sequence.

Where possible I attended all 'MR simulation' sessions in order to help facilitate the development process.

Patients were scanned on a 1.5T diagnostic MRI scanner (Aera, Seimens Healthcare, Erlangen, Germany). A hard couch similar to that used in radiotherapy was used when feasible. Patients underwent half their session with arms down and half with arms up. This was a pragmatic decision as it was not known how well tolerated the arms up position would be for the 40-60 minute scan time.

Patients 1-4 underwent imaging using a diagnostic protocol. This included a T2W coronal image acquired using multiple breath-holds, a transverse T2W HASTE sequence acquired in 2 breath-holds, a transverse 'triggered'⁷ (also known as a 'navigated') T2W sequence with a small field of view and a T1W transverse VIBE Dixon sequence taken in a single end-expiratory breath-hold pre and post gadolinium contrast (alongside other sequences acquired for research purposes outside the scope of this chapter). Further detail of sequence parameters is provided in appendix 5.1. Patients 5-9 underwent a similar protocol but with adaptations made following a review of the pros and cons of the sequences acquired for the first 4 patients. This review was performed by myself in collaboration with Dr Oliver Gurney-Champion (ICR MR Physicist). Areas of concern were highlighted and alterations to scanning parameters made which were then trialled on subsequent patients and their impact assessed.

Sequences were evaluated for their potential role within a radiotherapy workflow, whether that be to provide additional information for volume definition or as part

⁷ A triggered sequence is one where the image is acquired only at certain points of the respiratory cycle.

of a dedicated CT-MR simulation workflow where the MRI is fused to the planning CT. Use of MRI in an MR- only workflow was not assessed but will be investigated in future work.

5.2.2 Optimising sequences for online use on the Elekta Unity

In addition, I recruited patients to the PRIMER study⁸ (CCR4576). Eligible patients were those with a diagnosis of pancreatic cancer undergoing radiotherapy for this indication and without contraindication to MRI. The study's purpose is to aid development of an *online* MRgRT workflow. Patients underwent imaging sessions on the Elekta Unity lasting up to 40 minutes. Scanning occurred in the treatment position, with an abdominal coil and flat radiotherapy couch. At each session a variety of MRI sequences were trialled and assessed for their online workflow suitability. I completed this work in collaboration with Dr Oliver Gurney-Champion and Dr Andreas Wetscherek (ICR MR Physicists) alongside the MRL therapeutic radiographers. I was responsible for recruiting patients, reviewing the images obtained, evaluating their potential and implementing appropriate adjustments. I focused on their suitability for online re-contouring but other factors such as patient tolerability and workflow issues were also considered.

Patients were asked for feedback of their experience verbally and through the use of an experience questionnaire.

5.2.3 Evaluation of sequences optimised for the Elekta Unity

Sequences were evaluated for their suitability within an online MRgRT workflow using a 2-step process.

Step 1: Assessment by myself focussing on image clarity, patient tolerability and workflow factors. Unsuitable sequences were disregarded or adapted. This process was supplemented by input from wider members of the pancreatic working group (consisting of therapeutic radiographers, MR physicists, medical physicists and my supervisor Katharine Aitken).

⁸ PRIMER: Development of Daily Online Magnetic Resonance Imaging for Magnetic Resonance Image Guided Radiotherapy

Step 2: Promising sequences then underwent a formal assessment of image clarity using a visual graded analysis (VGA) tool (11).

In step 2, 3 clinical oncologists with an interest in pancreatic cancer radiotherapy (AH, KA and SB) used a 4-point Likert scale to evaluate sequence clarity. This assessment focussed on the clarity of the GTV, pancreas, stomach, duodenum and small bowel with respect to ease of online re-contouring. Sequences from 7 patients were evaluated to check for consistency across different body types. The evaluated sequences were the Elekta provided free-breathing T1W gradient ECHO, a breath hold mDixon (water component) and a radial gradient ECHO reconstructed to a time averaged position (3DVane). The patients' CBCT images were used as a comparator. Acquisition parameters of the MRI sequences reviewed are available in appendix 5.2.

Friedman's test followed by post hoc analysis using Wilcoxon signed rank test was carried out to assess for differences in structure visibility across the differing imaging sequences. A Bonferroni correction was applied for the Wilcoxon signed rank test resulting in a significance level set at $p < 0.008$. SPSS was used for statistical analysis as per previous chapters.

At the start of this project my plan had been to expand this work by asking the clinical oncologists taking part in the image clarity analysis to contour the GTV, pancreas, stomach, duodenum and small bowel on each of the image sets in order to compare contour agreement. This would have provided a more clinically relevant evaluation of image quality. I had planned to do this work around March 2020, however, the outbreak of the COVID-19 pandemic meant that the clinical oncologists involved were not able to commit to the significant amount of time contouring of this kind would have required.

5.3 Results

5.3.1 Development of radiotherapy simulation MRIs

Between January 2018- August 2019, 9 patients with pancreatic cancer were recruited to the Library study. Each patient underwent 1 imaging session on a diagnostic MRI scanner.

All patients tolerated their imaging sessions, verbal feedback indicated that the arms up position was less comfortable than the arms down position. The 'hard' radiotherapy couch top was felt to be acceptable.

A summary of the observations from the sequences acquired for patients 1-4 is shown in Table 5.3 with example images shown in Figure 5.1.

Table 5.3 Summary of observations from imaging session of patients 1-4 and their potential roles within an offline workflow.

Sequence name	Pros	Cons	Potential role in radiotherapy workflow
T2W coronal image, multiple breath holds	Clear views in coronal plane Limited respiratory artefact due to breath holds	No axial images Concern regarding reproducibility of multiple breath-holds and geometric accuracy 5.5mm slice thickness 2D acquisition (12)	Adjunct to volume delineation Not for use as standalone sequence in radiotherapy planning
T2W triggered, SFOV	Axial acquisition Good visualisation of pancreatic duct and duodenal bulb Limited respiratory artefact 3mm slice thickness	2D acquisition Triggered component makes it difficult to fuse with RT planning scan (13) Concerns regarding geometric accuracy Acquisition time dependent on respiratory rate- can be >10 minutes FOV too small for RT planning (does not	Adjunct to volume delineation Not for use as a standalone sequence in radiotherapy planning

		include external body contour)	
T2 Haste, 2 breath-holds	<p>Axial acquisition</p> <p>Good visualisation of pancreatic duct</p> <p>Limited respiratory artefact</p>	<p>2D acquisition</p> <p>Requires 2 breath-holds to acquire</p> <p>Concern re geometric validity</p> <p>Slice thickness 5mm</p>	<p>Adjunct to volume delineation</p> <p>Not for use as a standalone sequence</p>
T1W VIBE Dixon (water component) pre and post contrast	<p>T1W image is recommended as the primary dataset for MRI based contouring(14)</p> <p>3D acquisition (12)</p> <p>Slice thickness 1.5mm</p> <p>Clear image quality</p>	Small lateral FOV	<p>Preferred sequence to take forward as an MRI simulation scan (post contrast scan if only one sequence to be selected)</p> <p>Pre and late post contrast used as adjunct for delineation</p>

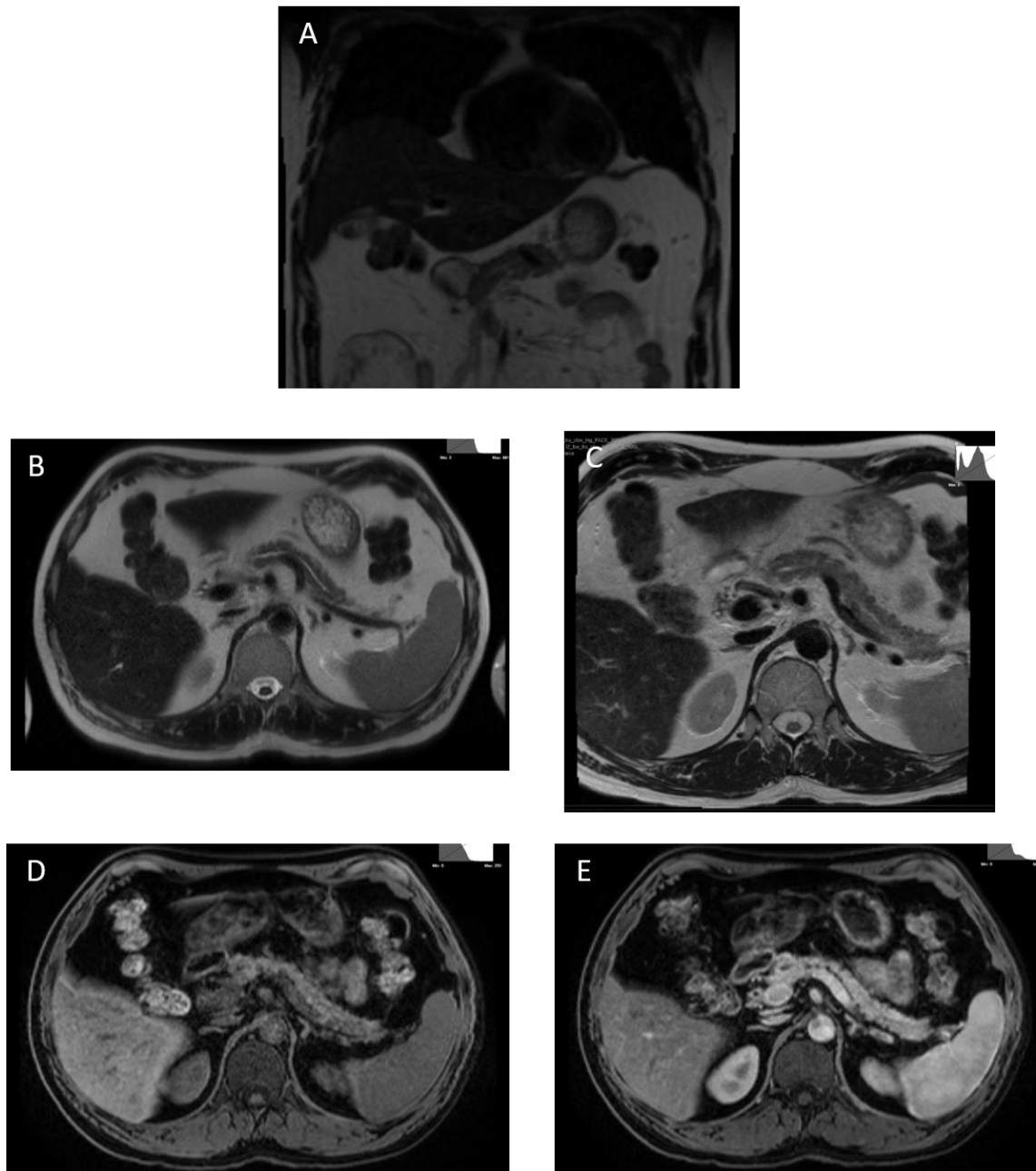


Figure 5.1 Examples of sequences acquired on the 1.5T diagnostic scanner.

A: T2W coronal image, multiple breath holds, B: T2 Haste, 2 breath-holds. C: T2W triggered, SFOV, D: T1W Dixon (water component) pre contrast, E: T1W Dixon (water component) post contrast.

From the initial review, the strongest contender for a MR simulation sequence was the T1 VIBE Dixon. This scan is taken at 3 time points in the standard diagnostic protocol, pre contrast, post contrast and delayed post contrast. It is quick to acquire (19 seconds) using a single breath-hold reducing the impact of respiratory artefact. Once acquired it is broken down into different components (in-phase, opposed-phase, water and fat). The water component would be the

preferred phase for delineation. The reasons this sequence is favoured are as follows:

1. T1W: T1W is the recommended primary sequence for GTV delineation when using MR simulation in pancreatic cancer (14). Normal pancreas returns a bright signal, tumour appears hypointense. Post contrast, the tumour enhances to a lesser degree than the surrounding healthy tissue.
2. Acquired in 3D: 3D acquisition is a necessary requirement for radiotherapy planning (12) so 3D is an advantage compared to other sequences that are acquired in 2D.
3. Slice thickness of 1.5mm: This is a similar slice thickness to a CT planning scan facilitating accurate fusion.
4. Clarity of GTV/OAR: Subjectively I felt the overall clarity of the GTV and dose sensitive OARs was best on this sequence. T2 images gave good clarity of the pancreatic duct or duodenal bulb but the small bowel was poorly defined. Objective assessment of image clarity (using VGA) was not carried out but can be included in future work.

A downside of the original version of this sequence was the relatively small superior/inferior field of view (compared to a standard radiotherapy planning CT) which might be problematic for patients with a larger body habitus. It is also acquired in breath-hold to reduce the impact of respiratory motion. This has the potential to introduce positioning errors if incorporated into an otherwise free-breathing radiotherapy protocol. However, as our current pancreatic protocol involves an end-expiratory breath-hold CT scan as the primary planning dataset the breath-hold could be viewed as an advantage in terms of fusion for our pathway.

The T2 sequences were not suitable as standalone sequences for radiotherapy planning for a range of reasons, namely concerns over geometric validity, acquisition time and slice thickness. However, they do provide additional information for tumour delineation and therefore could be used as an unfused adjunct for contouring.

For patients 5-7, iterative adjustments were made to the imaging protocol following the conclusions drawn from the imaging sessions of the previous 4 patients. The success of these changes were then confirmed in patients 8 and 9.

For example, we attempted to increase the superior/inferior field of view on the T1 VIBE Dixon to better accommodate taller patients. However, in order to keep the breath-hold at an acceptable length (20 seconds) this resulted in an increase in slice thickness to 1.6mm. This change was therefore rejected after it was tried for patients 5 and 6. Attempts to adjust the flip angle to better improve image quality were also rejected as this resulted in a worsening of image clarity.

Further adjustments were made for patient 7 to reduce the risk of geometric distortion, this included checking the constant deformation factor (requiring a switch from the pre-programmed 2D to a 3D correction (12)) and ensuring our bandwidth was acceptable (1, 9). These changes were then replicated for patients 8 and 9 to ensure results were consistent across different patients.

By the end of this process, we had a sequence (T1 VIBE Dixon) which from a clinical perspective could be used for a CT-MR simulation process. This sequence will then proceed to additional quality assurance testing to ensure that it is compatible with this type of workflow (7).

5.3.2 Evaluation of sequences for use in an online radiotherapy workflow on the MR Linac

Between January 2018- August 2019, 11 patients with pancreatic cancer undergoing radiotherapy were recruited to the PRIMER study.

Patients underwent between 1 and 7 imaging sessions. In total 44 imaging sessions were completed.

For the first 2 patients the Elekta provided sequences (technical parameters in Appendix 5.2) were assessed for their suitability for use within a fully adapted pancreatic online workflow. Figure 5.2 depicts axial slices of the 3 sequences. Images A and B are from the T1W and T2W sequence respectively, both taken in free breathing. Note the blurring of the organs due to respiratory and peristaltic

motion making accurate online re-contouring difficult. Blurring is improved in image C taken from the T2 navigated sequence as in this sequence data is only acquired at specific predetermined points in the respiratory cycle thus reducing the impact of respiration. However, the boundaries of key OARs are still difficult to discern. This navigated sequence also takes considerably longer to acquire (in the region of 6-10 minutes, dependent on the patient's respiratory pattern) compared to 3 minutes for the free-breathing scan thus reducing its utility in a time pressured online scenario.

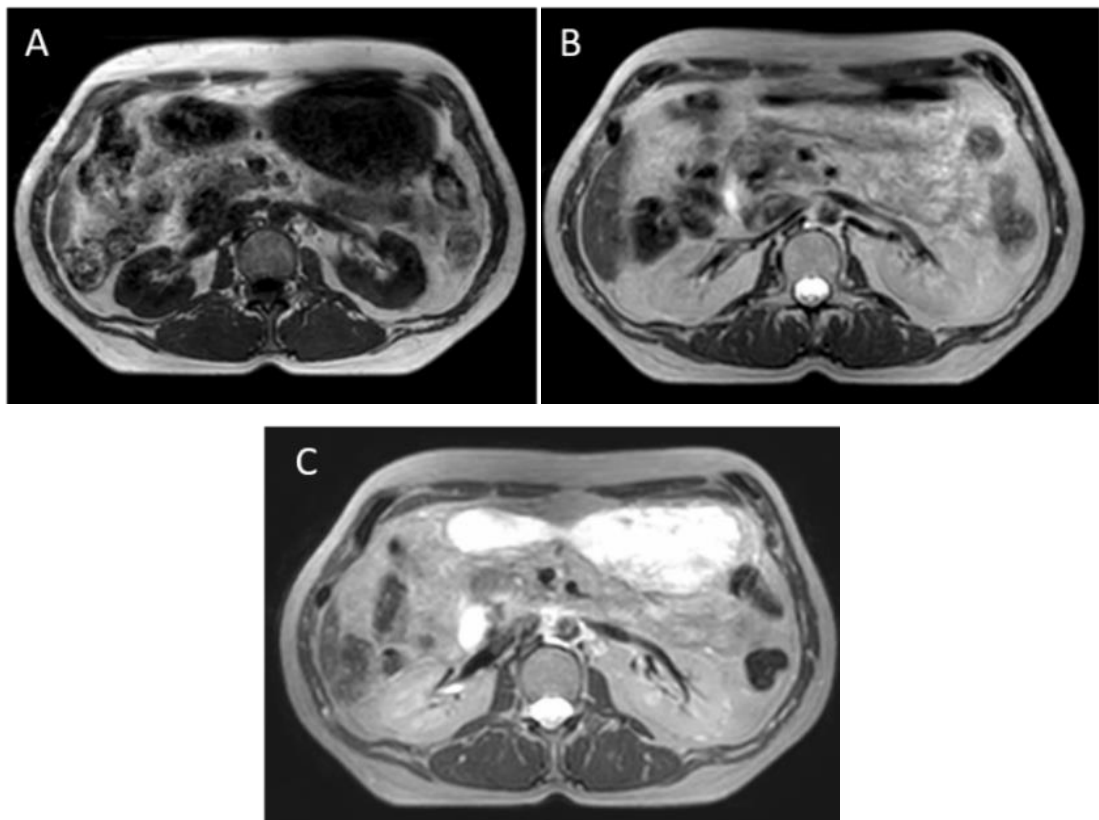


Figure 5.2 Axial slices of CE marked Elekta provided sequences.

A= 3D T1W image taken in free-breathing, B= 3D T2W image taken in free-breathing, C= 3D T2W navigated image taken in free-breathing.

The addition of water contrast (200mls taken 15 minute prior to imaging) resulted in some improvement in image clarity, for example, the duodenal bulb (especially on the T2W images) was easier to see, but the edges of the OARs were still difficult to define, see Figure 5.3. Therefore, it was concluded that in itself, the addition of a water bolus would not solve the image clarity issues.

The role of buscopan was considered to help reduce peristaltic motion and its associated image blurring. However, as this needs to be given intramuscularly (to work in a reliable time frame) after consideration, it was felt that this would not be acceptable to patients over multiple treatment fractions.

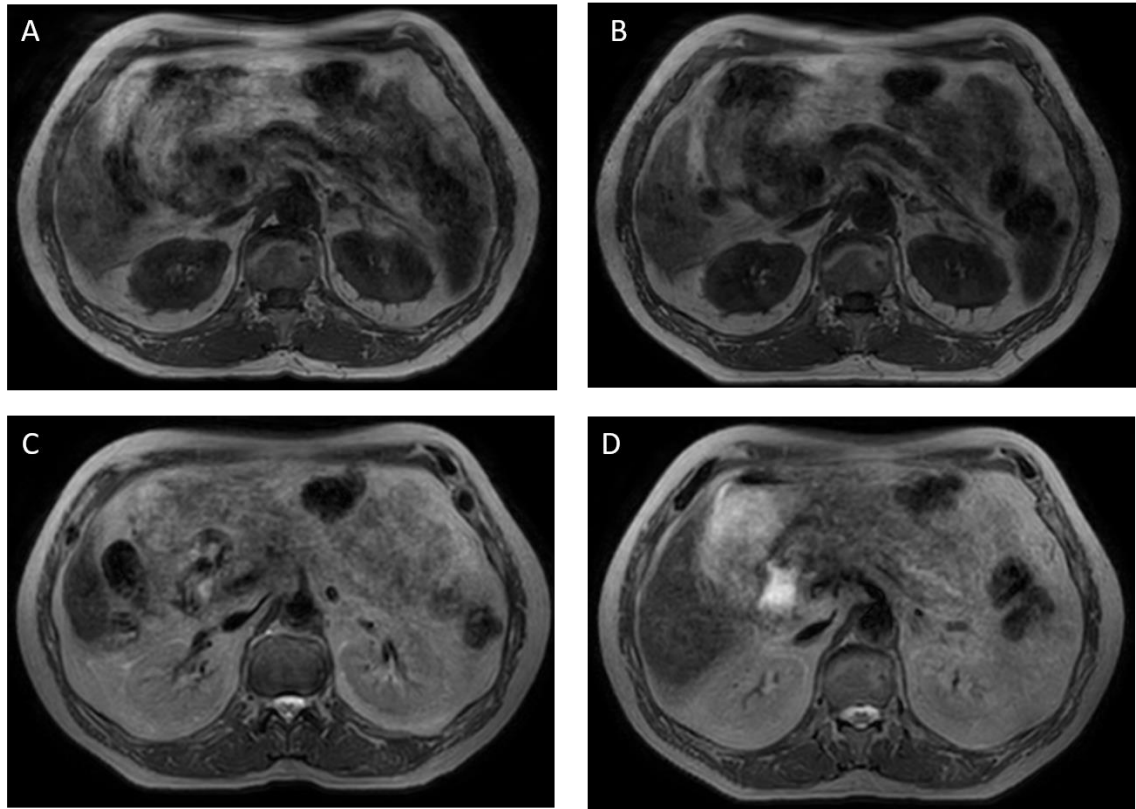


Figure 5.3 Impact of the addition of a water bolus given 15 minutes prior to imaging.

A= T1W acquired in free breathing without water bolus. B= T1W acquired in free breathing with water bolus. C= T2W acquired in free breathing without water bolus. D= T2W acquired in free breathing with water bolus. Note improvement in visibility of duodenal bulb (especially in T2W image) but boundaries of OARs still difficult to define.

Other free-breathing sequences were also trialled in the initial 3 patients. This included a free-breathing sequence developed by our collaborators at UMC Urtecht, Netherlands. However, this sequence also suffered from significant respiratory artefact (see Figure 5.4) limiting its use in an online adaptive pathway.

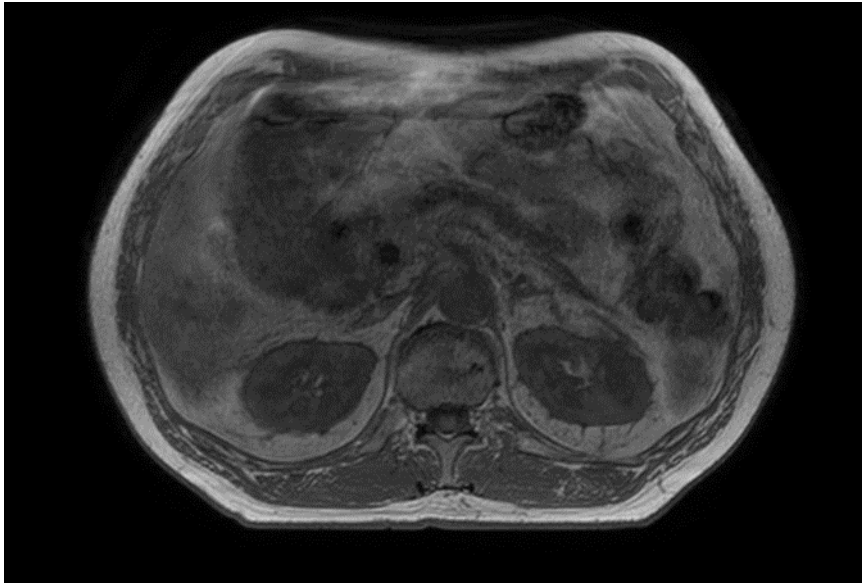


Figure 5.4 T1 mDixon (water component) developed by UMC Utrecht

Acquired in free breathing, note the impact of respiratory artefact which limits the ease of re-contouring.

It was therefore concluded that for subsequent patients alternative imaging sequences needed to be explored.

A potential solution to this problem was the use of a voluntary breath-hold sequence, similar to that utilised in the diagnostic protocol. The second potential solution involved a new sequence known as a 3DVane. This radial gradient ECHO sequence is acquired over multiple breathing cycles and is then reconstructed to a time averaged position with the aim of minimising the impact of respiratory motion on image clarity.

5.3.2.1 Investigation of breath-hold sequences

This involved the development and testing of sequences acquired in a short (<25 second) time period. From Patient 4 onwards various breath-hold sequences were trialled. These included an in-house sequence developed by our MR physics team with my input, and a breath-hold sequence from collaborators at the Medical College of Wisconsin, USA. The Wisconsin sequence was a T1W mDixon (similar to the VIBE Dixon used in the MR simulation protocol) which we adapted to give a wider field of view to ensure the lateral external body contour was included in its entirety (a necessity for online replanning).

On inspection, the image clarity of this sequence for online re-contouring was better than the Elekta provided free-breathing scans, see Figure 5.5. The sequence also had an acceptable acquisition time and field of view. However, the improved image clarity was achieved by compromising the slice thickness (6 mm, reconstructed to 3mm) which affected this sequence's suitability for online replanning. To rectify this, for patient 6 onwards the slice thickness was adjusted to 4 mm (reconstructed to 2 mm), however, in order to maintain both a short sequence acquisition time and similar image clarity, a reduction in the superior/inferior field of view (from 240 mm to 160 mm) was needed. Although not ideal, I felt that for the majority of patients this field size should be acceptable for online replanning. This 'thinner' slice Wisconsin sequence was taken forward to subsequent patients.

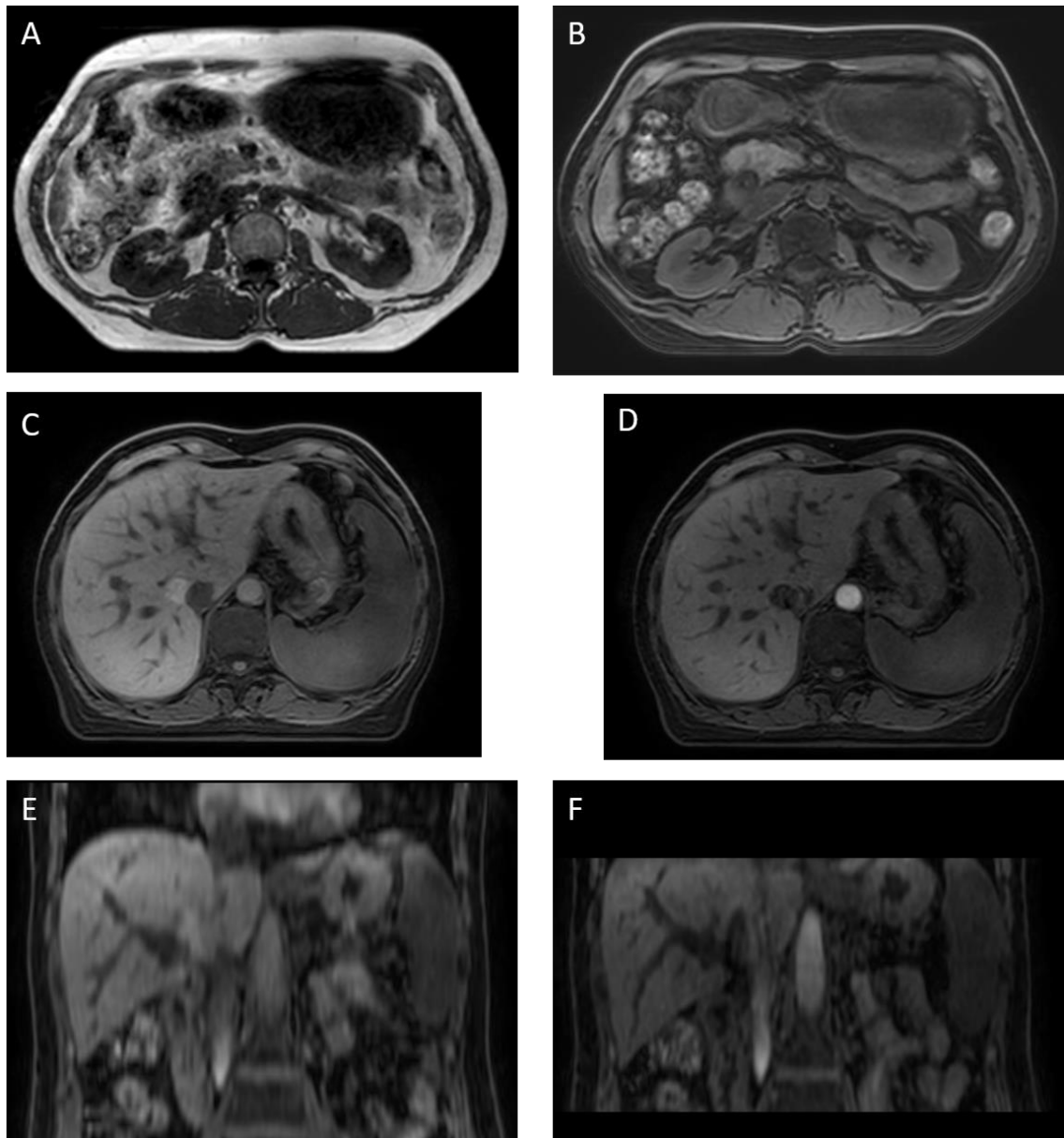


Figure 5.5 Imaging development of Wisconsin mDixon.

A= T1 free breathing scan for comparison. B= Wisconsin mDixon with wide FOV (water component), note the improved image clarity compared to A. C= Wisconsin mDixon with wide FOV. D= Wisconsin mDixon with wide FOV and reduced slice thickness, note maintained image clarity despite the decrease in slice thickness. Note however, reduction in superior/inferior FOV (E&F respectively).

Our in-house developed breath-hold scan was also an mDixon. Initially scanning parameters were set to an acquired voxel size of 2.5 x 2.5 mm and slice thickness of 1.5 mm. However, this resulted in an unacceptable compromise in superior/inferior field size (131 mm). After, numerous iterations, a compromise was reached with a sequence which took 21 seconds to acquire with acquired

voxel sizes of 2.5 x 2.5 mm and slice thickness of 3 mm. This gave a superior/inferior field of view of 165 mm similar to the Wisconsin sequence.

Attempts to improve sequence resolution further were then trialled in patient 6 by decreasing the voxel size at acquisition to 1.8 x 1.8 mm (compared to 2.5 x 2.5 mm) whilst maintaining the same field of view parameters and slice thickness, Figure 5.6. This 'high resolution' scan gave encouraging results and was taken forward in subsequent patients.

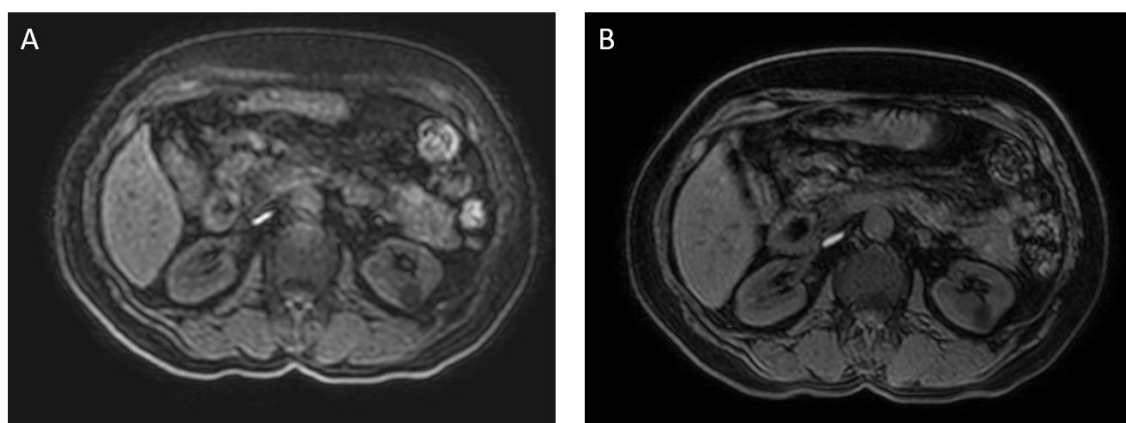


Figure 5.6 Comparison of in-house developed breath-hold Dixon.

Voxel size 2.5 x 2.5 mm (A), compared to higher resolution image with voxel size 1.8 x 1.8mm (B).

When comparing across patients, I felt both the finalised Wisconsin (thinner slice version) and the in-house breath-hold Dixon (higher resolution version) were an improvement compared to the Elekta provided sequences in terms of clarity. In my opinion, the difference between the 2 breath-hold scans in terms of image clarity was minimal, see Figure 5.7.

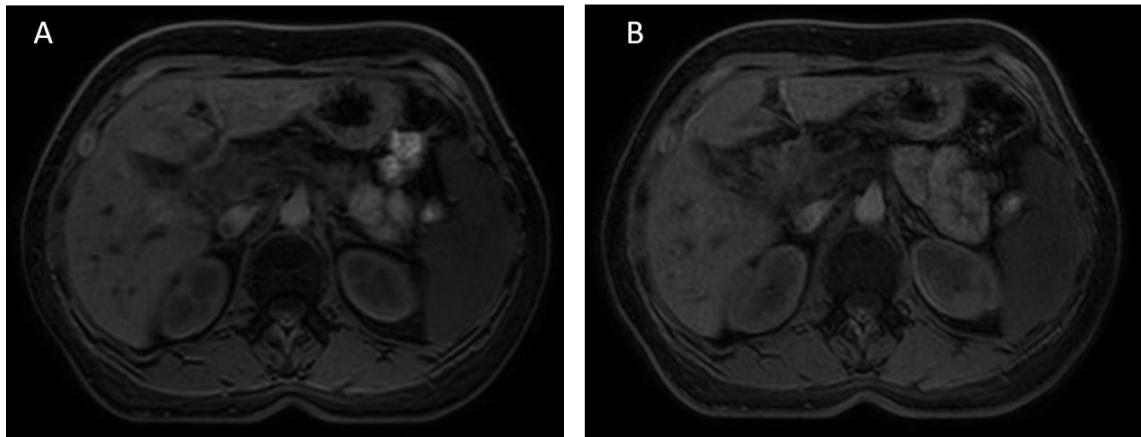


Figure 5.7 Comparison between finalised Wisconsin sequence (A) and In house version (B)

5.3.2.2 Investigation into 3DVane sequences

These sequences were available from patient 4 onwards. In total 4 different 3DVane sequences were trialled, all acquired in free-breathing. To limit the impact of respiratory motion, the sequences are post-processed to give an 'averaged' dataset. My preferred option was a balanced sequence (elements of T1W and T2W) with an acquired voxel size of 1.5 x 1.5 mm and a slice thickness of 3 mm. This gave a superior/inferior field of view size of 200 mm (therefore larger than the breath-hold scans). An example of this sequence, compared to a free breathing T1 sequence is shown in Figure 5.8. Note how the post-processing reduced the impact of respiratory artefact and improves image clarity, note also how the balanced nature of the sequence highlights the pancreatic duct.

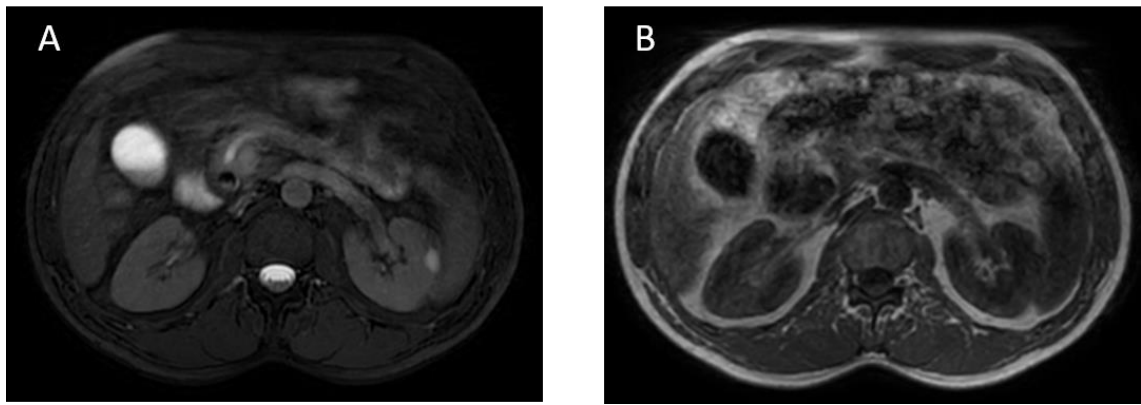


Figure 5.8 Comparison of 3DVANE vs T1W free breathing

A= 3DVANE, B= T1W free breathing

5.3.2.3 Patient tolerability

All patients were able to complete 40 minutes of scanning (the anticipated duration of an online fraction) in the arms up position. However, 2 patients (patient 11 and 12) reported transient worsening of their pre-existing peripheral neuropathy and queried the tolerability of this position over multiple fractions. As a result, for patient 11 we also trialled the preferred 3DVane and breath-hold sequences in the arms down position. The 3DVane was unaffected by this change. In comparison, the in-house Dixon required a change in phase encoding direction in order to resolve a wraparound artefact caused by the arms down position, see Figure 5.9. The Wisconsin sequence was also negatively affected by a wraparound artefact however this remained even when a phase encoding change was implemented.

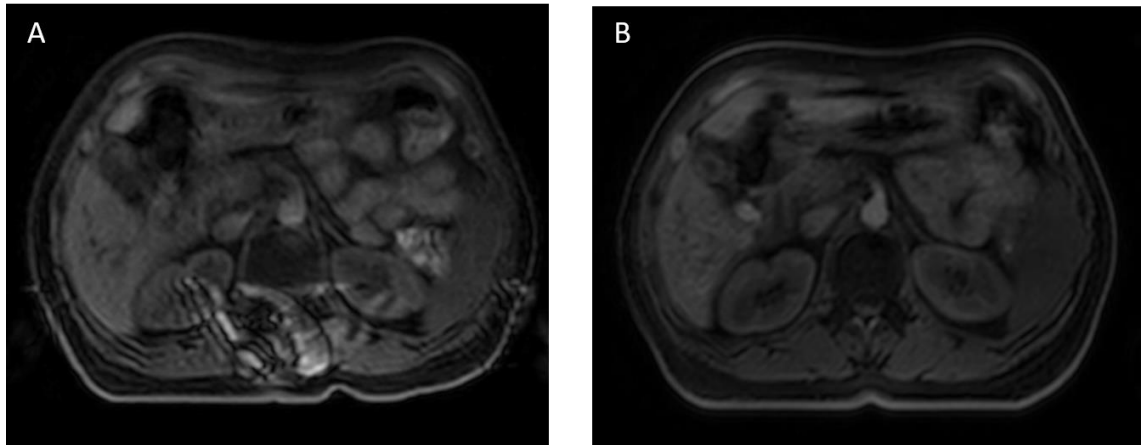


Figure 5.9 In house Dixon (high resolution) in arms down position with varying encoding directions.

A- With original phase encoding direction (right-left), B- with altered Ant/post phase encoding direction. Note wraparound artefact in A which is resolved in B.

With respect to the duration of breath-hold, all patients were able to complete the required 20 seconds. One patient (patient 5) needed to do this in end-inspiration rather than end-expiration.

5.3.2.4 Formal assessment of image clarity using visual graded analysis

A formal assessment of image clarity, undertaken by 3 observers using sequences from 7 patients (Patients 4-10) was performed. Due to time constraints one breath-hold (Wisconsin) and one 3DVane (the preferred balanced sequence) was assessed per patient. These were compared to a free breathing T1 and a CBCT. Sequences were acquired in the arms up position.

A statistically significant difference between the sequences was seen for all assessed structures, with the breath-hold mDixon and 3DVane sequences performing better than the free-breathing T1 and CBCT (Table 5.4). Post-hoc analysis using Wilcoxon signed ranks confirmed that there was a statistically significant improvement in clarity of all structures when comparing the breath-hold sequence and the 3DVane to the free-breathing and CBCT image set. There was no statistical difference between the image clarity of the breath-hold and 3DVane (Table 5.5) suggesting that from an image clarity perspective either the 3DVane or the breath-hold scan could be used in our online workflow.

Table 5.4 Results of formal image clarity assessment.

*A 4 point Likert scale was used (0= not visible, 1= unclear, 2= clear, 3= very clear) with each observer rating each structure separately. * Statistically significant result.*

Structure	Median Likert Score				Friedman Test (p-value)
	Free-breathing T1 (Interquartile range, IQR)	Breath-hold mDixon (IQR)	3DVane (IQR)	CBCT (IQR)	
GTV	1 (1.0-1.0)	2 (1.5-2.0)	2 (2.0-2.0)	0 (0.0-0.0)	<0.01*
Pancreas	1 (1.0-1.0)	2 (2.0-2.0)	2 (2.0-2.0)	0 (0.0-1.0)	<0.01*
Stomach	1 (1.0-2.0)	2 (2.0-2.5)	2 (2.0-2.0)	1 (0.0-1.0)	<0.01*
Duodenum	1 (1.0-1.0)	2 (1.75-2.0)	2 (2.0-2.0)	0 (0.0-1.0)	<0.01*
Small Bowel	1 (1.0-1.0)	2 (2.0-2.0)	2 (2.0-2.0)	0 (0.0-1.0)	<0.01*

Table 5.5 Wilcoxon Signed Ranks Test

*p value significance level set at < 0.008. * = statistically significant result*

Structure	Wilcoxon Signed Ranks Test (p value)					
	Breath-hold vs T1	3DVane vs T1	CBCT vs T1	CBCT vs Breath-hold	CBCT vs 3DVane	3DVane vs Breath-hold
GTV	< 0.001*	< 0.001*	0.001*	<0.001*	<0.001*	0.1
Pancreas	< 0.001*	< 0.001*	0.001*	< 0.001*	< 0.001*	0.16
Stomach	0.001*	0.001*	<0.001*	< 0.001*	<0.001*	0.41
Duodenum	< 0.001*	<0.001*	< 0.001*	< 0.001*	< 0.001*	0.76
Small Bowel	< 0.001*	<0.001*	< 0.001*	<0.001*	< 0.001*	0.71

5.4 Discussion

This development work had produced sequences which will be taken forward for offline and online MR guided radiotherapy workflows. They will now undergo additional physics quality assurance checks to confirm their suitability for treatment planning.

In the offline 'MR simulation' setting, the T1W VIBE Dixon with IV contrast is the preferred sequence. I envisage this being fused with the contrast enhanced breath-hold planning CT which is currently the primary dataset for our pancreatic cancer radiotherapy workflow. Although not discussed in this chapter, during the simulation sessions patients also underwent developmental 4D MRI scans. These 4D scans are still being optimised as current post-processing times (~24 hours) are not compatible with a clinical workflow. However, it is hoped that future

work will assess their possible integration into an MR simulation workflow as a partner to our currently acquired 4DCTs.

In the online setting, we have developed 3 contender sequences for integration into an online workflow. These are the 3DVane, the finalised in-house breath-hold Dixon and the adapted Wisconsin Dixon sequence. From an image clarity perspective, there is little to choose between these sequences.

However, an important weakness of both breath-hold sequences is our current inability to monitor the reproducibility of the breath-hold across fractions. Unlike some CT-based linacs and the ViewRay MRIdian, the Elekta Unity currently does not have a system to monitor the extent and consistency of a patient's breath-hold which raises concerns for the geometric accuracy of dose delivery. Despite initial optimism from Elekta, a solution to this problem is not currently forthcoming. There is also the issue of using a breath-hold scan for re-contouring and planning but treating in free-breathing due to the potential to introduce systematic errors in target position. This is a particularly acute problem in the context of SBRT, where precision is key. A solution to this problem would be to treat in breath-hold. However, due to the dose delivery rate of the MR Linac and the high dose per fraction used in SBRT treatments, this would require multiple breath-holds per fraction and again it is currently not feasible to monitor the consistency of these breath-holds in 3D during the beam on period. Accurate dose delivery therefore cannot be guaranteed.

Following discussions with members of the pancreatic working group the 3DVane has therefore been selected as our preferred sequence for online replanning and re-contouring. However, implementation of this sequence has its challenges. Firstly, as the sequence is not CE marked incorporation into a workflow has required a protocol amendment to our institution's PERMIT trial which is expected to be approved in early 2021. Encouragingly, Elekta have also indicated their preference for this sequence meaning that it is likely to be supported in future machine upgrades.

The sequence also requires post processing in order to produce the 'time averaged data set'. Initially, this needed to occur offline. An online solution has

now been developed by our MR physics team, but this solution requires switching between clinical and research modes on the MR Linac which is outside the current CE mark and needs the above protocol amendment. The need for post-processing will also extend the 'on couch' time for the patient. A potential work-around for this is to use the 3DVane for online re-contouring and replanning and then using a 'linker' sequence (which does not require post processing) as the verification image immediately prior to beam on. We have developed such a sequence by adapting the in-house high resolution breath-hold Dixon so that it is acquired multiple times while the patient is free-breathing and then an averaged dataset is produced. This is not as accurate as the 3DVane but would be suitable for use in verification.

Using an 'averaged' position for re-contouring and re-planning will require adaptation of our current offline planning model. This problem is not insurmountable and will be discussed further in the next chapter.

At the start of my thesis, I had hoped that we would be treating pancreatic cancer patients on the Elekta Unity during my research time. Unfortunately, this has not been possible, and this is largely due to the challenges which I have encountered as part of this development work. Firstly, low patient numbers impacted on the potential pool of trial candidates. This slowed trial recruitment and made it difficult to maintain momentum in the development process. This was exacerbated by an upgrade to the MRL which took place in the summer of 2018 which halted all scanning for several months and the COVID-19 outbreak which halted trial recruitment for a period.

Secondly, for patient comfort reasons, the trial protocol stipulated that each patient could only be scanned for a maximum of 40 minutes at a time. This limited the number of sequences which could be acquired in a single session and also limited the time available to make intra-session changes to sequences. I had planned for each patient to have multiple scanning sessions to enable intra-patient comparisons however, some patients were unable to commit to these additional sessions.

Thirdly, the CE marking issues and their impact on workflow development were only realised relatively late in the development process (2019). This was exacerbated by the fact that the promised time scale for an Elekta provided motion management system has been pushed back, with a firm date still not confirmed. This has made it more difficult for us as a department to plan resource allocation.

Finally, the outbreak of the COVID- 19 pandemic limited the time available to clinicians and other members of the MRL team for trial related activities. This meant that I was unable to complete some aspects of my work, such as an analysis of GTV contour variability on the differing sequences and the pace of workflow development in general was slowed.

Despite these challenges, I feel we now have suitable sequences for use in both an offline and online MR guided radiotherapy setting and so although slower than hoped, progress has been made.

5.5 Conclusion

In this chapter I have discussed the optimisation of MRI sequences for use in both an offline and online MR guided radiotherapy workflow. Future work will involve the integration of these sequences into pilot workflows for MRgRT for pancreatic cancer and will include evaluation of inter-observer contouring variability on the selected sequences. In addition, the role and integration of functional imaging in this setting is yet to be explored.

5.6 References

1. Kerkmeijer LGW, Maspero M, Meijer GJ, van der Voort van Zyp JRN, de Boer HCJ, van den Berg CAT. Magnetic Resonance Imaging only Workflow for Radiotherapy Simulation and Planning in Prostate Cancer. *Clinical oncology* (Royal College of Radiologists (Great Britain)). 2018;30(11):692-701.
2. Tyagi N, Fontenla S, Zelefsky M, Chong-Ton M, Ostergren K, Shah N, et al. Clinical workflow for MR-only simulation and planning in prostate. *Radiation oncology* (London, England). 2017;12(1):119.
3. Brock KK, Dawson LA. Point: Principles of magnetic resonance imaging integration in a computed tomography-based radiotherapy workflow. *Seminars in radiation oncology*. 2014;24(3):169-74.

4. Paulson ES, Erickson B, Schultz C, Allen Li X. Comprehensive MRI simulation methodology using a dedicated MRI scanner in radiation oncology for external beam radiation treatment planning. *Medical physics*. 2015;42(1):28-39.
5. Kay C, Roberts A, Guthrie A, Sheridan M. Recommendations for cross-sectional imaging in cancer management. Second Edition: Royal College of Radiologists; 2014.
6. Zhang L, Sanagapalli S, Stoita A. Challenges in diagnosis of pancreatic cancer. *World journal of gastroenterology*. 2018;24(19):2047-60.
7. Paulson ES, Crijns SP, Keller BM, Wang J, Schmidt MA, Coutts G, et al. Consensus opinion on MRI simulation for external beam radiation treatment planning. *Radiotherapy and oncology : journal of the European Society for Therapeutic Radiology and Oncology*. 2016;121(2):187-92.
8. White IM, Scurr E, Wetscherek A, Brown G, Sohaib A, Nill S, et al. Realizing the potential of magnetic resonance image guided radiotherapy in gynaecological and rectal cancer. *The British journal of radiology*. 2019;92(1098):20180670.
9. Pathmanathan AU, McNair HA, Schmidt MA, Brand DH, Delacroix L, Eccles CL, et al. Comparison of prostate delineation on multimodality imaging for MR-guided radiotherapy. *The British journal of radiology*. 2019;92(1095):20180948.
10. Schmidt MA, Payne GS. Radiotherapy planning using MRI. *Physics in medicine and biology*. 2015;60(22):R323-61.
11. Kember SA, Hansen VN, Fast MF, Nill S, McDonald F, Ahmed M, et al. Evaluation of three presets for four-dimensional cone beam CT in lung radiotherapy verification by visual grading analysis. *The British journal of radiology*. 2016;89(1063):20150933.
12. van der Heide UA, Frantzen-Steneker M, Astreinidou E, Nowee ME, van Houdt PJ. MRI basics for radiation oncologists. *Clinical and translational radiation oncology*. 2019;18:74-9.
13. Crijns SP, Raaymakers BW, Lagendijk JJ. Proof of concept of MRI-guided tracked radiation delivery: tracking one-dimensional motion. *Physics in medicine and biology*. 2012;57(23):7863-72.
14. Heerkens HD, Hall WA, Li XA, Knechtges P, Dalah E, Paulson ES, et al. Recommendations for MRI-based contouring of gross tumor volume and organs at risk for radiation therapy of pancreatic cancer. *Practical radiation oncology*. 2017;7(2):126-36.

Chapter 6

Investigation into the use of abdominal compression in pancreatic MR guided radiotherapy

Sections of this chapter have been published:

Abstract:

Alexander S, Lawes R, Adair Smith G, Barnes H, Hanson I, Herbert T, Huddart R, Lacey C, McNair H, Mitchell A, Nill S, Ockwell C, Oelfke U, Taylor H, Wetscherek A, Aitken K, Hunt A. PH-0164 Abdominal compression; development of a non-gated pancreas MRlgRT workflow. Radiotherapy and Oncology. 2021;161:S100-S1.

Chapter 6 Investigation into the use of abdominal compression in pancreatic MR guided radiotherapy

6.1 Introduction

Studies have shown that the pancreas can move in excess of 2cm in the superior-inferior direction due to respiration (1). This motion causes 2 main problems; firstly, it results in artefact, making MRI sequences more difficult to interpret. Secondly, it causes target motion. This necessitates larger treatment margins to ensure adequate target coverage throughout the respiratory cycle. Strategies mitigating against respiratory motion therefore allow for smaller treatment margins and give greater certainty over intra-fraction target and OAR position. This makes safe dose escalation easier to achieve and is a pre-requisite for successful dose escalated SBRT. Ideally, a motion management system would involve a form of advanced tumour tracking or beam gating solution (where the beam is only on when the target is in a pre-specified position). The ViewRay MRIdian device is equipped with gating and this is currently being deployed in the phase II SMART trial (Stereotactic MRI-guided On-table Adaptive Radiation Therapy (SMART) for locally advanced pancreatic cancer (NCT 03621644)). Currently, the Elekta Unity does not support such technology and despite initial optimism at the start of my thesis the time frame for an Elekta integrated tracking/gating solution is still unclear.

In the absence of gating/tracking, I investigated abdominal compression as an alternative solution to reduce respiratory motion and reduce treatment margins. Abdominal compression uses pressure on the abdomen to reduce the extent of abdominal breathing by restricting diaphragmatic motion. This should reduce the respiratory motion of intra-abdominal organs (2). Various abdominal compression devices are available and in the context of pancreatic cancer, such devices have been shown to reduce pancreatic tumour motion particularly in the superior/inferior direction (2-4). However, there is limited published data on the impact of different compression devices and their suitability for use in the context of MRgRT.

The aim of this chapter was therefore to examine the use of abdominal compression as a motion management solution for non-gated MRgRT in the upper abdomen. Successful integration of an abdominal compression device into our workflow would require this device to fulfil the following criteria:

1. MRI safe
2. Able to fit in the bore of the MRL alongside the coil bridge
3. Minimal/no adverse impact on image clarity
4. Result in a reduction in diaphragmatic motion (as a surrogate for pancreatic tumour motion)
5. Be compatible with our institution's 4DCT system
6. Be tolerated by wearer for the duration of a MRgRT fraction

Although parts of this project are still ongoing for example, the trial of abdominal compression in patient rather than non-patient volunteers and its impact on tumour motion (as opposed to abdominal surrogates), I will present the results available to date. My thanks to Rebekah Lawes and Sophie Alexander (therapeutic radiographers at RMH) for their help with data collection and analysis.

6.2 Methods

6.2.1 Volunteer selection

Due to the exploratory nature of this work, I opted to perform the initial stages using non-patient volunteers (with a view to moving to a patient cohort in the near future). Healthy volunteers were recruited to the PRIMER imaging study through staff communications at both The Royal Marsden Hospital and the Institute of Cancer Research. Volunteers were eligible if they had no significant past medical history, were not involved directly with MRL projects and had no contraindications to MRI. Volunteers were recruited in 2 cohorts. The first cohort of 5 volunteers (Volunteers 1-5) served as a pilot. These volunteers underwent between 3-5 MRL imaging sessions lasting up to 40 minutes. These pilot sessions were used to gain familiarity with the abdominal compression devices and their application, to check MRI sequence parameters and scanning levels, to develop techniques to optimise volunteer comfort (e.g. arms up versus arms down) and to look for an initial signal regarding an effect on respiratory motion.

Once the pilot was complete, a second cohort of volunteers (N=5, Volunteers 6-10) were recruited for a controlled evaluation of abdominal compression. Due to the coronavirus pandemic, volunteer numbers were restricted and in the second cohort, were limited to those working in the Royal Marsden Hospital radiotherapy department.

6.2.2 Identification of suitable abdominal compression devices

In order to investigate the impact of abdominal compression (AC) and assess the feasibility of integrating this technique into our MRgRT workflow, suitable AC devices needed to be identified. The device needed to be MRI compatible (MRI safe or conditional within the parameters of the MRL) and fit within the limited space of the MRL treatment bore. The first device trialled was an in-house adapted AC belt used by the CyberKnife department for selected upper abdominal treatments. This is essentially an abdominal support corset (Dynabelt, Thuasne, France) with additional support reinforcements removed (due to MRI incompatibility) and rudimentary markings added (see figure 6.1). The belt was available in 3 sizes and was appealing due to its simple design, relative low cost and familiarity within the department. We used this belt for our pilot cohort of non-patient volunteers and for one session per volunteer in our second cohort.

During the pilot period, while the Dynabelt appeared to show some benefit in abdominal motion reduction, it was felt that a custom built device might be able to improve on this further. In particular, the Dynabelt only had 3 compression graduations and it's 'tightness' was operator dependent. This meant that maximal compression was not necessarily achieved or consistent.

We therefore sort to identify a purpose built device. Through discussions with UK radiotherapy equipment distributors and other centres using AC in their radiotherapy workflows we identified the ZiFix™ system (Qfix, USA) as a suitable MRI compatible candidate. This device allows for more controlled and consistent compression through the use of a graduated belt plus an air bladder for additional compression (figure 6.1). Following an onsite demonstration by Qfix, we purchased a ZiFix for our study using grant money I had been awarded from the

BRC TPT Theme Pump Priming. This device was tested on volunteers in our second cohort (Volunteers 6-10).

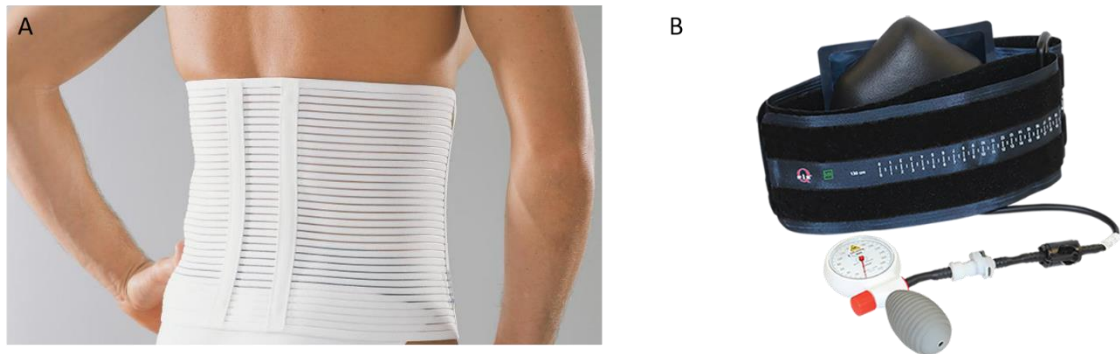


Figure 6.1 Abdominal compression devices tested.

A: Dynabelt, B: ZiFix

6.2.3 Assessment of the impact of abdominal compression on respiratory motion

Healthy volunteers from cohort 2, underwent 4 imaging session on the MRL. At each session T1W, mDixon (water), 3D Vane and coronal cine MRI sequences were acquired both with and without compression in free-breathing. In 3 out of 4 sessions, the volunteer wore the ZiFix (as this was felt to be the preferred device due to its more precise compression method) and for one session they wore the Dynabelt (for comparison). The T1W and cine coronal sequences were Elekta provided, the mDixon (water) and 3D Vane were those as described in Chapter 5 (the mDixon being the in-house 'linker' sequence). Volunteers were scanned in the arms down position.

To assess the impact of AC on respiratory motion, the cine coronal sequence with and without compression was used to measure the diaphragmatic peak to peak (superior-inferior) motion amplitude during each respiratory cycle. The cine image took 20.8 seconds to acquire with each scan consisting of between 3-6 respiratory cycles depending on the volunteers' pattern of breathing, see Figure 6.2 for measurement technique.

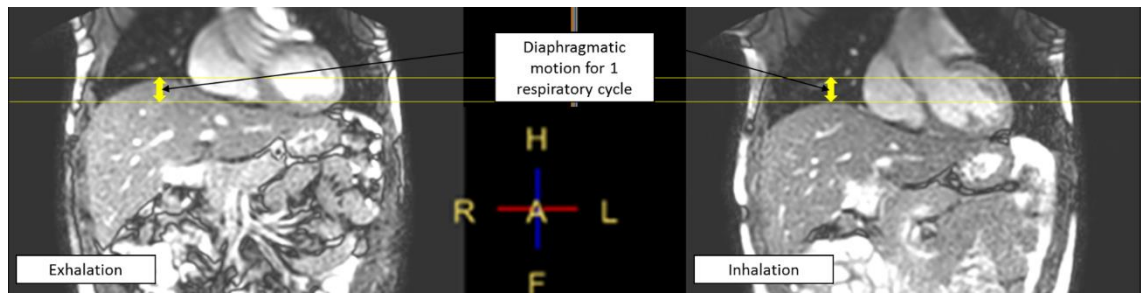


Figure 6.2 Measurement of diaphragmatic motion.

The distance between the most superior aspect of the liver dome/diaphragm at maximum exhalation compared to maximum inhalation was calculated. Image courtesy of Rebekah Lawes.

Diaphragmatic motion was used as a surrogate for pancreatic motion as imaging constraints meant it was not possible to accurately and reproducibly measure movement of the pancreas itself. It is accepted that this might represent an overestimate of target motion but this technique allowed us to perform a fair comparison of the efficacy of compression. Myself and Rebekah Lawes undertook all measurements together to reduce the impact of inter-observer variability.

Paired T-Tests (with a significance value set at 95%) were used to test for statistically significance differences in diaphragmatic motion comparing no compression versus Dynabelt and no compression versus ZiFix. Direct comparison between Dynabelt and ZiFix was not performed as, due to imaging time constraints, it was not possible to scan the volunteers wearing both Dynabelt and ZiFix during the same session and the impact of day to day variation in breathing was not known. Statistical tests were carried out using SPSS (version as per previously).

Although there are published studies looking at the use of AC to reduce abdominal motion (2-5), the majority used in-house developed devices. I was not able to find any published data using the specific devices used in this research. For the Dynabelt, this is not surprising as this is sold as an abdominal support garment and has been adapted by my institution. There was also no specific data on the extent that ZiFix reduced diaphragmatic motion. The data provided by the company (in limited abstract form with no citation) reported a reduction in

inspiratory capacity of 42% compared to no compression but did not mention the degree of diaphragmatic motion reduction.

6.2.4 Assessment of the impact of compression devices on image clarity

A visual graded analysis of the image quality of the T1W, mDixon (water) and 3DVane with and without compression was performed for each volunteer. Three assessors, two clinical oncologists (AH and KA) and one therapeutic radiographer (SA) reviewed the same randomly selected imaging sessions for each volunteer, one with no compression, one with ZiFix compression and one with Dynabelt compression. Image clarity was assessed using a 4 point Likert scale with anatomical structures (liver, pancreas, duodenum, stomach, small bowel and large bowel) graded as very clear (3), clear (2), unclear (1) or not visible (0). This was the same Likert scale as used in Chapter 5.

Statistically significant differences comparing image clarity with no compression versus Dynabelt versus ZiFix were tested for using Friedman test with additional post hoc analysis performed using Wilcoxon signed rank test. A Bonferroni correction was applied for the Wilcoxon signed rank test resulting in a significance level set at $p < 0.017$. SPSS was used as per previously for statistical analysis.

6.2.5 Assessment of volunteer tolerability

To assess AC device tolerability, qualitative data was collected from volunteers after every imaging session (questionnaire appendix 6.1). Volunteers were asked to record comments about the device in the free text area. Volunteers were able to terminate a session at any point if they experienced side effects or discomfort.

6.2.6 Assessment of compatibility with 4DCT

Our radiotherapy workflow includes a planning 4DCT which provides motion data for planning purposes. Therefore, AC devices need to be compatible with our in-house 4DCT technology. Volunteers in cohort 2 undertook one simulated session on our departmental CT scanner. The ability to pick up a 4D motion trace was assessed both with and without the compression devices. Volunteers did not undergo an actual CT scan.

6.3 Results

A total of 20 imaging sessions were completed in Cohort 2 (4 per volunteer). At each session sequences were acquired with and without the pre-specified compression device. Each volunteer completed 3 sessions wearing the ZiFix device and one session wearing the Dynabelt.

6.3.1 Assessment of the impact of abdominal compression on diaphragmatic motion

Use of the ZiFix compression device resulted in a statistically significant reduction in diaphragmatic motion as seen on cine MRI imaging. In matched data from sessions when volunteers used the ZiFix compared to the same session without compression, mean motion decreased from 11.6mm (S.D. 3.1) to 6.7 mm (S.D. 1.9), $p < 0.001$. See Figure 6.3.

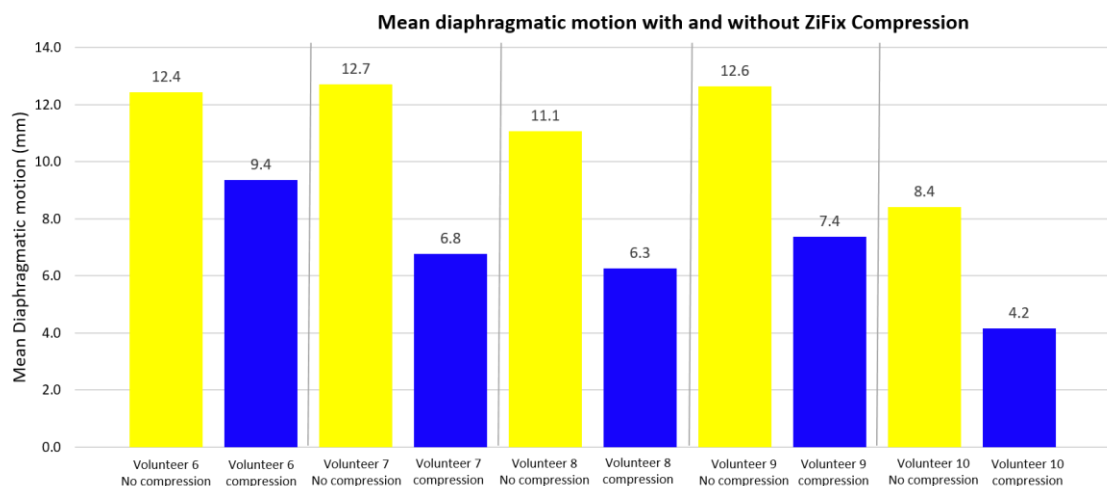


Figure 6.3 Graph showing the reduction in mean motion across the 5 volunteers in Cohort 2 with use of ZiFix compression device.

Yellow no compression, blue compression.

Use of the Dynabelt compression device also resulted in a statistically significant reduction in diaphragmatic motion. Mean motion with Dynabelt 7.6mm (S.D. 1.8) versus 12.7mm (S.D. 2.2) without compression during the same sessions, $p < 0.001$. See Figure 6.4.

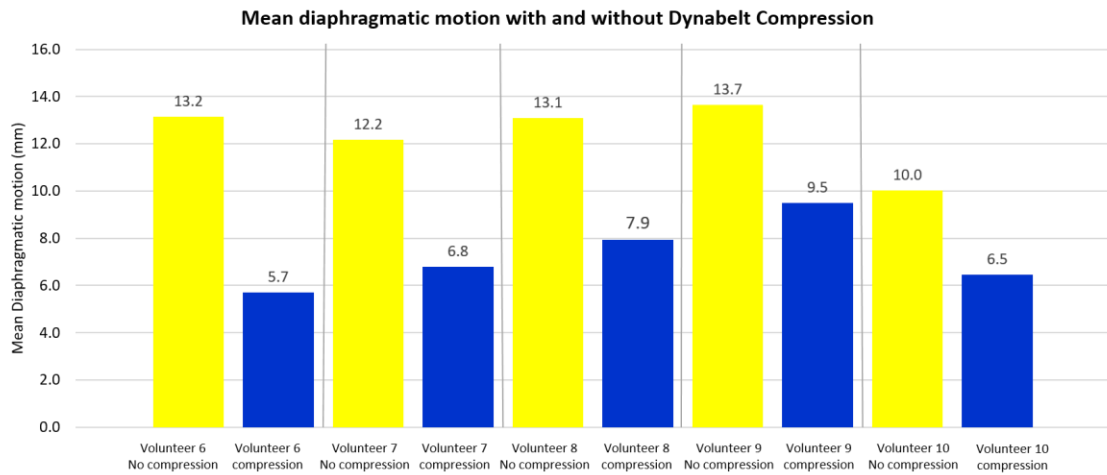


Figure 6.4 Graph showing the reduction in diaphragmatic motion across the 5 volunteers in Cohort 2 with use of the Dynabelt compression device.

Yellow no compression, blue compression.

6.3.2 Assessment of the impact on image clarity of the presence of compression devices

Imaging sequences from each volunteer were reviewed by 3 observers who assessed the image clarity of the abdominal organs. A total of 270 observations per sequence type were recorded.

There was no significant difference in the image clarity of the 3D Vane sequence (the sequence to be used in our workflow for re-contouring and treatment planning) comparing the 3 compression options (no compression versus Dynabelt versus ZiFix), $p = 0.07$. See Table 6.1.

The image quality of the T1W and mDixon (water) appeared to improve with the addition of a compression device with a statistically significant difference noted between the groups using Friedman test. On post hoc analysis, there was no statistical difference between the T1W image with the Dynabelt versus the ZiFix ($p = 1$) but a difference in favour of compression was seen between no compression and either Dynabelt or ZiFix use ($p < 0.01$).

In the case of the mDixon (water) sequence, although a statistical difference was seen between groups using the Friedman test, these differences were no longer

statistically significant after post hoc analysis with Wilcoxon Signed Ranks test (value for statistical significance $p < 0.02$).

Table 6.1 Median Likert score for the different sequences with the differing compression devices.

Imaging sequence	Median Likert (IQR) Compression Device			Friedman test
	No compression	Dynabelt	ZiFix	
T1W	1 (1-1)	1 (1-2)	1 (1-2)	$p < 0.01^*$
mDixon (water)	2 (2-2)	2 (2-2)	2 (2-2)	$p = 0.01^*$
3D Vane	2 (2-2)	2 (2-3)	2 (2-3)	$p = 0.07$

Likert scale: Not visible =0, unclear =1, clear =2, very clear =3. * = statistically significant result.

Table 6.2 Post hoc analysis of T1W and mDixon (water) comparisons.

** = statistically significant result.*

Imaging sequence	Wilcoxon Signed Ranks Test p value		
	No compression versus Dynabelt	No compression versus ZiFix	Dynabelt versus ZiFix
T1W	<0.01*	<0.01*	1.00
mDixon (water)	0.64	0.02	0.03

6.3.3 Assessment of volunteer tolerability

All imaging sessions were completed as planned with no sessions terminated early due to participant discomfort. A total of 20 experience questionnaires were completed, 5 from Dynabelt sessions and 15 from ZiFix sessions.

Dynabelt sessions were well tolerated with all volunteers strongly agreeing that they had no difficulties coping with the scan and would have had no concerns about having further scans in the future, Figure 6.4. Twenty percent of questionnaires reported some sweating or tingling. No specific concerns related to the belt itself were raised.

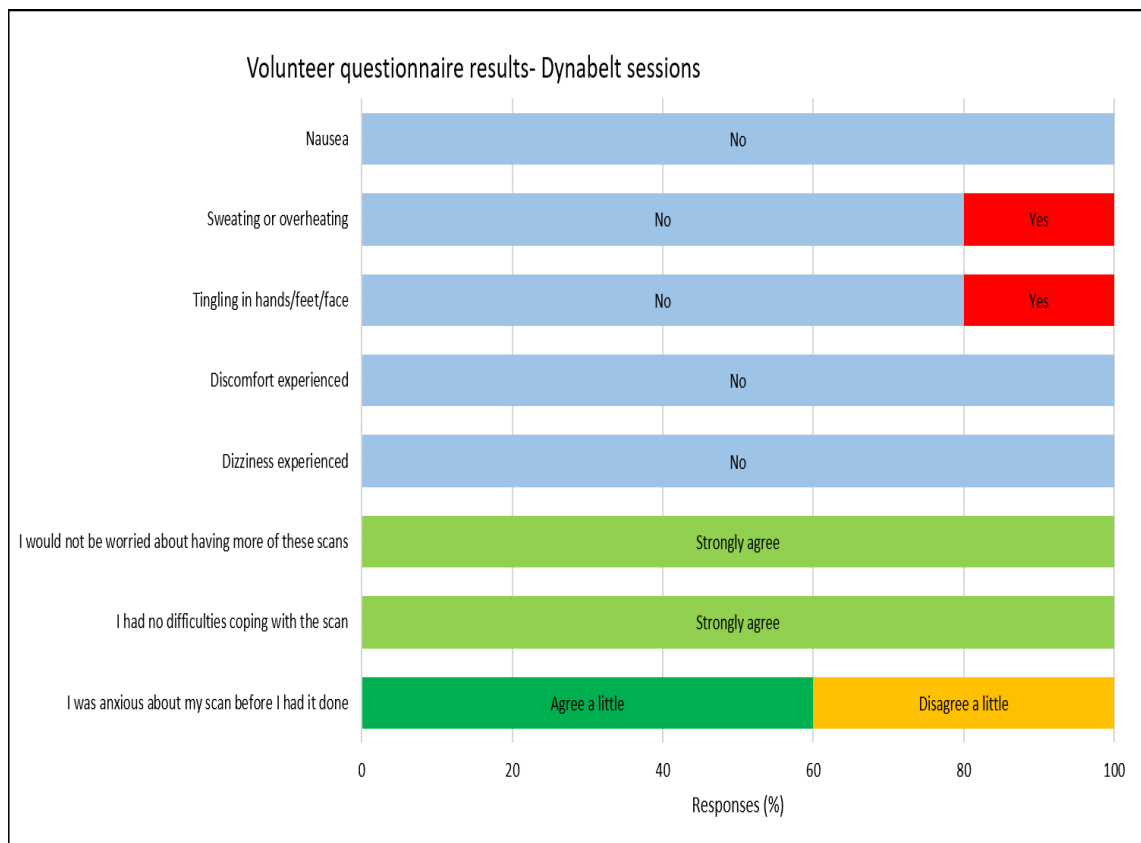


Figure 6.4 Results of volunteer questionnaires following Dynabelt sessions.

Top 5 questions yes/no answers permitted, bottom 3 questions scored on Likert scale strongly agree, agree a little, neither agree nor disagree, disagree a little, strongly disagree.

ZiFix sessions were also well tolerated although to a lesser extent to the Dynabelt. 87% of questionnaires reported no discomfort with 80% reporting that they strongly agreed with the statement that they would not be worried about having further scans and 60% strongly agreeing that they have no difficulties coping with the scan. Specific comments relating to the ZiFix included that it took a period of time to 'get used to the belt' and that it felt like they had 'eaten a large meal'. See Figure 6.5.

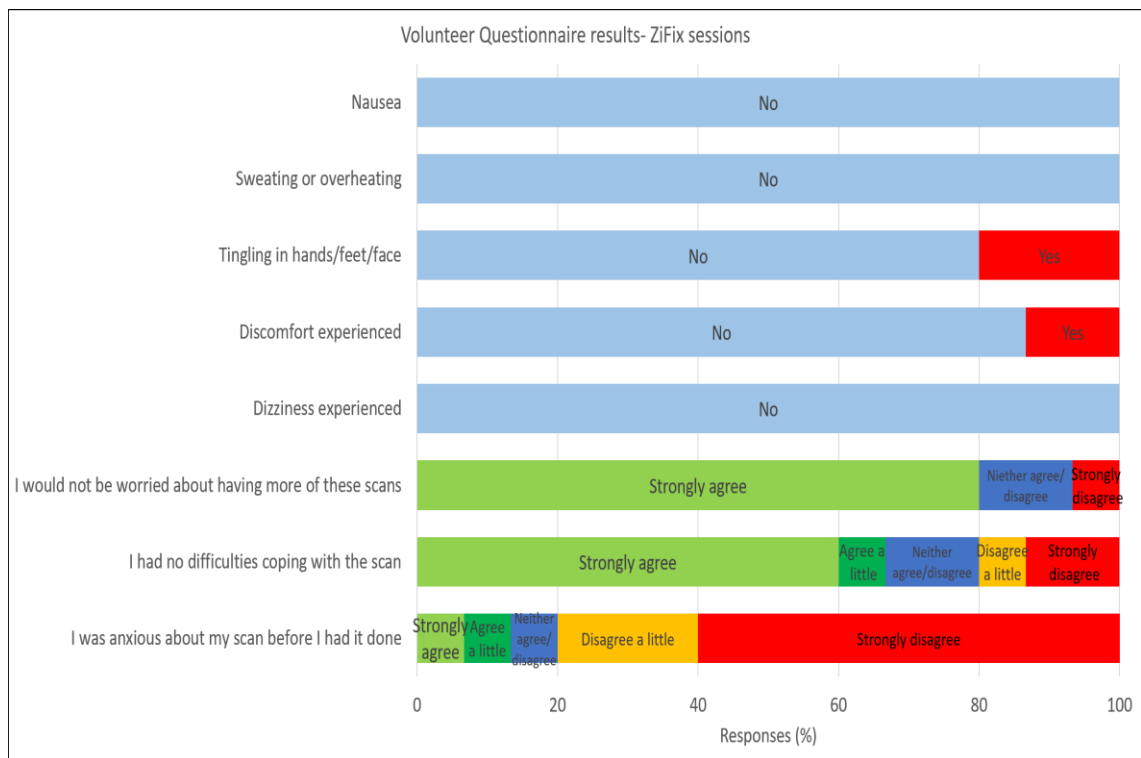


Figure 6.5 Results of volunteer questionnaires for ZiFix sessions.

Answer options as per Figure 6.4.

6.3.4 Assessment of compatibility with 4DCT

Assessment of the compatibility of the compression devices with our institution's 4DCT real time position management (RPM) system was carried out for 4/5 of the Cohort 2 volunteers. One volunteer had left the trust so was unable to participate. The RPM system was able to detect a suitable trace without compression and with the Dynabelt in situ for all 4 volunteers. However, when using the ZiFix device it was not possible to detect a suitable trace in 2 of the volunteers.

6.4 Discussion

This pilot study has identified 2 abdominal compression devices which met our pre-specified criteria and warrant further investigation within a patient cohort. Both devices were MR safe and able to fit with the MRL treatment bore. No negative impact on image clarity was noted and a reduction in diaphragmatic motion was seen. Both devices were tolerated by the wearer. The only area of

concern was the potential difficulty in acquiring a 4DCT trace whilst wearing the ZiFix system as this was only successful 50% of volunteers (although I acknowledge the small size of the tested cohort).

Our results are consistent with other studies looking at the impact of abdominal compression in the context of radiotherapy to the upper abdomen (2-5). Heerkens et al (3) used a customised abdominal corset to compress the abdomen of 10 pancreatic cancer patients. Using cine imaging and fiducial tracking they detected a statistically significant reduction in superior/inferior tumour motion with the addition of the corset (mean motion of 11.3 mm versus 7.2mm). This is comparable with the mean reduction seen in our study of 4.9mm when using the ZiFix. Similarly, Campbell et al (2) found that patients undergoing SBRT to the pancreas had a mean reduction in superior/inferior fiducial motion of 5 mm with the addition of compression.

In our study we did not measure pancreatic motion directly and instead relied on the diaphragm as a surrogate. This was because it was not possible to identify a reproducible point within the pancreas on our cine image to measure across the respiratory cycles and, as we used healthy volunteers, there were no trackable fiducials. It should be remembered therefore that the reduction in motion achieved in our study may not directly translate into the same reduction in pancreatic/pancreatic tumour motion.

It was encouraging that the results of our visual grading analysis did not show any negative impact on image clarity. This is important, as any erosion in image clarity would add to contour uncertainty. This would potentially result in the need for larger treatment margins to avoid inadvertent target miss negating any benefit in motion reduction. There are no other published studies looking at the impact of compression on MRI sequence clarity. However, from discussions within the Elekta consortium we do know of other centres that have successfully integrated compression within their MR guided workflows.

A weakness of this study is the use of non-patient volunteers and the small cohort size. This raises the possibility that our findings will not be reproducible in our patient population. However, the choice of cohort size and healthy volunteers was

a pragmatic one. Firstly, as we were unsure of the tolerability of the devices, the impact on respiratory motion and the impact on image clarity, we wanted to test the devices on volunteers without significant co-morbidity in the first instance to avoid exposing patients to unnecessary discomfort/time in the radiotherapy department. Secondly, as part of this project was carried out during the COVID pandemic, we needed to limit the number of people within the radiotherapy department for infection control reasons. We do however, plan to extend this work to a patient cohort when it is safe to do so.

In the patient cohort we will also pay particular attention to the impact of the compression devices on 4DCT acquisition. This was the only area of concern raised in our pilot cohort as in 50% of volunteers it was difficult to record a 4D trace whilst wearing the ZiFix device. In order for a 4DCT to be obtained the RPM at our centre relies on a minimum detectable abdominal wall excursion of approximately 4mm. This excursion is measured by placing a tracking box on the patient's abdomen, the movement of which is tracked by wall mounted lasers. It may be that the ZiFix device decreases abdominal wall motion in some patients to such an extent that a 4DCT trace is impossible to obtain or it may be that the shape of the ZiFix makes RPM box placement challenging. It should be noted that the Dynabelt had no issues with respect to 4DCT acquisition likely due to its thinner size and the larger area for RPM positioning. We may therefore find that with increased experience in RPM box positioning, acquisition rates for the ZiFix improve. It should also be noted that abdominal compression devices have been integrated into 4DCT non MRgRT workflows at other centres suggesting that this issue is not insurmountable.

6.5 Conclusion

In this chapter I have shown that the integration of an abdominal compression system within our workflow is likely to be feasible and shows promise as a way of reducing the impact of respiratory motion on target motion. In the future it could also be used as an adjunct to more advanced motion management techniques such as gating and tracking. This work will now be extended to confirm these findings in a patient cohort.

6.6 References

1. Huguet F, Yorke ED, Davidson M, Zhang Z, Jackson A, Mageras GS, et al. Modeling pancreatic tumor motion using 4-dimensional computed tomography and surrogate markers. *International journal of radiation oncology, biology, physics*. 2015;91(3):579-87.
2. Campbell WG, Jones BL, Schefter T, Goodman KA, Miften M. An evaluation of motion mitigation techniques for pancreatic SBRT. *Radiotherapy and oncology : journal of the European Society for Therapeutic Radiology and Oncology*. 2017;124(1):168-73.
3. Heerkens HD, Reerink O, Intven MPW, Hiensch RR, van den Berg CAT, Crijns SPM, et al. Pancreatic tumor motion reduction by use of a custom abdominal corset. *Physics and Imaging in Radiation Oncology*. 2017;2:7-10.
4. Lovelock DM, Zatcky J, Goodman K, Yamada Y. The effectiveness of a pneumatic compression belt in reducing respiratory motion of abdominal tumors in patients undergoing stereotactic body radiotherapy. *Technology in cancer research & treatment*. 2014;13(3):259-67.
5. Eccles CL, Patel R, Simeonov AK, Lockwood G, Haider M, Dawson LA. Comparison of liver tumor motion with and without abdominal compression using cine-magnetic resonance imaging. *International journal of radiation oncology, biology, physics*. 2011;79(2):602-8.

Chapter 7

Pancreatic cancer MRgRT
treatment protocol

Chapter 7 Pancreatic cancer MRgRT treatment protocol

7.1 Introduction

In the context of locally advanced pancreatic cancer (LAPC), the ultimate goal for MRgRT is to treat patients to a biological equivalent dose (BED₁₀) of >100Gy. However, for safety reasons, it is first necessary to gain experience at standard doses to avoid unexpected harm. In chapters 5 and 6 I have discussed my work on MRI sequence optimisation and the use of abdominal compression within an MRgRT workflow. In this chapter I discuss the integration of these elements into a non-dose escalated MRgRT protocol to be trialled at my centre.

In order to design this protocol, 2 key areas were explored:

1. The development of a 15 fraction regimen
2. The integration of optimised MRI sequences and abdominal compression into an online MRgRT workflow using a mid-ventilation planning technique.

7.2 Methods

7.2.1 Rationale for use of a non-dose escalated 15 fraction protocol.

Due to resource and workflow constraints, hypofractionated radiotherapy regimens are favoured on the MRL. Unlike for bladder cancer, at the start of my thesis there was no standard hypofractionated regimen for LAPC in the UK. However, there was interest amongst the UK radiotherapy community in the development of such a protocol. A 15 fraction approach was favoured (as opposed to a shorter fractionation) as this could be planned using an IMRT (rather than SBRT) technique and can be given alongside concurrent chemotherapy. In addition, at the start of my thesis, SBRT for pancreatic cancer was not commissioned by the NHS. The arrival of the Coronavirus pandemic accelerated the drive for a hypofractionation schedule. In fact, parts of the described protocol (applicable to standard linacs) have been incorporated into the Royal College of Radiologists recommendations for treating pancreatic cancer during the pandemic (1).

As a preliminary step to protocol development, I performed a literature search for both dose escalated and non-escalated 15 fraction regimens in use for pancreatic radiotherapy (appendix 7.1 summarises the papers reviewed).

Published retrospective data and protocols using 15 fractions come predominantly from US experience. 15 fraction protocols are typically used in the dose escalated setting alongside concurrent chemotherapy. A simultaneous integrated boost (SIB) technique is utilised with a central tumour dose of 67.5Gy/15# (2-6) integrated with a lower dose to the surrounding area. Centres employing this technique have strict patient selection criteria, utilise IMRT (or SBRT) with steep dose gradients, use high precision delivery (breath hold or gating) and often use GI planning OAR (GI PRV) structures. Without the benefit of breath hold or gating on the Elekta Unity (or indeed prior experience of treating pancreatic cancer patients on the MRL), dose escalation up to 67.5Gy would be too risky for our initial cohort of patients. However, elements of the techniques employed, such as the use SIBs, heterogeneous dose distributions and GI PRVs are relevant for a non-dose escalated protocol.

Lower dose 15 fraction protocols have also been published. Typically, they are used in the resectable/borderline resectable setting as an adjunct to surgery. In the phase III PREOPANC trial (7), 36Gy/15# with concurrent gemcitabine was compared to surgery alone. Although the trial failed to show a median OS benefit for the addition of CRT, 3 and 5 year OS was improved (8). In addition, in a predefined subgroup analysis for borderline resectable patients, an improved R0 resection rate (71% vs. 40%) was noted. Due to the lower doses utilised, the trial allowed both IMRT and 3D conformal radiotherapy and did not require use of advanced motion management strategies. However, with a BED₁₀⁹ of 44.64Gy, see Table 7.1, there is concern that such a protocol in LAPC would lead to under-dosing.

⁹ The exact α/β ratio for pancreatic cancer is unclear. Historically a value of 10 has been used which is in line with a recent literature review by Prior et al, placing the α/β at 9.5. 9. Prior PW, Chen X, Hall WA, Erickson BA, Li A. Estimation of the Alpha-beta Ratio for Chemoradiation of Locally Advanced Pancreatic Cancer. *Int J Radiat Oncol Biol Phys.* 2018;102(3):S97-S.

Table 7.1 Table of dose equivalence

(Not taking into account time factor)

Fractionation	BED α/β 10	BED α/β 3
50.4Gy/28# (UK standard)	59.47	80.64
54Gy/30#	63.72	86.4
36Gy/15#	44.64	64.8
45Gy/15#	58.5	90

BED = biologically effective dose, calculated using the following formula:

$BED = nd \left[1 + \frac{d}{\alpha/\beta} \right]$ Where n is the number of fractions, d is the dose per fraction and α/β is either 10 or 3.

Therefore, for this protocol a compromise was sought, aiming to provide sufficient dose to the tumour whilst minimising the risk to OARs.

A SIB technique was chosen with a boost dose of 45Gy/15# which is an equivalent BED₁₀ to 50.4Gy/28#, the current UK standard from the SCALOP trial (10). This is combined with a larger, low dose region receiving 40Gy/15# which is within GI OAR tolerance and designed to cover microscopic disease. This larger volume is similar to the CTV concept applied in the current SCALOP-2 trial (NCT02024009).

7.2.1.1 Rationale behind two dose level technique

The importance of including a larger, low dose target region is increasingly being recognised. Evaluation of SBRT series with small GTV to PTV margins suggest high rates of locoregional recurrence. In a retrospective evaluation of 510 patients treated with SBRT for operable, borderline resectable or locally advanced disease, 42% were found to have locoregional recurrences, most commonly in the region of the coeliac trunk, superior mesenteric artery and retroperitoneal space (11). Kharofa et al (12) reported higher than expected rates of local recurrence using 33Gy/5# with 3mm GTV to PTV margins in a borderline

resectable patient cohort. Rates of local recurrence decreased with the addition of a second, larger low dose PTV (25Gy/5#) which extended to include local vasculature. This is unsurprising given the high rates of perineural spread along mesenteric blood vessels seen in resected pancreatic cancer series (13). Two dose levels therefore allow adequate dose to be delivered to both macro- and microscopic disease whilst maintaining OAR constraints.

7.2.1.2 Rationale behind OAR dose constraints used in this protocol

The PREOPANC study (7) is the only reported phase III study which uses a 15# regimen. However, dose constraints for this trial are not applicable for this protocol as 36Gy/15# is below GI OAR tolerance.

Appendix 7.2 includes a breakdown of the dose constraints of published 15# protocols along with additional personal communication from clinicians utilising 15# protocols in the upper abdomen. Although there are slight variances between the studies, the majority converge around a maximum point dose of 45Gy to the duodenum, stomach and small bowel.

I opted to base the dose constraints for this protocol on those of Reyngold et al (3). This paper included the most detail on the implementation of an SIB approach. The paper's authors also have considerable experience in the use of both MR guided and standard linac pancreatic protocols. The paper advocates the use of PRVs around OARs as a way to mitigate against GI toxicity and as a result I have included these in the planning dose constraints. PRVs are also used in this context by Koay et al (6) and Goto et al (14). As Reyngold et al did not include constraints for the kidneys, liver or spinal cord these values were taken from the ABC-07 trial protocol which is a dose-escalated radiotherapy trial for cholangiocarcinoma currently recruiting in the UK (CRUK/14/029).

7.2.2 Integration of the optimised MRI sequences into the pancreatic workflow and PTV margin calculations

In keeping with MRL workflows at our centre, the pancreatic workflow includes an offline and online component.

Offline, the patient will undergo a CT planning scan which is contoured by the clinician. The CT provides relative electron densities of key structures contributing to the bulk density layering needed for dose calculation on the online MRIs. The CT is then used to generate a 'reference plan'. This will be based on a previously developed 'class solution'. This class solution will be designed to produce robust plans which, when personalised to an individual's anatomy, will require minimal or no change to the optimisation parameters during online adaption. This is similar to my centre's technique for MRgRT to the bladder. On the day of treatment, the patient will undergo a 'session' MRI (MRI_{session}) which will be registered to the CT planning scan using soft tissue matching. Contour propagation from the CT to the MRI_{session} will occur and necessary adjustments made before a new online plan is optimised. Prior to beam on, a second MRI ($MRI_{\text{verification}}$) will be performed to confirm patient positioning and target coverage.

As described in Chapter 5, following the MRI sequence development process, the favoured sequence for use as the MRI_{session} is the 3DVane. This sequence, acquired over multiple breathing cycles, produces an image which depicts the anatomy in its 'average' position over these cycles. However, the 3DVane itself does not provide information with respect to the variance around this position and therefore cannot inform an individualised motion margin. This information will therefore come from the offline planning CT.

Standardly at our centre an internal target volume (ITV) approach is used to account for respiratory motion for conventionally fractionated regimens. Here a respiratory correlated 4DCT is acquired over a single respiratory cycle. The images produced are 'binned' into the different phases of this respiratory cycle. The GTV is contoured on the maximum inhale and exhale bins of the 4DCT and combined with the GTV from the contrast CT to create an ITV which takes into account the tumour's deformation and position change over the respiratory cycle. To this, isotropic margins are then added to account for microscopic spread, creating the CTV, with an additional margin added for the PTV.

A weakness to this approach is that as the ITV encompasses all possible motion during the respiratory cycle, (even though the tumour spends relatively little time

at the extreme ends of this motion) it is often large and can encompass excess amounts of normal tissue increasing the risk of toxicity (15). An alternative to the ITV approach is the use of a mid-ventilation (MidV) or mid-position scan for delineation and planning. In the mid-ventilation scenario, a computer algorithm is used to identify the 4DCT bin which most closely matches the time-averaged position of the GTV, akin to the position seen on the 3DVane. This bin is used for contouring and treatment planning with individualised probability based GTV-PTV margins added based on the peak-to-peak motion throughout the respiratory cycle. This technique has been modelled for use in the context of LAPC (16) and has been shown to reduce overall treatment margins. It is also in use in the Netherlands for lung SBRT (15) and has been shown to facilitate dose escalation in the context of liver SBRT (17).

In addition, as the MidV 4DCT bin most closely represents the ‘average position’ of the anatomy during a respiratory cycle, it is most akin to the position as seen on the 3DVane (the sequence being used as the MRI_{session}). This should allow for propagation of contours from the 4DCT to the MRI_{session} of higher quality than if the breath-hold CT component was used as variation in anatomical position will be less. Contours would therefore require less adjustment during the online workflow enabling the workflow to be completed in a timelier manner.

The methodology for MidV margin generation has been previously described by Wolthaus et al (18). However, as this approach has not previously been used at RMH/ICR in the context of pancreatic cancer, centre specific adaption was needed.

For this work I collaborated with wider members of the pancreatic working group at RMH/ICR. These included Dr Dualta McQuaid (Medical Physicist) who developed the computer script for the identification of the MidV bin on pancreatic 4DCTs and Sophie Alexander (Therapeutic Radiographer) who helped run the script on 10 test patients. Additional members of the working group were Dr Katharine Aitken (Consultant Clinical Oncologist), Dr Helen McNair (Head Research Radiographer) and Dr Simeon Nill (Medical Physicist).

To test the suitability of the in-house algorithm, the deformed computer-generated GTVs (which are used to determine the MidV bin) were checked for accuracy. To do this, I contoured the GTV on each respiratory bin for 10 test patients. This contouring was completed prior to the computer-generated contours so as not to introduce bias. My GTVs were then compared to the computer-generated GTVs using the DICE coefficient (DCE) metric. Across the 100 GTVs analysed (10 per patient) a median DCE of 0.8 was recorded. This is comparable to that reported by Hall et al (19) in a planning study comparing the CT based pancreatic volumes of 12 radiation oncologists (DCE 0.73) and was therefore felt to be acceptable.

The peak-to-peak motion of the GTV across the respiratory cycle as reported by the script was also sense checked against published studies reporting pancreatic motion on 4DCT. Mean motion in this cohort was 3.4mm superior/inferior, 2.0 mm anterior/posterior and 0.7mm left/right which is broadly in keeping with similar published series (20-24).

Finally, the centre specific components of the MidV margin formula were agreed within the working group. The margin formula used was from Lens et al (16) in their paper modelling the use of MidV in pancreatic radiotherapy (equation 1). This is based on the Van Herk's equation (25) which ensures a minimum dose to the CTV of 95% for 90% of patients.

$$\text{Margin} = 2.5 \Sigma + 1.64 \sigma - 1.64 \sigma_p \text{ (mm)} \quad \text{Equation 1}$$

Where Σ is the standard deviation of the systematic errors, σ is the standard deviation of the random errors and σ_p represents the width of the penumbra in water which, by general international consensus is **3.2mm**.

Σ is calculated using the following formula:

$$\Sigma = \sqrt{\Sigma_{del}^2 + \Sigma_{midV}^2} \quad \text{Equation 2}$$

Where:

Σ_{del} = delineation uncertainty. In Lens et al this was set at 3mm based on values from a prostate study at their institution. In our case we set this value to **0mm** in line with previous work at our institution using MidV planning for lung cancer¹⁰.

Σ_{midV} = the difference between the true tumour position and the position on the MidV bin. In Lens et al this was set at **0.5mm** which was determined by taking the standard deviation of the difference seen in their 18 trial patients. We opted to use this value as it closely matched the standard deviation of the difference seen in our 10 patient cohort (0.6mm).

σ is calculated using the following formula:

$$\sigma = \sqrt{\sigma_{setup}^2 + \sigma_{midV}^2 + \sigma_{inter}^2 + \sigma_{pen}^2 + (0.358 A)^2}$$

Equation 3

Where:

σ_{setup} = setup error, set as 3mm by Lens but we used **0mm** as we would be using daily adaption.

$\sigma_{mid V}$ = uncertainty in tumour position, set as **0.5mm** (same as the value used in the systematic error calculation).

σ_{inter} = image registration errors. In Lens et al the value used was 1mm based on an estimate from a previous study at their institution in patients with fiducial markers in situ. We opted to increase this to **3mm** as our patients will not have fiducials and we anticipate additional CT-MR registration error, (based on preliminary work by Sophie Alexander looking at registrations carried out by differing radiographers).

¹⁰ Previous work was carried out by Dr Hannah Bainbridge as part of her PhD on novel approaches to lung radiotherapy at ICR/RMH. Her findings are published in her PhD thesis available in the ICR library

σ_{pen} = beam penumbra, by general international consensus this is deemed to be **3.2mm** in water.

A = peak to peak tumour motion, which will be based on the individual motion seen for each patient in each direction (and will be calculated by the MidV script).

By inputting these values into equations 1-3, along with different degrees of motion the following PTV margins are produced (Table 7.2).

Table 7.2 Initial margin calculations

Peak to peak motion (mm)	Margin (mm)
0	3.24
1	3.27
2	3.34
3	3.45
4	3.61
5	3.81
6	4.05
7	4.33
8	4.63
9	4.97
10	5.32
11	5.70
12	6.10
13	6.52
14	6.96

As a group we subsequently agreed that it would be pragmatic to group these results as such precise measurements are unnecessary. As a result, the final proposed PTV margins are shown in Table 7.3

Table 7.3 Proposed PTV margins.

This will be calculated separately for motion in the superior/inferior, anterior/posterior and left/right directions.

Motion	Corresponding margin
0 mm-5 mm	4 mm
5.1 mm-9 mm	5 mm
9.1 mm-11 mm	6 mm
11.1 mm-14 mm	7 mm

Abdominal compression will be used to keep respiratory motion to a minimum. Patients with motion greater than 14mm despite compression will not be offered MRgRT and will be offered an alternative treatment technique.

7.3 Results- The protocol

I have developed the following protocol to treat patients with LAPC on the Elekta Unity. This protocol includes details of patient indications, pre-treatment investigations, therapeutic schemata, volume definition and principles of treatment planning and delivery. It does not however go into the detail of treatment planning which will be covered in separate radiotherapy planning documents devised by the medical physics team at RMH.

7.3.1 Objectives and Scope

To summarise the planning and treatment of patients receiving 15 fraction hypofractionated radiotherapy for pancreatic malignancies on the Elekta Unity MR-Linac.

7.3.2 Indications

Patients with locally advanced adenocarcinoma of the pancreas (as defined by MDT) who have not progressed following up-front chemotherapy and are fit to receive chemoradiotherapy.

The dose is 45Gy/15# with concomitant capecitabine (using a simultaneous integrated boost technique with 40Gy/15# given to lower dose volume).

7.3.3 Pre-radiotherapy investigations

A PET/CT should be performed to rule out metastatic disease. A DMSA scan may be required if renal dose is likely to be significant.

Patients may require an MRI to aid tumour definition if not well defined on contrast enhanced CT (discretion of clinician).

7.3.4 Therapeutic schemata

7.3.4.1 Dose prescriptions

The dose to PTV₄₅₀₀ will be 45Gy in 15 fractions (3 Gy per fraction) delivered over 3 weeks (Monday-Friday). The dose to PTV₄₀₀₀ will be 40Gy in 15 fractions (2.67 Gy per fraction) delivered over 3 weeks (Monday-Friday).

7.3.4.2 Chemotherapy

Concurrent oral capecitabine, 830mg/m² BD will be given on days receiving radiotherapy.

7.3.5 Pre-treatment

7.3.5.1 Patient simulation and immobilisation

An IV contrast enhanced exhale breath-hold pancreatic protocol CT (CECT) should be obtained, followed by a 4DCT. The patient will be scanned arms down with knee immobilisation. Abdominal compression should be used, utilising the ZiFix device in the first instance followed by the Dynabelt if a 4DCT cannot be obtained.

Patients should be nil by mouth for 2 hours prior to scan and each treatment. Patients should then drink ~200 ml of water or oral contrast 10-15 minutes prior to scanning/treatment to aid the visualisation of the upper GI tract.

If being used, a planning MRI should ideally be performed on the same day of planning CT, with the patient immobilized in the treatment position and similar drinking instructions followed.

7.3.6 Volume definition

7.3.6.1 Targets

GTV

On the 3D CECT, outline GTV_T:

GTV_T = the macroscopic pancreatic tumour visible on imaging plus peritumoural lymph nodes (> 1cm in short axis diameter and considered suggestive of involvement on diagnostic imaging).

This structure should then be replicated on each respiratory bin of the 4DCT, labelling as GTV_T_10%, GTV_T_20% etc.

Use the pancreatic mid-ventilation computer script, to generate a deformed GTV_T on each respiratory bin. The clinician should compare this to the corresponding clinician drawn GTV_T_10% etc. with changes made to the deformed version as necessary.

The script will calculate the mid-ventilation (MidV) position and bin. If agreed this bin will be used for radiotherapy planning as the primary dataset. The script will report the 3D motion of GTV_T over the respiratory cycle. This will enable creation of an individualised anisotropic margin.

CTV

$CTV_{4000} = GTV_T + 5\text{mm}$ in all directions, edited back to exclude areas of overlap with uninvolved GI tract.

PTV

$PTV_{4500} = GTV_T + \text{motion adapted margin}$ (see Table 7.4)

$PTV_{4000} = CTV_{4000} + \text{motion adapted margin (see Table 7.4)}$

Table 7.4 PTV motion adapted margin.

Based on motion provided by the script. This margin is applied separately in each direction superior/inferior, anterior/posterior, left/right directions.

Motion Bin	Corresponding margin
0 mm-5 mm	4 mm
5.1 mm-9 mm	5 mm
9.1 mm-11 mm	6 mm
11.1 mm-14 mm	7 mm

7.3.6.2 OARs

Duodenum: The whole of the duodenum from below the pylorus to the fourth part of duodenum (up to the ligament of Treitz) should be outlined.

Duodenum PRV: Duodenum + 5mm

Stomach: The whole stomach should be outlined

Stomach PRV: Stomach + 5mm

Small bowel: Individual loops of small bowel should be outlined on all slices from 2cm above to 2cm below the PTV not including colon and duodenum.

Small bowel PRV: Small bowel + 5mm

Large Bowel: Outline all large bowel from 2cm above to 2cm below the PTV

Large Bowel PRV: Large bowel + 5mm

Liver: Outline the whole liver

Kidneys: Both kidneys should be outlined separately

Spinal Cord: The spinal cord from 2cm above to 2cm below the PTV

Spinal Cord PRV: Spinal cord + 5mm

7.3.7 Treatment planning

Full planning details will be provided in a dedicated radiotherapy planning document. A VMAT/IMRT technique will be used.

OAR constraints take priority over PTV coverage.

Table 7.5 PTV constraints for 45Gy/15# simultaneous integrated boost

Structure	Constraint	Optimal	Mandatory
PTV ₄₅₀₀	D95%		≥95% (42.75Gy)
	D98%	≥95% (42.75Gy)	
	D2%	≤105% (47.25Gy)	≤107% (48.15Gy)
	D50%		≥ 100% (45Gy) +/- 1%
PTV ₄₀₀₀	D95%		≥95% (38Gy)
	D98%	≥95% (38Gy)	
	D50%		≥ 100% (40Gy)

Table 7.6 OAR constraints.

**Adapted from Reyngold et al (3)*

OAR	Dose Constraint Gy
Stomach PRV Dmax 0.5cc	≤ 45
Duodenum PRV Dmax 0.5cc	≤ 45
Small Bowel PRV Dmax 0.5cc	≤ 40
Large Bowel PRV Dmax 0.5cc	≤ 50
Liver (mean)	≤ 24
Kidneys Mean combined If one kidney or one kidney mean dose > 12Gy	≤ 15 V12Gy $\leq 10\%$
Spinal cord PRV Dmax 0.5cc	≤ 37.5
Spleen (mean)	< 6

7.3.8 Treatment delivery

Patients should follow the same fasting and drinking instructions as used prior to radiotherapy planning CT.

Treatment will be delivered on the Elekta Unity using an online adapt to shape protocol. Patients will be treated arms down wearing the compression belt used for planning. They will undergo a 3DVane MRI_{session} scan which will be used for re-contouring and replanning. Re-contouring will focus on adjustment of GI OARs within 2cm of PTV₄₅₀₀. An MRI_{verification} (in-house developed 'linker sequence') will enable position check prior to beam on. Further details on the online adapt to shape protocol will be detailed in a separate planning document.

Prophylactic anti-emetic and PPI should be considered

7.3.9 Follow up after treatment

CTCAE v5.0 should be used for prospective evaluation of toxicity with recommended time points of data collection at 4 weeks, 3 months and then 3 monthly until 2 years of follow up is reached. Follow up should be annual thereafter up to 5 years. CT imaging is recommended at 3 months. Ca 19-9 should be measured at each visit.

Table 7.7 Follow up schedule for locally advanced pancreatic cancer

Time Point				
	4 weeks	3 months	3 monthly until 2 years	2-5 years
Toxicity assessment	√	√	√	Annual
CT		√		
Ca 19-9		√	√	√

7.4 Discussion

The above protocol is designed as a bridge to our department's ultimate goal of delivering dose escalated MRgRT for LAPC. Compared to the pancreatic protocols in use at our institution pre 2020 it has 2 new elements, the use of 15 fractions and the use of the mid-ventilation approach to devising PTV margins.

The rationale behind the development of a 15 fraction protocol has been described in the methods section. I began this work in 2019 with a view to developing a protocol for use at my institution. However, with the arrival of the Coronavirus pandemic the development of a 15 fraction protocol for use across the UK became more pressing. In 2020 I was included in a UK wide working group to address this issue and elements of this protocol have therefore been included in the current Royal College of Radiology (RCR) guidance on the

treatment of pancreatic cancer during the pandemic (1). There are some differences however between the RCR's final guidance and that written above particularly in relation to the OAR dose constraints and the use of planning at risk volumes. This is because in this protocol I have opted to follow as closely as possible the dose constraints/planning techniques used in published LAPC series (3) which have been showed to be well tolerated by patients (4). Centres employing these constraints use PRVs to help reduce the chance of a GI OAR accidentally moving into higher dose areas. Although not strictly necessary at the doses used here, given our lack of experience with this fractionation schedule, I felt it was important to follow the published methodology to reduce the risk of unexpected toxicity to our patients. I also felt this would make the transition to dose-escalated treatments more straightforward as PRVs are an important safety measure in this context. Differences in the OAR dose constraints also exist between this protocol and that adopted by the RCR. Here, I opted to follow the dose constraints of the published pancreatic series whilst the RCR consensus group preferred to use the constraints listed in the ABC-07 trial. The ABC-07 constraints were selected by the RCR as some centres were already using these in the context of cholangiocarcinoma and therefore there was some familiarity of them within the group.

Use of the mid-ventilation approach in treatment planning was included in this protocol for two reasons. Firstly, it enabled individualised, motion dependent treatment margins to be added to the online GTV/CTV. Secondly, the mid-ventilation position was felt to more closely match the position seen on the 3DVane reducing the variability of the anatomy online compared to offline thus helping to reduce the time needed for online plan re-optimisation. Although not used as standard in the UK, the mid ventilation margin generation approach has been shown to reduce treatment margins in the LAPC setting (16) compared to an ITV approach. This provides a dosimetric advantage when trying to dose escalate close to dose limiting OARs. The PTV margin created is also less sensitive to day-to-day changes in respiratory motion which should ensure better target coverage (16). In the absence of more advanced motion management techniques such as gating or tracking, the mid-ventilation approach was therefore

felt to offer a way of individualising treatment margins without excessive dose to normal tissue.

The protocol described above is a steppingstone towards improving outcomes for patients with LAPC. It will enable my institution to move towards dose escalated treatments for this patient group and the potential overall survival benefit that this might bring. I do not envisage this protocol being used in the longer term instead I see its use as a way to build experience and confidence in the delivery of MRgRT to the pancreas whilst minimising the risk of unexpected toxicity. Once this experience has been gained, I envisage a move initially to 5 fraction SBRT followed by dose escalated treatments in either 5 or 15 fractions.

Concurrent capecitabine has been used in this protocol as this is the current UK standard of care (10). The continued use of capecitabine versus or in addition to novel radiosensitizers is an area of active research, for example the SCALOP-2 trial (26). The greater precision offered by MRgRT may enable 'stronger' radiosensitizers to be used in the future as less normal tissue will be receiving higher doses of radiation. Through the use of functional MRI, it may also be possible to tailor radiosensitizer use to the individual patient. For example, tumours noted to have higher levels of hypoxia on MRI may benefit more from radiosensitizers targeting hypoxia.

With respect to dose escalation, there are no clinical studies directly comparing outcomes from 5 versus 15 fraction regimens. A planning study I authored (27) did not find a significant difference in dose escalation potential between 50Gy/5# versus 67.5Gy/15# in the study population as a whole, but on an individual patient level, differences in target volume coverage were seen. This suggests that having institutional access to both a 5 and 15 fraction dose escalated protocol and selecting the best protocol for the individual patient would be of benefit. Although 5 fraction protocols may be more appealing due to their shorter treatment duration, 15 fraction protocols are given with radiosensitizers. It may be that some patients benefit more from a 15 fraction approach due to the use of radiosensitization over and above the degree of dose escalation that can be

achieved and exploring whether this is the case should be an area of active research.

Regardless of the dose escalated protocol that is chosen, the experience gained from use of this protocol with respect to motion management, online recontouring, imaging parameters and online plan review will be valuable.

7.5 Conclusion

This chapter focusses on the development of a 15 fraction protocol for pancreatic MRgRT at RMH/ICR. At the time of writing, development of a pancreatic ‘class solution’ is ongoing but it is hoped that the first patients will be treated in the near future. The success of this workflow will then be evaluated, and changes made as needed. It is hoped that the experience gained during this time period will enable the safe transition to dose escalated treatments once a gating/tracking solution becomes available on the Elekta Unity.

7.6 References

1. Jones CM, Radhakrishna G, Aitken K, Bridgewater J, Corrie P, Eatock M, et al. Considerations for the treatment of pancreatic cancer during the COVID-19 pandemic: the UK consensus position. *British journal of cancer*. 2020;123(5):709-13.
2. Krishnan S, Chadha AS, Suh Y, Chen HC, Rao A, Das P, et al. Focal Radiation Therapy Dose Escalation Improves Overall Survival in Locally Advanced Pancreatic Cancer Patients Receiving Induction Chemotherapy and Consolidative Chemoradiation. *International journal of radiation oncology, biology, physics*. 2016;94(4):755-65.
3. Reyngold M, Parikh P, Crane CH. Ablative radiation therapy for locally advanced pancreatic cancer: techniques and results. *Radiation oncology (London, England)*. 2019;14(1):95.
4. Colbert LE, Moningi S, Chadha A, Amer A, Lee Y, Wolff RA, et al. Dose escalation with an IMRT technique in 15 to 28 fractions is better tolerated than standard doses of 3DCRT for LAPC. *Advances in radiation oncology*. 2017;2(3):403-15.
5. Crane CH. Hypofractionated ablative radiotherapy for locally advanced pancreatic cancer. *Journal of radiation research*. 2016;57 Suppl 1:i53-i7.
6. Koay EJ, Hanania AN, Hall WA, Taniguchi CM, Rebueno N, Myrehaug S, et al. Dose-Escalated Radiation Therapy for Pancreatic Cancer: A Simultaneous Integrated Boost Approach. *Practical radiation oncology*. 2020.
7. Versteijne E, Suker M, Groothuis K, Akkermans-Vogelaar JM, Besselink MG, Bonsing BA, et al. Preoperative Chemoradiotherapy Versus Immediate Surgery for Resectable and Borderline Resectable Pancreatic Cancer: Results of

- the Dutch Randomized Phase III PREOPANC Trial. *Journal of clinical oncology : official journal of the American Society of Clinical Oncology*. 2020;Jco1902274.
8. Eijck CHJV, Versteijne E, Suker M, Groothuis K, Besselink MGH, Busch ORC, et al. Preoperative chemoradiotherapy to improve overall survival in pancreatic cancer: Long-term results of the multicenter randomized phase III PREOPANC trial. *Journal of Clinical Oncology*. 2021;39(15_suppl):4016-.
 9. Prior PW, Chen X, Hall WA, Erickson BA, Li A. Estimation of the Alpha-beta Ratio for Chemoradiation of Locally Advanced Pancreatic Cancer. *Int J Radiat Oncol Biol Phys*. 2018;102(3):S97-S.
 10. Mukherjee S, Hurt CN, Bridgewater J, Falk S, Cummins S, Wasan H, et al. Gemcitabine-based or capecitabine-based chemoradiotherapy for locally advanced pancreatic cancer (SCALOP): a multicentre, randomised, phase 2 trial. *The Lancet Oncology*. 2013;14(4):317-26.
 11. Zhu X, Ju X, Cao Y, Shen Y, Cao F, Qing S, et al. Patterns of Local Failure After Stereotactic Body Radiation Therapy and Sequential Chemotherapy as Initial Treatment for Pancreatic Cancer: Implications of Target Volume Design. *International journal of radiation oncology, biology, physics*. 2019;104(1):101-10.
 12. Kharofa J, Mierzwa M, Olowokure O, Sussman J, Latif T, Gupta A, et al. Pattern of Marginal Local Failure in a Phase II Trial of Neoadjuvant Chemotherapy and Stereotactic Body Radiation Therapy for Resectable and Borderline Resectable Pancreas Cancer. *American journal of clinical oncology*. 2019;42(3):247-52.
 13. Schorn S, Demir IE, Haller B, Scheufele F, Reyes CM, Tieftrunk E, et al. The influence of neural invasion on survival and tumor recurrence in pancreatic ductal adenocarcinoma - A systematic review and meta-analysis. *Surgical oncology*. 2017;26(1):105-15.
 14. Goto Y, Nakamura A, Ashida R, Sakanaka K, Itasaka S, Shibuya K, et al. Clinical evaluation of intensity-modulated radiotherapy for locally advanced pancreatic cancer. *Radiation oncology (London, England)*. 2018;13(1):118.
 15. Peulen H, Belderbos J, Rossi M, Sonke JJ. Mid-ventilation based PTV margins in Stereotactic Body Radiotherapy (SBRT): a clinical evaluation. *Radiotherapy and oncology : journal of the European Society for Therapeutic Radiology and Oncology*. 2014;110(3):511-6.
 16. Lens E, van der Horst A, Versteijne E, van Tienhoven G, Bel A. Dosimetric Advantages of Midventilation Compared With Internal Target Volume for Radiation Therapy of Pancreatic Cancer. *International journal of radiation oncology, biology, physics*. 2015;92(3):675-82.
 17. Velec M, Moseley JL, Dawson LA, Brock KK. Dose escalated liver stereotactic body radiation therapy at the mean respiratory position. *International journal of radiation oncology, biology, physics*. 2014;89(5):1121-8.
 18. Wolthaus JW, Sonke JJ, van Herk M, Damen EM. Reconstruction of a time-averaged midposition CT scan for radiotherapy planning of lung cancer patients using deformable registration. *Medical physics*. 2008;35(9):3998-4011.
 19. Hall WA, Heerkens HD, Paulson ES, Meijer GJ, Kotte AN, Knechtges P, et al. Pancreatic gross tumor volume contouring on computed tomography (CT) compared with magnetic resonance imaging (MRI): Results of an international contouring conference. *Practical radiation oncology*. 2018;8(2):107-15.
 20. Shiinoki T, Shibuya K, Nakamura M, Nakamura A, Matsuo Y, Nakata M, et al. Interfractional reproducibility in pancreatic position based on four-dimensional computed tomography. *International journal of radiation oncology, biology, physics*. 2011;80(5):1567-72.

21. Goldstein SD, Ford EC, Duhon M, McNutt T, Wong J, Herman JM. Use of respiratory-correlated four-dimensional computed tomography to determine acceptable treatment margins for locally advanced pancreatic adenocarcinoma. *International journal of radiation oncology, biology, physics*. 2010;76(2):597-602.
22. Hallman JL, Mori S, Sharp GC, Lu HM, Hong TS, Chen GT. A four-dimensional computed tomography analysis of multiorgan abdominal motion. *International journal of radiation oncology, biology, physics*. 2012;83(1):435-41.
23. Cattaneo GM, Passoni P, Sangalli G, Slim N, Longobardi B, Mancosu P, et al. Internal target volume defined by contrast-enhanced 4D-CT scan in unresectable pancreatic tumour: evaluation and reproducibility. *Radiotherapy and oncology : journal of the European Society for Therapeutic Radiology and Oncology*. 2010;97(3):525-9.
24. Minn AY, Schellenberg D, Maxim P, Suh Y, McKenna S, Cox B, et al. Pancreatic tumor motion on a single planning 4D-CT does not correlate with intrafraction tumor motion during treatment. *American journal of clinical oncology*. 2009;32(4):364-8.
25. van Herk M, Remeijer P, Rasch C, Lebesque JV. The probability of correct target dosage: dose-population histograms for deriving treatment margins in radiotherapy. *International journal of radiation oncology, biology, physics*. 2000;47(4):1121-35.
26. Strauss VY, Shaw R, Virdee PS, Hurt CN, Ward E, Tranter B, et al. Study protocol: a multi-centre randomised study of induction chemotherapy followed by capecitabine \pm nelfinavir with high- or standard-dose radiotherapy for locally advanced pancreatic cancer (SCALOP-2). *BMC cancer*. 2019;19(1):121.
27. Bertholet J, Hunt A, Dunlop A, Bird T, Mitchell RA, Oelfke U, et al. Comparison of the dose escalation potential for two hypofractionated radiotherapy regimens for locally advanced pancreatic cancer. *Clinical and translational radiation oncology*. 2019;16:21-7.

Chapter 8

Conclusions

Chapter 8 Summary, conclusions and future directions

Magnetic resonance guided radiotherapy has many postulated benefits over conventional radiotherapy treatment techniques. Its improved soft tissue definition, lack of imaging related ionising radiation and the ability to perform online adaptive replanning offers the potential for greater treatment accuracy and the possibility of dose escalation with minimal toxicity. However, safe and effective delivery of MRgRT is not without its challenges.

Within this thesis I have developed and examined different aspects of the MRgRT pathway in relation to the treatment of muscle invasive bladder and locally advanced pancreatic cancer. Within this chapter I summarise my findings and discuss future research opportunities.

8.1 MRI based inter-observer contouring variability in bladder cancer radiotherapy and consensus guidance generation

The degree of inter-observer MRI based contouring variability within 31 members of the bladder cancer radiotherapy community has been explored. Pre guidance generation the greatest variation was seen in the GTV structure (median DCE 0.68). CTV and bladder wall variability was minimal, with a median DCE of 0.95. Education and guidance generation were subsequently shown to reduce GTV variability, the study's primary endpoint. However, an analysis of simulated target coverage has shown that GTV contour variation can lead to gold standard target underdosing and extra dose to non-target tissue. Interobserver contouring variation should therefore be considered when deciding on treatment margins.

A consensus guideline has been developed for contouring using MRI with input from 26 clinicians. This guideline will now be published with the hope that it can become an educational resource for the bladder cancer radiotherapy community.

The work discussed in Chapter 1 is important as clinician contouring is considered the 'weak link' within the radiotherapy pathway (1). As technical advances allow for ever more conformal and precise treatment, accurate

definition of target structures becomes more important. It is reassuring that interobserver variability of the whole bladder CTV is minimal and that education can help to improve contouring of the more poorly performing GTV structure. However, acknowledgement and awareness of remaining inter-observer variability is important. This is particularly true if dose escalation to a boost region is considered or in the context of treatment margin reduction. Dose escalation to a poorly defined target could result in excess toxicity whilst treatment margins which fail to account for contouring error could lead to target miss. My work so far has not identified the exact margin needed to account for current levels of variation. However, it has highlighted that, particularly in the case of the GTV structure, variation is a potential concern. Future work could explore this further.

When using a 2-dose level treatment technique, different margins may be required to ensure optimal coverage of the boost (GTV) target versus the remaining bladder. For example, it might be possible to use a smaller margin to cover the whole bladder CTV structure where variation is minimal, whilst using a larger margin to cover the boost region. The data set acquired during my thesis could be used for this analysis.

This chapter focused on contouring variability using MRI. A direct comparison between MRI and CT contour variability was not performed. Future work could explore whether there is a difference in the variation seen. It is hypothesised that MRgRT can improve radiotherapy treatment due to improved soft tissue definition and the use of online adaptive replanning. CT guided online adaptive replanning is now also available, for example through use of the Varian Ethos (Varian, Palo Alto, CA) which uses integrated iterative CBCT for online adaptive replanning. Given the limited number of MR Linacs in the UK, deciding which groups of patients would benefit most from this limited resource is important. If bladder contouring variation can be shown to be reduced when using MRgRT versus CT guided treatment, then this would favour the use of MRgRT for this patient group at least until direct treatment related outcome comparisons can be made.

Finally, this chapter has highlighted the role of education in improving contouring variability. I hope that when published the guidance generated through this work

will be useful to all clinicians treating bladder cancer whether or not they have access to an MR Linac. MRI is increasingly being used in the bladder cancer diagnostic pathway and has been shown to improve staging accuracy compared to CT and TURBT (2-4). Interpretation of MRI is therefore a valuable skill for all those involved in bladder radiotherapy contouring.

8.2 Workflow development for the treatment of bladder cancer on the Elekta Unity.

In order to treat bladder cancer patients on the Elekta Unity new radiotherapy workflows were required. Suitable intra-fraction treatment margins covering the anticipated time of an MRgRT fraction were needed along with a strategy for online recontouring of OARs. In Chapter 3 I describe my work on this subject. I have shown that an anisotropic CTV to PTV margin of 1.5cm superiorly and anteriorly, 1cm posteriorly and 0.5cm inferiorly and laterally can encompass >90% of intra-fraction bladder (target) change over 30 minutes. A smaller, 0.5cm isotropic margin encompassed only 68% of intra-fractional excursions over this time period. I have shown that bladder filling correlates with intra-fractional target position change and can be used to predict inadequate coverage by a 0.5cm isotropic margin. These findings have directly influenced my centre's choice of treatment margin when using MRgRT for bladder cancer patients.

I have evaluated differing re-contouring strategies for key organs at risk showing that it is not necessary to contour OARS in their entirety in order to ensure sufficient target coverage whilst still maintaining OAR dose constraints. This work has influenced our current re-contouring strategy within our hypofractionated workflow.

Moving forward, future work in this area will involve personalisation of treatment margins to the individual concerned. I have set up an imaging protocol for bladder cancer patients undergoing treatment on the MRL to track the anatomy pre-treatment (day 0) and on an intra- and inter- fractional basis. I hope that these datasets can then be used to look at predictors of inter- and intra-fractional target position change. For example, does tumour position effect the degree and direction of bladder filling or position change? Is this effect consistent across a

treatment course? Can this be used to predict the most appropriate intra-fraction treatment margin for that individual prior to treatment? Individualisation of treatment margins in this way would allow for greater treatment conformity and less normal tissue in the high dose region. This could reduce the risk of treatment related toxicity especially when considering dose escalation in patients with large volumes of bowel in the pelvis. Equally, identification of factors which predict for large day-to-day variations in target size and position would be useful in predicting which patients have most to gain from an adaptive versus a standard plan of the day workflow. As technology develops and dose tracking (5) becomes an option further personalisation will be possible however, this technology is some way off at present.

8.3 Feasibility of Magnetic Resonance Guided Radiotherapy for the Treatment of Muscle-Invasive Bladder Cancer.

In a world first, I have demonstrated that MRgRT to the bladder is clinically feasible on the Elekta Unity. A full online adaptive workflow was delivered in a timely manner with maintained target coverage and acceptable patient tolerance. These findings will now be confirmed in a larger cohort of patients including those eligible for 55Gy in 20 fractions with concurrent chemotherapy. Collaboration with other members of the MR Linac consortium is ongoing to ensure findings are reproducible across centres. There are also plans to begin treatment using a 2-dose level technique with a boost to the tumour or tumour bed (60Gy/20#), and a lower dose to the remaining bladder (46Gy/20#). This will require delineation of a GTV or tumour bed boost region. The consensus guidance developed in Chapter 2 will provide guidance on how this should be delineated minimising the impact of inter-observer variability and ensuring contouring consistency across different treating sites.

Based on a comparison between treatment conformity for my patient cohort versus a similar patient cohort enrolled in the Hybrid bladder study (treated using a C-arm linear accelerator and a library of plans technique), it appears that use of MRgRT improves treatment conformity. Whether this improves outcomes for patients is yet to be seen. We are prospectively collecting survival and toxicity data in all patients treated on the MRL so although a direct head-to-head trial has

not yet been performed this information will provide some insight into the potential benefit of MRgRT to this patient group.

Understanding which bladder cancer patients might benefit most from MRgRT is an important consideration. As discussed in Chapter 4, we elected to treat patients suitable for 36Gy/6# in our first cohort for pragmatic reasons not because we thought this patient group was likely to benefit most from this new style of treatment. In fact, therapeutic gains are most likely to be found in those suitable for radical radiotherapy given the greater non cancer related life expectancy and therefore the greater impact of treatment failure (especially if salvage cystectomy is not an option). It is in this group that the benefits of dose escalation are currently being explored within the RAIDER trial (6) and moving forward, it is this group which will become our team's primary focus.

Efforts to improve patient outcomes will concentrate on the unique selling points of MRgRT such as improved treatment accuracy (allowing safer dose escalation) and the use of functional imaging to guide treatment planning. For example, use of real-time imaging during the beam on period will enable greater understanding of intra-fractional target position changes. Advances in real time dose tracking will enable further personalisation of treatment margins and a greater understanding of the true delivered dose. The use of online diffusion weighted imaging (DWI) to facilitate boost volume delineation as well as predicting response to radiotherapy will be examined. Quantitative DWI analysis using images from diagnostic scanners has shown promise in providing a non-invasive assessment of bladder radiotherapy response (7) but due to difference in imaging protocols separate validation would be needed for online sequences acquired on the MRL. If successfully validated, this information could be used to help stratify patients into relapse risk defined follow up groups, potentially sparing low risk patients unnecessary cystoscopies whilst ensuring those with evidence of poor response are offered quick access to surgical salvage if appropriate. Use of DWI may also allow for more accurate definition of potentially radioresistant areas of tumour which can then be boosted more effectively. Incorporation of DWI information into online recontouring and plan adaption could therefore further personalise treatment plans, potentially reducing the risk of treatment failure.

It is likely that not all patients will benefit equally from dose escalation or require treatment on an MRL in order to achieve their best radiotherapy related outcome. Based on the results of the BC2001 and BCON trial meta-analysis (8) local control rates using standard, non dose escalated radiotherapy techniques are in the region of 72% at 5 years. Rates of 5 year late rectal toxicity (grade 3-4) are in the region of 3-7%. Identifying those patients who are likely to experience local failure or significant toxicity using standard techniques (and therefore are most likely to benefit from dose escalation or greater treatment accuracy) is an important challenge. Factors known to predict local regional recurrence include age, tumour stage and the use of radiosensitization (8). However, there are likely other factors at play such as genetic and molecular differences within cancers which are predictive of treatment response. Although there are currently no predictive biological biomarkers for bladder radiotherapy response in clinical use, a number of potential candidates have been identified and are awaiting validation (9). If validated, biomarkers such as these could be used to help triage patients towards the most appropriate treatment strategy and platform for their cancer.

In the future, novel imaging biomarkers beyond DWI, may also prove useful in improving our ability to select patients most likely to benefit from MRgRT and dose escalation. As discussed in the introduction, sequences such as BOLD and TOLD which quantify tumour hypoxia might prove useful in identifying areas to boost within a tumour or they may help to select patients most likely to benefit from hypoxia modification for example in the form of carbogen radiosensitization. The MRL is well placed research tool to help in the development of new imaging biomarkers as it will be possible to closely correlate anatomical, functional and delivered dose data. This will be discussed in more detail later.

With respect to toxicity, there is a known dose-volume relationship for late rectal toxicity particularly at higher doses (10). Strategies which can reduce rectal doses especially to those with challenging anatomy may help to reduce longer term toxicity. Although current dose constraints take into account the known dose volume relationship, in standard radiotherapy techniques, plan approval is based on the anatomy at the time of planning and does not take into account inter- or intra- fraction variation in OARs. Therefore, the true delivered dose to OARs may

be significantly higher than planned. Identifying patients whose anatomy is most likely to cause failure of OAR constraints based on true delivered dose prior to commencing treatment may allow those patients to be directed towards MRgRT and adaptive replanning with a potential improvement in long term toxicity rates. This will require additional understanding of the degree of inter- and intra- fraction rectal motion seen in the bladder cancer community and whether there are any predictive factors which can be used to select out those patients where this change is likely to result in long term toxicity. Similarly, when considering late bladder toxicity, greater confidence in the position of the tumour versus normal bladder wall may allow for lower total doses to the uninvolved bladder when using a 2-dose level technique. Again, identification of factors which predict for greater variability in bladder position prior to treatment should help to triage patients towards the most appropriate treatment platform.

8.4 MRI sequence optimisation for pancreatic MR guided radiotherapy.

In Chapter 5 I discussed the development of MRI sequences for use within the locally advanced pancreatic cancer radiotherapy pathway. I have assessed their suitability for inclusion in both the offline and online components of our workflow and made recommendations for sequences which can be taken forward into clinical use. This work is an important first step in the development of an MRgRT workflow as without suitable sequences for online recontouring and replanning, online adaptive radiotherapy for pancreatic cancer will not be possible on the Elekta Unity. Future work in this area will involve integration of these sequences into pilot clinical workflows along with an assessment of contouring variability on the 3DVane sequences. There is also an ongoing dialogue with Elekta regarding the delivery of timely and high-quality sequence upgrades to ensure sequence quality continues to improve and that any updates fall within the CE marking of the treatment machine. Compared to CBCT, the imaging sequences developed thus far have improved image clarity. This highlights the benefit of pursuing MR guided online adaptive techniques compared to CBCT based alternatives for this patient group.

Since completing my research time, my centre has begun to examine how 4D MRI sequences reconstructed from the 3DVane sequence might be used to assess target and organ motion prior to each fraction. Currently, our workflow uses motion information gained from a single 4DCT at the time of planning to individualise treatment margins. However, this represents motion from a single breathing cycle and does not necessarily correlate with the motion seen during a course of treatment (11). By taking a 3DVane just prior to treatment (which averages motion over a few breathing cycles) and using this information to decide on the margins for that day correlation with the motion seen during treatment should be improved. Use of the 3DVane in this way will require improvements in current computing technology, but it is hoped that these advances are not too far away. In the longer term, gated or tracked treatments will hopefully become a reality on Elekta Unity. Gating is currently used on the ViewRay MRIdian allowing dose delivery only when the target is within a predefined treatment window. Tracked treatments are not yet available on either platform but CT based planning studies have shown the potential dosimetric gains of this technique in the context of pancreatic cancer (12). Use of these advanced motion management techniques combined with adaptive replanning, should enable even greater scope for dose escalation particularly for those patients with the most challenging anatomy.

As with bladder cancer, the role of functional imaging in optimising radiotherapy for locally advanced pancreatic cancer patients should be explored. Despite showing promise as a predictor of chemotherapy response (13), so far DWI has failed to show efficacy in radiotherapy response assessment for pancreatic cancer. However, studies conducted to date have been small and larger studies are warranted (14).

The use of radiomics to interrogate images acquired on MRLs is also an area of interest particularly in the context of pancreatic cancer (15, 16). Radiomics is an auto- or semi-automated quantitative image analysis technique where perceptible and imperceptible information is extracted from radiographic images using mathematical analysis (17). This analysis has the potential to identify patterns or 'textures' within images that can monitor or predict response to treatment. Pilot

studies from imaging acquired on the ViewRay MRIdian platform have highlighted the feasibility of this approach in predicting response to stereotactic radiotherapy in locally advanced pancreatic cancer (15) . Larger studies are needed including those using images acquired on the Elekta Unity. If found to be successful, this technique could then provide a valuable tool in identifying predictors of response or prognosis which can drive treatment decisions. For example, in the case of LAPC patients, imaging response predictors may help to identify those patients most likely to achieve R0 surgical resection post radiotherapy, with the improved survival outcomes this is associated with.

8.5 Investigation into the use of abdominal compression in pancreatic MR guided radiotherapy

In Chapter 6, I discuss the integration of abdominal compression into the pancreatic MRgRT workflow. In order to safely deliver dose escalated treatment to the pancreas, strategies to mitigate against the impact of respiratory motion must be deployed. Without access to advanced motion management techniques such as gating or tracking, other methods of motion reduction are needed. I demonstrate that abdominal compression is tolerated by volunteers and causes a statistically significant reduction in intra-abdominal motion without detriment to image clarity.

Due to restrictions in place as a result of COVID, it was not possible to validate this work in a patient cohort during my research period. However, this work is now taking place. The plan therefore remains to incorporate abdominal compression into our clinical workflow. This should allow us to use smaller treatment margins sparing dose to organs at risk.

8.6 Pancreatic cancer MRgRT treatment protocol

Chapter 7 focusses on the development of a non-dose escalated 15 fraction MRgRT protocol which utilises a mid-ventilation planning solution.

This protocol is designed to be the first step in our department's ultimate goal of delivering dose escalated MRgRT for patients with locally advanced pancreatic cancer. It was necessary to develop such a protocol as at the start of my research

period we did not have a 15 fraction protocol at my institution and internationally there was no Elekta Unity specific protocol in existence. Due to workforce and platform related constraints, treatment using our existing 30 fraction regimen was not an option.

I do not envisage this protocol being used in the long term instead I see its use as a way to build experience and confidence in the delivery of MRgRT to locally advanced pancreatic cancer patients whilst minimising the risk of unexpected toxicity. Once this experience has been gained, I envisage a move initially to 5 fraction SBRT (given its shorter treatment time and emerging evidence of superiority over CRT (18)) and then to dose escalated treatments in either 5 or 15 fractions. Delivery of dose escalated treatments will likely require the use of gated treatment delivery, technology that will hopefully be shortly available on the Elekta Unity.

Once MR-guided treatment is technically feasible, focus should shift to demonstrating whether this treatment is superior to current standards of care. Data on the use of MR-guided treatment for pancreatic cancer currently comes from retrospective series predominantly from centres using the ViewRay MRIdian. A systematic review by Hall et al (19) found just 3 studies published post 2014 with 20 patients or more. All were retrospective series using doses varying between 30-67.5Gy in 5-28 fractions. MR guided radiotherapy was shown to be technically feasible, to be well tolerated and give good rates of local control. Rudra et al (20), reported on the outcomes of 44 patients receiving a variety of doses. They found that those receiving a higher dose ($BED_{10} > 70\text{Gy}$), had an improved OS compared to those receiving lower doses without any increase in toxicity. Chuong et al (21) using doses between 35-50Gy in 5 fractions demonstrated 1 year local control rates of 87.8%, however, median OS was 9.8 months (from the time of RT completion not diagnosis) which is not a significant improvement compared to non MR-guided SBRT pancreatic series. Similarly, Hassanzadeh et al (22) reported on the outcomes of 44 patients receiving dose escalated 50Gy in 5 fractions. Again, excellent local control was seen (84.3% at one year) but this failed to translate into an improvement in OS (median OS 15.7 months from diagnosis) compared to historical non dose escalated and non-MR-

guided SBRT series. It is hoped that prospective trials such as the currently recruiting Phase II SMART trial which aims to deliver dose escalated treatment (50Gy/5#) to patients with LAPC (NCT03621644), will help to build the argument for dose escalation and MRgRT in LAPC and provide a platform for future randomised studies comparing MR versus CT guided treatments.

Although the hope is that dose escalation will lead to an overall survival benefit across the board, it is likely that the gains from dose escalation and MRgRT will not be uniform across the LAPC patient cohort, and the challenge will be identifying those patients who are most likely to benefit. For example, whilst the majority of LAPC patients die from distant metastatic progression and potentially harbour micrometastatic disease at the time of diagnosis, one third will die from predominantly local disease (23). It is this cohort who potentially have the most to gain from improvements in local control through the use of dose escalation. As there appears to be a dose response curve favouring higher doses (24), the radiotherapy platform that can deliver the highest dose (without excessive toxicity) is potentially the best platform for that patient. Given the advantages in terms of online image quality compared to CBCT and the potential this allows for greater accuracy in dose delivery, it would follow that the best platform would therefore be one which utilises MR guidance. However, identifying this group at the time of diagnosis remains a challenge. Currently, given the high rates of occult metastasis, patients with LAPC are generally given upfront chemotherapy in the first instance followed by radiotherapy if their disease remains localised. This 'trial of biology' allows those with poorly responding occult disease to declare themselves prior to undergoing radiotherapy. However, despite this approach, the majority will still go on to develop metastatic disease in a relatively short timeframe. Genomic analysis of pancreatic cancer samples has highlighted potential markers of poor prognosis such as loss of expression of SMAD4 (25) but no definitive biomarkers for local disease failure have so far been identified. Further genomic analysis work is ongoing with umbrella studies such as the Precision Panc platform (NCT04161417) working towards personalisation of treatment based on genomic analysis of individual patients and their tumours. In the future, this work could be complemented by radionomic information from patients undergoing treatment on the MRL allowing the development of novel

prognostic and predictive biomarkers. These biomarkers could then be used to help tailor treatment to an individual patient. For example, a biomarker which predicts a good response to radiotherapy could be used to triage patients towards radiotherapy platforms which allow dose escalation even if this means the patient travelling further to receive treatment. In contrast, those less likely to respond or where dose escalation has not been showed to be beneficial would benefit more from optimisation of their systemic therapy or if radiotherapy was deemed appropriate more standard doses delivered at their local and therefore more convenient centre.

8.7 The future of MRgRT

MRgRT is a new technology which holds promise in improving patient outcomes through greater accuracy and personalisation of radiotherapy treatment. So far in this Chapter I have discussed how my work has contributed to workflow development and treatment feasibility studies in relation to MIBC and LAPC patients. Relevant future research questions for these two tumour sites have been discussed. However, it is important to also consider where MRgRT sits within the broader context of radiotherapy as a whole.

Given the finite nature of healthcare budgets and resources, ensuring that the most cost-effective treatment is offered is important. MRgRT is expensive and resource intensive. In a US study looking at hepatocellular carcinoma SBRT, delivery of an MRgRT treatment course was found to be 18% more expensive than a comparable CT guided treatment (26). A review of prostate cancer SBRT showed a 5 fraction course of MRgRT to be almost \$1500 more expensive than an equivalent CT guided course (27). However, increased expense can be justified if MRgRT results in improvements in patient outcomes. It is therefore important that prospective and ideally randomised studies comparing CT and MR guided treatments are conducted.

In the UK, cost, space and resource implications mean that it is unlikely there will ever be sufficient capacity for all radiotherapy patients to undergo their treatment on an MR Linac. To ensure equitable delivery of treatment, it will therefore be necessary to understand which patient groups should be prioritised for treatment

on this versus other radiotherapy platforms. Priority should be given to those cancers where the MR Linac can offer significant gains in patient outcomes over and above that which can be achieved on other treatment platforms. Consideration should also be given to the effectiveness of other non-radiotherapy based treatment options for that tumour type. Cancers of the upper abdomen, and in particular the pancreas, are strong contenders to benefit the most from online MR-guide adaptive techniques given their close proximity to dose sensitive organs at risk, their poor visualisation on CBCT imaging and their (and nearby OARs) unpredictable inter and intra-fraction motion. The poor prognosis of pancreatic cancer and its projected increasing impact on the population's health over the next few years (28) also means that this is a cancer in need of new and more effective treatment options. However, this potential benefit should not be assumed, and studies should be conducted which confirm this hypothesis.

Although it may not be possible (or beneficial) to treat all patients on an MRL, research using the MRL could still benefit the wider cancer population. MRLs are well placed to lead in the development of prognostic and predictive imaging biomarkers. Each patient treated on an MRL will have numerous scans during their treatment period. These scans will be in the treatment position with a close temporal relationship to the delivered dose. If these scans and their linked patient characteristic, dose, and outcome data can then be safely archived together this opens up the possibility of 'big data' radionomic analysis. Given the inherent downtime in the online workflow, MRgRT also provides an excellent opportunity to develop new functional imaging sequences, as new sequences can be trialled without the need for the patient to spend additional time in hospital. These new sequences and the findings from radionomic analysis could offer insight into the behaviour of cancers more broadly or offer cancer specific information which can then be translated into prognostic, predictive or therapeutic interventions for the cancer population as a whole not just those who have treatment on an MRL. For patients treated on an Elekta Unity, the MOMENTUM Study aims to provide such a platform for data collection, storage and analysis (29). This study is an international registry open to all patients treated on an Elekta Unity at select hospitals (members of the initial MR-linac Consortium). Those patients that consent will have their clinical, technical and outcome data pseudonymized and

stored in an international registry which can be accessed by researchers according to data access rules. It is hoped that this registry, which has over 70000 MRI scans and 25000 plans uploaded to date, will provide a valuable resource in the drive to improve tumour control, survival and quality of life for all patients with cancer.

8.8 Conclusion

MRgRT is entering an exciting new era as we move from theoretical discussions around treatment delivery into actual delivered treatments. There is however, still much to understand and ongoing work is needed to realise the full potential of this new technology. Key to this is developing an understanding as to which patient groups are most likely to benefit from MRgRT compared to other radiotherapy treatment techniques and how to best utilise the 'big data' potential of the vast numbers of MRI scans which will be obtained during the course of patients' treatments. The hope is that this new technology will enable the development of ever more personalized radiotherapy treatments culminating in significant improvements in patient outcomes.

8.9 References

1. Roques TW. Patient selection and radiotherapy volume definition - can we improve the weakest links in the treatment chain? *Clinical oncology (Royal College of Radiologists (Great Britain))*. 2014;26(6):353-5.
2. Woo S, Suh CH, Kim SY, Cho JY, Kim SH. Diagnostic performance of MRI for prediction of muscle-invasiveness of bladder cancer: A systematic review and meta-analysis. *European journal of radiology*. 2017;95:46-55.
3. Gandhi N, Krishna S, Booth CM, Breau RH, Flood TA, Morgan SC, et al. Diagnostic accuracy of magnetic resonance imaging for tumour staging of bladder cancer: systematic review and meta-analysis. *BJU international*. 2018;122(5):744-53.
4. Huang L, Kong Q, Liu Z, Wang J, Kang Z, Zhu Y. The Diagnostic Value of MR Imaging in Differentiating T Staging of Bladder Cancer: A Meta-Analysis. *Radiology*. 2018;286(2):502-11.
5. Hunt A, Hansen VN, Oelfke U, Nill S, Hafeez S. Adaptive Radiotherapy Enabled by MRI Guidance. *Clinical oncology (Royal College of Radiologists (Great Britain))*. 2018;30(11):711-9.
6. Hafeez S, Webster A, Hansen VN, McNair HA, Warren-Oseni K, Patel E, et al. Protocol for tumour-focused dose-escalated adaptive radiotherapy for the radical treatment of bladder cancer in a multicentre phase II randomised controlled trial (RAIDER): radiotherapy planning and delivery guidance. *BMJ open*. 2020;10(12):e041005.

7. Hafeez S, Koh M, Jones K, El Ghzal A, D'Arcy J, Kumar P, et al. Assessing Bladder Radiotherapy Response With Quantitative Diffusion-Weighted Magnetic Resonance Imaging Analysis. *Clinical oncology (Royal College of Radiologists (Great Britain))*. 2022.
8. Choudhury A, Porta N, Hall E, Song YP, Owen R, MacKay R, et al. Hypofractionated radiotherapy in locally advanced bladder cancer: an individual patient data meta-analysis of the BC2001 and BCON trials. *The Lancet Oncology*. 2021;22(2):246-55.
9. Song YP, McWilliam A, Hoskin PJ, Choudhury A. Organ preservation in bladder cancer: an opportunity for truly personalized treatment. *Nature reviews Urology*. 2019;16(9):511-22.
10. Gulliford SL, Foo K, Morgan RC, Aird EG, Bidmead AM, Critchley H, et al. Dose-volume constraints to reduce rectal side effects from prostate radiotherapy: evidence from MRC RT01 Trial ISRCTN 47772397. *International journal of radiation oncology, biology, physics*. 2010;76(3):747-54.
11. Lens E, van der Horst A, Kroon PS, van Hooft JE, Davila Fajardo R, Fockens P, et al. Differences in respiratory-induced pancreatic tumor motion between 4D treatment planning CT and daily cone beam CT, measured using intratumoral fiducials. *Acta oncologica (Stockholm, Sweden)*. 2014;53(9):1257-64.
12. Karava K, Ehrbar S, Riesterer O, Roesch J, Glatz S, Klock S, et al. Potential dosimetric benefits of adaptive tumor tracking over the internal target volume concept for stereotactic body radiation therapy of pancreatic cancer. *Radiation oncology (London, England)*. 2017;12(1):175.
13. Qu C, Zeng PE, Wang HY, Yuan CH, Yuan HS, Xiu DR. Application of Magnetic Resonance Imaging in Neoadjuvant Treatment of Pancreatic Ductal Adenocarcinoma. *Journal of magnetic resonance imaging : JMRI*. 2022;55(6):1625-32.
14. Zimmermann C, Distler M, Jentsch C, Blum S, Folprecht G, Zöphel K, et al. Evaluation of response using FDG-PET/CT and diffusion weighted MRI after radiochemotherapy of pancreatic cancer: a non-randomized, monocentric phase II clinical trial-PaCa-DD-041 (Eudra-CT 2009-011968-11). *Strahlentherapie und Onkologie : Organ der Deutschen Röntgengesellschaft [et al]*. 2021;197(1):19-26.
15. Simpson G, Spieler B, Dogan N, Portelance L, Mellon EA, Kwon D, et al. Predictive value of 0.35 T magnetic resonance imaging radiomic features in stereotactic ablative body radiotherapy of pancreatic cancer: A pilot study. *Medical physics*. 2020;47(8):3682-90.
16. Tomaszewski MR, Latifi K, Boyer E, Palm RF, El Naqa I, Moros EG, et al. Delta radiomics analysis of Magnetic Resonance guided radiotherapy imaging data can enable treatment response prediction in pancreatic cancer. *Radiation oncology (London, England)*. 2021;16(1):237.
17. van Timmeren JE, Cester D, Tanadini-Lang S, Alkadhi H, Baessler B. Radiomics in medical imaging-"how-to" guide and critical reflection. *Insights into imaging*. 2020;11(1):91.
18. Tchelebi LT, Lehrer EJ, Trifiletti DM, Sharma NK, Gusani NJ, Crane CH, et al. Conventionally fractionated radiation therapy versus stereotactic body radiation therapy for locally advanced pancreatic cancer (CRiSP): An international systematic review and meta-analysis. *Cancer*. 2020;126(10):2120-31.

19. Hall WA, Small C, Paulson E, Koay EJ, Crane C, Intven M, et al. Magnetic Resonance Guided Radiation Therapy for Pancreatic Adenocarcinoma, Advantages, Challenges, Current Approaches, and Future Directions. *Frontiers in oncology*. 2021;11:628155.
20. Rudra S, Jiang N, Rosenberg SA, Olsen JR, Roach MC, Wan L, et al. Using adaptive magnetic resonance image-guided radiation therapy for treatment of inoperable pancreatic cancer. *Cancer medicine*. 2019;8(5):2123-32.
21. Chuong MD, Bryant J, Mittauer KE, Hall M, Kotecha R, Alvarez D, et al. Ablative 5-Fraction Stereotactic Magnetic Resonance-Guided Radiation Therapy With On-Table Adaptive Replanning and Elective Nodal Irradiation for Inoperable Pancreas Cancer. *Practical radiation oncology*. 2021;11(2):134-47.
22. Hassanzadeh C, Rudra S, Bommireddy A, Hawkins WG, Wang-Gillam A, Fields RC, et al. Ablative Five-Fraction Stereotactic Body Radiation Therapy for Inoperable Pancreatic Cancer Using Online MR-Guided Adaptation. *Advances in radiation oncology*. 2021;6(1):100506.
23. Iacobuzio-Donahue CA, Fu B, Yachida S, Luo M, Abe H, Henderson CM, et al. DPC4 gene status of the primary carcinoma correlates with patterns of failure in patients with pancreatic cancer. *Journal of clinical oncology : official journal of the American Society of Clinical Oncology*. 2009;27(11):1806-13.
24. Moraru IC, Tai A, Erickson B, Li XA. Radiation dose responses for chemoradiation therapy of pancreatic cancer: an analysis of compiled clinical data using biophysical models. *Practical radiation oncology*. 2014;4(1):13-9.
25. Shugang X, Hongfa Y, Jianpeng L, Xu Z, Jingqi F, Xiangxiang L, et al. Prognostic Value of SMAD4 in Pancreatic Cancer: A Meta-Analysis. *Translational oncology*. 2016;9(1):1-7.
26. Parikh NR, Lee PP, Raman SS, Cao M, Lamb J, Tyran M, et al. Time-Driven Activity-Based Costing Comparison of CT-Guided Versus MR-Guided SBRT. *JCO oncology practice*. 2020;16(11):e1378-e85.
27. Parikh NR, Clark MA, Patel P, Kafka-Peterson K, Zaide L, Ma TM, et al. Time-Driven Activity-Based Costing of CT-Guided vs MR-Guided Prostate SBRT. *Applied radiation oncology*. 2021;10(3):33-40.
28. Rahib L, Smith BD, Aizenberg R, Rosenzweig AB, Fleshman JM, Matrisian LM. Projecting cancer incidence and deaths to 2030: the unexpected burden of thyroid, liver, and pancreas cancers in the United States. *Cancer research*. 2014;74(11):2913-21.
29. de Mol van Otterloo SR, Christodouleas JP, Blezer ELA, Akhiat H, Brown K, Choudhury A, et al. The MOMENTUM Study: An International Registry for the Evidence-Based Introduction of MR-Guided Adaptive Therapy. *Frontiers in oncology*. 2020;10.

Appendix 2.1

Bladder Contouring Study

Participant information

Aim

The aim of this study is to develop a consensus on the use of MR in the contouring of bladder cancers. The study will take place in several stages. This information sheet pertains to the first stage of the study which aims to assess current levels of interobserver variability with respect to tumour GTV and CTV and bladder wall. Subsequent stages will involve a consensus meeting and discussion, followed by a further contouring study to establish the impact of the new guidance created at the consensus meeting. It is hoped that this work will provide an educational tool for the use of MR in bladder cancer radiotherapy and provide a consensus for outlining in future radiotherapy trials which use MR.

Method

This stage of the study aims to establish current outlining practice. It contains the following tasks:

1. Questionnaire related to your current practice
2. 3 MR based cases- to delineate the GTV and CTV and outer bladder wall
3. 1 CT based cases- to delineate the GTV and CTV

Instructions

Task 1

Please complete the attached experience questionnaire- please email this back to me at arabellahunt@icr.ac.uk

Task 2

There are 3 MR based GTV/CTV contours to complete (cases 1, 2 and 3)

Unless otherwise stated please contour your GTV and CTV on the **T2 SFOV transverse** sequence. You will be provided with a case vignette and additional sequences to aid your delineation. Please assume all patients are being treated radically.

Please contour the following structures:

GTV= visible tumour/tumour bed- **please ignore** any potentially positive lymph nodes, concentrate instead on the tumour related to the bladder itself. For MR cases contour on the T2 SFOV image set unless otherwise stated

CTV= as defined in the international RAIDER trial- GTV plus the whole bladder plus any areas of extravesical spread. If the tumour is at the base of the bladder or distant CIS was/is present, the CTV should include 1.5cm of the prostatic urethra in males or 1cm of the urethra in females. Ignore any lymph node disease. For MR cases contour on the T2 SFOV image set unless otherwise stated

Outer Bladder Wall= contour as you would the bladder as **an organ at risk**. Contour on the T1 dataset

In order to complete the tasks you will need to login into the Monaco Cloud system remotely. You should have been sent separate login information.

Once logged in, go to open patient, under Bladder you should find an account with your name on it. Open up each case as needed.

Please note you can open up different sequences at the same time to help aid your delineation- please do not try to fuse these images as the bladder filling changes will make this difficult. This will keep the contouring exercise consistent between participants.

Please ensure that when you are completing your contours the correct sequence is 'active' ie that any contour you create are being saved onto the correct image data set.

Case 1 (labelled as Case 1 on Monaco Treatment Planning System):

78 year old male. G3 T3 N0 (no CIS) TCC bladder. CT: abnormal thickening of the antero-superior aspect of the urinary bladder. Irregularity of the bladder surface anteriorly suggesting full thickness disease. MRI: Antero-superior disease extending over at least 60mm, no involvement of adjacent bowel loops. Cystoscopy: Thickening at the dome in keeping with mural mass. Slice thickness of T2 SFOV: 3mm.

Case 2 (labelled as Case 2 on Monaco Treatment Planning System):

82 year old female. G3 T3 N0 (No CIS) TCC bladder. CT: Tumour present at the right anterior lateral wall measuring approx. 20mm in ant/post diameter. MRI: thickening seen in the right anterior lateral bladder wall, up to 8mm in thickness extending over 4.5cm in transverse diameter on the coronal images. Cystoscopy: right sided tumour, patent ureteric orifices. Slice thickness of T2 SFOV: 4mm

Case 3 (labelled as case 4 in Monaco Treatment Planning System):

78 year old male. T3b N0 (with CIS) TCC bladder. Cystoscopy: multiple papillary tumours involving left lateral and anterior bladder wall. MRI: Left bladder wall shows area of restricted diffusion and intermediate T2 signal, tumour extends anteroposterior for at least 5cm and probably involves the left VUJ. Tumour extends towards the prostate but does not invade the capsule. **Contour GTV/CTV on T2 LFOV.** Slice thickness of T2 LFOV: 5mm

Task 3

Case 4 involves CT derived contours. Please outline the GTV and CTV, please contour on the axial CT slices. Patient vignettes are included to aid delineation.

Case 4 (labelled as case 12 on Monaco Treatment Planning System):

68 year old male, T2b/3N0M0, No CIS, TCC bladder, CT: involvement of anterior and left lateral aspect of bladder, minimal perivesical fat invasion difficult to rule out. Cystoscopy- large solid looking tumour on anterior and lateral wall, no involvement of ureteric orifices. CT slice thickness 2.5mm

Thank you for your time. Once you have completed your contours please let me know and I can arrange for them to be analysed.

In the meantime if you have any questions please do not hesitate to get in touch.

Dr. Arabella Hunt

Clinical Research Fellow to Professor Robert Huddart and Dr. Shaista Hafeez

The Institute of Cancer Research

arabella.hunt@icr.ac.uk

07786198863

Bladder Contouring Study- Post Consensus

Participant information

Aim

The aim of this study is to develop a consensus on the use of MR in the contouring of bladder cancers. Stage 1 (pre consensus contouring) is now complete. Stage 2 involved the creation of a consensus guidance which has been circulated to you. This is the 3rd and final stage of the study which is looking at the impact of the consensus guidance on interobserver contouring variation.

Method

This stage of the study consists of 3 MR based cases on which you need to delineate the GTV and CTV as per the guidance in the consensus guideline. **Please familiarise yourself with this guidance prior to undertaking the contouring and complete the Delphi guidance questionnaire.**

Instructions

There are 3 MR based GTV/CTV/ bladder wall contours to complete (cases 13, 14, 15.)

Unless otherwise stated please contour your GTV and CTV on the **T2 TSE TRA SFOV transverse** sequence (for **case 15** please contour on the **T2 TSE TRA LFOV sequence**). You will be provided with a case vignette and additional sequences to aid your delineation. Please assume all patients are being treated radically.

Please contour the following structures:

GTV= visible **tumour/tumour bed-** please ignore any potentially positive lymph nodes, concentrate instead on the tumour related to the bladder itself.

CTV= as defined in the international RAIDER trial- GTV plus the whole bladder plus any areas of extravesical spread. If the tumour is at the base of the bladder or distant CIS was/is present, the CTV should include 1.5cm of the prostatic urethra in males or 1cm of the urethra in females. Ignore any lymph node disease.

Outer Bladder Wall= contour as you would the bladder as **an organ at risk**

Case 13: 70 year old male. T3 (no CIS) TCC of the bladder. Cystoscopy shows large tumour at the anterior wall. MRI: large tumour with full thickness invasion of the anterior bladder wall, small bowel overlies this area but is not directly involved. **Contour on axial T2 TSE TRA SFOV**, slice thickness 4mm.

Case 14: 60 year old male. T3 (no CIS) TCC of the bladder. Cystoscopy shows a right sided lateral wall mass. MRI: right sided bladder wall lesion, with extravesical extension, reaching but not involving the right vesico-ureteric junction. No extension into the bladder base or prostate. **Contour on axial T2 TSE TRA SFOV**. Slice thickness 4mm.

Case 15

78 year old male. T3b N0 (with CIS) TCC bladder. Cystoscopy shows multiple papillary tumours involving left lateral and anterior bladder wall. MRI: Left bladder wall shows area of restricted diffusion and intermediate T2 signal, tumour extends anteroposterior for at least 5cm and probably involves the left VUJ. Tumour extends towards the prostate but does not invade the capsule. **Contour on T2 TSE TRA LFOV**. Slice thickness of T2 LFOV: 5mm

Thank you for your time, please feel free to email me if you have any questions.

Dr. Arabella Hunt

Clinical Research Fellow to Professor Robert Huddart and Dr. Shaista Hafeez

The Institute of Cancer Research

arabella.hunt@icr.ac.uk

Appendix 2.2

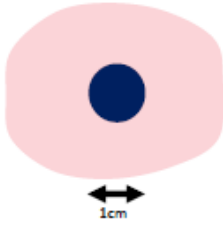
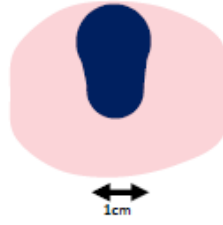
Contouring guidance for MR in bladder cancer radiotherapy

This draft guidance has been written to support target volume delineation on MR for bladder radiotherapy. It was developed following live, interactive web-based video conference discussions on the 30th January 2019.

Final agreed guidance will be developed using a Delphi survey and consensus conference approach amongst participants. Each structure item below will be scored by the reviewer as 1-3 (disagree), 4-6 (equivocal), 7-9 (agree) and 'unable to score'. Consensus will be defined as those items scored 'agree' (7-9) by $\geq 70\%$ of participants.

MR-based contouring guidance

Structure	Volume definition	MR interpretation (hints/pitfalls)
Gross tumour volume (GTV)	<ul style="list-style-type: none"> Prior to outlining, diagnostic images and surgical bladder map should be referred to where available in order to assist tumour localisation. All extravesical tumour and pathological bladder wall thickening due to cancer should be included in the GTV. Initial pre-treatment disease should be included in the GTV. If no tumour is visible (i.e. post transurethral resection of the bladder tumour, TURBT and, or following chemotherapy), the tumour bed is reconstructed at the appropriate bladder wall position using available diagnostic imaging, surgical bladder map, or fiducial markers. 	<ul style="list-style-type: none"> T2 weighted (T2W) imaging should be used for GTV delineation. On T2W imaging urine appears bright, normal detrusor muscle appears dark, and tumour has intermediate signal. T1 weighted (T1W) imaging should not be used for GTV delineation as distinguishing between GTV and normal bladder wall is difficult. Tumour and normal bladder wall both have intermediate signal. Tumour with high cellular density will appear as regions of low signal intensity with restricted diffusion on apparent diffusion coefficient (ADC) maps. Tumours can exhibit high signal intensity on diffusion weighted imaging (DWI). The signal intensity of background tissue is well suppressed. High b-value images produce better tumour to normal tissue contrast. Greater image distortion means it should not be used in isolation but in conjunction with T2W images. Some normal pelvic structures can demonstrate high signal intensity physiologically on DWI and should not be mistaken for tumour. This risk is minimised by using also using T2W images. Tumours show early enhancement on dynamic contrast-enhanced (DCE) image. Multiplanar views should be used for target delineation. Consideration should be paid to bladder tumour mimickers on MRI which include <ol style="list-style-type: none"> post TURBT inflammation or fibrosis on T2W or DCE image (distinguished from tumour using DWI) high cellularity associated with pyuria produces high signal intensity on DWI (distinguished from tumour by fluid level with normal urine and presence of high signal intensity on T2W image) clots can show high signal intensity on DWI and T1W prostatic inflammation causes high signal intensity on DWI and T2W image benign lesions and artefacts can show high signal intensity therefore DWI should be compared to T2W and DCE image where available

Clinical target volume (CTV)	<ul style="list-style-type: none"> This should encompass the entire tumour, (or tumour bed where appropriate), the whole bladder and any area of extravesical spread. If GTV is at the base of bladder or if distant CIS is present the CTV should also include 1.5cm of prostatic urethra in males or 1cm of urethra in females. The urethra is difficult to visualise without catheterisation <ol style="list-style-type: none"> In the male pelvis using a 1cm roller ball (diameter) begin at bladder neck extending the contouring caudally to the start of penile urethra so total length is 1.5cm. <p>If prostatic urethra is not visible within the prostate gland, central positioning of the roller ball within the prostate gland on axial slice is acceptable surrogate for true position (Figure 1a). Acceptable variation is extension of prostatic urethra volume anteriorly (Figure 1b).</p> <p>Figure 1. Acceptable variation of prostatic urethra contour (blue) on axial representation through prostate (pink).</p> <p>a.</p>  <p>b.</p>  <ol style="list-style-type: none"> In the female pelvis begin contouring using a 1cm roller ball at the internal urethral orifice extending the structure caudally to the perineum along the anterior wall of the vagina so total length is 1cm. 	<ul style="list-style-type: none"> T1W imaging may assist with normal outer bladder wall delineation. Normal bladder has intermediate signal intensity, and urine has low signal intensity (appears dark). On DCE normal bladder has late enhancement.
Rectum	<ul style="list-style-type: none"> The rectum is outlined to include the full circumference and rectal contents. Outlining should extend from the lowest level of ischial tuberosities to the recto-sigmoid junction. The recto-sigmoid junction will be defined by the most inferior of the following three landmarks <ol style="list-style-type: none"> the point at which the rectum loses its round shape in the axial plane and turns anteriorly into the sigmoid colon (often best appreciated on the sagittal image); the bifurcation of the inferior mesenteric artery into the sigmoid and superior rectal arteries; the S2/S3 junction. 	<ul style="list-style-type: none"> Susceptibility artefact from air in the rectum or colon may cause false positive by producing high signal intensity on DWI with no identifiable abnormality on T2W.

Appendix 2.3

Experience Questionnaire

Name:

Institution:

1. How many bladder cancer patients are treated with radiotherapy (radical/palliative) per year at your institution?
2. How many years of experience do you have in bladder radiotherapy?
3. What do you usually include in your GTV and CTV for a node negative patient being treated radically?
4. What is the current role of MRI in bladder cancer patients at your institution?
5. Would you be happy for your name to appear on paper documenting the results of this study?

Appendix 4.1

Study Name:_____ Study Number:_____ Date:-_____

Patient Experience Questionnaire; MRLinac (Unity) Radiotherapy treatment

Radiotherapy treatment delivered on the MR Linac (Unity) using Magnetic Resonance Imaging (MRI) is a new technology.

We would like to find out your views about having treatment on Unity. This may help us improve the experience for you and other patients.

We would be grateful if you would complete this questionnaire after your treatment and return it to us before you leave.

Please circle the response that best fits your experience

	0	1	2	3
	Not at all	Slightly	Moderately	Very
I needed more detailed information before my treatment	Not at all	Slightly	Moderately	Very
I found the treatment position comfortable	Not at all	Slightly	Moderately	Very
I found the treatment bed comfortable	Not at all	Slightly	Moderately	Very
I found it easy it to stay still and maintain the treatment position	Not at all	Slightly	Moderately	Very
I wanted to come out of the machine during my treatment	Not at all	Slightly	Moderately	Very
I felt calm during my treatment	Not at all	Slightly	Moderately	Very
I found the noise in the room easy to tolerate	Not at all	Slightly	Moderately	Very

I found the lighting in the room easy to tolerate	Not at all	Slightly	Moderately	Very
I found the time taken for the treatment easy to tolerate	Not at all	Slightly	Moderately	Very
I felt dizzy during my treatment	Not at all	Slightly	Moderately	Very
I felt dizzy immediately after my treatment	Not at all	Slightly	Moderately	Very
I felt hot during my treatment	Not at all	Slightly	Moderately	Very
I felt tingling sensations during my treatment	Not at all	Slightly	Moderately	Very
I experienced a metallic taste during my treatment	Not at all	Slightly	Moderately	Very
I needed more communication from staff during my treatment	Not at all	Slightly	Moderately	Very
I forced myself to manage the situation	Not at all	Slightly	Moderately	Very
I found listening to the music helpful whilst having my treatment	Not at all	Slightly	Moderately	Very
I understood the procedure	Not at all	Slightly	Moderately	Very
Comments:				

Appendix 5.1

Technical details of MRI sequence acquisition on the 1.5T Seimens Aera

Sequence name	TR (ms)	TE (ms)	Flip angle	Sequence plane	Voxel size (mm x mm)	Slice thickness (mm)	FOV (mm)	Number of Slices	Pixel bandwidth	2D vs 3D
T2W TSE coronal, multi BH	2800	82	150	Coronal	1.64x1.64	5	208x256	35	300	2D
T2W TSE triggered, SFOV	5076	76	134	Transverse	1.0x 1.0	3	256x256	30	200	2D
T2 Haste, 2 BH	1000	87	170	Transverse	1.18x1.18	5	320x260	42	490	2D
T1W VIBE pre and post contrast	6.69	2.39	10.0	Transverse	1.48x1.48	1.5	256x208	160	475	3D

Original diagnostic exam card TR= repetition time, TE= ECHO time, FOV= field of view, 2D= 2 dimensional, 3D = 3 dimensional, T2W= T2 weighted, TSE= turbo spin ECHO, BH= breath-hold, T1W= T1 weighted, VIBE volumetric interpolated breath-hold examination

Appendix 5.2

Technical details of the MRI sequences evaluated for use using visual graded analysis tool. TR= repetition time, TE= ECHO time, FOV= field of view, 2D= 2 dimensional, 3D = 3 dimensional, T2W= T2 weighted, BH= breath-hold, T1W= T1 weighted, Tra = transverse ¹ used for patient 1 and 2, ² used for patients 3-7. Voxel size and slice thickness are reconstructed values.

Sequence name	TR (ms)	TE (ms)	Flip angle	Sequence plane	Voxel size (mm x mm)	Slice thickness (mm)	FOV, RLxAPxFH (mm)	Number of Slices	Pixel bandwidth	2D vs 3D
T1 3D Tra	7.61	4.5	30	Transverse	0.94x 0.94	1	452x320x300	300	433	3D
T1 mDixon BH (water) ¹	7.18	0	15	Transverse	1.12 x 1.12	3	393x375x240	78	432	3D
T1 mDixon BH (water) ²	7.17	0	15	Transverse	1.12 x 1.12	2	393x375 x160	83	432	3D
3D Vane	3.48	1.34	40	Transverse	0.69x 0.69	1.5	500x500x200	133	866	3D

Technical details of Elekta provided sequences

Sequence name	TR (ms)	TE (ms)	Flip angle	Sequence plane	Voxel Size (mm x mm)	Slice thickness (mm)	FOV, RLxAPxFH (mm)	Number of slices	Pixel bandwidth	2D vs 3D
T1 3D Tra	7.61	4.5	30	Transverse	0.94x 0.94	1	452x320x300	300	433	3D
T2 3D Tra	2100	205	90	Transverse	0.56x 0.56	1.2	448x320x300	250	1221	3D
T2 3D Tra Navigated	2100	247	90	Transverse	0.72x 0.72	1.2	457x340x279	233	1154	3D

Appendix 6.1

PRIMER – Participant Experience Questionnaire

Participant Study Number: _____

Session number: _____ Date of Session: _____

PART ONE:

Please complete the following about TODAY's MR Linac Scan:

	Strongly agree	Agree a little	Neither agree nor disagree	Disagree a little	Strongly disagree
I was anxious about my scan before I had it done	<input type="checkbox"/>	<input type="checkbox"/>	<input type="checkbox"/>	<input type="checkbox"/>	<input type="checkbox"/>
I had no difficulties coping with the scan	<input type="checkbox"/>	<input type="checkbox"/>	<input type="checkbox"/>	<input type="checkbox"/>	<input type="checkbox"/>
I would not be worried about having more of these scans	<input type="checkbox"/>	<input type="checkbox"/>	<input type="checkbox"/>	<input type="checkbox"/>	<input type="checkbox"/>

If you did not like your scan today, please give the reason/s:

Did you experience any of the following during your MR Linac scan today:

Dizziness Yes ☐ No ☐

Discomfort Yes ☐ No ☐

If yes, please give details: _____

Tingling in hands/feet/face Yes ☐ No ☐

If yes, please give details: _____

P.T.O.

Sweating or Overheating Yes ☐ No ☐

If yes, please give details:

Nausea Yes ☐ No ☐

If you answered 'yes' to any of the above, have the feelings gone now that the scan is over?

Yes ☐ No ☐

PART TWO:

Please answer the following questions about any recent DIAGNOSTIC MR Scan you have had

Have you had a diagnostic MRI within the last two months?

Yes ☐ **Please complete the questions below**

No ☐ This questionnaire is now complete. Thank you for your time.

Please tick the appropriate box below (if yes answered above):

Compared to my diagnostic MRI, the MR Linac scan was:	Less Difficult	<input type="checkbox"/>
	No Different	<input type="checkbox"/>
	More Difficult	<input type="checkbox"/>
	Not Sure	<input type="checkbox"/>

This questionnaire is now complete. Thank you for your time.

Appendix 7.1

Results from literature search of 15 fraction pancreatic radiotherapy protocols

Author	Title	Main Focus	Methodology	Key Results
Small Jr et al 2007 DOI: 10.1200/JCO.2007.13.9014	Full-dose gemcitabine with concurrent radiation therapy in patients with nonmetastatic pancreatic cancer: A Multicentre Phase II trial	Phase II trial looking at the safety and efficacy of concurrent Gemcitabine with 36Gy/15# using 3D conformal radiotherapy	39 patients with non-metastatic pancreatic cancer, 16 resectable, 9 borderline resectable, 14 unresectable at time of enrolment Concurrent Gemcitabine dose: 1000mg/m ² D1, D8, D15 GTV= gross tumour + involved lymph nodes. CTV= GTV+5mm PTV= CTV +5mm 3D CRT planning, no IMRT allowed No specific dose constraints for liver, small bowel, colon Spinal cord no more than 104% dose Combined kidney D50% < 20Gy	Overall response rate 5.1% Disease control rate 84.6% 1 year OS 73% 25.6% G3/4 treatment related non-haematological toxicity
Passoni et al 2013 doi.org/10.1016/j.ijrobp.2013.09.012	Hypofractionated Image-Guided IMRT in Advanced Pancreatic Cancer With	Phase I trial- single Italian institution	25 LAPC without progression post chemo 4DCT	Achieved low levels of toxicity

	Simultaneous Integrated Boost to Infiltrated Vessels Concomitant With Capecitabine: A Phase I Study	Safety of SIB dose escalation using Tomotherapy 44.25Gy/15# to tumour Boost to 58Gy to vessels within tumour mass	<p>GTV1= tumour GTV2= subvolume of GTV1 around vessels (area to get boost) ITVs created PTV1 received fixed dose of 44.25Gy in 15# PTV2 was dose escalated</p> <p>Concomitant capecitabine 1250mg/m2 given daily</p> <p>The overlaps between stomach and duodenum and PTVs were also defined as "target" volumes, but they received a reduced prescription dose depending on their absolute volume: 43.25 Gy, 42.25 Gy, and 40 Gy when overlap volume were <30cc, 30-50cc >50 cc, respectively</p>	Median OS from start of CRT 12.3 months
<p>Krishnan 2015 et al (Chris Crane team)</p> <p>doi.org/10.1016/j.ijrobp.2015.12.003</p>	Focal Radiation Therapy Dose Escalation Improves Overall Survival in Locally Advanced Pancreatic Cancer Patients Receiving Induction Chemotherapy and Consolidative Chemoradiation	Retrospective review of local practice at single institution in US using a variety of fractionations including 67.5Gy in 15 fractions	All had induction chemo before (folfirinox or gem based). Concurrent chemo was gemcitabine or capecitabine based	<p>Escalating to BED > 70 positive impact on survival</p> <p>Those undergoing 15 # (7 patients) had concurrent chemo</p>
<p>Crane 2016</p> <p>doi: 10.1093/jrr/rrw016</p>	Hypofractionated ablative radiotherapy for locally	Review of hypofractionated pancreatic radiotherapy	Description of dose escalated programme	Only use 15# in those where tumour > 1cm from OAR,

	advanced pancreatic cancer	and description of local practice at single institution in US	<p>1. Utilises gating, intentional dose heterogeneity and simultaneous integrated protection</p> <p>2. Patients treated in inspiratory BH (if reliable) or gated end expiration with fiducials</p> <p>3. Uses CT on rails for online verification</p> <p>4. Simultaneous protection: subtraction of a planning 4D OAR vol +5mm from high dose volume</p> <p>37.5Gy/15# to 'microscopic area', CTV= GTV +10mm, PTV= CTV+5mm</p> <p>67.5Gy/15 to boost region = GTV+0-5mm</p> <p>Max point 45Gy for stomach and duodenum, 40Gy for jejunum</p>	
<p>Colbert et al 2017 (Chris Crane team)</p> <p>doi.org/10.1016/j.adro.2017.02.004</p>	Dose escalation with an IMRT technique in 15 to 28 fractions is better tolerated than standard doses of 3DCRT for LAPC	<p>Comparison between standard dose 3DCRT and escalated dose radiation using IMRT</p> <p>Retrospective review of single US centre</p>	<p>59/ 154 patients had a dose escalated treatment or which 10 were treated in 15 fractions</p> <p>Dose escalated patients were treated with image guidance (usually a CT on rails) and respiratory gating</p>	<p>No G4/5 acute or late toxicity in dose escalated group with lower rates of G3 toxicity compared to standard dose group</p> <p>Importance of image guidance, and motion management highlighted</p>

<p>Goto et al 2018</p> <p>doi.org/10.1186/s13014-018-1063-5</p>	<p>Clinical evaluation of intensity-modulated radiotherapy for locally advanced pancreatic cancer</p>	<p>Comparison between 3DCRT and IMRT</p> <p>Retrospective review of single centre experience (Japan)</p> <p>Same team as Iwai et al</p>	<p>80 3D CRT patients, median dose 54Gy/30# with 250mg/m² Gemcitabine compared to 27 IMRT patients received median dose of 48Gy/15# with full dose weekly Gemcitabine</p> <p>GTV= gross disease CTV = GTV + 5mm + potential PA LN and neuroplexus involvement PTV= CTV + 5mm margin (breath hold used) PTV boost = PTV – (Stomach + 5-10mm and Duodenum + 5-10mm)</p> <p>Prescription dose= D95 to PTV boost individualised between 39 and 51 Gy</p> <p>Stomach/Duodenum V45Gy <1cc V42Gy <5cc, V39Gy <25 cc</p> <p>Stomach+PRV/duodenum + PRV V39Gy <30cc, V36Gy <45cc</p> <p>Spinal cord Dmax 36Gy, spinal cord PRV D2cc<39Gy</p> <p>Kidney V20 Gy<30% Liver Dmean <30Gy</p>	<p>Use of hypofractionated IMRT resulted in improved OS and LRPFS without increased GI toxicity compared to conventionally fractionated regimen</p>
<p>Reyngold, Parikh, Crane 2019</p>	<p>Ablative radiation therapy for locally advanced</p>	<p>Explanation of current techniques and dose</p>	<p>High dose PTV (67.5Gy/15) = GTV +0-5mm margin</p>	<p>Dose escalated treatment requires use of advanced</p>

doi.org/10.1186/s13014-019-1309-x	pancreatic cancer: techniques and results	constraints used at authors institutions (US)	excluding GI OAR +5-7mm margin Microscopic extension PTV (37.5Gy/15#)= CTV+5mm CTV= GTV +1cm +CA, SMA, +/- porta hepatis +/- splenic hilum basins Stomach and duodenum segments 1 and 2 +3-5mm: Dmax 45Gy Small bowel PRV (3-5mm) max dose <40Gy Large bowel PRV +3-5mm Dmax <50Gy	motion management technique, good image guidance and adaptive replanning PRVs used as avoidance structures during planning
Versteijne et al 2020 doi.org/10.1200/JCO.19.02274	Preoperative chemoradiotherapy versus immediate surgery for resectable and borderline resectable pancreatic cancer: Results of the Dutch randomized phase III PREOPANC trial	Phase III trial comparing chemoradiotherapy to upfront surgery in resectable/borderline resectable disease Locally advanced patient not included	246 patients, 1:1 ratio CRT vs immediate surgery GTV delineated on all phases of the 4D CT scan. CTV= the GTV plus possible tumour extension of 5 mm. ITV= summation of CTV's in all phases of respiration PTV= ITV + 10mm 36Gy/15# with 1000mg/m2 Gemcitabine D1,8 and 15 No dose constraints for small bowel as total dose below tolerance Mean kidney <16.8Gy, mean liver dose < 26.4Gy	No OS benefit for addition of CRT (HR 0.78, CI 0.58-1.05, P=0.96 Improved R0 resection rate with CRT(71% vs 40% P<0.001)

			Primary end point: OS	
<p>Iwai et al 2020</p> <p>(same team as Goto et al)</p> <p>doi.org/10.1186/s13014-020-01712-2</p>	<p>Hypofractionated intensity-modulated radiotherapy with concurrent chemotherapy for elderly patients with locally advanced pancreatic carcinoma</p>	<p>Retrospective analysis of LAPC patients aged ≥ 75 years receiving hypofractionated IMRT (48Gy/15# with concurrent weekly gemcitabine) at single institution in Japan</p>	<p>15 patients</p> <p>Respiratory motion managed with breath-hold, respiratory gating or dynamic tumour tracking</p> <p>GTV= primary tumour +involved lymph nodes CTV= GTV +5mm + prophylactic lymph node region PTV standard= CTV + 5mm PTV boost= PTV minus (stomach + 5-10mm) minus duodenum + 3-5mm) PTV boost = 48Gy/15# PTV standard = ≥ 36Gy/15# OAR constraints prioritised Weekly Gemcitabine 1000mg/m² followed by maintenance Gemcitabine OAR dose constraints as per Goto et al</p>	<p>Median OS 20.4 months</p> <p>3 cases of G3 non-haematologic toxicity- 1 RT related</p>

<p>Koay et al 2020</p> <p>doi.org/10.1016/j.prro.2020.01.012</p>	<p>Dose-escalated radiation therapy for pancreatic cancer: A simultaneous integrated boost approach</p>	<p>Paper on practical approach to dose-escalated radiotherapy for pancreatic cancer</p>	<p>Includes a case study using 15 fraction regimen and simultaneous integrated boost technique</p> <p>Utilises boost to 67.5Gy but with wider volume receiving 37.5Gy, however should aim for the portion of GTV not overlapping with the GI PRV to receive 45Gy</p>	<p>Uses planning at risk volumes (GI OAR +5mm) to reduce risk of toxicity</p> <p>OAR dose constraints take priority over target coverage</p>
<p>Parag Parikh</p> <p>Personal correspondence</p>	<p>Prospective Phase I Study of nab-Paclitaxel plus Gemcitabine with Concurrent MR-Guided IMRT in Patients with Locally Advanced Pancreatic Cancer</p>	<p>In recruitment</p> <p>Utilising dose escalated RT (MR guidance and gating) with gemcitabine plus abraxane</p> <p>Lowest 15# fraction dose they will test will be 50Gy/15#</p>		<p>Results awaited</p>

Appendix 7.2

Dose constraints from 15 fraction protocols

Organ	PREOPANC	Goto et al 2018		Parag Parikh personal correspondence	ABC-07 trial (dose escalated radiotherapy of cholangiocarcinoma) personal correspondence from Maria Hawkins			Koay et al 2020	Primus-002 trial		Reygolds, Crane, Parikh
Duodenum	Nil given as "36Gy/15# below tolerance"	Dmax 1.0cc	<45Gy	Dmax <45Gy		Optimal	Mandatory	Dmax <45Gy	Dmax 0.5cc	≤45Gy	Dmax <45Gy Parts 1 and 2 as a PRV With 3-5mm margin
		D5cc	<42Gy		Dmax 0.5cc	≤45Gy	≤48Gy				
		D25cc	<39Gy								
		Duodenum +PRV	V39 < 30cc V36 <45cc		D5cc	≤36Gy	-		D5cc	≤35Gy	
Stomach	Nil given as "36Gy/15#	Dmax 1.0cc	<45Gy	Dmax <45Gy		Optimal	Mandatory	Dmax <45Gy	Dmax 0.5cc	≤40Gy	Dmax <45Gy

	below tolerance"	D5cc	<42Gy		Dmax 0.5cc	≤40Gy	≤45Gy		D5cc	≤36Gy	as a PRV With 3-5mm margin
		D25cc	<39Gy								
		Stomach + PRV	V39 < 30cc V36 <45cc		D5cc	≤36Gy	-				
Small bowel	Nil given as "36Gy/15# below tolerance"	Not reported		Dmax <45Gy		Optimal	Mandatory	Dmax <45Gy	Dmax 0.5cc	≤45Gy	Dmax <40Gy as a PRV With 3-5mm margin
					Dmax 0.5cc	≤45Gy	≤48Gy		D5cc	≤36Gy	
					D5cc	≤36Gy	-				
Large bowel	Nil given as "36Gy/15# below tolerance"	Not reported	Not reported			Optimal	Mandatory	Dmax <45Gy	Dmax 0.5cc	≤48Gy	Dmax <50Gy as a PRV With 3-5mm margin
					Dmax 0.5cc	≤48Gy	≤51Gy				

Liver	Mean ≤ 26.4Gy	Mean dose <30Gy	Mean dose <25Gy	Mean ≤ 24Gy			Mean <24Gy	Mean ≤22Gy V10 ≤70%	Not reported
Kidneys	If mean to one kidney > 16.8Gy avoid contralateral	V20 <30% (at least one)	D25% <18Gy If one kidney D33% <18Gy and D50% <13Gy		Optimal	Mandatory	Mean <18Gy V20 <33% each	Mean ≤18Gy If mean to one kidney >18Gy then remaining kidney V12 <10%	Not reported
				Mean combined	≤12Gy	≤15Gy			
				If one kidney or one kidney mean dose >12Gy		V12Gy ≤10%			
Spinal cord	Nil given as "36Gy/15# below tolerance"	Dmax <36Gy Cord +PRV D2cc <39Gy	Dmax 0.03cc <45Gy		Optimal	Mandatory	Dmax <30Gy	Dmax 0.5cc to PRV ≤37.5Gy	Not reported
				Dmax 0.5cc PRV	≤35Gy	≤37.5Gy			
Common bile duct	Not reported	Not reported	Not reported	Not reported			Dmax <70Gy	Not reported	Not reported

Spleen	Not reported	Not reported	Not reported	Not reported	Mean <6Gy	Not reported	Not reported
--------	--------------	--------------	--------------	--------------	-----------	--------------	--------------